EN/DDCV

①

MULTIVARIABLE CONTROL LAWS FOR THE

AFTI/F-16

THESIS

AFIT/GE/EE/83S-4   A. Finley Barfield

DTIC
ELECTE
DEC 1 4 1983

S   D

B

DEPARTMENT OF THE AIR FORCE

AIR UNIVERSITY (ATC)

AIR FORCE INSTITUTE OF TECHNOLOGY

Wright-Patterson Air Force Base, Ohio

83   12   13   233

MULTIVARIABLE CONTROL LAWS FOR THE

AFTI/F-16

THESIS

AFIT/GE/EE/83S-4   A. Finley Barfield

DTIC
S ELECTE D
DEC 1 4 1983

B

Approved for public release; distribution unlimited.

AFIT/GE/EE/83S-4

MULTIVARIABLE CONTROL LAWS FOR THE

AFTI/F-16

THESIS

Presented to the Faculty of the School of Engineering

of the Air Force Institute of Technology

Air University

in Partial Fulfillment of the

Requirements for the Degree of

Master of Science

by

A. Finley Barfield, B.S.E.E.

Graduate Electrical Engineer

July 1983

Preface

Emphasis in this thesis is on the development of a preliminary design for a flight control system using recently evolved multivariable techniques and considering real world constraints. Such an approach is important because of concerns that exist in the engineering community about the application of modern control system designs with high gains and wide bandwidths.

The AFTI vehicle is chosen because of my experience with the control law development and knowledge of the implementation constraints. I would like to thank Mr. Jim Ramage, Chief Engineer for the AFTI/F-16 ADPO, for sponsoring this effort along with the ADPO Engineers for providing assistance and guidance during the study.

The theoretical background is based on techniques developed by Professor Brian Porter from the University of Salford, England. I would like to express my appreciation to Professors John J. D'Azzo and Constantine H. Houpis of the Department of Electrical Engineering at the Air Force Institute of Technology. The thesis would not have been possible without their guidance and suggestions.

This research was accomplished in parallel with four fellow students. I found the numerous and enlightening discussions with this group to be most helpful during the

ii

thesis effort. My sincere thanks to Captain Jon Bauschlicker, Lieutenant Tom Lewis, Captain Mike Masi and Lieutenant Dan Russ who comprised this group.

Finally, I want to express my love and appreciation to my wife, Diane, for her patience and understanding during this research effort. I would also like to thank my parents and my brother, Travis, for all their love and support.

A. Finley Barfield

Accession For	
NTIS GRA&I	✓
DTIC TAB	☐
Unannounced	☐
Justification	

By	
Distribution/	
Availability Codes	
Dist	Avail and/or Special
A-1	

DTIC COPY INSPECTED 3

Contents

List of Figures

xi

List of Tables

List of Symbols

$\underline{A}$ Continuous-time plant matrix

AC   Aerodynamic center

A_n Longitudinal acceleration (positive upward along the negative z body axis)

$A_{n_{cg}}$ Longitudinal acceleration at the center of gravity

A_{n_p} Longitudinal acceleration at the pilot's station

A_y Side acceleration (positive out the right wing along the y body axis)

$A_{y_{cg}}$ Side acceleration at the center of gravity

A_{y_p} Side acceleration at the pilot's station

α Angle of attack, perturbation angle of attack in perturbation equations

α_T Trim angle of attack

α_1 Independent fuselage pitch pointing mode

$\bar{\alpha}$ Ratio of proportional to integral feedback

$\underline{B}$ Continuous-time plant matrix

b   Wing span

BW   Bandwidth

β Sideslip angle

β_1 Independent fuselage yaw pointing mode

$\underline{C}$ Continuous-time Output Matrix

c   Mean Aerodynamic Cord

CG,cg   Center of gravity

C_D Nondimensional coefficient of drag (along velocity vector)

C_{D_α} Nondimensional variation of drag with angle of attack

C_{D_δ} Nondimensional variation of drag with elevator (δe) or flaperon (δf)

C_{D_0} Nondimensional bias coefficient of drag at zero angle of attack

C_{D_u} Nondimensional variation of drag with forward velocity perturbations from trim velocity

C_L Nondimensional coefficient of lift (normal to velocity vector)

C_{L_α} Nondimensional variation of lift with angle of attack

$C_{L_{\dot{\alpha}}}$ Nondimensional variation of lift with the rate of change of angle of attack

C_{L_δ} Nondimensional variation of lift with elevator (δe) or flaperon (δf)

C_{L_0} Nondimensional bias coefficient of lift at zero angle of attack

C_{L_q} Nondimensional variation of lift with pitch rate

C_{ℓ_β} Nondimensional variation of rolling moment with sideslip angle

C_{ℓ_δ} Nondimensional variation of rolling moment with aileron (δa), rudder (δr), canard (δc), or differential tail (δ_{DT})

C_{ℓ_p} Nondimensional variation of rolling moment with roll rate

C_{ℓ_r} Nondimensional variation of rolling moment with yaw rate

C_m Nondimensional coefficient of pitching moment

C_{m_α} Nondimensional variation of pitching moment with angle of attack

C_{m_δ} Nondimensional variation of pitching moment with elevator (δe) or flaperon (δf)

C_{m_0} Nondimensional bias coefficient of pitching moment at zero angle of attack

C_{m_q} Nondimensional variation of pitching moment with pitch rate

C_{m_u} Nondimensional variation of pitching moment with forward velocity perturbations

cmd   Command

C_{n_β} Nondimensional variation of yawing moment with sideslip angle

C_{n_δ} Nondimensional variation of yawing moment with aileron (δa), rudder (δr), canard (δc), or differential tail (δ_{DT})

C_{n_p} Nondimensional variation of yawing moment with roll rate

C_{n_r} Nondimensional variation of yawing moment with yaw rate

cos   Cosine

C_x Nondimensional x-force coefficient

C_{x_α} Nondimensional variation of x-force with angle of attack

C_{x_δ} Nondimensional variation of x-force with elevator (δe) or flaperon (δf)

C_{x_0} Nondimensional bias x-force coefficient at zero angle of attack

C_{x_q} Nondimensional variation of x-force with pitch rate

C_{x_u} Nondimensional variation of x-force with forward velocity perturbation

C_{y_β} Nondimensional variation of y-force with sideslip angle

C_{y_δ} Nondimensional variation of y-force with aileron (δa), rudder (δr), canard (δc), or differential tail (δ_{DT})

C_{y_p} Nondimensional variation of y-force with roll rate

C_{y_r} Nondimensional variation of y-force with yaw rate

C_z Nondimensional z-force coefficient

C_{z_α} Nondimensional variation of z-force with angle of attack

$C_{z_{\dot\alpha}}$ Nondimensional variation of z-force with the rate of change of angle of attack

C_{z_δ} Nondimensional variation of z-force with elevator (δe) or flaperon (δf)

C_{z_0} Nondimensional bias coefficient of z-force at zero angle of attack

C_{z_q} Nondimensional variation of z-force with pitch rate

C_{z_u} Nondimensional variation of z-force with forward velocity perturbation

deg   Degree

δa Aileron deflection

δc Canard deflection

δ_{DT} Differential horizontal tail deflection (rolling tail)

δe Elevator or horizontal tail deflection

δf Flap deflection

$e(t),\underline{e}$ Error vector

$\underline{e}(kT)$ Discrete error vector

ϵ Epsilon scalar multiplier

F_s Stick input

ft   Feet

F_y Sideforce in y-body axis

F_z Force in z-body axis

$F_{z_{cg}}$ z-force at center of gravity

f Sampling frequency

g Gravity, type of pilot command, gain constant

xvi

$\underline{G}(s)$ Transfer function matrix

I_{xx} Moment of inertia about x-axis

I_{yy} Moment of inertia about y-axis

I_{zz} Moment of inertia about z-axis

I_{xz} Product of inertia about xz-axes

$\underline{I}$ Identity matrix

K_i Gain constant on surface position feedbacks

$\underline{K}_0$ Proportional control law feedback matrix

$\underline{K}_1$ Integral control law feedback matrix

K_p Gain constant in pilot model

Lat-Dir   Lateral-Directional

lbs   pounds

Long   Longitudinal

ℓ_x Distance from CG to sensor location along x-axis

ℓ_y Distance from CG to sensor location along y-axis

ℓ_z Distance from CG to sensor location along z-axis

L_β Dimensional variation of rolling moment with sideslip angle

L_δ Dimensional variation of rolling moment with aileron (δa), rudder (δr), canard (δc), or differential tail (δ_{DT})

L_p Dimensional variation of rolling moment with roll rate

L_r Dimensional variation of rolling moment with yaw rate

$\underline{M}$ Measurement matrix

m   Aircraft mass, number of inputs

MAC   Mean Aerodynamic Cord

M_α Dimensional variation of pitching moment with angle of attack

$M_{\dot{\alpha}}$	Dimensional variation of pitching moment with the rate of change of angle of attack
M_c	Controllability matrix
MD	MULTI Design
M_o	Observability matrix
M_q	Dimensional variation of pitching moment with pitch rate
M_θ	Dimensional variation of pitching moment with pitch angle
M_x	Moment about the x-axis
M_y	Moment about the y-axis
M_z	Moment about the z-axis
n	Number of states
N_β	Dimensional variation of yawing moment with sideslip angle
N_δ	Dimensional variation of yawing moment with aileron (δa), rudder (δr), canard (δc), or differential tail (δ_{DT})
N_r	Dimensional variation of yawing moment with yaw rate
N_p	Dimensional variation of yawing moment with roll rate
p	Number of outputs, roll rate
PR	Pilot Rating
q	Pitch rate
$\bar{q}$	Dynamic pressure
r	Yaw rate
rad	Radians
S	Surface area
s	Laplace operator
sec	Seconds

sin	Sine
σ	Elements of the Sigma (Σ) matrix
$\underline{\Sigma}$	Sigma Gain Weighting matrix
$\underline{T}$	Transformation matrix
T	Sampling period, Thrust
TWeaD, TWEAD	Tactical Weapon Delivery
U	Velocity along x-axis
$\Delta u, u$	Perturbation velocity along x-axis
$\underline{u}$	Input vector
V	Velocity along y-axis
v	Perturbation velocity along y-axis
$\underline{v}$	Command input vector
V_T	Forward Velocity
W	Velocity along z-axis, aircraft weight
w	Perturbation velocity along z-axis
$\underline{w}$	Controller output vector
$\underline{x}$	State vector
X_α	Dimensional variation of x-force with angle of attack
$X_{\dot{\alpha}}$	Dimensional variation of x-force with the rate of change of angle of attack
X_δ	Dimensional variation of x-force with elevator (δe) or flaperon (δf)
X_q	Dimensional variation of x-force with pitch rate
X_u	Dimensional variation of x-force with forward velocity perturbation
$\underline{y}$	Output vector
Y_β	Dimensional variation of y-force with sideslip angle

Y_δ Dimensional variation of y-force with aileron (δa), rudder (δr), canard (δc), and differential tail (δ_{DT})

Y_p Dimensional variation of y-force with roll rate

Y_r Dimensional variation of y-force with yaw rate

$\underline{z}(t),\underline{z}$ Integral of error vector

$\underline{z}(kT)$ Discrete Integral of error vector

Z_α Dimensional variation of z-force with angle of attack

$Z_{\dot{\alpha}}$ Dimensional variation of z-force with the rate of change of angle of attack

Z_δ Dimensional variation of z-force with elevator (δe) or flaperon (δa)

Z_q Dimensional variation of z-force with pitch rate

Z_u Dimensional variation of z-force with forward velocity perturbation

Z_t Transmission zeros

$Z_{1,2}$ Finite system roots

Z_3 Infinite system roots

θ Pitch angle

θ_c Pitch angle command

θ_e Pitch angle error

ϕ Roll angle

ψ Yaw angle

$\Gamma(\lambda)$ Asymptotic transfer function matrix

Abstract

Recently evolved multivariable design techniques are used to develop control laws for the AFTI/F-16. The techniques were developed by Professor Brian Porter of the University of Salford, England. In the study, designs are investigated to provide pilot control of vehicle rotational rates and accelerations. This line of inquiry is in contrast to the angle control concepts required in previous applications of these new techniques. A computer-aided design package called "MULTI" is used in refining the control laws to the preliminary design stage. It proves to be invaluable.

An aircraft model is developed in state space form for the AFTI vehicle from linearized aerodynamic data. This is accomplished at several points in the flight envelope. After validation, these models are used for the design and evaluation of the control laws.

AFTI is equipped with additional control surfaces to provide Direct Force (CCV) control. A requirement of the design is to demonstrate specific CCV capabilities. Major emphasis is placed on the ability to properly blend CCV and conventional control capabilities for combat maneuvering.

The methods employed to obtain a design are presented along with the evaluations of the final control laws.

Several instabilities encountered during the investigation are discussed. The multivariable techniques are shown to provide good designs with a very moderate expenditure of manpower. Additional areas of research are discussed along with proposed modifications to the "MULTI" package.

MULTIVARIABLE CONTROL LAWS FOR

THE AFTI/F-16

I.   Introduction

Background

The advent of digital fly-by-wire control on advanced
high performance aircraft has provided the pilot with control
over pertinent motion variables. A stick input no longer
simply commands a control surface deflection. The pilot's
task is not restricted by the basic aerodynamic characteris-
tics of the vehicle. The designer has the ability to develop
a system which allows the pilot to command the type of air-
craft response that has been found to be most useful. Such
developments have opened the door to tailoring the control
system for accomplishing specific mission phases with the
promise of significant performance improvements. For a num-
ber of years, control theory has been applied to the design
of limited authority augmentation systems to improve an air-
craft's inherent short period and dutch roll damping through-
out the flight envelope. Also, it has been employed in the
design of autopilots to perform functions such as altitude
hold, Mach hold, or heading hold and in the development of
automatic landing systems. In the 1960 time period, flight

1

testing on the TWeaD F-4 program demonstrated active control could improve the ability of the pilot to use the aircraft as a weapons platform (Ref 1).

Recent emphasis has been on the incorporation of control concepts early in the aircraft design cycle to improve flight performance. The aerodynamic design is no longer restricted by requirements to provide natural damping and stability. In the case of statically unstable aircraft, the control system provides complete artificial stability and acceptable flying qualities.

The use of fly-by-wire requires the "electrical flight control system" to be as reliable and endurable as the mechanical system it replaces. This establishes rather severe requirements for the system, since flight safety is a paramount issue. The flight control system has to be designed to operate after several failures. In some cases this results in the use of four identical (redundant) channels within the flight control system so that monitoring and majority voting can identify and isolate failures. The required reliability is in the order of 1×10^{-7} failures per flight hour. Thus, only one failure is permitted for every 10 million flight hours (Ref 2).

Such stringent requirements result in the philosophy of having very few signal sources external to the system. Aircraft motion sensors used by the flight control system, although not possessing great accuracy, are extremely

2

reliable. Linear Variable Differential Transformers (LVDT) which are magnetically coupled are used as position sensors. Potentiometers are avoided because of their high failure rates and tendency to generate noisy signals.

This type of reliability is not necessary for other avionics systems or for limited authority outer-loop control functions such as autopilots. In these cases a failure is easily detected by the pilot and corrective action taken to counter the failure until the system can be removed from operation. This is not practical for full authority fly-by-wire systems. Because of their high authority and fast response, failures can result in aircraft loss.

Recent developments in Direct Force capabilities have provided the pilot with an additional dimension in maneuvering response resulting in a "new way to fly" (Ref 3). The proper application of these new Control Configured Vehicle (CCV) abilities to enhance combat effectiveness has been the subject of several research programs (Ref 4; 5).

Control design has been complicated by these new abilities. The designer is now faced with multiple input/output systems and an ever increasing number of feedback loops. Although classical methods can provide a means of design, application of these methods is becoming more and more time-consuming. Many iterations are required, as each new loop is closed, to satisfy the many varied and sometimes conflicting requirements.

The CCV YF-16 program carried such a classical design through flight testing with exceptionally good results. Attempts to design with modern control techniques have given less impressive results. This is unfortunate since these methods offer the potential of improved performance with a reduction in the design complexity. Requirements such as use of full state feedback, definition of a proper performance index, or selection of desired eigenvectors leave much to be desired in the currently available modern control techniques.

Recent theoretical work by Professor Brian Porter at the University of Salford, England, on high-gain error actuated methods has shown promise of enabling the design of exceptionally good performing systems without many of the drawbacks of current modern control methods. The theory of Professor Porter's work is presented in Chapter III and can also be found in Reference 6.

The problem undertaken in this thesis research is the development of an air-to-air combat control system for the AFTI/F-16 aircraft. Emphasis is placed on considerations for a practical implementation. The design is accomplished at several points in the flight envelope as shown in Figure 1. The point at 0.9 Mach and 20,000 feet is the primary design case. This is the condition where aerial combat generally begins. The other points are chosen to give a good variation in both the aerodynamic characteristics and static

4
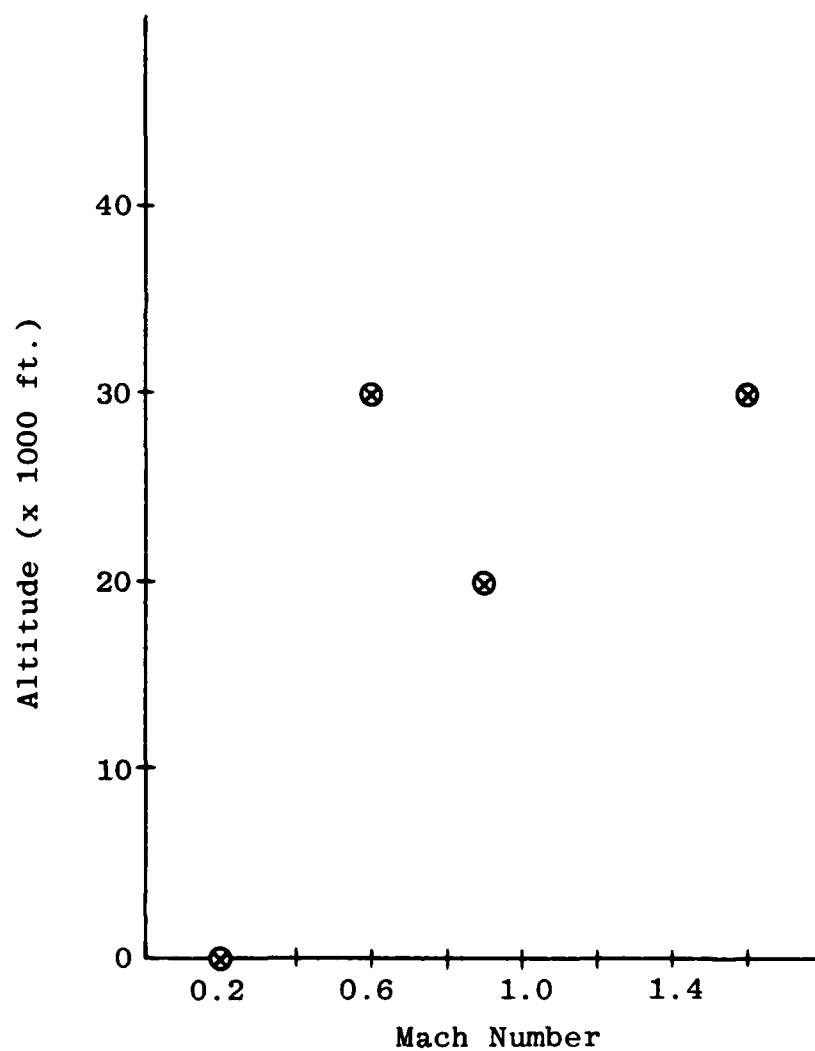
Figure 1.   Flight Envelope Design Points

stability. Only cursory data is collected at the 0.2 Mach, sea level condition since combat capability is being stressed. This condition is included in the evaluation because it provides information on operation at elevated angle of attack. The 1.6 Mach, 30,000 feet point is selected due to the high "$\overline{q}$" condition and since some encounters actually begin supersonically. However, for such encounters, should a maneuvering engagement develop, airspeed drops quickly, and the subsonic region is entered.

Assumptions

Basic assumptions in the design effort are established to reduce the design complexity to a level equivalent to that of a "preliminary design" effort. These assumptions are listed below.

* The aircraft is a rigid body, and mass is constant.

* Thrust is not changing.

* The earth's surface is an inertial reference frame.

* The atmosphere is assumed fixed with respect to the earth.

* The equations of motion can be decoupled into a longitudinal and a lateral-directional set of equations.

* Linearization about an operating condition is acceptable for point designs.

* Aerodynamics are fixed for Mach and altitude.

A rigid aircraft model is employed in which any two points in the airframe remain fixed with respect to one

6

another. Flexibility due to structural modes of the air-craft are not considered in this study. However, requirements are developed with a consideration of such effects. As an example, flight control-structural interactions can cause several problems ranging from unwanted vibrations or control surface activity to structural failure and aircraft loss. With this in mind, the design goals are established to provide good performance at a minimum gain and bandwidth. In seeking to prevent structural interaction, the system is limited in bandwidth to only the range needed to do the job. High frequencies, where structural resonances are usually encountered, are attenuated. It is noted that flexibilized aerodynamic data is used in developing the linear aircraft model. In this way control surface deformation due to air loads is accounted for as dynamic pressure changes.

Mass variations for the aircraft are fairly large because of fuel usage during a mission. However, the control system responses being studied are in the range of one to ten seconds compared to a 1.5 hour mission. Fuel usage and the resulting mass change during a specific maneuver are very small and can be neglected.

Thrust is held constant throughout each maneuver to reduce the number of variables being altered in the design. It also provides a means of comparing design attempts. With constant thrust, the variation in velocity provides an indication of the drag penalty and energy loss for the same

maneuver for several candidate designs. In addition, an apriori scheme for varying thrust during a maneuver is not apparent. Although thrust adjustment can be added as an input to control velocity, it is felt that pilot control of thrust during combat maneuvering is very active and not easily predicted for use in design studies of this level. Such an extension can be examined for application to an auto-mated or semi-automated attack system.

The inertial frame of reference is established as the earth's surface. This greatly simplifies the equation development and is valid for two reasons. First, the sensors used for flight control systems, although highly reliable, are not sensitive enough to detect the earth's rotational rate or the coriolis acceleration. Secondly, the maneuvers being considered have short durations compared to earth rate. Relative to the earth they are also "local" responses, and thus a flat earth with constant gravity gives fairly accurate results.

For this design effort, the atmosphere is assumed fixed to the surface of the earth. The limited scope of this preliminary design did not cover random gust, steady winds, or wind sheers during maneuvers. However, the effect of gust upset is considered in establishing design restraints that lead to a limited bandwidth control system with reduced gains. It also directs the selection of feedback signals to those which are not overly gust sensitive.

The full nonlinear equations of motion are developed in Appendix B and then simplified for the study. The first basic simplification is to assume that for this preliminary design work the equations can be broken into a set of longitudinal equations and a set of lateral-directional equations which do not interact. Since air combat maneuvering is a design goal, this assumption of being decoupled must be kept in mind. At times the assumption is altered to allow for consideration of special maneuvers such as the ability to roll about the velocity vector of the aircraft. That ability is very desirable for fighter aircraft and is addressed later.

Multiple design points are established in the flight envelope, and the simplified equations are linearized at these points. Perturbation equations about these points are then employed in the design phase. Such a strategy assumes that such point designs are fairly accurate representations at the selected points. To accomplish a full envelope design requires many such point designs with gain scheduling between points. This approach has been used for several existing aircraft control system designs and requires a great many points to be considered. The further the deviation from such "design" points, the less likely that the design is adequate since the model used for such designs becomes less and less realistic. In this study, only four design points are used as shown in Figure 1. These are

9

selected to provide a full range of aerodynamic variations for the controller design effort. For a practical design, a great many more points must be considered with a number of trimmed acceleration levels at each point being studied.

Although perturbations in velocity and altitude about trim are examined, the aerodynamic model is fixed at the trim point. Aerodynamic coefficients are constant through-out a maneuver. In general, the aerodynamic coefficients vary rather slowly (except in the transonic region), and the approximation is valid for reasonably small variations about the trim point.

The above assumptions with their resulting restric-tions are typical of simplifications used in developing a preliminary design for an aircraft control system. They are considered to be appropriate for this study.

Pertinent Observations

Previous efforts applying Professor Porter's method have centered on the command of output functions such as pitch angle, flight path angle, or roll angle. That approach presents two problems for the application being considered in this thesis. First, these angular quantities are ref-erenced to inertial space which in this case is the local earth coordinate system. Such measurements are usually obtained from an inertial navigation system or inertial measurements system which has a significantly lower relia-bility and failure detection capability than the flight

control system. Second, the pilot feels aircraft body
angular rates and accelerations since he is physically
attached to the aircraft. In actuality, he controls these
quantities in flying the aircraft. For a right stick input,
a fighter pilot expects to develop a proportional "right
wing down" roll rate. Release of the stick input results
in zero roll rate while the aircraft roll angle remains at
a constant value. In pitch, the pilot expects constant
stick force to result in a constant acceleration with an
associated pitching rate. It is important to note that the
pilot actually feels (and desires to command) accelerations
at his position in the aircraft. This acceleration, A_{n_p} ,
is a combination of aircraft acceleration measured at the
center of gravity, $A_{n_{cg}}$, and rotational acceleration, $\dot{q}$,
as shown in the following simplified equation. The ℓ_x term
is the distance from the center of gravity to the pilot's
position.

$$A_{n_p} = A_{n_{cg}} + \ell_x(\dot{q}) \qquad (1.1)$$

For rudder commands, yaw rate is developed with a corres-
ponding side acceleration (A_y) and sideslip (β). Based on
such observations, the controller design strives to command
these same inputs.

Recent flight testing on a highly modified F-16 has
demonstrated some rather unique new capabilities. These
capabilities are provided to the pilot through the use of

11

multiple control surfaces. The use of these control surfaces, coupled with the flight control system, allow "direct forces" to be developed by the aircraft (Figure 2). The direct force term is meant to imply the development of forces which are uncoupled from or not related to the aircraft's rotation. Using direct forces, six new control modes are available to the pilot as illustrated in Figures 3 and 4.

The "direct lift" mode provides a longitudinal acceleration while holding angle of attack constant. In this mode a pilot's command to the system causes the aircraft to change its flight trajectory by developing an additional lift force without an angle of attack change.

The "pitch pointing" mode allows the pilot to command an angle of attack change without developing an acceleration. With this mode, the pilot can actually point the nose of the aircraft up or down without changing the direction of flight.

"Longitudinal translation" results in the aircraft changing altitude or translating upward without rotating. A constant upward velocity is developed while maintaining a zero pitch rate.

These same capabilities also exist in the lateral-directional axis. The use of canards in conjunction with the rudder and various control system feedbacks allows direct force to be developed while moments are balanced on the aircraft. Ailerons are also used to counter unwanted rolling moments.
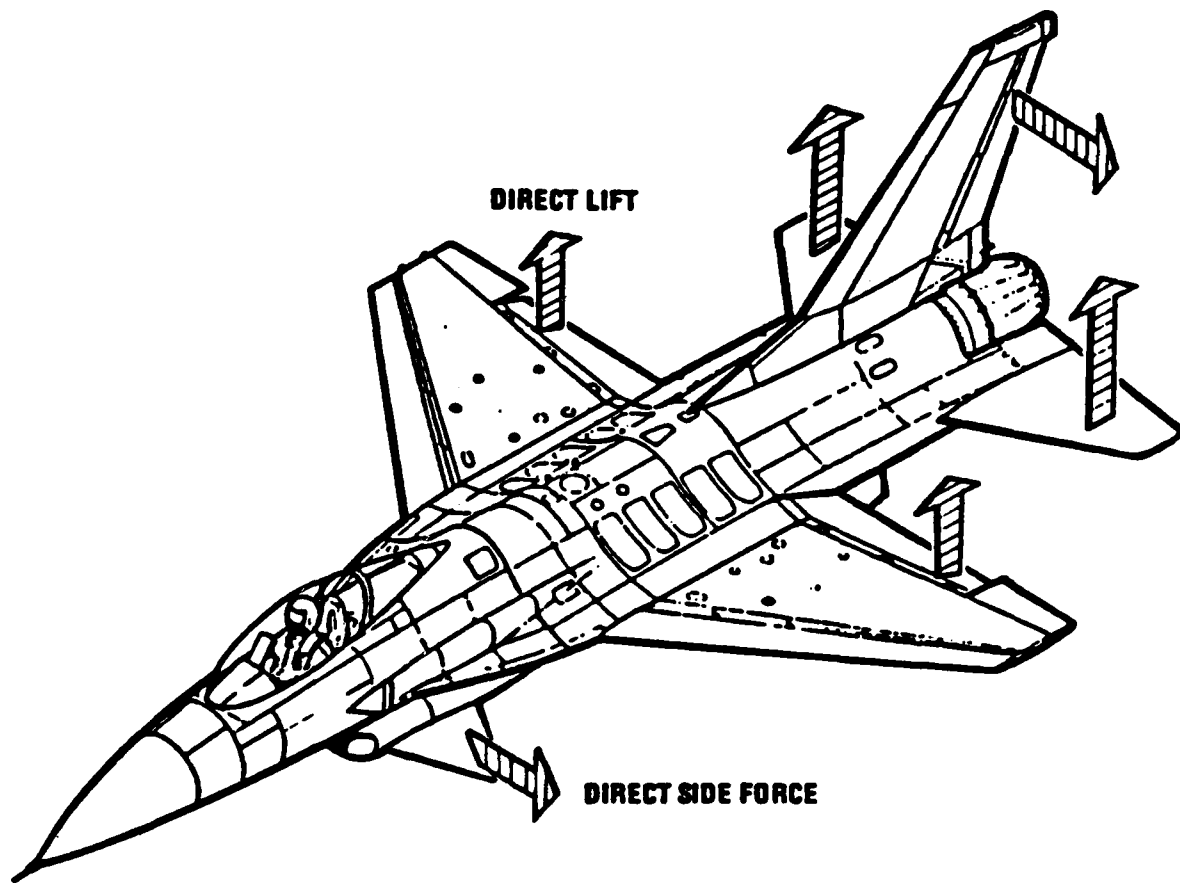
Figure 2. Direct Force Development Using
         Multiple Surfaces
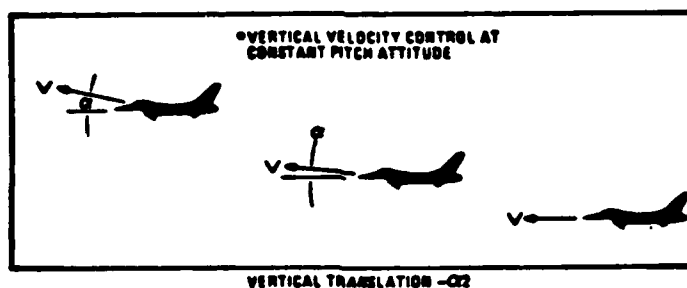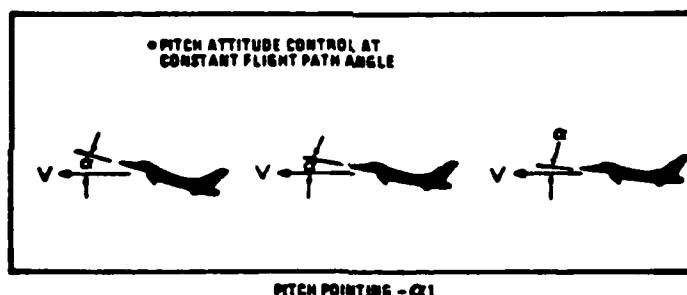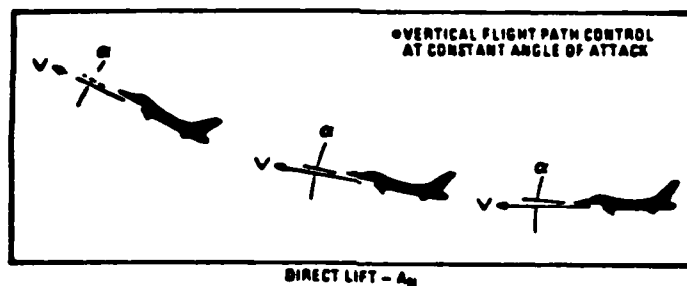
Figure 3. Longitudinal Direct Force Modes

14
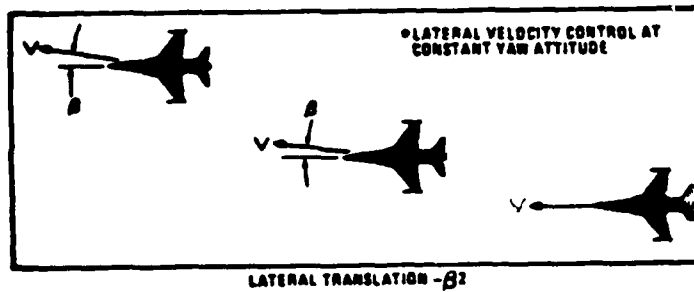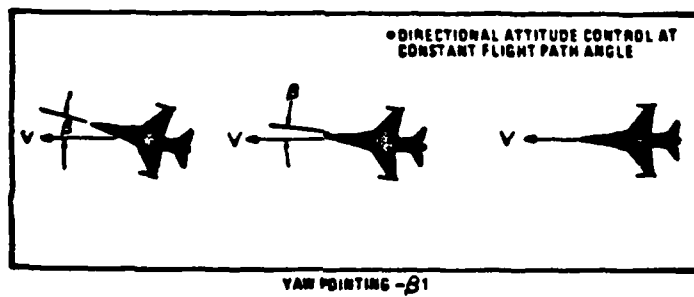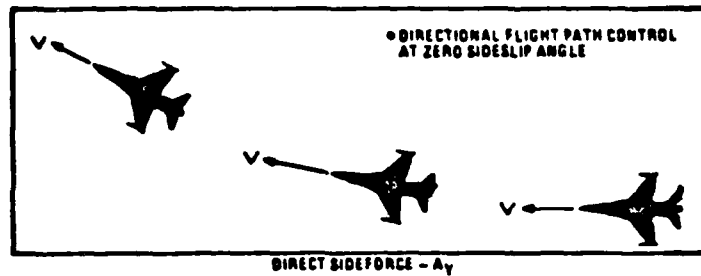
Figure 4.   Lateral-Directional Direct Force Modes

A "direct sideforce" mode provides lateral acceleration to the pilot without inducing a sideslip angle. Using such a mode allows wings level turns to be performed in which a turn rate is developed without banking the aircraft or developing a sideslip. As in the longitudinal case, the aircraft is turning with the velocity vector as opposed to leading it in conventional maneuvers.

"Yaw pointing" provides the pilot with independent control over sideslip, beta. The aircraft's nose can be pointed right or left without developing a side acceleration or changing the direction of travel.

"Lateral translation" results in the aircraft being able to execute side-step maneuvers without having to bank. In this case, a constant side velocity is developed while maintaining a zero yaw rate.

These modes of operation are called Control Configured Vehicle (CCV) maneuvers in this report. It is acknowledged that the CCV concept encompasses much more than unconventional flight modes (Ref 7). The above descriptions of the unconventional modes differ from the definitions found in the open literature by the lack of the use of terms relative to an inertial reference such as flight path angle or pitch angle. This is deemed desirable since such definitions, while being correct for limited portions of flight, are not proper in maneuvering situations. As an example, consider the case of pitch pointing. This can be defined as changing

the aircraft's pitch attitude while maintaining flight path angle and heading angle. In wings level flight such a system provides the desired fuselage pointing. Should the aircraft be in a high "g" turn requiring a large bank angle, such a system cannot be employed. Heading angle is continually changing due to the turn. For a descending turn, flight path angle is also changing. Pitch attitude (θ) is defined as the angle between the local horizon and the x-axis of the aircraft. Should the aircraft be banked at 88 or 89 degrees, changing theta results in a yawing motion. This is clearly not what is intended. It is advantageous to mechanize such CCV capabilities for "all aspect" operation. This was accomplished for the majority of modes on the CCV YF-16. Using the definitions specified in this report, a system is specified which is able to develop a change in angle of attack without an accompanying normal acceleration change. In this way fuselage pointing can be obtained without interfering with maneuvering turns. In fact, it can be commanded simultaneously with the turn.

Study Approach and Design Requirements

The general approach for this study is to design a multivariable control system for the AFTI/F-16 vehicle for combat maneuvering. Major emphasis is on the development of a controller with equivalent or improved performance as compared with the current AFTI Air-to-Air gunnery control mode but with reduced complexity. Each design attempt begins

17

with a very simple design and slowly increases in complexity
until a realistic result is obtained. For example, at the
0.9 Mach, 20,000 feet case a short period approximation of
the aircraft is initially employed in order to arrive at a
basic design with the fewest variables to adjust. The
design then proceeds to treating the full equations of motion
and includes actuator and sensor models. Any time an
unforeseen result or problem is encountered, the simplistic
model is reinvestigated. This allows determination of the
cause of such a result as either being inherent in the basic
design or as having been created in the manipulation of
variables or in the modeling of the more complex system.
It also results in a tremendous time saver in finding prob-
lems and errors as shown later in the report.

Early in the study, a set of general design require-
ments is established to form a basis for the work. These
requirements are listed below.

* The design will provide control and stability
  augmentation.

* Responses are to be fast and well-behaved.

* Surface position and rate limits must not be
  exceeded.

* Aircraft rates and accelerations will be
  directly controlled.

* Feedbacks can be reliably obtained with
  existing sensors.

* Conventional and specific CCV maneuver capa-
  bilities are available.

A brief discussion on the development of each of these requirements follows.

The controller is to augment the basic aircraft stability and in some cases, such as in the subsonic region, provide artificial stability for a statically unstable aircraft. In addition, it should provide the pilot with control over motion parameters that are important for the specific mission task of air-to-air gunnery.

In target acquisition and tracking, certain basic characteristics have been found to be advantageous. The main pilot task is precise pointing. The task can be broken into an acquisition phase and a fine tracking phase. Acquisition requires large roll and pitch changes. This translates into being able to pull onto the target rapidly, and thus, the acceleration response must be fast and well damped. Fine tracking requires precise attitude control which indicates that the pitch rate response must be fast and well damped.

In conventional aircraft, the pitch and acceleration responses are coupled, and this results in conflicting requirements. Generally, a fast "g" response produces a fast pitch rate response with large overshoots and low damping. If the design emphasizes a fast and well-damped pitch rate response, then it results in a relatively slow "g" response. The actual design which is implemented is usually a compromise of both responses, providing the best

overall results. Direct lift provides the designer with the capability of altering this basic relationship. Pitch rate and normal acceleration can be "decoupled." In this way, both responses can be tailored to provide fast well-damped behavior within the direct lift capability limits. Once these limits are exceeded, such decoupling is not possible.

The restrictions on surface position and rate limiting are imposed at the preliminary design stage as opposed to the conventional tendency for a new system to include them later in the design cycle. This restriction is established after a review of several applications of the design technique. In those cases it has been apparent that the exceptionally fast aircraft responses achieved were developed through large and extremely fast surface movements.

A design is sought that results in surface activity that does not encounter either of these limits. Running into a position limit results in loss of decoupling and prevents the required command from being reached. In cases where the control system is providing artificial stability, this results in loss of that stability. Rate limiting pre-sents a problem that is a little more sinister but just as dangerous. Rate limiting is a nonlinear function that can result in a significant increase in phase lag in a feedback system. Such phase lag has been shown to cause loss of control and divergent oscillations that can result in air-craft loss for a full authority fly-by-wire system.

It is interesting to note that in early multivariable designs such as the CCV YF-16 (in which classical design techniques were used), aircraft stability and control, and basic flying qualities were provided by conventional control surfaces with appropriate feedbacks. Additional surfaces were used to provide the direct force capabilities. Rate or surface limiting of these additional surfaces resulted in loss of the direct force function with less than the desired responses, but augmentation was not impaired. Rate and position limiting is important for the conventional surfaces and such limiting is prevented in the design. In the current multivariable designs, surface rate and position limiting is an important consideration on all surfaces since the stability function, as well as the direct force function, is performed by the combination of all surfaces.

The desirability of controlling aircraft body rates and accelerations becomes more apparent when considering the complexity of interface to the pilot. The multivariable theory applied in this thesis allows as many independent aircraft states or linear combinations of states to be commanded as there are control surfaces (inputs). For the AFTI vehicle there are two longitudinal surfaces, and thus, it is possible to control two system outputs. It should be noted that both must be commanded to some value even if that value is zero. Suppose the command parameters are selected to be angle of attack and pitch angle. In maneuvering flight,

21

pitch angle is not completely a longitudinal parameter. In the case of a constant altitude turn, theta stays at zero. Additionally, how does the pilot know what value of these two parameters to command in order to perform the maneuver he desires? One answer is to develop a model of the aircraft. Conventional pilot commands can be input, and the resulting model parameters can provide the command inputs to the multivariable controller. This requires that a simple model must be developed which exhibits the response desired of the actual aircraft. With the wide variation of aerodynamic parameters, gain scheduling might be required in the model. If the control system is to be tailored to the specific task, the model must also be tailored.

If pitch rate and normal acceleration are employed for the command parameters, the problem can be eliminated. The pilot generally desires a specific "g" level and a corresponding pitch rate can be determined from the following relationship $q = (1845/U)(A_n)$. The choice of rate and acceleration makes sense as far as reliability, availability, pilot preference, interface complexity, and workload are concerned.

The required reliability of a flight control system which provides stability and control augmentation is discussed earlier in this chapter. Rate gyros and accelerometers that sense body motion can be incorporated in the flight control system design where redundant electrical

power and signal processing are available. They are low enough in cost and size that multiple sensors can be used for redundancy. Such redundancy considerations are not meant to infer that selection of feedback signals is limited to only rates and accelerations. It is to focus attention on the careful selection of signals. In the F-16, angle of attack is deemed necessary for use in the flight control system. A means of developing multiple independent and reliable sources has been found. In addition, the F-16 uses four longitudinal accelerometers, four lateral accelerometers, four pitch rate gyros, and four roll rate gyros. These are required to meet mission reliability and failure tolerance requirements.

Through several research and development programs, the CCV control modes have been examined for usefulness in combat scenarios. From this work, several of the modes are selected for design applications in this thesis.

The first of these is blending of the conventional maneuvering capability of the aircraft with the direct lift function in the longitudinal axis to provide improved performance. The decoupling of direct lift from aircraft rotation can be used to tailor the aircraft response in a conventional maneuver to provide optimum response for both acceleration and pitch rate. Thus, the longitudinal design is aimed at using direct lift and conventional aircraft blending. Fuselage pointing holds promise for automatically

23

nulling small aiming errors during target tracking or in
obtaining a lock-on by the weapons system. The feasibility
of providing longitudinal fuselage pointing by commanding
rates and accelerations is examined. Direct sideforce has
also been shown to be promising in air-to-air gunnery and
may have possibilities for air-to-ground bombing applica-
tions. It may also be useful for evasive maneuvering or
limited terrain avoidance maneuvers. Thus, it is selected
for the directional design. Conventional roll rate control
is selected for the lateral design. The controller design
being sought is to provide the above combination of uncon-
ventional and conventional capabilities to the aircraft.

Presentation Sequence

The material in this thesis consists of a description
of the aircraft chosen for the study in Chapter II. The
process of developing a model for the design, and the means
of validating such a model is also presented. Chapter III
contains a brief description of the multivariable design
theory developed by Professor Brian Porter of the University
of Salford, England. An important area of bounded stability
is included. The design method and representative results
at selected points in the flight envelope are presented in
Chapter IV. A proposed design procedure is established.
Inadequacies of the design method as well as advantages are
discussed. The final design is evaluated in Chapter V against
several criteria and compared with current state-of-the-art

designs. Conclusions are discussed in Chapter VI with recommendations for future efforts. A complete set of aerodynamic and transformed aircraft model data is included in Appendix A. Development of the equations of motion is covered in detail in Appendix B. Controller responses to the maximum estimated inputs to verify surface rate and position limits are presented in Appendix C. The last three Appendices document the three programs used in conjunction with MULTI in the designs. The programs provide methods to: (1) convert and transform aerodynamic data into the form necessary for developing a state space aircraft model; (2) calculate transmission zeros; and (3) determine the closed-loop system matrix. The last program is useful in obtaining both closed-loop roots and system transfer functions.

II.   The AFTI/F-16 Aircraft

Aircraft Description

The AFTI vehicle is a highly modified F-16 aircraft.
It has been changed to allow flight demonstration of the
benefits possible from the integration of advanced tech-
nology features. Among the advanced features selected for
demonstration are triple redundant digital flight control
computers, and a flight control system tailored to the spe-
cific mission phase. Tailoring has resulted in eight
separate control modes being implemented in the digital com-
puters with extensive gain scheduling to provide unprece-
dented performance. Asynchronous computer operation is
employed in which each of the three computers operates
independently in calculating the flight control laws. A
redundancy management system has been developed that uses
comparison monitoring of the three computers along with
internal self-test features to detect failed system elements,
and provides a two-fail/operate capability. This means the
system can withstand two similar failures and still continue
to operate.

AFTI's major external modifications to date have
been the addition of twin vertical canards mounted under
the engine inlet and the installation of a dorsal fairing
or "back pack" between the cockpit and vertical tail. The
dorsal fairing houses avionics and instrumentation necessary

26

for the flight test effort. Although receiving an entirely
new flight control system, the original F-16 sensors are
retained. Body accelerations are measured at the pilot's
station by longitudinal and lateral accelerometers. There
are four identical sensors for each axis for redundancy.
The F-16 flight control system employs all four since it is
quadruply redundant. AFTI uses only three of these sensors
to provide essentially the same fail/operate capability as
the F-16. The fourth provides signals for flight test
instrumentation. Body rotational rates are sensed by rate
gyros located very close to the aircraft's center of gravity.
There are four identical pitch rate gyros, four roll rate
gyros, and four yaw rate gyros. In addition, angle of
attack is sensed by two fuselage side-mounted cones, as well
as, by a hemispherical differential pressure probe extending
from one side of the aircraft. Although sideslip angle,
beta, is not employed in the F-16, plans called for its use
in the AFTI system. The same type of conical sensors used
for angle of attack were to be installed to measure sideslip.
Unfortunately, a suitable location, free of airflow irregu-
larities around the fuselage, could not be found to provide
good sideslip information.

The aircraft is shown in the drawing in Figure 5.
The control surfaces used in this study are denoted by solid
black. These consist of two fully movable horizontal tail
surfaces which can be deflected symmetrically as an elevator

27
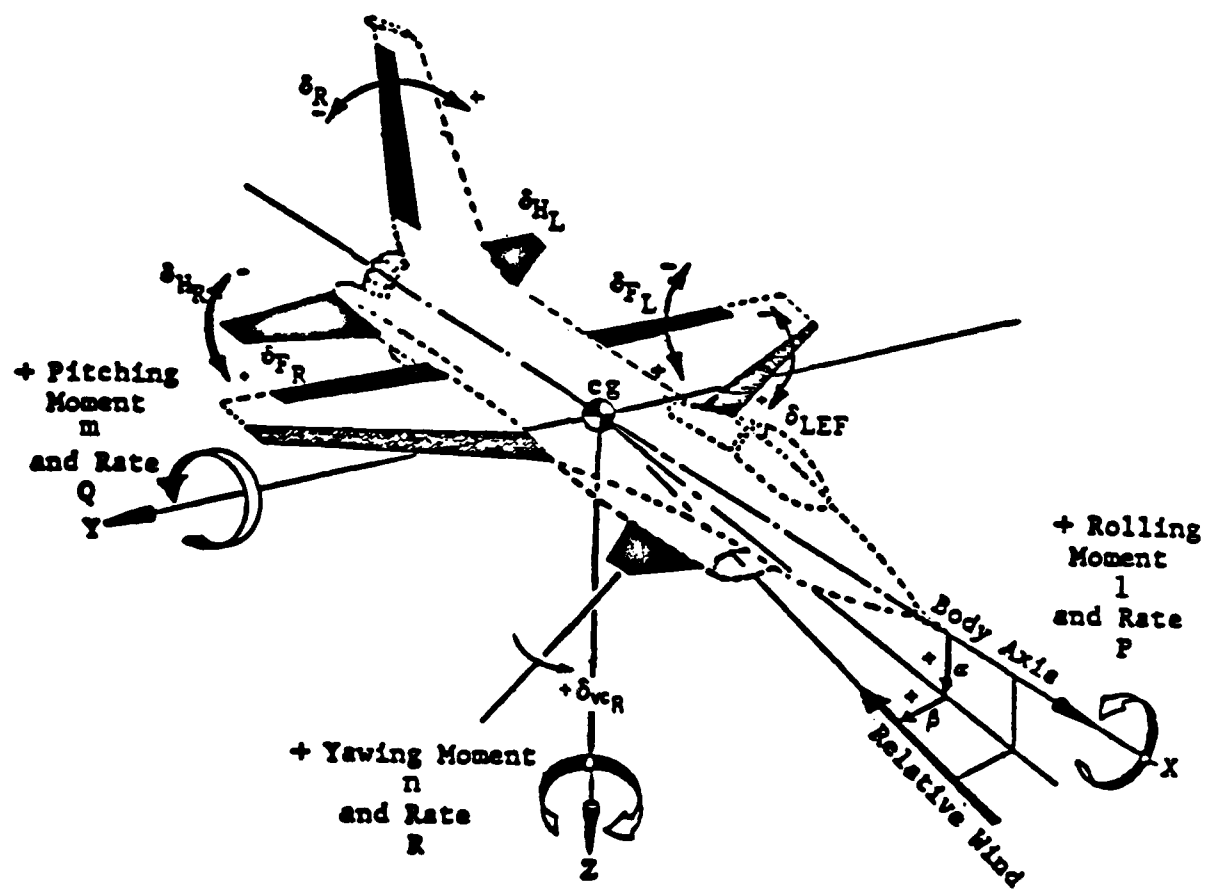
Figure 5. AFTI/F-16 Control Surface Location

or asymmetrically for augmenting roll control. Flaperons on the trailing edge of each wing can be moved symmetrically to act as flaps or asymmetrically as ailerons for primary roll control. The canards are used for sideforce control. Sign convention used in this study is also displayed in the figure.

Longitudinally the unaugmented aircraft (no control system) is statically unstable at subsonic flight conditions as illustrated in Figure 6. The center of gravity (CG) is located behind the aerodynamic center (AC) by design. The difference between the CG and AC is generally measured in percent of the mean aerodynamic cord (MAC). The figure shows the aircraft to be approximately three percent unstable subsonically. In the transonic region, the aircraft is neutrally stable. Although stable at supersonic speeds, there is also a reduction in stability when compared to conventional aircraft. The unstable condition eliminates the requirements for the elevator to continually develop a down load in trimmed flight. The tail is actually adding lift to the aircraft. Because of this design feature, the aircraft can obtain higher load factors and has reduced drag. This translates into faster turn rates and longer operational ranges. The unaugmented aircraft pitch angle-to-elevator deflection transfer function for the 0.9 Mach 20,000 feet condition is shown below. It should be noted that the short period roots of the aircraft are real, and

29
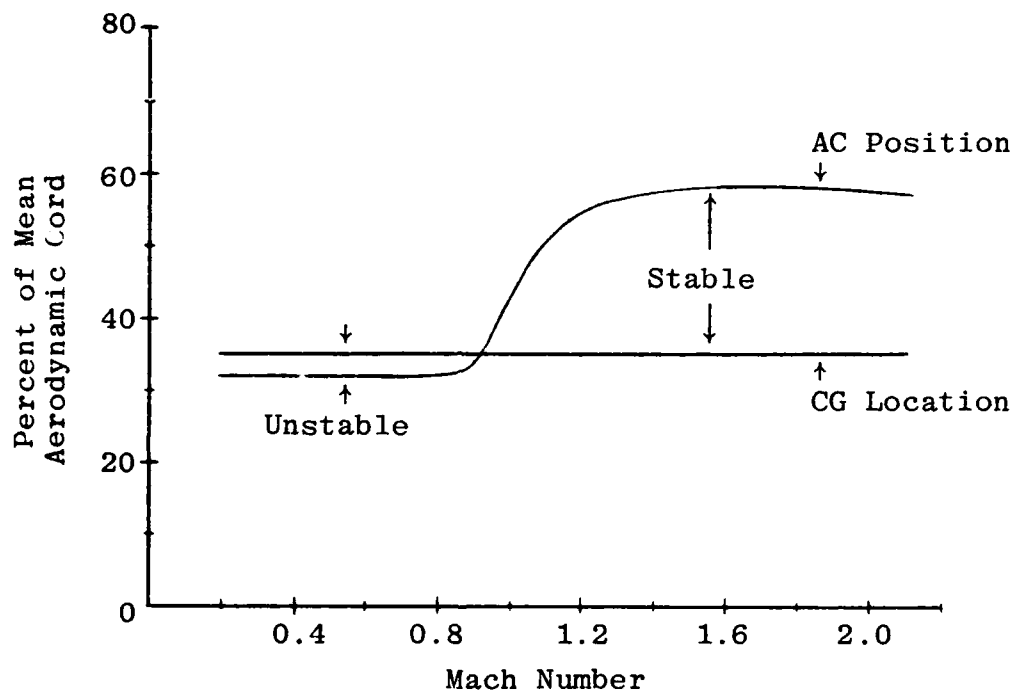
Figure 6.   Longitudinal Static Stability Plot

one is unstable. This is the manner in which static instability is manifested.

$$\frac{q}{\delta_e} = \frac{-24.06(s)(s+0.0126)(s+1.51)}{(s+0.00757\pm j0.0543)(s-0.964)(s+3.222)} \qquad (2.1)$$

Phugoid   Short Period

In the lateral-directional axis, the aircraft has very light dutch roll damping. This can be seen by examining the yaw rate-to-rudder deflection transfer function for the aircraft computed at the 0.9 Mach 20,000 feet point.

$$\frac{r}{\delta_r} = \frac{-5.81(s+0.323\pm j0.623)(s+2.482)}{(s+0.0272)(s+0.391\pm j2.961)(s+2.697)} \qquad (2.2)$$

Spiral   Dutch Roll   Roll

In its smallest sense, the control system design must provide longitudinal stability and improve dutch roll damping. In a larger sense, this is desired while providing an aircraft control system combination that is of most benefit to the pilot in performing specific tasks during a mission. The task considered in this study is air-to-air gunnery.

Aerodynamic Model

An extensive aerodynamic data package was developed by the General Dynamics Corporation of Fort Worth, Texas, for the AFTI/F-16 vehicle. The work was performed under contract to the AFTI/F-16 Advanced Development Program Office (ADPO) of the Flight Dynamics Laboratory. Wind

31

tunnel testing in both low and high speed tunnels provided data throughout the flight envelope for angle of attack ranges of 90 degrees to -40 degrees and large sideslip angles. F-16 wind tunnel data and flight test data were used as a baseline for the package.

A General Dynamics program was used to obtain linearized aerodynamic coefficients by trimming the aircraft at various flight conditions and load factors. Aircraft weight and inertias were also provided by the program. This data is listed in Table 1 for the major design point at 0.9 Mach and 20,000 feet. A complete set of data for all the points considered in the study is given in Appendix A. It should be noted that by convention, the static derivatives (C_{m_α} , C_{L_α} , etc.) are listed in units of per degree (1/deg). The dynamic derivatives, such as C_{L_q} , $C_{L_{\dot\alpha}}$, C_{n_p} , are listed in units of per radian (1/rad). Also by convention, the aerodynamic derivatives are presented in the stability axis while mass properties, such as moments and products of inertias, and the position of the sensors, are referenced to the body axis of the aircraft. Figure 7 provides a definition of the axis systems. The data must be converted to a consistent reference frame to permit analyses to be conducted.

For conditions where angle of attack is small, such as in trimmed straight and level flight, the differences between body and stability axes can usually be ignored. In

32

Table 1

Aircraft Data for the 0.9 Mach and 20,000 Feet
Flight Condition

Aircraft Parameters

$\bar{q}$ (dynamic pressure - lbs/ft^2) = 552.113

S (wing reference area - ft^2) = 300.0

c (wing mean aerodynamic cord - ft) = 11.32

b (wing span - ft) = 30.0

V_T (trim velocity - ft/sec) = 933.23

W (weight - lbs) = 21,018.0

Inertias: I_{xx} (slug - ft^2) = 10,033.4

I_{yy} (slug - ft^2) = 53,876.3

I_{zz} (slug - ft^2) = 61,278.5

I_{xz} (slug - ft^2) = 282.132

Aircraft Aerodynamic Coefficients in the Stability Axis

α(deg) = 1.86

C_L = 0.1262	C_m = 0.0	C_D = 0.02377
$C_{L_\alpha}(\frac{1}{deg})$ = 0.09481	$C_{m_\alpha}(\frac{1}{deg})$ = 0.001938	$C_{D_\alpha}(\frac{1}{deg})$ = 0.002636
$C_{L_{\delta_e}}(\frac{1}{deg})$ = 0.009578	$C_{m_{\delta_e}}(\frac{1}{deg})$ = -0.01209	$C_{D_{\delta_e}}(\frac{1}{deg})$ = 0.000173
$C_{L_{\delta_f}}(\frac{1}{deg})$ = 0.01572	$C_{m_{\delta_f}}(\frac{1}{deg})$ = -0.003280	$C_{D_{\delta_f}}(\frac{1}{deg})$ = 0.000351

33

Table 1 (continued)

$C_{L_q}(\frac{1}{\text{rad}})$ = 3.1617	$C_{m_q}(\frac{1}{\text{rad}})$ = -2.3822	
$C_{L_{\dot{\alpha}}}(\frac{1}{\text{rad}})$ = -1.3578	$C_{m_{\dot{\alpha}}}(\frac{1}{\text{rad}})$ = -1.3076	
$C_{L_u}(\frac{1}{\text{ft/sec}})$ = -0.000442	$C_{m_u}(\frac{1}{\text{ft/sec}})$ = -0.00006	$C_{D_u}(\frac{1}{\text{ft/sec}})$ = 0.00016
$C_{y_\beta}(\frac{1}{\text{deg}})$ = -0.02205	$C_{n_\beta}(\frac{1}{\text{deg}})$ = 0.001675	$C_{\ell_\beta}(\frac{1}{\text{deg}})$ = -0.001901
$C_{y_p}(\frac{1}{\text{rad}})$ = 0.05756	$C_{n_p}(\frac{1}{\text{rad}})$ = -0.005541	$C_{\ell_p}(\frac{1}{\text{rad}})$ = -0.3512
$C_{y_r}(\frac{1}{\text{rad}})$ = 0.5576	$C_{n_r}(\frac{1}{\text{rad}})$ = -0.2791	$C_{\ell_r}(\frac{1}{\text{rad}})$ = 0.02194
$C_{y_{\delta_r}}(\frac{1}{\text{deg}})$ = 0.002377	$C_{n_{\delta_r}}(\frac{1}{\text{deg}})$ = -0.001272	$C_{\ell_{\delta_r}}(\frac{1}{\text{deg}})$ = 0.000331
$C_{y_{\delta_a}}(\frac{1}{\text{deg}})$ = -0.000088	$C_{n_{\delta_a}}(\frac{1}{\text{deg}})$ = -0.00016	$C_{\ell_{\delta_a}}(\frac{1}{\text{deg}})$ = -0.001804
$C_{y_{\delta_{DT}}}(\frac{1}{\text{deg}})$ = -0.001708	$C_{n_{\delta_{DT}}}(\frac{1}{\text{deg}})$ = -0.000997	$C_{\ell_{\delta_{DT}}}(\frac{1}{\text{deg}})$ = -0.001816
$C_{y_{\delta_c}}(\frac{1}{\text{deg}})$ = 0.001716	$C_{n_{\delta_c}}(\frac{1}{\text{deg}})$ = 0.001256	$C_{\ell_{\delta_c}}(\frac{1}{\text{deg}})$ = 0.00023

Figure 7.   Axis Definition

stability analyses, it is often easier to convert a few
inertia terms into stability axis data than to convert all
of the aerodynamic derivatives into the body axis. Since
the characteristic equation and corresponding aircraft roots
are unaffected by this axis transformation, the determina-
tion of quantities such as short period damping can be made
in either axis system.

However, as is shown later, there are major draw-
backs to choosing the stability axis for design work. Con-
version of inertia data to the stability axis yields numbers
with no physical significance. In some cases, the converted
products of inertia are negative. Thus, valuable insight
into the mechanics of maneuvering flight needed by the design
engineer is lost.

In fighter aircraft, fast rolls about the body axis
at large angles of attack can result in unacceptably large
sideslip angles. The design problem is to use body-sensed
data in the flight control system to cause the aircraft to
roll about the velocity vector. In this way, alpha remains
essentially constant, and beta stays close to zero. If the
design is accomplished in the stability axis, which is
aligned with the velocity vector, rolling about the x axis
produces the desired results. The signal being fed back to
accomplish this is actually stability axis roll rate (a
quantity which is not usually available within the flight
control system). Thus, design in the stability axis can

36

lead to problems in implementation unless extreme care is taken. Designing in the body axis yields the same results but requires the engineer to explicitly attack the problem of obtaining an appropriate feedback signal. The signal must cause the proper rolling action with the available sensor information. As is shown later, this is usually accomplished by using body axis measurements of angle of attack, roll rate, yaw rate and side acceleration.

In this research, maneuvering flight characteristics are of primary interest. In elevated load factor or high "g" maneuvers, angle of attack can be a relatively large value, and the difference between body and stability axes becomes more significant. The body axis is chosen for this design for two main reasons in addition to those given in the previous discussions. First, the sensors providing feedback signals are actually measuring body accelerations and rates. Second, the pilot desires to control variables that he actually feels which are body accelerations and rates.

The transformation equations to convert to the body axis are based on data from Reference 20 and are given in Appendix B. The coefficients must also be dimensionalized for use in the equations of motion. These calculations are time-consuming and must be carried out for each flight condition being investigated. To aid in the conversion and transformation at a number of flight conditions, a computer

program called Conversion And Transformation (CAT) is developed to perform the necessary mathematical operations.

For the design effort, the equations of motion must be written as state equations in the form $\underline{\dot{x}} = \underline{A}\underline{x} + \underline{B}\underline{u}$. They represent a set of first-order differential equations. This operation is also carried out by the CAT program. The program's outputs are designated as primed derivatives. They are of the proper form to be directly inserted into the $\underline{A}$ matrix. The equations used in the conversion are presented in Appendix B. The computer listing is given in Appendix D.

The states in these equations do not include acceleration. Additional transformations are manually performed to obtain a state vector that includes accelerations at the pilot's station. The results of these transformations for the four flight conditions are listed in Appendix A. An example of the transformation method is shown below for the side velocity equation.

$$\dot{V} = \frac{\bar{q}S}{m}\left[C_{y_\beta}\beta + \{C_{y_{\dot{\beta}}}\dot{\beta} + C_{y_p}p + C_{y_r}r\}\frac{b}{2V_T} + C_{y_{\delta_a}}\delta_a \right.$$
$$\left. C_{y_{\delta_r}}\delta_r + C_{y_{\delta_c}}\delta_c\right] - rU + pW + g\cos\theta\sin\phi \quad (2.3)$$

or

$$\dot{V} = (Y_\beta)\beta + (Y_p)p + (Y_r)r + (Y_{\delta_a})\delta_a + (Y_{\delta_r})\delta_r$$
$$+ (Y_{\delta_c})\delta_c - rU + pW + g\cos\theta\sin\phi \quad (2.4)$$

Dividing by U and letting $\beta = V/U$, $\dot{\beta} = \dot{V}/U$, and $\alpha = W/U$ yields

$$\dot{\beta} = (\frac{Y_\beta}{U})\beta + (\frac{Y_p}{U})p + (\frac{Y_{\delta_a}}{U})\delta_a + (\frac{Y_{\delta_r}}{U})\delta_r + (\frac{Y_{\delta_c}}{U})\delta_c + (\frac{Y_r}{U})r$$

$$- r + p\alpha + \frac{g}{U}\cos\theta\sin\phi \qquad (2.5)$$

Also, let $\sin\phi = \phi$ in radians and $\alpha = 0.0$, which gives

$$\dot{\beta} = (\frac{Y_\beta}{U})\beta + (\frac{Y_p}{U})p + (\frac{Y_r}{U} - 1)r + (\frac{Y_{\delta_a}}{U})\delta_a$$

$$+ (\frac{Y_{\delta_r}}{U})\delta_r + (\frac{Y_{\delta_c}}{U})\delta_c + (g\frac{\cos\theta}{U})\phi \qquad (2.6)$$

Redefining the coefficients yields

$$\dot{\beta} = (Y_\beta{}')\beta + (Y_p{}')p + (Y_r{}')r + (Y_{\delta_a}{}')\delta_a$$

$$+ (Y_{\delta_r}{}')\delta_r + (Y_{\delta_c}{}')\delta_c + (Y_\phi{}')\phi \qquad (2.7)$$

These equations are simplified, and the restrictions discussed in Chapter I are applied. The resulting states represented by the simplified equations are pitch angle, theta, forward velocity, angle of attack, and pitch rate in the longitudinal axis and roll angle, sideslip angle, roll rate, and yaw rate in the lateral-directional axes. In applying the restrictions, it is assumed that coupling between longitudinal, and lateral-directional axes can be neglected. Although this is not entirely correct for a high-performance fighter, the assumption is still generally applied in preliminary design efforts in order to simplify the problem. Exceptions are taken when necessary. Once a

preliminary design is complete, it is evaluated in a simulation with full nonlinear coupled equations of motion. Unfortunately, such an evaluation is beyond the scope of this research effort.

Acceleration at the pilot station is not one of the resulting states in the equations available for feedback design. Since this is a function which must be commanded, the solution to this dilemma is found by using the following relationships. The longitudinal force equation in the z body direction can be written as

$$F_{z_{cg}} = m(\dot{W} + pV - qU - g\cos\theta\cos\phi) \qquad (2.8)$$

thus

$$A_{z_{cg}} = \frac{F_{z_{cg}}}{m} = \dot{W} + pV - qU - g\cos\theta\cos\phi \qquad (2.9)$$

This is longitudinal acceleration in the z direction at the center of gravity. From Appendix B

$$\dot{W} = (Z_\alpha)\alpha + (Z_{\dot{\alpha}})\dot{\alpha} + (Z_q)q + (Z_u)\Delta U + (Z_{\delta_e})\delta_e$$
$$+ (Z_{\delta_f})\delta_f - pV + qU + g\sin\theta\cos\phi \qquad (2.10)$$

Letting $\alpha = W/U$ and $\dot{\alpha} = \dot{W}/U$, this becomes

$$\dot{\alpha} = [\frac{1}{U}] [(Z_\alpha)\alpha + (Z_{\dot{\alpha}})\dot{\alpha} + (Z_q)q + (Z_u)\Delta U + (Z_{\delta_e})\delta_e$$
$$+ (Z_{\delta_f})\delta_f - pV + qU + g\sin\theta\cos\phi] \qquad (2.11)$$

40

Gathering the terms with $\dot{\alpha}$ on the left-hand side of the equation yields

$$\dot{\alpha}(1 - \frac{Z_{\dot{\alpha}}}{U}) = \frac{1}{U} \, [(Z_{\alpha})\alpha + (Z_q)q + (Z_u)\Delta U + (Z_{\delta_e})\delta_e$$

$$+ (Z_{\delta_f})\delta_f - pV + qU + g\sin\theta\cos\phi] \qquad (2.12)$$

Note: $\frac{Z_{\dot{\alpha}}}{U}$ is extremely small and is neglected.

From Equation (2.9)

$$A_{z_{cg}} = U(\dot{\alpha} + p\frac{V}{U} - q\frac{U}{U} - \frac{g}{U}\cos\theta\cos\phi) \qquad (2.13)$$

and using Equation (2.12), gives

$$A_{z_{cg}} = U\{(\frac{1}{U})[(Z_{\alpha}\alpha + Z_q q + Z_u\Delta U + Z_{\delta e}\delta e + Z_{\delta f}\delta f - pV$$

$$+ qU + g\sin\theta\cos\phi)] + \frac{pV}{U} - \frac{qU}{U} - \frac{g}{U}\cos\theta\cos\phi\} \qquad (2.14)$$

Simplification by cancelling terms yields

$$A_{z_{cg}} = (Z_{\alpha})\alpha + (Z_q)q + (Z_u)u + (Z_{\delta e})\delta e + (Z_{\delta f})\delta f \qquad (2.15)$$

Acceleration at the center of gravity can be expressed as a combination of the available states previously defined plus contributions from the control surfaces. At this point, two methods of expressing acceleration in state space format are apparent.

41

The easiest and least complex method is to use the previously developed $\underline{\dot{x}} = \underline{A}\underline{x} + \underline{B}\underline{u}$ equations and form an output equation $\underline{y} = \underline{C}\underline{x} + \underline{D}\underline{u}$ where the output being sought is acceleration. The contributions from the control surfaces are included in the $\underline{D}$ matrix. The state space model has the form

$$
\begin{bmatrix} \dot{\theta} \\ \dot{u} \\ \dot{\alpha} \\ \dot{q} \end{bmatrix} = \begin{bmatrix} 0 & 0 & 0 & 1 \\ X_\theta{}' & X_u{}' & X_\alpha{}' & X_q{}' \\ Z_\theta{}' & Z_u{}' & Z_\alpha{}' & Z_q{}' \\ M_\theta{}' & M_u{}' & M_\alpha{}' & M_q{}' \end{bmatrix} \begin{bmatrix} \theta \\ u \\ \alpha \\ q \end{bmatrix} + \begin{bmatrix} 0 & 0 \\ X_{\delta e}{}' & X_{\delta f}{}' \\ Z_{\delta e}{}' & Z_{\delta f}{}' \\ M_{\delta e}{}' & M_{\delta f}{}' \end{bmatrix} \begin{bmatrix} \delta e \\ \delta f \end{bmatrix}
\qquad (2.16)
$$

$$
\begin{bmatrix} A_{z_{cg}} \\ q \end{bmatrix} = \begin{bmatrix} 0 & Z_u & Z_\alpha & Z_q \\ 0 & 0 & 0 & 1 \end{bmatrix} \begin{bmatrix} \theta \\ u \\ \alpha \\ q \end{bmatrix} + \begin{bmatrix} Z_{\delta e} & Z_{\delta f} \\ 0 & 0 \end{bmatrix} \begin{bmatrix} \delta e \\ \delta f \end{bmatrix}
\qquad (2.17)
$$

Unfortunately, the design method used in this report does not consider a $\underline{D}$ matrix. The problem is, therefore, to develop the equations of motion with a zero $\underline{D}$ matrix but with the contributions from the control surfaces included. The method used in this design effort is to augment the $\underline{A}$ matrix with the actuator states. In this manner an augmented state vector is produced which includes surface deflection as shown below. Using a first-order actuator transfer function model of $[20/(s+20)]$ for both the elevator and

42

flaperon surfaces results in the following equations.

$$\delta e = [\frac{20}{s + 20}] \ \delta e_{cmd} \tag{2.18}$$

$$\delta e(s + 20) = 20 \ \delta e_{cmd} \tag{2.19}$$

$$\delta \dot{e} + 20 \ \delta e = 20 \ \delta e_{cmd} \tag{2.20}$$

$$\delta \dot{e} = -20 \ \delta e + 20 \ \delta e_{cmd} \tag{2.21}$$

In a similar computation, the flaperon actuator model results in a first-order equation of $\delta \dot{f} = -20 \ \delta f + 20 \ \delta f_{cmd}$. The input vector $\underline{u}$ is now the actuator command instead of surface position as shown previously. The state and output equations are

$$
\begin{bmatrix} \dot{\theta} \\ \dot{u} \\ \dot{\alpha} \\ \dot{q} \\ \delta \dot{e} \\ \delta \dot{f} \end{bmatrix} =
\begin{bmatrix}
0 & 0 & 0 & 1 & 0 & 0 \\
X_\theta{}' & X_u{}' & X_\alpha{}' & X_q{}' & X_{\delta e}{}' & X_{\delta f}{}' \\
Z_\theta{}' & Z_u{}' & Z_\alpha{}' & Z_q{}' & Z_{\delta e}{}' & Z_{\delta f}{}' \\
M_\theta{}' & M_u{}' & M_\alpha{}' & M_q{}' & M_{\delta e}{}' & M_{\delta f}{}' \\
0 & 0 & 0 & 0 & -20 & 0 \\
0 & 0 & 0 & 0 & 0 & -20
\end{bmatrix}
\begin{bmatrix} \theta \\ u \\ \alpha \\ q \\ \delta e \\ \delta f \end{bmatrix} +
\begin{bmatrix} 0 & 0 \\ 0 & 0 \\ 0 & 0 \\ 0 & 0 \\ 20 & 0 \\ 0 & 20 \end{bmatrix}
\begin{bmatrix} \delta e_{cmd} \\ \delta f_{cmd} \end{bmatrix}
\tag{2.22}
$$

$$
\begin{bmatrix} A_{z_{cg}} \\ q \end{bmatrix} =
\begin{bmatrix}
0 & Z_u & Z_\alpha & Z_q & Z_{\delta e} & Z_{\delta f} \\
0 & 0 & 0 & 1 & 0 & 0
\end{bmatrix}
[\theta \ \ u \ \ \alpha \ \ q \ \ \delta e \ \ \delta f]^T
\tag{2.23}
$$

43

In this case, $A_{z_{cg}}$ can be controlled as an output of the system without having a $\underline{D}$ matrix. Unfortunately, to develop the output requires a combination of all but one longitudinal state. At this point a transformation is employed to provide $A_{z_{cg}}$ as a state in place of angle of attack. As shown earlier,

$$A_{z_{cg}} = Z_\alpha \alpha + Z_q q + Z_u u + Z_{\delta e}\delta e + Z_{\delta f}\delta f \qquad (2.15)$$

thus

$$\begin{bmatrix} \theta \\ u \\ A_{z_{cg}} \\ q \\ \delta e \\ \delta f \end{bmatrix} = \begin{bmatrix} 1 & 0 & 0 & 0 & 0 & 0 \\ 0 & 1 & 0 & 0 & 0 & 0 \\ 0 & Z_u & Z_\alpha & Z_q & Z_{\delta e} & Z_{\delta f} \\ 0 & 0 & 0 & 1 & 0 & 0 \\ 0 & 0 & 0 & 0 & 1 & 0 \\ 0 & 0 & 0 & 0 & 0 & 1 \end{bmatrix} \begin{bmatrix} \theta \\ u \\ \alpha \\ q \\ \delta e \\ \delta f \end{bmatrix} \qquad (2.24)$$

$$\underline{z} \qquad\qquad\qquad \underline{T} \qquad\qquad\qquad \underline{x}$$

$\underline{z} = \underline{T}\underline{x}$ where $\underline{T}$ is a transformation matrix to develop a $\underline{z}$ state vector containing $A_{z_{cg}}$ from the original state vector $\underline{x}$. The complete set of equations is transformed using $\underline{x} = \underline{T}^{-1}\underline{z}$. Thus

$$\underline{\dot{x}} = \underline{A}\underline{x} + \underline{B}\underline{u} \qquad (2.25)$$

$$\underline{T}^{-1}\underline{\dot{z}} = \underline{A}\underline{T}^{-1}\underline{z} + \underline{B}\underline{u} \qquad (2.26)$$

$$\underline{\dot{z}} = \underline{T}\underline{A}\underline{T}^{-1}\underline{z} + \underline{T}\underline{B}\underline{u} \qquad (2.27)$$

44

and
$$\underline{y} = \underline{C}\underline{x} \qquad (2.28)$$

$$\underline{y} = \underline{C}\underline{T}^{-1}\underline{z} \qquad (2.29)$$

The output equation is actually not needed. It gives the relationship for expressing the old states as a linearized combination of the new states. Since interest is in the acceleration as an output and a state, a new $\underline{C}$ matrix is formed to allow using $A_{z_{cg}}$ as a feedback.

Acceleration at another point on the aircraft other than the center of gravity can be computed as follows:

Note:
$$A_n = -A_z \qquad (2.30)$$

$$A_n = A_{n_{cg}} - (\ell_x)(pr - \dot{q}) - (\ell_y)(rq + \dot{p})$$
$$+ (\ell_z)(p^2 + q^2) \qquad (2.31)$$

where ℓ_x, ℓ_y, and ℓ_z are distances in the body axis from the point to the center of gravity.

Since ℓ_y and ℓ_z are much smaller than ℓ_x for the AFTI vehicle and since the assumption is made that the longitudinal and lateral-directional axes can be decoupled, the equation reduces to

$$A_n = A_{n_{cg}} + (\ell_x)\dot{q} \qquad (2.32)$$

The units are ft/sec^2 for acceleration, feet for the ℓ_x distance, and rad/sec for the rotational acceleration term ($\dot{q}$). In a similar manner, the lateral acceleration at a point

other than the center of gravity is computed as

$$A_y = A_{y_{cg}} - (\ell_x)(pq - \dot{r}) - (\ell_y)(p^2 + r^2)$$

$$+ (\ell_z)(qr - \dot{p}) \qquad (2.33)$$

which, using the same assumptions, becomes

$$A_y = A_{y_{cg}} + (\ell_x) \dot{r} \qquad (2.34)$$

Equations (2.32) and (2.34) are used to develop relation-ships for acceleration at the pilot's station in the air-craft. Since acceleration at the center of gravity is now a state and the equations developed from the last transfor-mation give $\dot{q}$ as a summation of the new state vector $\underline{z}$, a final transformation can be made to obtain accelerations at the pilot's station for the z and y axes.

An example of the transformations at the design points of 0.9 Mach and 20,000 feet is presented below for the longitudinal axis. The complete transformations for this point are given in Appendix B. For the other flight conditions, only the final resulting state equations are listed in the appendix in the interest of brevity. The same transformation method is used in each case.

Using the primed aerodynamic coefficients from the CAT program, the following state equation is developed.

46

$$
\begin{bmatrix} \dot{\theta} \\ \dot{u} \\ \dot{\alpha} \\ \dot{q} \\ \dot{\delta e} \\ \dot{\delta f} \end{bmatrix} =
\begin{bmatrix}
0 & 0 & 0 & 1 & 0 & 0 \\
-32.1831 & -0.0120748 & 38.2418 & -30.135 & 2.001 & 2.3087 \\
-0.0011187 & -0.000022 & -1.4845 & 0.994789 & -0.149227 & -0.244924 \\
0.0003086 & -0.00013 & 4.27172 & -0.777221 & -24.0581 & -6.47269 \\
0 & 0 & 0 & 0 & -20 & 0 \\
0 & 0 & 0 & 0 & 0 & -20
\end{bmatrix}
\begin{bmatrix} \theta \\ u \\ \alpha \\ q \\ \delta e \\ \delta f \end{bmatrix} +
\begin{bmatrix} 0 & 0 \\ 0 & 0 \\ 0 & 0 \\ 0 & 0 \\ 20 & 0 \\ 0 & 20 \end{bmatrix}
\begin{bmatrix} \delta e_{cmd} \\ \delta f_{cmd} \end{bmatrix}
$$

(2.35)

From the unprimed dimensional coefficients, the $\underline{T}_1$ matrix is formed.

$$
\underline{T}_1 =
\begin{bmatrix}
1 & 0 & 0 & 0. & 0 & 0 \\
0 & 1 & 0 & 0 & 0 & 0 \\
0 & -0.0207687 & -1385.34 & -4.86336 & -139.263 & -228.57 \\
0 & 0 & 0 & 1 & 0 & 0 \\
0 & 0 & 0 & 0 & 1 & 0 \\
0 & 0 & 0 & 0 & 0 & 1
\end{bmatrix}
$$

(2.36)

Performing the transformation yields the following state equations.

$$
\begin{bmatrix} \dot{\theta} \\ \dot{u} \\ \dot{A}_{z_{cg}} \\ \dot{q} \\ \dot{\delta e} \\ \dot{\delta f} \end{bmatrix} =
\begin{bmatrix}
0 & 0 & 0 & 1 & 0 & 0 \\
-32.18 & -0.01265 & -0.02760 & -30.27 & -1.843 & -4.0 \\
2.311 & 0.001208 & -1.469 & -1381 & 2904 & 4606 \\
0.000309 & -0.000194 & -0.003084 & -0.7922 & -24.49 & -7.177 \\
0 & 0 & 0 & 0 & -20 & 0 \\
0 & 0 & 0 & 0 & 0 & -20
\end{bmatrix}
\begin{bmatrix} \theta \\ U \\ A_{z_{cg}} \\ q \\ \delta e \\ \delta f \end{bmatrix} +
\begin{bmatrix} 0 & 0 \\ 0 & 0 \\ -2785 & -4571 \\ 0 & 0 \\ 20 & 0 \\ 0 & 20 \end{bmatrix}
\begin{bmatrix} \delta e_{cmd} \\ \delta f_{cmd} \end{bmatrix}
$$

(2.37)

47

Using the $\dot{q}$ expression from this state matrix in Eq. (2.32) results in the expression for acceleration at the pilot's station.

$$A_{n_p} = A_{n_{cg}} + [\ell x] \begin{bmatrix} 0.000309 & -0.000194 & 0.003084 & -0.7922 & -24.49 & -7.177 \end{bmatrix} \begin{bmatrix} \theta \\ u \\ A_{n}-g \\ q \\ \delta e \\ \delta f \end{bmatrix}$$

(2.38)

where $\quad \ell_x = 13.95$ ft $\qquad\qquad$ (2.39)

With Eq. (2.9), an expression can be developed for $\dot{\alpha}$ using the states available after the last transformation. Assuming $pV = 0$ and $\phi = 0$ results in

$$A_{z_{cg}} = \dot{W} - qU - g\cos\theta \qquad (2.40)$$

Dividing by forward velocity, U, and letting $\alpha = \frac{W}{U}$ gives

$$\frac{A_{z_{cg}}}{U} = \dot{\alpha} - q - \frac{g}{U}\cos\theta \qquad (2.41)$$

Solving for $\dot{\alpha}$ yields

$$\dot{\alpha} = \frac{A_{z_{cg}} + g\cos\theta}{U} + q \qquad (2.42)$$

Expressed using incremental acceleration from 1g trimmed flight, the equation becomes

$$\dot{\alpha} = \frac{A_{z_{cg}}}{U} + q \qquad (2.43)$$

The $\dot{\alpha}$ equation is added to the state equations, and a second transformation matrix T_2 is formed from Eq. (2.38).

48

Thus,

$$
\begin{bmatrix} \dot{\alpha} \\ \dot{\theta} \\ \dot{u} \\ \dot{A}_{z_{cg}} \\ \dot{q} \\ \dot{\delta e} \\ \dot{\delta f} \end{bmatrix} = \begin{bmatrix} 0 & 0 & 0 & 0.001072 & 1 & 0 & 0 \\ 0 & 0 & 0 & 0 & 1 & 0 & 0 \\ 0 & -32.18 & -0.01265 & -0.0276 & -30.27 & -1.843 & -4.0 \\ 0 & 2.311 & 0.001208 & -1.469 & -1387 & 2904 & 4606 \\ 0 & 0.000309 & -0.000194 & -0.003084 & -0.7922 & -24.49 & -7.177 \\ 0 & 0 & 0 & 0 & 0 & -20 & 0 \\ 0 & 0 & 0 & 0 & 0 & 0 & -20 \end{bmatrix} \begin{bmatrix} \alpha \\ \theta \\ u \\ A_{z_{cg}} \\ q \\ \delta e \\ \delta f \end{bmatrix} + \begin{bmatrix} 0 & 0 \\ 0 & 0 \\ 0 & 0 \\ -2785 & -4571 \\ 0 & 0 \\ 20 & 0 \\ 0 & 20 \end{bmatrix} \begin{bmatrix} \delta e_{cmd} \\ \delta f_{cmd} \end{bmatrix}
$$

(2.44)

and

$$
T_2 = \begin{bmatrix} 1 & 0 & 0 & 0 & 0 & 0 & 0 \\ 0 & 1 & 0 & 0 & 0 & 0 & 0 \\ 0 & 0 & 1 & 0 & 0 & 0 & 0 \\ 0 & 0.00043 & -0.000271 & 1.043 & -1.105 & -341.64 & -100.12 \\ 0 & 0 & 0 & 0 & 1 & 0 & 0 \\ 0 & 0 & 0 & 0 & 0 & 1 & 0 \\ 0 & 0 & 0 & 0 & 0 & 0 & 1 \end{bmatrix}
$$

(2.45)

The transformation results in

$$
\begin{bmatrix} \dot{\alpha} \\ \dot{\theta} \\ \dot{u} \\ \dot{A}_{z_p} \\ \dot{q} \\ \dot{\delta e} \\ \dot{\delta f} \end{bmatrix} = \begin{bmatrix} 0 & 0 & 0 & 0.001027 & 1.001 & 0.3510 & 0.1029 \\ 0 & 0 & 0 & 0 & 1 & 0 & 0 \\ 0 & -32.18 & -0.01266 & -0.02646 & -30.3 & -10.88 & -6.649 \\ 0 & 2.419 & 0.001801 & -1.466 & -1447 & 9388 & 6668 \\ 0 & 0.00031 & -0.000195 & -0.002957 & -.7955 & -25.5 & -7.473 \\ 0 & 0 & 0 & 0 & 0 & -20 & 0 \\ 0 & 0 & 0 & 0 & 0 & 0 & -20 \end{bmatrix} \begin{bmatrix} \alpha \\ \theta \\ u \\ A_{z_p} \\ q \\ \delta e \\ \delta f \end{bmatrix} + \begin{bmatrix} 0 & 0 \\ 0 & 0 \\ 0 & 0 \\ -9738 & -6770 \\ 0 & 0 \\ 20 & 0 \\ 0 & 20 \end{bmatrix} \begin{bmatrix} \delta e_{cmd} \\ \delta f_{cmd} \end{bmatrix}
$$

(2.46)

49

and the output equation is:

$$
\begin{bmatrix} A_{z_p} \\ q \end{bmatrix} = \begin{bmatrix} 0 & 0 & 0 & 1 & 0 & 0 & 0 \\ 0 & 0 & 0 & 0 & 1 & 0 & 0 \end{bmatrix} = [\alpha \ \ \theta \ \ u \ \ A_{z_p} \ \ q \ \ \delta e \ \ \delta f]^T
$$

(2.47)

The transformation to acceleration at the aircraft center of gravity is performed as an intermediate step at which point the $\dot{\alpha}$ equation is added. The same results are obtained by writing the $\dot{\alpha}$ equation twice in the original system equations and forming a combined transformation matrix to directly obtain acceleration at the pilot's station from Eqs. (2.15) and (2.32) as follows:

$$
A_{n_p} = A_{n_{cg}} + \ell_x(\dot{q})
$$

(2.48)

and

$$
A_{n_{cg}} = -A_{z_{cg}} = -Z_\alpha \alpha - Z_q q - Z_u u - Z_{\delta e}\delta e - Z_{\delta f}\delta f
$$

(2.49)

Both $A_{n_{cg}}$ and $\dot{q}$ are expressed as combinations of the original state variables and can be combined to yield:

$$
\begin{aligned}
A_{n_p} = (\ell_x M_\theta{}')\theta + (\ell_x M_u{}' - Z_u)\Delta U + (\ell_x M_\alpha{}' - Z_\alpha)\alpha \\
+ (\ell_x M_q{}' - Z_q)q + (\ell_x M_{\delta e}{}' - Z_{\delta e})\delta e \\
+ (\ell_x M_{\delta f}{}' - Z_{\delta f})\delta f
\end{aligned}
$$

(2.50)

Thus,

$$
\begin{bmatrix} \alpha \\ \theta \\ u \\ A_{n_p} \\ q \\ \delta e \\ \delta f \end{bmatrix} = \begin{bmatrix} 1 & 0 & 0 & 0 & 0 & 0 & 0 \\ 0 & 1 & 0 & 0 & 0 & 0 & 0 \\ 0 & 0 & 1 & 0 & 0 & 0 & 0 \\ 0 & (\ell_x M_\theta{'}) & (\ell_x M_u{'} - Z_u) & (\ell_x M_\alpha{'} - Z_\alpha) & (\ell_x M_q{'} - Z_q) & (\ell_x M_{\delta e}{'} - Z_{\delta e}) & (\ell_x M_{\delta f}{'} - Z_{\delta f}) \\ 0 & 0 & 0 & 0 & 1 & 0 & 0 \\ 0 & 0 & 0 & 0 & 0 & 1 & 0 \\ 0 & 0 & 0 & 0 & 0 & 0 & 1 \end{bmatrix} \begin{bmatrix} \alpha \\ \theta \\ u \\ \alpha \\ q \\ \delta e \\ \delta f \end{bmatrix}
$$

$$(2.51)$$

This method is used on all subsequent transformations to develop pilot station acceleration as a state. In either method of arriving at this final state vector, the addition of the $\dot{\alpha}$ equation results in a transmission zero at the origin. The significance of transmission zeros is discussed in Chapter III. This does not affect the designs that are developed. They are evaluated with and without the $\dot{\alpha}$ equation. Transfer function checks show that with the inclusion of the $\dot{\alpha}$ equation both a pole and a zero are added to the system at the origin. This pole-zero combination cancels and contributes nothing to the output responses.

The equations are modified to have states, inputs and outputs in convenient units such as "g" for accelerations and degrees for surface deflections. In the resulting system equations, the B matrix is partitioned as shown below.

$$
\underline{B} \;=\; \begin{bmatrix} 0 & 0 \\ 0 & 0 \\ 0 & 0 \\ -9738 & -6770 \\ 0 & 0 \\ \text{-}\ \text{-}\ \text{-}\ \text{-}\ \text{-}\ \text{-} \\ 20 & 0 \\ 0 & 20 \end{bmatrix} \;=\; \begin{bmatrix} \underline{B}_1 \\ \\ \text{-}\ \text{-}\ \text{-} \\ \underline{B}_2 \end{bmatrix} \qquad (2.52)
$$

The row dimension of $\underline{B}_2$ is equal to the number of inputs or, in this case, surface commands. Thus, it is always a square matrix. For the design work, the system is transformed once more so that $\underline{B}_1$ is a zero matrix. Such an arrangement is hereafter referred to as the zero-B_2 form. Although not necessary for application of the design principles, this conversion is accomplished for the following reasons.

First, a knowledge of the location of transmission zeros of the system is desired. A relatively simple and reliable means of calculating transmission zeros is available for systems in the zero-B_2 form (Ref 6). The method of computation of transmission zeros is discussed in Chapter III. This method is computerized using macro programming of the TOTAL program. A listing of the macro program is included in Appendix E.

The second reason is based on a previous unfortunate implementation of the design equations in the MULTI program which has been corrected at the time of this report. The problem is discussed in Chapter IV after the design

equations are presented in Chapter III. With the original
MULTI program, the design obtained without this last trans-
formation results in a system that is not adequately
decoupled to meet the design objectives.

A note of caution is necessary at this point. Trans-
formation to the zero-B_2 form results in a new set of states.
Unfortunately, pilot station acceleration is altered by the
transformation. Since this is one of the states to be used
for feedback, the design implementation is unduly complicated.
With the modified MULTI program, the same design results can
be obtained without transformation to this form. It is
advantageous to design with A_{n_p} and A_{y_p} as states and to
transform the final design only to check for transmission
zeros which are not altered by such transformations.

Validation Methods

One major concern in the development of the linear
models for multivariable designs is the complexity of per-
forming multiple conversions and transformations. Each
operation can become a source of errors. Validation of the
final model as a true representation of the aircraft becomes
a paramount issue. Such validation is handled in the follow-
ing manner.

The linearized aerodynamic data obtained from General
Dynamics are checked for reasonableness of coefficient
values. Any discrepancies are checked with the nonlinear

data plots available in the AFTI/F-16 ADPO. All discrepancies are resolved with the help of ADPO engineers.

The linearized data is used as input for the Transfer Function Program (TRANSF). This is an ADPO program that is available at AFIT. The program allows direct input of the data and provides stability axis transfer functions for each aircraft state to surface input. These are open-loop or unaugmented aircraft transfer functions. The results are compared with known aircraft data developed by General Dynamics such as longitudinal static stability and dutch roll damping at each flight condition.

Since linear transformations do not change a system's characteristic equation, this provides a general test of each transformation in the development of the desired state-space model. In addition, the transformations are hand calculated for one case and used to check each computer operation. The actual sequence consists of using the CAT program to go from nondimensional coefficients to dimensional body axis "primed" derivatives for the $\underline{A}$ matrix. The system states available at this point are shown below.

$$\underline{x}(\text{Long.}) = \begin{bmatrix} \theta \\ u \\ \alpha \\ q \end{bmatrix} \quad \text{and} \quad \underline{x}(\text{Lat.-Dir.}) = \begin{bmatrix} \phi \\ \beta \\ p \\ r \end{bmatrix} \quad (2.53)$$

The **A** matrix is then augmented to include the actuator states assuming a first-order actuator. The state vectors are now

$$
\underline{x}(\text{Long.}) = \begin{bmatrix} \theta \\ u \\ \alpha \\ q \\ \delta e \\ \delta f \end{bmatrix} \qquad \underline{x}(\text{Lat.-Dir.}) = \begin{bmatrix} \phi \\ \beta \\ p \\ r \\ \delta a \\ \delta r \\ \delta c \end{bmatrix} \qquad (2.54)
$$

This system is then transformed to include accelerations at the center of gravity as previously discussed and finally transformed to acceleration at the pilot's station. The last transformations have replaced angle of attack and sideslip with longitudinal and side acceleration. Both angle of attack and sideslip are important parameters to monitor in maneuvering flight. To allow this, two new equations are added that express alpha and beta as a combination of the existing states. The final resulting state vectors are shown below.

$$\underline{x}(\text{Long.}) = \begin{bmatrix} \alpha \\ \theta \\ U \\ A_{n_p} \\ q \\ \delta e \\ \delta f \end{bmatrix} \qquad \underline{x}(\text{Lat.-Dir.}) = \begin{bmatrix} \beta \\ \phi \\ A_{y_p} \\ p \\ r \\ \delta a \\ \delta r \\ \delta c \end{bmatrix} \qquad (2.55)$$

The TOTAL program is employed to perform the above trans-
formations. System transfer functions are checked after
every transformation. The transformations can be combined
to simplify the effort. This is also done for each of the
other flight conditions. Finally, prior to design, the
state model is altered to provide the states, inputs, and
outputs in convenient units. Accelerations are expressed
in "g" units; rates are given in degrees per second; angles
and surface deflections are in degrees; and velocities have
units of feet per second. Transformation to zero-B_2 form
is accomplished and results in the following set of states.

$$\underline{x}(\text{Long.}) = \begin{bmatrix} \alpha \\ \theta \\ U \\ A_{n_p} + K_1 \delta e + K_2 \delta f \\ q \\ \delta e \\ \delta f \end{bmatrix} \qquad (2.56)$$

$$\underline{x}(\text{Lat.-Dir.}) = \begin{bmatrix} \beta \\ \phi \\ A_{y_p} + K_1 \delta a + K_2 \delta r + K_3 \delta r \\ p \\ r \\ \delta a \\ \delta r \\ \delta c \end{bmatrix} \qquad (2.57)$$

III. Multivariable Control Law Theory

Overview

The designs in this thesis are the result of the application of control law methods developed by Professor Brian Porter of the University of Salford, England. The techniques are presented in Reference 6. This chapter provides a summary of the techniques used in the design of high performance tracking systems for aircraft control. It also includes a discussion of important facets in their application. The theoretical discussions cover the discrete case and the corresponding continuous design equations. This approach is taken because, although the designs are for a digital implementation, the insight and experience with continuous design principles can be used effectively. The methods are essentially identical for continuous and discrete designs. It is often more meaningful to consider the s-plane root locations and migrations as opposed to z-plane analysis. For those cases where the continuous methods are employed, it should be kept in mind that sampling effects and discrete time delay must be examined prior to design acceptance.

The plant to be controlled is described by first-order linear differential equations written in state-space format:

$$\underline{\dot{x}} = \underline{A}\underline{x} + \underline{B}\underline{u} \qquad (3.1)$$

$$\underline{y} = \underline{C}\underline{x} \qquad (3.2)$$

where

      A = the continuous-time plant matrix (n x n)

      B = the continuous-time control matrix (n x m)

      C = the continuous-time output matrix (p x n)

The dimensions are defined as n being the number of states, m the number of inputs, and p the number of outputs.

The $\underline{A}$, $\underline{B}$ and $\underline{C}$ matrices are partitioned to yield the following equations:

$$\begin{bmatrix} \underline{\dot{x}}_1 \\ \hline \underline{\dot{x}}_2 \end{bmatrix} = \begin{bmatrix} \underline{A}_{11} & \underline{A}_{12} \\ \hline \underline{A}_{21} & \underline{A}_{22} \end{bmatrix} \begin{bmatrix} \underline{x}_1 \\ \underline{x}_2 \end{bmatrix} + \begin{bmatrix} \underline{B}_1 \\ \underline{B}_2 \end{bmatrix} \underline{u} \qquad (3.3)$$

$$\underline{y} = \begin{bmatrix} \underline{C}_1 & \underline{C}_2 \end{bmatrix} \begin{bmatrix} \underline{x}_1 \\ \underline{x}_2 \end{bmatrix} \qquad (3.4)$$

$\underline{B}_2$ is a square matrix with a row and column size equal to the number of inputs in the vector $\underline{u}$. $\underline{C}_2$ is also square with the number of rows and columns equal to the number of outputs. The designation of "inputs" for the aircraft model usually refers to the control surfaces, such as the elevator or rudder, available to command changes in the aircraft states. However, in designs where the $\underline{A}$ matrix is augmented with surface actuator states, "inputs" denote the

surface actuator input commands. Outputs are states or combinations of states of the aircraft such as angle of attack or pitch rate.

A requirement of the design method is that the number of inputs must equal the number of outputs, thus $\underline{B}_2$ and $\underline{C}_2$ have the same row and column dimensions. $\underline{A}_{22}$ also has the same dimensions. Knowing these dimensions allows the system matrices to be easily partitioned as shown above.

Two design methods are applicable to the aircraft under study using the regular and irregular designs. The design method used is determined by the type of plant being considered.

Regular Versus Irregular Design

To be considered as a "regular" plant, the matrix representing the first Markov parameter, $[\underline{CB}]$, must have rank equal to the number of outputs. Since $\underline{C}$ is of order $(p \times n)$, and $\underline{B}$ is of order $(n \times m)$ with $p=m$, $[\underline{CB}]$ is a square matrix and must have full rank to fulfill the requirement of a regular plant. The gain matrix for feedback control is formed using the inverse of $[\underline{CB}]$. This cannot be accomplished without full rank.

Plants in which the first Markov parameter, $[\underline{CB}]$, is rank deficient are designated as "irregular." To allow the design to be accomplished, an $\underline{F}$ matrix is formed as shown and used in place of the $\underline{C}$ matrix:

60

$$\underline{F} = [\ \underline{F}_1 \ \vdots \ \underline{F}_2 \ ] \qquad (3.5)$$

where

$$\underline{F}_1 = [\ \underline{C}_1 + \underline{MA}_{11} \ ] \qquad (3.6)$$

$$\underline{F}_2 = [\ \underline{C}_2 + \underline{MA}_{12} \ ] \qquad (3.7)$$

The elements of the measurements matrix $\underline{M}$ are selected to obtain a matrix $[\underline{FB}]$ having full rank and thus being invertable.

The control law is a proportional plus integral output feedback law expressed as:

$$\underline{u}(kT) = (1/T)[\underline{K}_0 \underline{e}(kT) + \underline{K}_1 \underline{z}(kT)] \qquad (3.8)$$

where

$1/T$ is the sampling frequency

$\underline{K}_0$ is the proportional gain matrix for the error signal $\underline{e}(kT)$

$\underline{K}_1$ is the gain matrix for the backward difference of the error signal, which is designated as $\underline{z}(kT)$.

For the continuous case, the law is expressed as

$$\underline{u} = g(\underline{K}_0 \underline{e} + \underline{K}_1 \int \underline{e} \ dt) \qquad (3.9)$$

where

g is the forward path gain

$\underline{K}_0$ is the proportional gain for the error signal

$\underline{K}_1$ is the gain for the integral of the error signal.

61

A block diagram of the system with this control
law is presented in Figures 8 and 9 for both the continuous
and discrete cases. The portion in broken lines is present
only for irregular designs.

The gain factor in the figure is the sampling fre-
quency (1/T) for the discrete system or a gain constant (g)
for the continuous system. For the regular design the
error vector $\underline{e}$ is expressed as $\underline{e} = \underline{v} - \underline{y}$. Each command
in the $\underline{v}$ vector is summed with its corresponding output
element in the $\underline{y}$ vector and is the input for the proportional
plus integral gain paths. Thus, there exists a bank of
integrators, one for each error signal developed. These
integrators insure that the error signals are always driven
to zero, resulting in the final value of the output equaling
the input for step type commands.

In the irregular design the $\underline{e}$ vector is defined by

$$\underline{e} = \underline{v} - \underline{w} \tag{3.10}$$

where

$$\underline{w} = \underline{y} + \underline{M}\underline{\dot{x}} \tag{3.11}$$

These outputs $\underline{w}$ are developed with the measurement matrix $\underline{M}$
and the derivatives $\underline{\dot{x}}$ of the system states. Again for step
inputs, the error signal is driven to zero. Rates of the
system states also go to zero and, as before, the resulting
output equals the commanded input.

62
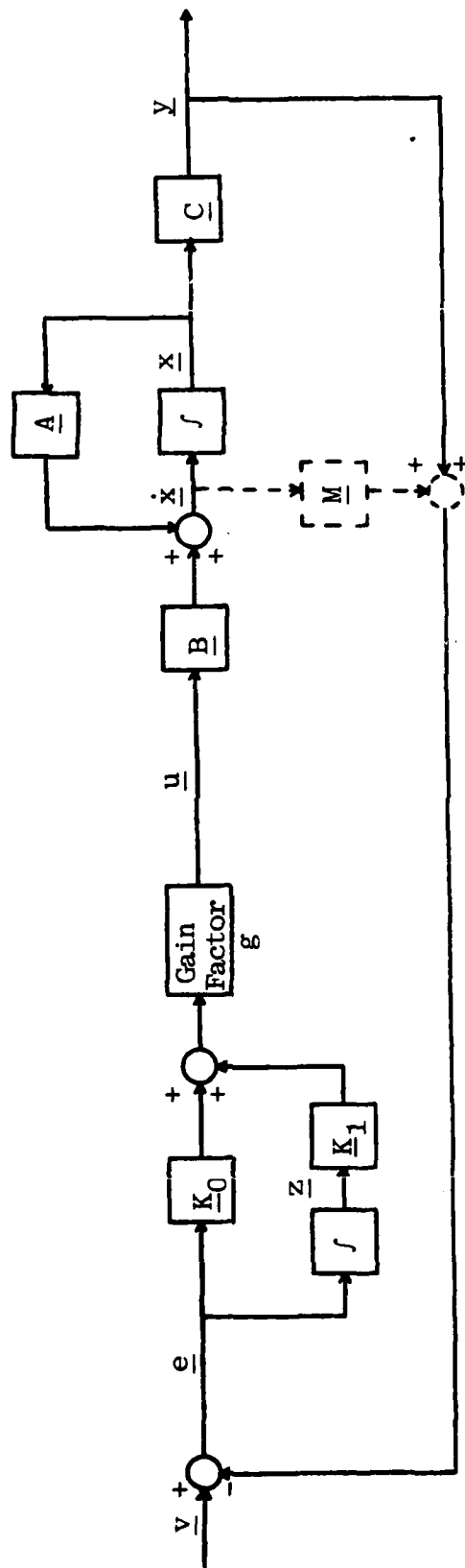
Figure 8. System Block Diagram - Continuous Design
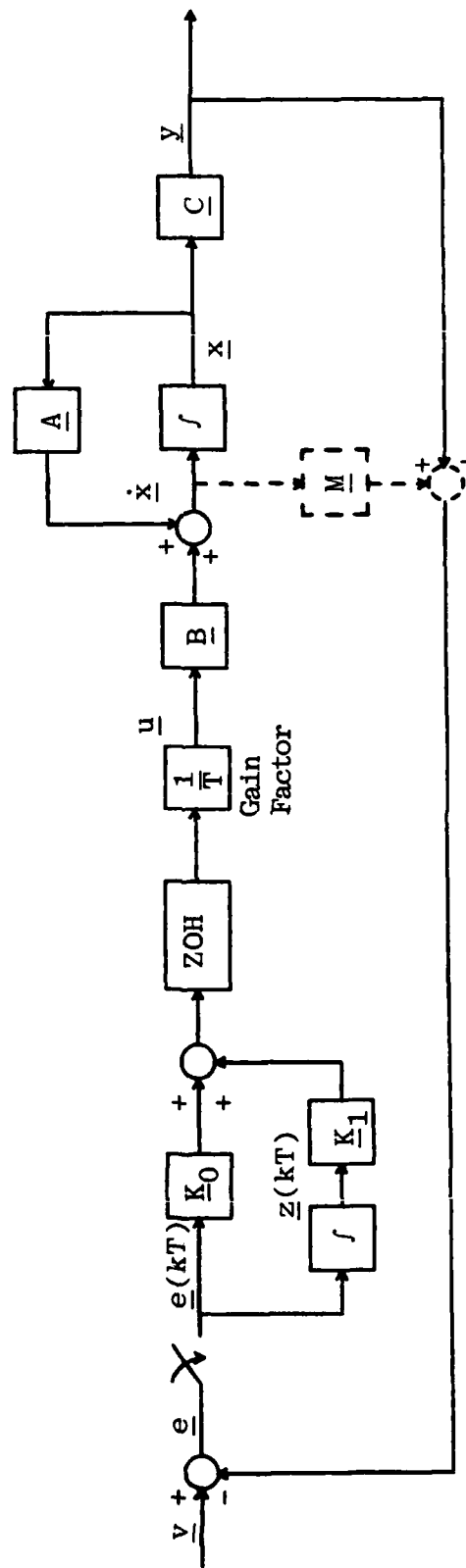
Figure 9. System Block Diagram - Discrete Design

64

At this point, the question of "do the state derivatives always go to zero as desired" must be asked. The answer is a qualified yes. For step commands to the system in which the outputs are states or linear combinations of states, the derivatives go to zero with one exception. This is precisely the reason for the large effort in this study developing state representation for quantities that are to be commanded. By establishing acceleration and pitch rate as system states, these quantities can be commanded, and for step inputs, the derivatives of the quantities go to zero in steady state. The exception concerns the situation in which one of the state derivatives is set equal to a state that is to be controlled. If the state is commanded to a constant value, the derivative reaches this constant value in the steady state. For example, consider a longitudinal design where, due to simplifying assumptions, the rate of change of pitch angle θ is set equal to body axis pitch rate q. It is assumed that q is a state of the system as well as an output. If it is desired to command a step in q, the state derivative $\dot{\theta}$ will eventually reach a constant value. This situation is one in which the system has a transmission zero at the origin. The significance of transmission zeros is discussed later in this chapter. For the time being, it is asserted that this situation provides an acceptable design if the measurement matrix elements are chosen so the system does not feed back the $\dot{\theta}$ state derivative.

65

Output Feedback and the M Matrix

One of the major advantages of this design method is that it uses output feedback. Thus, all the states of the system are not required to be fed back for the design. The outputs are usually quantities of interest that are easily measured by existing sensors. Unfortunately, a measurement matrix is needed for all but the simplest design cases encountered. A number of points must be considered in selecting this measurement matrix as discussed later in this chapter. One such point relates to output feedback and is examined at this time.

It is important to select matrix elements that cause state derivatives to be fed back which can be either measured or derived from existing measurements. If this cannot be accomplished, the alternative is to form the derivative according to the state equation. In general, most of the derivative state equations involve combinations of essentially all the system states. Thus, to develop the proper state derivative, full-state or essentially full-state feedback is needed. This eliminates the tremendous advantage of output feedback and is avoided for design applications in this report. For the designs considered here, elements in the measurement matrix are selected to result in rotational accelerations being used as the rate derivative signals to be fed back. These signals are available from an inertial measurement system; however, such an approach for obtaining

rotational acceleration is not recommended due to reliability considerations. The technique selected for this study is as follows: considering the longitudinal case, $\dot{q}$ is selected as the derivative to be fed back as shown in Chapter IV. Equation (2.48) from Chapter II is repeated below:

$$A_{n_p} = A_{n_{cg}} + (\ell_x)\dot{q} \qquad (2.48)$$

The acceleration at the pilot station, A_{n_p}, is sensed by flight control accelerometers. Acceleration at the center of gravity, $A_{n_{cg}}$, can also be sensed by another set of flight control accelerometers. Using the above expression, a reasonably good approximation of $\dot{q}$ can be developed for use in the system. This same technique is used in the lateral-directional design.

Movement of the CG during flight introduces errors into the results. The CG variation in the x-body axis is approximately one percent of the MAC or 1.1 feet. Another source of error exists in the simplification used to develop Equation (2.48). Roll rate can be relatively large on the aircraft and may have to be considered in developing an expression for $\dot{q}$ using Equation (2.31). Time was not available in this study to evaluate the effects of such errors.

Asymptotic Characteristics

For the design shown in Figure 8, as the gain factor increases, the system transfer function $\underline{G}(s) = \underline{C}(s\underline{I} - \underline{A})^{-1}\underline{B}$ assumes the asymptotic form

$$\underline{\Gamma}(\lambda) = \underline{\tilde{\Gamma}}(\lambda) + \underline{\hat{\Gamma}}(\lambda) \qquad (3.12)$$

where

$\underline{\tilde{\Gamma}}(\lambda)$ is the "slow" transfer function matrix and

$\underline{\hat{\Gamma}}(\lambda)$ is the "fast" transfer function matrix.

The poles of these transfer functions fall into three groups designated Z_1, Z_2, and Z_3. The slow modes correspond to poles contained in Z_1 and Z_2. As gain factor increases towards infinity, the poles of Z_1 become uncontrollable and the poles of Z_2 become unobservable. As this happens, the system response is increasingly dominated by the fast modes which correspond to the poles Z_3. Expressions for the asymptotic modes are given in Table 2.

As the gain factor is increased, tracking of the system's output to input commands becomes increasingly "tight." Reference 6 shows that with only moderate increases in gain factor, the output resembles an extremely fast first-order response. Although the dominant finite (fast) roots can be made complex, much of the experience to date has been with real roots.

The gain $\underline{K}_0$ is chosen such that

$$\underline{CBK}_0 = \text{diagonal} \{ \sigma_1, \sigma_2, \ldots \sigma_n \} \qquad (3.13)$$

68

Table 2

Asymptotic Equations for Zero-B_2 Form

System is represented by:

$$\begin{bmatrix} \dot{x}_1 \\ \dot{x}_2 \end{bmatrix} = \begin{bmatrix} \hat{A}_{11} & \hat{A}_{12} \\ \hline \hat{A}_{21} & \hat{A}_{22} \end{bmatrix} \begin{bmatrix} x_1 \\ x_2 \end{bmatrix} + \begin{bmatrix} 0 \\ \hline \hat{B}_2 \end{bmatrix} u \quad \text{and} \quad y = [\ \hat{C}_1 \ \hat{C}_2 \ ] \begin{bmatrix} x_1 \\ x_2 \end{bmatrix}$$

Continuous Case	Discrete Case
Gain Factor = g	Gain Factor = $1/T$
(Poles are in the s-plane)	(Poles are in the z-plane)

$$\tilde{\Gamma}(\lambda) = \underline{C}_o (\lambda \underline{I}_n - \underline{A}_o)^{-1} \underline{B}_o = 0 \qquad\qquad \tilde{\Gamma}(\lambda) = \underline{C}_o (\lambda \underline{I}_n - \underline{A}_o)^{-1} \underline{B}_o$$

$$\hat{\Gamma}(\lambda) = (\lambda \underline{I}_m + g\ \hat{\underline{C}}_2 \hat{\underline{B}}_2\ \underline{K}_0)^{-1} g\ \hat{\underline{C}}_2 \hat{\underline{B}}_2\ \underline{K}_0 \qquad \hat{\Gamma}(\lambda) = (\lambda \underline{I}_m - \underline{I}_m + \hat{\underline{C}}_2 \hat{\underline{B}}_2\ \underline{K}_0)^{-1} \hat{\underline{C}}_2 \hat{\underline{B}}_2\ \underline{K}_0$$

(Finite roots)

$$\underline{Z}_1 = |\ \lambda\ \underline{K}_0 + \underline{K}_1\ | = 0 \qquad\qquad\qquad \underline{Z}_1 = |\lambda \underline{I}_m - \underline{I}_m + T\ \underline{K}_0^{-1} \underline{K}_1| = 0$$

$$\underline{Z}_2 = |\lambda \underline{I}_{n-m} - \hat{A}_{11} - \hat{A}_{12}\ \hat{\underline{C}}_2^{-1} \hat{\underline{C}}_1| = 0 \qquad \underline{Z}_2 = |\lambda \underline{I}_{n-m} - T\ \hat{A}_{11} + \hat{A}_{12}\ \hat{\underline{C}}_2^{-1} \hat{\underline{C}}_1| = 0$$

(Infinite roots)

$$\underline{Z}_3 = |\lambda \underline{I}_m + g\ \hat{\underline{C}}_2 \hat{\underline{B}}_2\ \underline{K}_0| = 0 \qquad\qquad \underline{Z}_3 = |\lambda \underline{I}_m - \underline{I}_m + \hat{\underline{C}}_2 \hat{\underline{B}}_2\ \underline{K}_0| = 0$$

69

Table 2 (continued)

$$\underline{A}_o = \begin{bmatrix} -\underline{K}_0^{-1}\underline{K}_1 & 0 \\ \underline{A}_{12}\underline{C}_2^{-1}\underline{K}_0^{-1}\underline{K}_1 & \underline{A}_{11}-\underline{A}_{12}\underline{C}_2^{-1}\underline{C}_1 \end{bmatrix}$$

$$\underline{B}_o = \begin{bmatrix} 0 \\ \underline{A}_{12}\,\underline{C}_2^{-1} \end{bmatrix}$$

$$\underline{C}_o = [\underline{K}_0^{-1}\underline{K}_1 \,|\, 0]$$

where:

70

Equation (3.13) is used to calculate the proportional gain
matrix $\underline{K}_0$. The elements of the $\underline{\Sigma}$ matrix, which is selected
as a diagonal matrix, are chosen by the designer. These
values determine the respective gains or the weighting of
each error signal on the control surface or the system
input being commanded by the control law.

$$\underline{K}_0 = [\underline{CB}]^{-1}\underline{\Sigma} \tag{3.14}$$

The integral gain matrix $\underline{K}_1$ is often determined by a scalar
multiplication of the $\underline{K}_0$ matrix.

$$\underline{K}_1 = \overline{\alpha}\underline{K}_0 \tag{3.15}$$

The system transfer function G(s) approaches a
diagonal asymptotic form of increasingly noninteracting
control. Thus, the output responses become decoupled as gain
increases. The asymptotic closed-loop transfer function of
the digital system has the form:

$$\underline{\Gamma}(\lambda) = \text{diagonal } \{ \frac{\sigma_1}{\lambda-1+\sigma_1}, \frac{\sigma_2}{\lambda-1+\sigma_2}, \cdots \frac{\sigma_n}{\lambda-1+\sigma_n} \} \tag{3.16}$$

For the continuous system, the asymptotic transfer function
has the form:

$$\underline{\Gamma}(\lambda) = \text{diagonal } \{ \frac{g\sigma_1}{\lambda+g\sigma_1}, \frac{g\sigma_2}{\lambda+g\sigma_2}, \cdots \frac{g\sigma_n}{\lambda+g\sigma_n} \} \tag{3.17}$$

For the irregular plant, the above equations are
applied by replacing the $\underline{C}$ matrix with an $\underline{F}$ matrix. The

71

component $\underline{C}_1$ is replaced by $\underline{F}_1$ and $\underline{C}_2$ is replaced by $\underline{F}_2$ as calculated in Equations (3.6) and (3.7).

In the equations in Table 2 , the gain values $\underline{K}_0$ and $\underline{K}_1$ are the same as those developed from the equations that are not in zero-B_2 form. This is because

$$[\underline{CB}] = [\underline{C}_2\underline{B}_2] \quad \text{or} \quad [FB] = [\underline{F}_2\underline{B}_2] \tag{3.18}$$

The asymptotic closed-loop system roots can be calculated from the equations in Table 2 and are composed of the sets Z_1, Z_2 and Z_3. In the limit as gain approaches infinity, the following rules can be used to estimate root locations in the s-plane.

The Z_1 finite roots are m in number and equal to the ratio of integral to proportional gain values. The Z_2 finite roots are n-m in number and located at transmission zero locations.

The Z_3 infinite roots are m in number and for the continuous case they are located at a position on the real axis equal to $-g\sigma_i$ where g is the gain factor and σ_i is the respective weighting element selected by the designer in the $\underline{\Sigma}$ matrix. For the discrete case the roots are located at $1-\sigma_i$ and are located near the origin.

Transmission Zeros

Transmission zeros are considered as regions in either the s-plane or the z-plane. These regions are asymptotic locations for certain finite or slow roots of the

72

system. Output feedback does not alter the location of transmission zeros (Ref 8). Such locations may coincide with conventional single input/single output transfer function zeros, or they may simply be regions in the plane that attract finite poles. Since the basic system transmission zeros cannot be altered by the controller design and since infinite gain cannot be used, the location of roots migrating towards these zeros does produce an effect on the system response.

Designing for a system with an unstable transmission zero is possible, but it means an upper stability limit must be established. Operation is possible only below that limit. Increasing gain eventually results in a pole migrating to the unstable location.

Using the zero-B_2 form, transmission zeros can be calculated from the equation in Table 2 where $Z_t = Z_2$. Although they cannot be altered by output feedback, transmission zeros can be changed in two ways. First, should the location of transmission zeros of the system be unacceptable, it is sometimes possible to select another $\underline{C}$ matrix that is acceptable for the design and yields different zero locations. Second, the measurement matrix modifies the transmission zeros, and it may be possible to alter the matrix elements to give both acceptable performance and acceptable transmission zero location.

Measurement Matrix Elements

Some guidelines are available for the selection of the measurement matrix. Reference 9 presents a systematic approach to their selection for optimum decoupling. In addition, the following suggestions are offered:

1. make the measurement matrix as sparse as possible adding only enough non-zero elements to yield an F matrix and an [FB] matrix of full rank;

2. select values for the non-zero elements that give acceptable transmission zeros. In most cases, the values of the measurement elements result in transmission zero locations that are equal to the reciprocal of the element value. However, cases are encountered in this design effort in which this rule does not hold. This usually occurs when more than the minimum number of elements is specified. In these cases, the macro program in Appendix E proved to be a necessity in selecting proper elements; and

3. select the location of the non-zero elements to use a state derivative that can be easily obtained and is zero for steady-state step commands as discussed previously.

Closed-Loop Roots

The design technique does not guarantee stability of the system unless it has stable transmission zeros and infinite gain. Even with stable transmission zeros, the root migrations can cross into the unstable region as the gain increases, and then return to the stable transmission

74

zero. With the desire to develop a system with only enough
gain to do the job and being unfamiliar with the effects of
design parameter variations on the system, it is desirable
to be able to evaluate the closed-loop system roots for each
design.

The equations for computing closed-loop roots are
presented below. They are given for both the zero-B_2 and
non-zero-B_2 formats. The zero-B_2 format solution is mech-
anized using macro programming of TOTAL. A listing of the
program and instructions for its use are given in Appendix F.

Partitioning of the $\underline{A}$ and $\underline{B}$ system matrices is
accomplished as before to yield $\underline{B}_2$ and $\underline{A}_{22}$ of order (m x m),
where m is the number of inputs.

$$\underline{\dot{x}} = \left[\begin{array}{c|c} \underline{A}_{11} & \underline{A}_{12} \\ \hline \underline{A}_{21} & \underline{A}_{22} \end{array} \right] \underline{x} + \left[\begin{array}{c} \underline{B}_1 \\ \hline \underline{B}_2 \end{array} \right] \underline{u} \tag{3.3}$$

$$\underline{y} = [\ \underline{C}_1 \ | \ \underline{C}_2 \ ] \ \underline{x} \tag{3.4}$$

or

$$\underline{\dot{x}}_1 = \underline{A}_{11}\underline{x}_1 + \underline{A}_{12}\underline{x}_2 + \underline{B}_1\underline{u} \tag{3.19}$$

$$\underline{\dot{x}}_2 = \underline{A}_{21}\underline{x}_2 + \underline{A}_{22}\underline{x}_2 + \underline{B}_2\underline{u} \tag{3.20}$$

$$\underline{y} = \underline{C}_1\underline{x}_1 + \underline{C}_2\underline{x}_2 \tag{3.21}$$

$$\underline{e} = \underline{v} - \underline{y} \quad \text{and} \quad \underline{u} = g\underline{K}_0\underline{e} + g\underline{K}_1\int\underline{e}dt \tag{3.22}$$

75

let $\dot{\underline{z}} = \underline{e}$ and $z = \int \underline{e} dt$ (3.23)

then $\dot{\underline{z}} = \underline{v} - \underline{y}$ (3.24)

$$\dot{\underline{z}} = -\underline{C}_1 \underline{x}_1 - \underline{C}_2 \underline{x}_2 + \underline{v} \qquad (3.25)$$

$$\underline{u} = g\underline{K}_0 \dot{\underline{z}} + g\underline{K}_1 \underline{z} = g\underline{K}_0(-\underline{C}_1 \underline{x}_1 - \underline{C}_2 \underline{x}_2 + \underline{v})$$
$$+ g\underline{K}_1 \underline{z} \qquad (3.26)$$

$$\underline{u} = -g\underline{K}_0 \underline{C}_1 \underline{x}_1 - g\underline{K}_0 \underline{C}_2 \underline{x}_2 + g\underline{K}_0 \underline{v} + g\underline{K}_1 \underline{z} \qquad (3.27)$$

$$\dot{\underline{x}}_1 = \underline{A}_{11} \underline{x}_1 + \underline{A}_{12} \underline{x}_2 - \underline{B}_1 g\underline{K}_0 \underline{C}_1 \underline{x}_1 - \underline{B}_1 g\underline{K}_0 \underline{C}_2 \underline{x}_2$$
$$+ \underline{B}_1 g\underline{K}_0 \underline{v} + \underline{B}_1 g\underline{K}_1 \underline{z} \qquad (3.28)$$

$$\dot{\underline{x}}_1 = (\underline{A}_{11} - \underline{B}_1 g\underline{K}_0 \underline{C}_1)\underline{x}_1 + (\underline{A}_{12} - \underline{B}_1 g\underline{K}_0 \underline{C}_2)\underline{x}_2$$
$$+ (\underline{B}_1 g\underline{K}_0)\underline{v} + (\underline{B}_1 g\underline{K}_1)\underline{z} \qquad (3.29)$$

$$\dot{\underline{x}}_2 = \underline{A}_{21} \underline{x}_1 + \underline{A}_{22} \underline{x}_2 - \underline{B}_2 g\underline{K}_0 \underline{C}_1 \underline{x}_1 - \underline{B}_2 g\underline{K}_0 \underline{C}_2 \underline{x}_2$$
$$+ \underline{B}_2 g\underline{K}_0 \underline{v} + \underline{B}_2 g\underline{K}_1 \underline{z} \qquad (3.30)$$

$$\dot{\underline{x}}_2 = (\underline{A}_{21} - \underline{B}_2 g\underline{K}_0 \underline{C}_1)\underline{x}_1 + (\underline{A}_{22} - \underline{B}_2 g\underline{K}_0 \underline{C}_2)\underline{x}_2$$
$$+ (\underline{B}_2 g\underline{K}_0)\underline{v} + (\underline{B}_2 g\underline{K}_1)\underline{z} \qquad (3.31)$$

Writing Equations (3.25), (3.29) and (3.31) in matrix notation provides the description of the closed-loop system where $\underline{v}$ is the input command vector to the control system.

76

$$
\begin{bmatrix} \dot{\underline{z}} \\ \dot{\underline{x}}_1 \\ \dot{\underline{x}}_2 \end{bmatrix} = \begin{bmatrix} 0 & -\underline{C}_1 & -\underline{C}_2 \\ \underline{B}_1 g \underline{K}_1 & \underline{A}_{11} - \underline{B}_1 g \underline{K}_0 \underline{C}_1 & \underline{A}_{12} - \underline{B}_1 g \underline{K}_0 \underline{C}_2 \\ \underline{B}_2 g \underline{K}_1 & \underline{A}_{21} - \underline{B}_2 g \underline{K}_0 \underline{C}_1 & \underline{A}_{22} - \underline{B}_2 g \underline{K}_0 \underline{C}_2 \end{bmatrix} \begin{bmatrix} \underline{z} \\ \underline{x}_1 \\ \underline{x}_2 \end{bmatrix} + \begin{bmatrix} \underline{I} \\ \underline{B}_1 g \underline{K}_0 \\ \underline{B}_2 g \underline{K}_0 \end{bmatrix} \underline{v}
$$

$$(3.32)$$

Note that $\underline{z}$ is a vector of dimension (number of inputs) x 1. For irregular designs replace $\underline{C}_1$ and $\underline{C}_2$ with $\underline{F}_1$ and $\underline{F}_2$, respectively.

Some caution should be exercised in using these closed-loop equations. For the digital system, the control is piecewise continuous between samples and thus, by letting $1/T = g$, these equations can be used to evaluate stability in a general sense. However, the effects of sampling such as quantization and zero order hold are not considered. Also, in any system using a real digital machine, such things as the computational time delay, harmonics generated by sampling, and the apparent rate limiting due to maximum sampling speed can cause instabilities. These effects are not considered in these equations. Nevertheless, the computation of the closed-loop roots provides an understanding of the effects of design changes on the system and can be the basis for realistic stability checks.

MULTI Computer-Aided Design

The MULTI program was created by previous AFIT thesis research (Ref 10) and allows real-time computer-aided designs to be accomplished with the control law theories presented in this chapter. A users' guide is presented in

77

Reference 10. This design effort would have been impractical without such a package, along with the TOTAL program. Iterations and refinements are necessary as the design progresses. Time response data provide the basis for design decisions. The program allows on-line design changes and provides response plots to defined command inputs.

There are several differences between the MULTI program computations and the theoretical equations presented in this chapter which must be pointed out.

In the computation of the gain matrices, a number of flexibilities are provided. The actual MULTI computations are shown below.

For the regular design case:

$$\underline{K}_0 = \overline{\alpha} \; \epsilon \; [\underline{CB}]^{-1} \underline{\Sigma} \qquad (3.33)$$

$$\underline{K}_1 = \epsilon \; [\underline{CB}]^{-1} \underline{\Sigma} \qquad (3.34)$$

Both $\overline{\alpha}$ and ϵ are scalars, and $\overline{\alpha}$ is used to set the ratio of proportional to integral gain. Unfortunately, it is the inverse of the usual method of varying this relationship. ϵ is a scalar that can be used to change all the gain elements by any desired amount. For the digital design case, this proves useful for cases where the sampling frequency has been fixed by other design considerations. The system response can be altered by increasing ϵ, resulting in the same effect as increasing $1/T$.

For the irregular design:

$$\underline{K}_0 = \overline{\alpha} \ \epsilon \ [\underline{F}_2\underline{B}_2]^{-1}\underline{\Sigma} \tag{3.35}$$

$$\underline{K}_1 = \epsilon \ [\underline{F}_2\underline{B}_2]^{-1}\underline{\Sigma} \tag{3.36}$$

It should be noted that the $[\underline{FB}]$ matrix must be used for the calculations if $\underline{B}$ is not in $\begin{bmatrix} 0 \\ \underline{B}_2 \end{bmatrix}$ form.

IV. Philosophy and Details of the

Design Method

Requirements

The following requirements must be satisfied in applying the design method:

1. The number of inputs must equal the number of outputs.

2. The system must be controllable and observable.

3. All transmission zeros must be stable.

4. Integral plus proportional control is applied to all forward loop signals.

Each of these requirements is considered in detail in the following paragraphs.

Inputs and Outputs

The "inputs" refer to the number of controls that can be commanded to alter the aircraft's states. These are inputs to the aerodynamic (plant) model. For the AFTI/F-16 longitudinal case, the inputs consist of the flaperon and the horizontal tail (elevator) surface positions. For the lateral-directional case, they are the canard, aileron and rudder surface positions. These are designated by the $\underline{u}$ vector in the system equation. The "outputs" are the variables contained in the $\underline{y}$ vector and are the responses which are to be controlled. The outputs can be states of the

system or linear combinations of states. For this study, two sets of outputs for the longitudinal axis are considered. The first set is angle of attack and pitch rate. The second set consists of normal acceleration at the pilot's station and pitch rate. The lateral-directional outputs are chosen to be side acceleration at the pilot's station, roll rate, and yaw rate. An explanation of this selection is given in the design procedure section.

For each aircraft response that is to be independently controlled, a separate surface must be available. This is a requirement for a decoupled response and is independent of the design method. For a conventional pull up, only one surface is employed, the elevator, and the pilot has independent control of one aircraft state, normal acceleration. The angle of attack and pitch rate, which are developed, are directly related to the normal acceleration being commanded. In order to independently control both acceleration and angle of attack for a decoupled response such as Direct Lift, the use of an additional control surface, the flaperon, is required. A direct lift force can be developed with the flaps without rotating the aircraft, since the moments generated by the flaps are balanced by the elevator. Thus, to enable control of two outputs (responses), two inputs (surfaces) are required. This holds true for the multivariable techniques employed in this thesis. The procedure for selection of the proper commands for each control

81

parameter in order to perform specified maneuvers is dis-
cussed in detail later in the chapter.

Controllability and Observability

Controllability and observability are properties
of the state-space representation of a system. Controlla-
bility implies that the inputs can affect each mode of the
system. For a time invariant linear system, controllability
can be checked by evaluating the rank of the controllability
matrix $\underline{M}_c$ (Ref 11) where

$$\text{Rank } \underline{M}_c = \text{Rank } [\underline{B} \quad \underline{AB} \quad \ldots \quad \underline{A}^{n-1}\underline{B}] = n$$

Observability implies that the outputs are affected
by every mode. It also implies that the effects on the out-
puts of one state variable can be distinguished from the
effects of other state variables. For a time invariant
linear system, this property can be determined by evaluating
the rank of the observability matrix $\underline{M}_o$, (Ref 11) where

$$\text{Rank } \underline{M}_o = \text{Rank } [\underline{C}^T \quad \underline{A}^T\underline{C}^T \quad \ldots \quad \underline{A}^{T(n-1)}\underline{C}^T] = n$$

Controllability and observability are evaluated for
each design. This is accomplished by employing the CESA
(Ref 12) computer-aided design package available as an AFIT
program on the CDC6600 system. In cases where the criteria
are not met, the system model is redefined until controlla-
bility and observability are achieved. The majority of the

cases under investigation are found to be controllable and observable.

Transmission Zeros

As discussed in Chapter III, transmission zeros of the system are considered as regions toward which system roots migrate with increasing gain. As gain approaches infinity or sampling time approaches zero, the affected roots asymptotically approach the transmission zero ca-tions. Output feedback does not alter transmission ..us. In the strictest sense, it is desired that all such be stable in order to insure system stability with high gain. Such a selection does not guarantee stability for all system gain values since the locus of system roots may journey into the unstable region before arriving in the vicinity of the transmission zeros. Thus, for stable transmission zeros, stable operation is only assured for gain values approaching infinity. A controller design for a system with unstable transmission zeros can be developed with these techniques, but in such cases an upper gain boundary is established to prevent system roots from moving into the unstable region. Thus, the restriction is not absolute; however, failing to meet it does impose additional design considerations.

For irregular designs, when $\underline{CB}$ does not have full rank, additional transmission zeros are introduced by the measurement matrix $\underline{M}$. These can be altered by changing the matrix elements. If the measurement matrix is very sparse,

the location of the additional transmission zeros in the
s-plane is the inverse of the values of the elements in the
measurement matrix. Thus, a 0.25 element in the measurement
matrix produces a transmission zero at -4.0 in the s-plane.
This simple relationship breaks down as the number of
measurement matrix elements increases. Reference 9 provides
a guide to the selection of the measurement matrix. A com-
puterized method to directly calculate the transmission zero
locations is developed using equations from Reference 6 and
macro programming of TOTAL. The program is discussed later
in the report and is listed in Appendix E.

At this point the concept of global stability is
considered, and its influence in the design method examined.
Global stability or "bounded input-bounded output" stability
implies that for any and all bounded inputs to a system, the
outputs are also bounded. Because of the assumptions made in
the equation development, controlling angular rate and
acceleration results in the existence of a transmission zero
at the origin. This is one of the major reasons previous
efforts have not pursued rate or acceleration controllers.
As discussed previously, controllers of this type are desired
for fighter aircraft, and classical experience shows that
such designs perform very well. The question that must be
answered is, "Is global stability necessary?" By carefully
considering the dynamics of a maneuver, the answer is a
resounding no. For example, the transmission zero at the

origin results in an unbounded pitch attitude (θ) response for a bounded pitch rate (q) input. This is exactly what is sought. For the simplified equations, the pitch angle is the integral of pitch rate, and thus a pitch rate step command should cause the pitch angle to ramp to infinity. For all other conceivable inputs, this is the only "unbounded output." The integration due to a pole located exactly at the transmission zero causes the unbounded output and is both predictable and desirable. In conventional fighter aircraft, a step change or bounded output of pitch attitude is manually obtained by the pilot developing a pitch rate and then reducing it to zero through the use of a pulse input.

In conclusion, for this application to the aircraft control problem, a transmission zero at the origin is not only acceptable but highly desirable. The system is considered conditionally stable, and such stability is appropriate for the designs under study. In all cases, any instability encountered during the design work is investigated to define its cause. Also, gain and phase margins are established for the system which must be met both analytically and by test of the actual implementation. This approach is used for classical designs, and the military specification governing control system design, MIL-F-9490D, establishes such margins for a system. Those margins are adopted for use in this investigation.

It is of interest to consider "guaranteed stability." Much has been said in the literature about control design methods that guarantee stability. If a set of conditions is met, then the system is always stable. Such a guarantee has been espoused as a major advantage for designs developed by linear quadratic methods (either the deterministic LQR or the nondeterministic LQG approach). In these approaches, the stability is "guaranteed" only for full state feedback. Such full state feedback is almost impossible to implement. States not contributing significantly to the response are generally eliminated to arrive at a practical design. In addition, a model of the process to be controlled is developed for design. As long as the model and process are exactly the same, and assuming full state feedback, stability is guaranteed. For aircraft applications, such models are only approximations to the real aircraft. Stability is not guaranteed for processes which do not exactly match the design model.

Early in a design cycle, such "guaranteed stability" is useful since the engineer does not have to continually check stability margins for each proposed concept. However, at this point the models are usually very simple, and an evaluation of stability is not a difficult task. Later in the cycle, when the full plant is considered with its inherent nonlinearities, stability checks must be made irrespective of any implied guarantee. The advantage of

guaranteed stability is more an academic nicety than a practical design benefit. For any realistic flight control application, gain and phase margins are specified, and testing is accomplished to prove compliance.

Integral Plus Proportional Compensation

The requirement of integral plus proportional control on all forward loops is not considered a severe restraint. In fighter aircraft applications, integral plus porportional compensation is generally used in the pitch axis for the primary variable controlled by the pilot. For aircraft such as the F-16, this variable is normal acceleration. Pitch rate and angle of attack are fed back to tailor the response and to augment stability. Their values are not directly commanded by the pilot. The relationship between pitch rate, angle of attack, and acceleration varies with flight condition. This variation is natural for a pilot and provides a cue to his operating point in the flight envelope. Thus, use of integral plus proportional compensation is generally not necessary for these feedbacks. In the roll axis, a roll rate command system is used, but the response to a pilot input changes with flight conditions. Again, this variation is generally very natural for the pilot, and such compensation is not needed.

In redundant control systems, the integrators must be equalized. Consider the F-16 again as an example. The pitch axis has four separate but identical control channels

87

with exactly the same feedbacks. Four integral plus proportional networks exist in the path from pilot input to surface command; however, due to the signal selection method, multiple duplicates of only one channel are actually controlling the aircraft. The others are active and provide comparison signals with the ability to instantaneously take over control in the event of a failure. With such an arrangement, only one of the integrators can actually drive its input to zero by matching the aircraft's response to the pilot's command.

Although all the channels are trying to provide the same control, tolerance differences in the components in each channel cause the signals to be slightly different. The inputs to the three integrators that are not in direct control never go completely to zero.

With a constant input, these integrators ramp to infinity. In real applications, they simply saturate. The solution of the dilemma is to have the integrators equalize one another. Such equalization, although necessary, adds complexity. It also creates points in an otherwise separated system where failures can be propagated from one channel to another.

Thus, the addition of integral plus proportional compensation where it is not entirely necessary, increases complexity, and may endanger redundancy. Only through more complexity and a substantial amount of additional testing

can the integrity of the redundant system be preserved. As noted above, use of the compensation on all forward control paths can remove useful cues from the pilot relating to flight condition by forcing the steady-state response to equal the command.

When decoupled operation is desired, the addition of integrators to the forward paths is highly desirable. This is because, in such decoupling, several parameters must be exactly controlled. The use of integral plus proportional compensation on each forward signal path insures that the specified values commanded are reached in steady state.

Unfortunately, the decoupled capabilities are only auxiliary flight modes that aid in certain specific tasks. They are limited in authority and do not replace conventional controls, only augment them. For this reason, the requirement for integral plus proportional compensation on all feed forward paths may be a disadvantage.

A Design Procedure

A procedure for developing a design is established, based on the efforts in this thesis. The basic steps in this procedure are outlined below and are then discussed in detail.

1. Formulate the aircraft design model into the proper format.

2. Validate the model.

3. Select the outputs to be controlled and the feedback signals that are required.

4. Check controllability and observability.

5. Calculate the transmission zeros and select the measurement matrix.

6. Estimate the maximum maneuvers.

7. Scale gains for stable response.

8. Vary weighting matrix elements for desired responses and to meet control input restraints.

9. Adjust proportional plus integral gain for timely steady-state behavior.

The Aircraft Model

Chapter II covers the formulation of an aircraft model in state space format necessary for this design application. It also covers the methods used to validate the model. These are two extremely important and usually error prone steps in the design process. Time spent in developing a controller design is wasted effort if the model for the plant is not an adequate representation. Each step in the model development must be checked and rechecked for accuracy. Automated methods are extremely useful in actual design efforts since multiple point designs at a number of flight conditions are accomplished. The model development for each of these points is usually very similar. However, such programs must themselves be adequately validated.

90

Output Feedback Choices

Selection of the outputs to be commanded and the feedbacks to be used is dependent on three main items:

1. Pilot interface requirements.

2. Reliability and redundancy considerations.

3. Practicality of measuring the feedback signals required.

In the early design stage, selection of feedback signals is, at times, an arbitrary decision. Such decisions can have a dramatic impact on cost, complexity, and the reliable operation of the resulting system when it enters production. Use of easily obtained reliable signals is recommended.

Checking the System Properties

Controllability and observability are checked for both the open-loop aircraft and the closed-loop design model prior to performing design variations. This is another area prone to error due to the tedium of performing operations on matrices with realistic elements. Automation can significantly reduce the computational burden. The CESA program available as an AFIT Library program is used throughout this investigation to check controllability and observability.

Transmission Zeros and the M Matrix

The selection of measurement matrix elements and the calculation of transmission zeros are steps that are interrelated in the design. An initial selection is made for the

measurement matrix elements using data from Reference 6
and from previous study efforts. The transmission zeros
are then calculated. Based on their locations, refinement
of the measurement matrix elements is made. In some cases,
unstable transmission zeros that are not created by the
measurement matrix can be removed by redefining the $\underline{C}$ output
matrix. The calculation is performed using the matrix
methods of the TOTAL interactive program available at AFIT.
A Macro program called AKEY 's employed on TOTAL when the
$\underline{B}$ matrix of the state equation is in the "zero-B_2" format
shown at the top of Table 2 . After the system matrices
are stored, AKEY requires only the entering of the measure-
ment matrix elements for each trial calculation of transmis-
sion zeros. The equation implemented for irregular designs
is shown below:

$$\underline{Z}_t = |\lambda \underline{I}_{n-\ell} - \underline{A}_{11} + \underline{A}_{12}\underline{F}_2^{-1}\underline{F}_1| = 0 \qquad (4.1)$$

For regular designs, the same program is used except that
$\underline{C}_1$ and $\underline{C}_2$ are entered in place of $\underline{F}_1$ and $\underline{F}_2$, respectively.
A zero matrix of size n-ℓ by ℓ is entered for the measure-
ment matrix. The program for TOTAL can be quickly created
and kept on a permanent computer file for access throughout
the design. A listing of the Macro steps is given in
Appendix E. An alternate program called ZERO is also avail-
able for determining transmission zeros, but has not been
completely debugged (Ref 13).

92

For the first design attempt, the $\overline{\alpha}$, Σ and ε parameters are set to one in MULTI. In almost all cases, this results in an unstable system. The gain is then reduced by decreasing ε until stable operation is obtained. For those cases that are initially stable, gain is increased until the instability point is found. The gain is then reduced by the required margin.

Initial design attempts using the techniques of Professor Porter usually result in systems that respond rapidly to commands. The quickness of the response may require large control surface deflections and excessive surface rates. Therefore, the design must be modified. The control surface limits for the AFTI/F-16 are shown in Table 3.

Table 3

Surface Position and Rate Limits

Surface	Position Limit (deg)	No Load Rate Limit (deg/sec)
Elevators	±25	60
Flaperons	±20	52
Rudder	±30	120
Canards	±27	100

Maximum Maneuver Estimates

To stay within position limits, a method based on maximum commands is developed. At each condition, the maximum maneuvers that can be commanded are estimated. These estimated maximum maneuvers are used as inputs, and individual weighting matrix elements are varied until less than maximum surface positions are reached. The weighting matrix elements are also adjusted (ratioed with respect to one another) at the same time to provide the type of responses desired. Then, the proportional plus integral ratio $(1/\bar{\alpha})$ is adjusted so that steady-state behavior is reached within a desired time.

Maximum capability for conventional maneuvers may be limited by structural ability, pilot physiological constraints, control authority or departure limits. Table 4 lists the maximum longitudinal and roll commands used in the thesis.

Table 4

Maximum Command Estimates

Flight Condition		Axis (units)	
Mach	Altitude (ft)	Pitch (g)	Roll (deg/sec)
0.2	30	+3.1	150
0.6	30000	+4.7	300
0.9	20000	+9.0	300
1.2	30000	+8.5	210

CCV maneuvers are limited by the direct force capability of the control surfaces. To develop the CCV maximum estimates, the equations of motion are solved for each maneuver of interest. Longitudinal authority is limited by the maximum deflection of the symmetric flaperons for both the direct lift and pitch pointing modes. In the lateral-directional modes, the canard deflection sets the maximum sideforce capability while the rudder deflection limit establishes the maximum yaw pointing capability. For the translational modes, a velocity is produced by developing a direct force and then, after an established time, reducing the force to zero. Thus, the maximum translational capabilities are determined by the integral of the direct forces. Since the time for direct force to be commanded is an arbitrary design selection, maximum estimates for translation are not shown. The solution of the system of equations for the CCV maximum estimates is found at each flight condition. Table 5 is a compilation of the results.

The input commands are very closely tracked by the controllers developed using this design method. For step inputs, the control surfaces are commanded instantaneously to maximum deflection. This would result in rate limiting in any actual implementation. Inclusion of an actuator model reduces the surface rates, but not to values within acceptable limits. Rates are kept below the limit by slowing down the input command. It is recommended that this be

Table 5

CCV Maximum Capabilities

Flight Condition		Mode	Capability
Mach	Altitude (ft)		
0.9	20000	A_n	2.07 g
		α_1	2.72 deg
		A_y	0.84 g
		β_1	4.30 deg
0.2	0	A_n	0.16 g
		α_1	3.22 deg
		A_y	0.05 g
		β_1	2.77 deg
0.6	30000	A_n	0.70 g
		α_1	4.0 deg
		A_y	0.20 g
		β_1	4.68 deg
1.6	30000	A_n	0.94 g
		α_1	1.00 deg
		A_y	0.60 g
		β_1	1.48 deg

accomplished by placing a first-order lag in each command input path. Output from the lag device is a continuous, well-behaved function that the controller tracks with good accuracy. This approach is used in classical designs presently being flown. The lag or "pilot command prefilter" does not interfere with the closed-loop stability but matches the aircraft's response to the pilot's response. Time delays from 1/4 second to 1/10 second are generally used. Higher-order filters can be used, but they tend to increase phase lag at higher frequencies. As discussed in Chapter V, it is beneficial to keep the phase lag as low as possible from such a filter in order to reduce pilot workload.

The MULTI computer-aided design program, at the time of this research, does not have the ability to handle filters on the command inputs to the controller. In work on a related thesis, a method has been developed to represent command inputs as ramp hold waveforms (Ref 14). The ramp hold input is used to approximate an input prefilter by slowing down the command and providing acceptable surface rates. This is not a one-to-one relationship since rates are also affected by feedback signals. However, the technique does result in acceptable surface rates and output responses. The time duration for the ramp is calculated from the maximum surface position divided by the maximum surface rate.

Gain Scaling and the Weighting Matrix

Initially, responses are obtained for a given design to a maximum step input, and the surface rates are examined. The surface with the highest rate is used to establish the ramp time for the input. Then interactive fine tuning is performed to establish the fastest ramp that provides surface rates below the specified limits. The same ramp is used for all inputs.

Weighting matrix elements are varied to develop the desired time responses. After selection of the matrix elements, rate and position limits are again checked and iterated to result in a system that meets the requirements and provides the desired response.

At this point in a design attempt, it is very useful to understand the designation of the elements in the gain matrices. With such knowledge during the gain iteration step, it is possible to trace an undesirable response to its cause or to correct surface saturation problems with minimal impact on performance.

Figure 10 illustrates the element designation for the two input-two output longitudinal AFTI design, i.e.:

$$\underline{K}_0 = \begin{bmatrix} P_{11} & P_{12} \\ P_{21} & P_{22} \end{bmatrix} \quad \text{and} \quad \underline{K}_1 = \begin{bmatrix} I_{11} & I_{12} \\ I_{21} & I_{22} \end{bmatrix} \qquad (4.2)$$

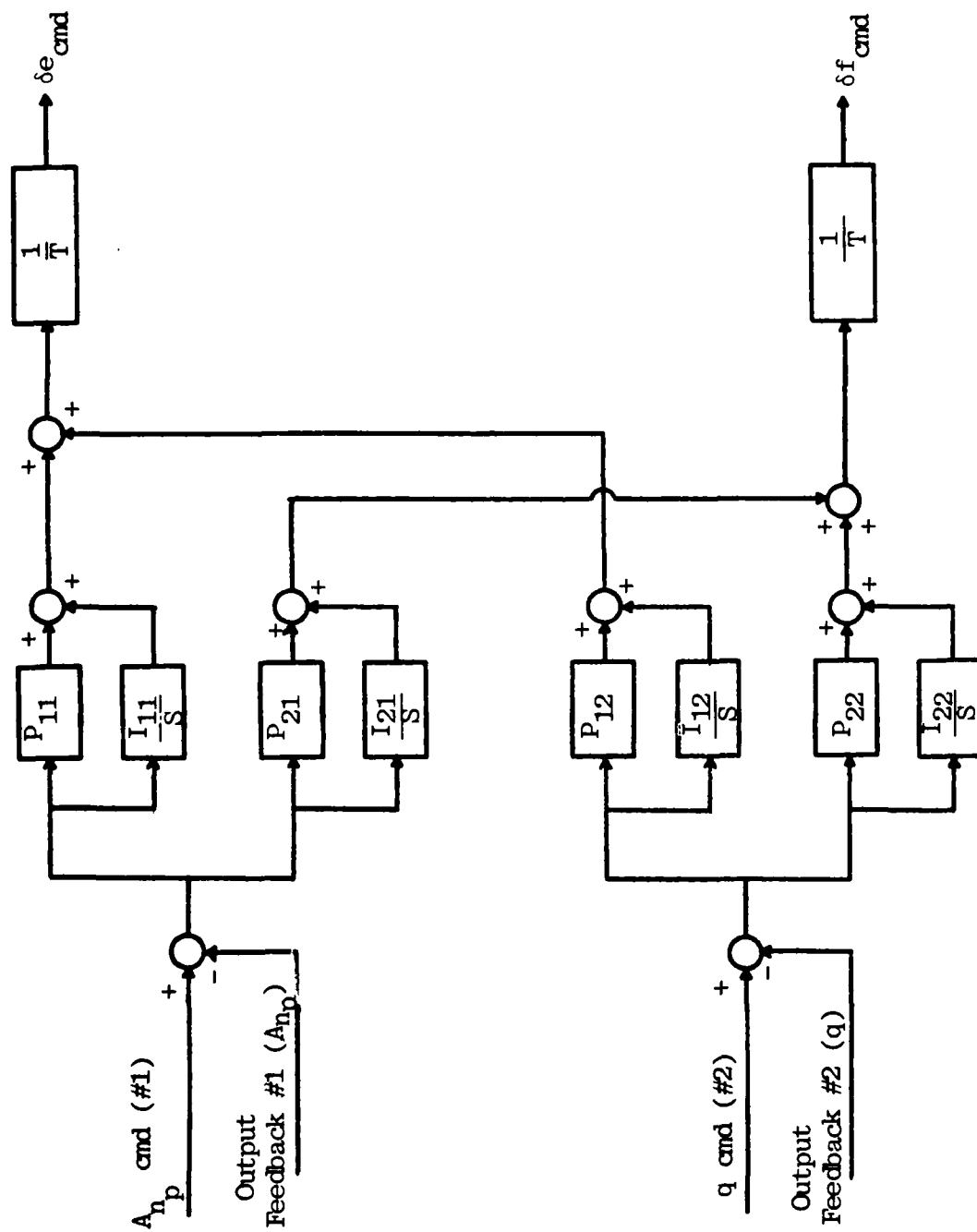The $\underline{C}$ matrix specifies the outputs to be used as feedbacks.

98

Figure 10. Longitudinal Two Input--Two Output Controller Block Diagram

99

$$y = \begin{bmatrix} 0 & 0 & 0 & 1 & 0 & 0 & 0 \\ 0 & 0 & 0 & 0 & 1 & 0 & 0 \end{bmatrix} \begin{bmatrix} \alpha \\ \theta \\ u \\ A_{n_p} \\ q \\ \delta_e \\ \delta_f \end{bmatrix} = \underline{cx} \qquad (4.3)$$

Feedback number one is the longitudinal acceleration at the pilot's station, A_{n_p}, and feedback number two is pitch rate. The elevator surface position is determined by the equation:

$$\delta_{e_{cmd}} = \{(A_{n_p} \text{ error})(P_{11})\} + \{\int(A_{n_p} \text{ error})(I_{11})\}$$
$$+ \{(q \text{ error})(P_{12})\} + \{\int(q \text{ error})(I_{12})\} \qquad (4.4)$$

Integral Plus Proportional Adjustment

The proportional plus integral ratio is adjusted until the system reaches the desired steady-state value in the time required. It is important to realize that the $\bar{\alpha}$ parameter in MULTI is the inverse of the ratio of integral to proportional gain. As shown in Chapter III:

$$\underline{K}_0 = \bar{\alpha} \; \varepsilon \; [\underline{F}_2\underline{B}_2]^{-1}\underline{\Sigma} \qquad (4.5)$$

and

$$\underline{K}_1 = \varepsilon \; [\underline{F}_2\underline{B}_2]^{-1}\underline{\Sigma} \qquad (4.6)$$

Varying α directly affects the proportional gains and system stability. What is actually desired is to hold the proportional gains constant while varying the integral gains to improve steady-state response. The method developed is to select the ratio of proportional to integral gain by varying the $\bar{\alpha}$ parameter and then modifying the gain matrix to return to the original proportional gain. This becomes a time-consuming process and can be eliminated by altering MULTI to move the parameter into the equation for the integral gains.

Gain and Phase Margins

Although not actually listed as part of the design method, gain and phase margins must be checked for any design. In real applications, there is no "guaranteed" stability. The model used in a design is, as the name states, just a model of the aircraft. All the inputs and states of the aircraft are never included in any design model. Aeroelastic interactions, gust disturbances, and nonlinear characteristics of the aircraft or control system can all result in unexpected instabilities.

The only guarantee is that produced by requiring a margin be established and to base the margin on the best estimate of the uncertainties in the model. The military flight control design specification establishes such margins for systems being developed. The table below is extracted from Reference 15. One of the easier methods to check gain

101

Table 6

Gain and Phase Margin Requirements

Airspeed / Mode Frequency Hz	Below $V_{O_{MIN}}$	$V_{O_{MIN}}$ To $V_{O_{MAX}}$	At Limit Airspeed (V_L)	At 1.15 V_L
$f_M < 0.06$	GM = 6 db (No Phase Requirement Below $V_{O_{MIN}}$)	GM = ±4.5 PM = ±30	GM = ±3.0 PM = ±20	GM = 0 PM = 0 (Stable at Nominal Phase and Gain)
$0.06 \le f_M <$ First Aero-Elastic Mode		GM = ±6.0 PM = ±45	GM = ±4.5 PM = ±30	
$f_M >$ First Aero-Elastic Mode		GM = ±8.0 PM = ±60	GM = ±6.0 PM = ±45	

NOTE: Gain is in dB; Phase is in degrees.

where: V_L = Limit Airspeed (MIL-A-8860).

$V_{O_{MIN}}$ = Minimum Operational Airspeed (MIL-F-8785).

$V_{O_{MAX}}$ = Maximum Operational Airspeed (MIL-F-8785).

Mode = A characteristic aeroelastic response of the aircraft as described by an aeroelastic characteristic root of the coupled aircraft/FCS dynamic equation-of-motion.

102

Table 6 (continued)

GM = Gain Margin   = The minimum change in loop gain, at nominal phase, which
                         results in an instability beyond that allowed as a
                         residual oscillation.

PM = Phase Margin   = The minimum change in phase at nominal loop gain which
                         results in an instability.

f_M = Mode frequency in Hz (FCS engaged).

Nominal Phase and   = The contractor's best estimate or measurement of FCS
Gain   and aircraft phase and gain characteristics available
                         at the time of requirement verification.

and phase margins is to use frequency domain analysis
methods (Bode plots or Nyquist plots). These are not pres-
ently available within MULTI but may be achieved with other
programs such as TOTAL.

Note that the required margins in Table 6 are
specified for all aerodynamically closed loops of the flight
control system. In multiple loop systems, variations are
made with all gain and phase values in the feedback paths
held at nominal values except for the path under investiga-
tion.

In preliminary designs, since structural mode data
may not be available, a general guideline is to use ±6db gain
margin and ±45 degrees phase margin. The specified gain
margin must be large enough to account for: (1) uncertain-
ties in the aircraft model, and (2) system changes from age
through the operating life. As more testing is accomplished
with the aircraft and the uncertainties are removed, the
margins may be reduced. In recent years, airframes have
become more efficient, being manufactured with less strength
and weight. At the same time, control system designs have
increased in authority and gain. This trend has signifi-
cantly increased the possibility of adverse interactions
between the control system and the structure (servoelastic
problems). At times such interactions include the aerody-
namic feedback paths resulting in aeroservoelastic insta-
bilities (Ref 21).

As a guard against such instabilities, it is prudent to limit the control system bandwidth. Most structural modes occur at higher frequencies than the functions of the control system. Thus, once a control bandwidth is found that provides acceptable performance, it is advisable to provide gain attenuation at all higher frequencies. Structural modes or interactions within the control system bandwidth must be handled with either notch filters or phase compensation techniques.

For this study, the ±6db gain margin and 45 degrees phase margin are specified. Bandwidth limiting is seen as a desirable characteristic for the system. This limiting is accomplished with the actuators. Compensation is not allowed to counter the gain roll off above the actuator break frequency in order to provide the desired bandwidth limiting. Even with this concept, it should be noted that both the F-16 and the AFTI/F-16 control system designs require the addition of notch filters to alleviate structural interactions.

As a final note on stability margins, the MULTI design package does not provide a means for altering individual system gains. The elements of the weighting matrix change all the gains associated with each output being fed back. Thus, to check stability, the elements of the gain matrix must be manually changed outside the MULTI program. Although not difficult, this is a time-consuming process. The

unavailability of frequency domain analysis methods in the MULTI package make phase measurements very difficult.

One method used in actual on-aircraft testing is to insert a compensation element of the form $[1-\tau s]/[1+\tau s]$ into each loop being tested. The time constant is increased until divergence occurs or until the 45 degree phase margin is demonstrated. It is desirable to include compensation filters within the MULTI design package. Presently, use of this approach requires regeneration of the aircraft model to include the compensation. The model has to be modified to allow evaluation with this element in each individual feedback loop. This addition to MULTI can provide a convenient means of measuring gain and phase margins. Only cursory phase margin checks are accomplished for the designs due to this limitation.

Evolution of a Final Design

The design procedure is illustrated with a simple case in order to develop an understanding of the method being applied. Several interesting facts come to light from this approach. Many details of the design process are included in order to show the evolutionary process which leads to a successful design.

Trial 1. The longitudinal equations at 0.9 Mach and 20,000 feet are considered first. By arranging the equations with theta as the first state and by neglecting the drag

equation, a short period approximation is developed which is in the zero-B_2 form:

$$\begin{bmatrix} \dot{\theta} \\ \dot{\alpha} \\ \dot{q} \end{bmatrix} = \begin{bmatrix} 0 & 0 & 1 \\ -0.001187 & -1.4845 & 0.9948 \\ 0.000309 & 4.2717 & -0.7772 \end{bmatrix} \begin{bmatrix} \theta \\ \alpha \\ q \end{bmatrix} + \begin{bmatrix} 0 & 0 \\ -0.1492 & -0.2249 \\ -24.058 & -6.4727 \end{bmatrix} \begin{bmatrix} \delta_e \\ \delta_f \end{bmatrix} \quad (4.7)$$

$$\underline{y} = \begin{bmatrix} \alpha \\ q \end{bmatrix} = \begin{bmatrix} 0 & 1 & 0 \\ 0 & 0 & 1 \end{bmatrix} \begin{bmatrix} \theta \\ \alpha \\ q \end{bmatrix} \quad (4.8)$$

The system is controllable and observable with a transmission zero at the origin. The $\underline{C}$ matrix is created to provide control of angle of attack and pitch rate. The concept is to control pitch rate and longitudinal acceleration. Rewriting Equation (2.43)

$$A_{z_{cg}} = (\dot{\alpha} - q)U \quad (4.9)$$

Remembering that $A_n = -A_z$ and using Equation (2.32) yields

$$A_{n_p} = (q - \dot{\alpha})U + (\ell_x)\dot{q} \quad (4.10)$$

In a steady state pitch maneuver with constant acceleration, $\dot{\alpha}$ and $\dot{q}$ are zero. Converting the equation to the desired units of "g" and "degrees per second" yields

$$A_{n_p}(g) = \left[\frac{U(ft/sec)}{1845} \right] q(deg/sec) \quad (4.11)$$

107

This method can be applied to the lateral-directional axes giving a similar expression relating sideforce and yaw rate.

$$A_{y_p}(g) = \left[\frac{U(ft/sec)}{1845}\right] r(deg/sec) \qquad (4.12)$$

These two relationships are useful in meeting pilot interface requirements discussed later in this chapter. Since longitudinal acceleration is directly related to pitch rate, it is assumed that acceptable acceleration results by exercising proper control over pitch rate.

An initial value of one is selected for $\bar{\alpha}$, Σ and the ε elements. This results in an unstable design as shown in Figures 11 and 12. Adjustment of the weighting matrix elements produces the responses shown in Figures 13 and 14. In this case, the design parameters are:

$$\bar{\alpha} = 1.0 \qquad (4.13)$$

$$\varepsilon = 1.0 \qquad (4.14)$$

$$\Sigma = \begin{bmatrix} 0.1 & 0.0 \\ 0.0 & 2.35 \end{bmatrix} \qquad (4.15)$$

The inputs are step commands for angle of attack and pitch rate. The steps are not applied instantaneously. They are ramped in over a 0.4 second time interval. The interval is established by the flaperon rate limit and position limit.
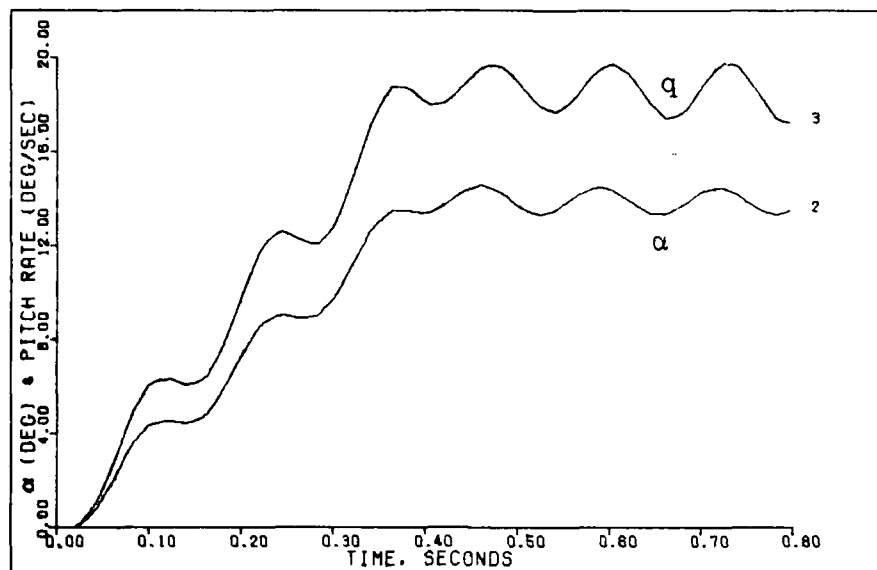
108

Figure 11. Response Plot for Initial Rate Controller
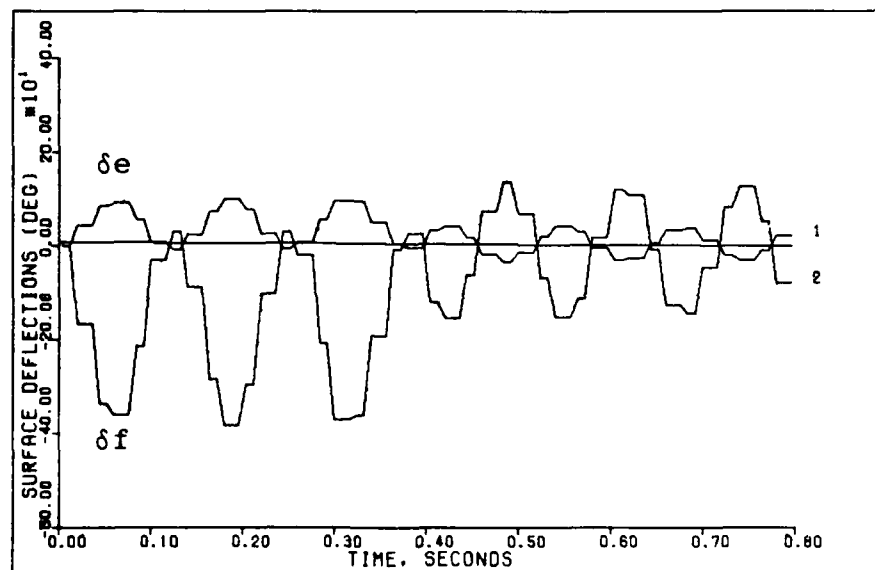Design with Short Period Approximation

Figure 12. Surface Position Plot for Initial Rate
Controller Design with Short Period Approximation
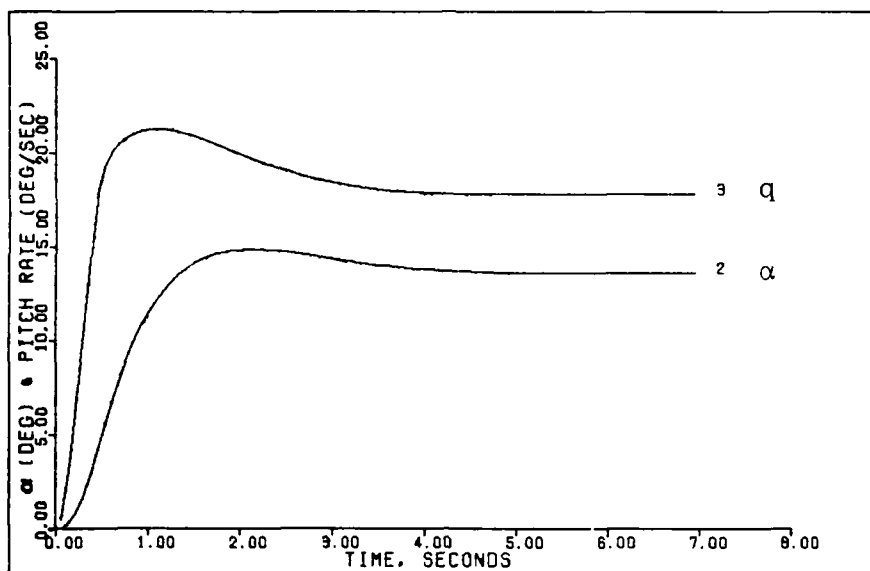
109

Figure 13.   Response Plot for Rate Controller with
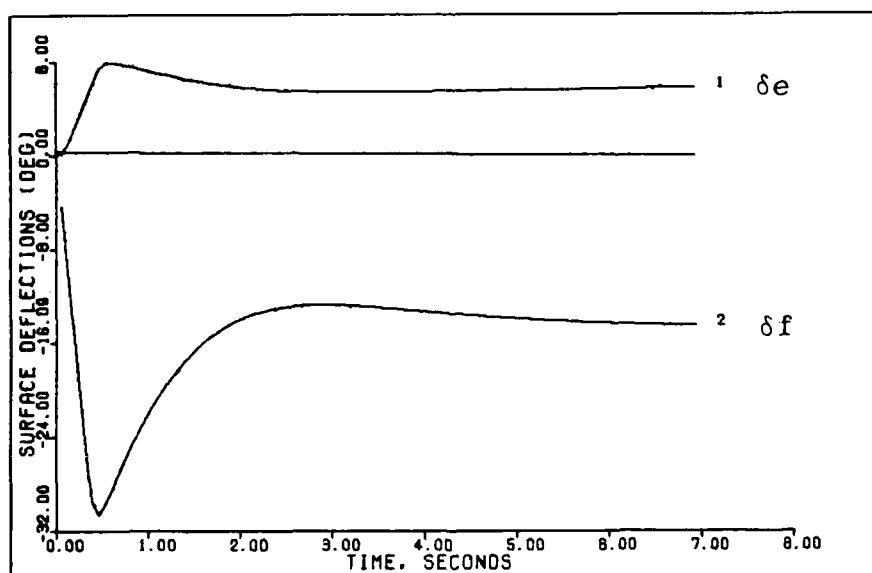Short Period Approximation

Figure 14.   Surface Position Plot for Rate Controller
with Short Period Approximation

110

$$\text{Ramp time} = \frac{\text{rate limit}}{\text{position limit}} \qquad (4.16)$$

The steady-state angle of attack command is determined by solving the aircraft equations for a trim solution at the desired acceleration level. This is a necessary calculation to obtain a coupled longitudinal maneuver with this type of design.

The responses appear acceptable, but two problems are evident. First, the required alpha command must be computed. Thus, pilot inputs must be converted into pitch rate and angle of attack commands through an aircraft model prior to input to the controller.

Second, the flaperons are deflecting in the wrong direction in Figure 14. The flaps are intended to aid in the maneuver by creating a positive instantaneous direct lift. For positive direct lift the flaps must be commanded to a positive position. By driving the flaperon in a negative direction, as shown, the controller is rotating the aircraft as rapidly as possible to develop the commanded pitch rate and angle of attack. The negative flaps are decreasing lift and adversely affecting acceleration. This appears to be contrary to the intended operation. Actually, the controller designed is responding exactly as specified. The step commands of angle of attack and pitch rate are in effect saying to rotate the aircraft rapidly. This is exactly what is being achieved.

111

Trial 2. The problem is in the concept of what
should be happening. The concept assumes that by commanding
alpha and q, acceleration is adequately controlled, based
on Equation (4.11). However, the equation assumes a coupled
aircraft, and this design method develops an essentially
decoupled aircraft. Care must be exercised in selecting the
states to be commanded, and in developing the proper rela-
tionship of these commands to recoupling the aircraft. The
other problem is that the concept assumes for a specific load
factor there is a unique value for both α, q, and the ele-
vator position in steady state. With two surfaces, there
are multiple solutions to the steady-state trim problem.
What is actually desired is a crisp, well-behaved step in
pitch rate and acceleration with a corresponding step in
angle of attack. What is commanded is a quick step in alpha
and q irrespective of the acceleration. In other words, fast
rotation is commanded and provided by the design, but it is
really not desired.

The solution is to restructure the problem to
actively command acceleration and pitch rate. Angle of
attack is still important, and is monitored in the responses.
The speed of response of acceleration and pitch rate deter-
mine the resulting angle of attack. Using Equation (2.43)
and (2.32), the relationship can be defined by

$$\dot{\alpha} = \frac{A_{n_p}}{U} - \left(\frac{}{}\right) \qquad (4.17)$$

In the steady state $\dot{q}$ is zero, thus

$$\dot{\alpha} = \frac{A_{n_p}}{U} + q \qquad (4.18)$$

This solution requires a transformation of states
to obtain acceleration. When performing the transformation
as outlined in Chapter II, the angle of attack state is
replaced by acceleration as a state. The importance of
angle of attack must not be overlooked in the design. Too
large a value can result in loss of directional stability
and departure from controlled flight. Too small an angle of
attack results in the use of a larger flaperon deflection
than necessary to perform the desired maneuver. To allow
angle of attack to be observed in the design attempts, it
can be added as a redundant state equation as outlined in
Chapter II, although this complicates the design. It
increases the dimensions of the system matrices, adds a
transmission zero at the origin, and results in the addition
of a pole and a zero at the origin in the system transfer
function. An alternative is to establish the proper $\underline{C}$ matrix
which produces an acceleration output as well as an angle of
attack output. This eliminates the need for augmenting the
system matrix with redundant equations. MULTI cannot pres-
ently accept such a $\underline{C}$ matrix, since only those outputs that
are commanded can be obtained. This is a proposed modifica-
tion for MULTI.

A design with acceleration as a state is shown in Figures 15, 16 and 17. This illustrates that the same undesired response is obtained if care is not exercised in selecting elements of the measurement matrix. In the case shown, acceleration can now be observed and is initially negative. This is definitely not desirable. It is a result of the use of the flaps in the wrong direction causing an instantaneous loss of lift as the aircraft rotates. Rotation eventually results in an increase in alpha and an associated increase in lift. Figures 18 through 20 show response to a step for the same system with a measurement matrix selected to be as sparse as possible. The desired responses are obtained.

A cautionary note is provided. The maneuvers shown thus far are for step commands approximating the maximum aircraft capability. This is not to imply that the linearized perturbation equations used for the design are accurate for these maneuvers. It is only meant to give a general indication of the maximum surface rates and surface deflections commanded by the controller. Much smaller step responses are used to demonstrate the design. Responses with the full equations of motion and a 1g command are shown in Figures 21 through 25.

A pointing system is developed by using the same rate and acceleration commands. For fuselage pointing, a pulse command is input for pitch rate while a zero
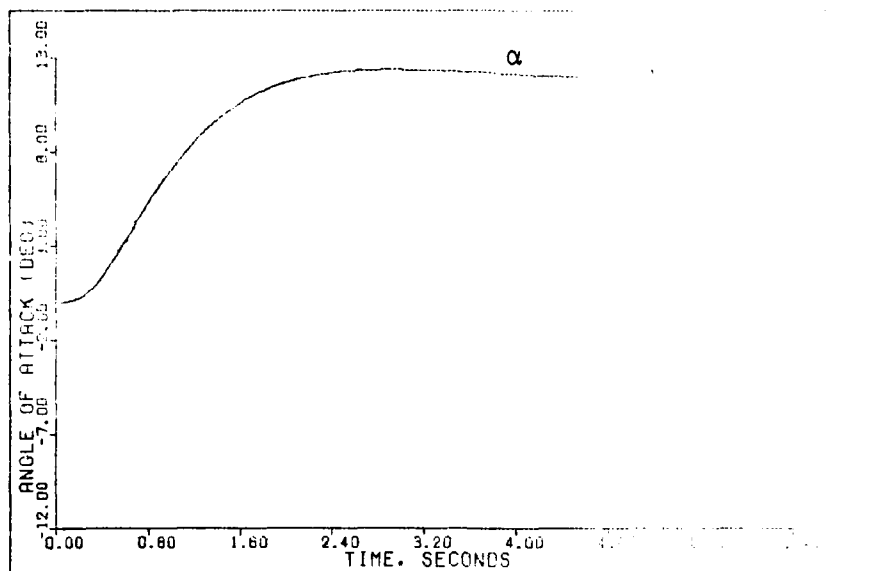
114

Figure 15. α Response of the Trial 2 Design
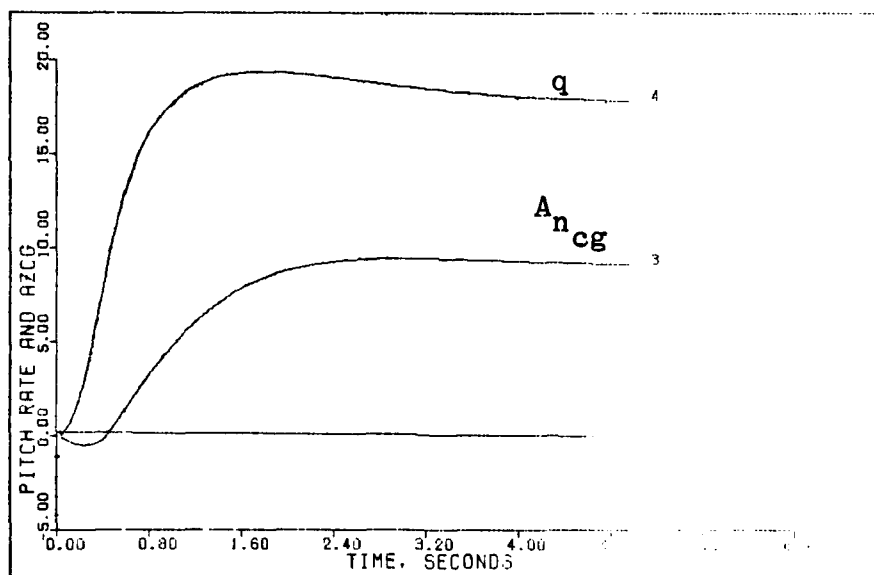to a 9g Step Command
(0.9 Mach 20,000 feet)

Figure 16. Pitch Rate and Acceleration Response
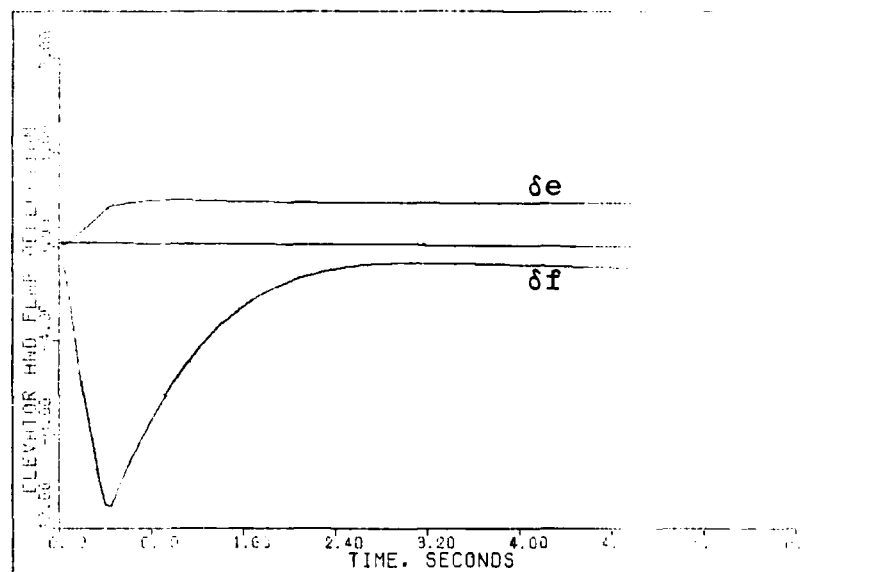of the Trial 2 Design to a 9g Step Command
(0.9 Mach 20,000 feet)

115

Figure 17. Surface Response of the Trial 2
Design to a 9g Step Command
(0.9 Mach 20,000 feet)

116

Figure 18.   α Response of the Desired Preliminary
Design to a 9g Step Command
(0.9 Mach 20,000 feet)

Figure 19.   Pitch Rate and Acceleration Response
of the Desired Preliminary Design to a 9g Step
Command
(0.9 Mach 20,000 feet)

117

Figure 20. Surface Response of the Desired Prelimi-
nary Design to a 9g Step Command
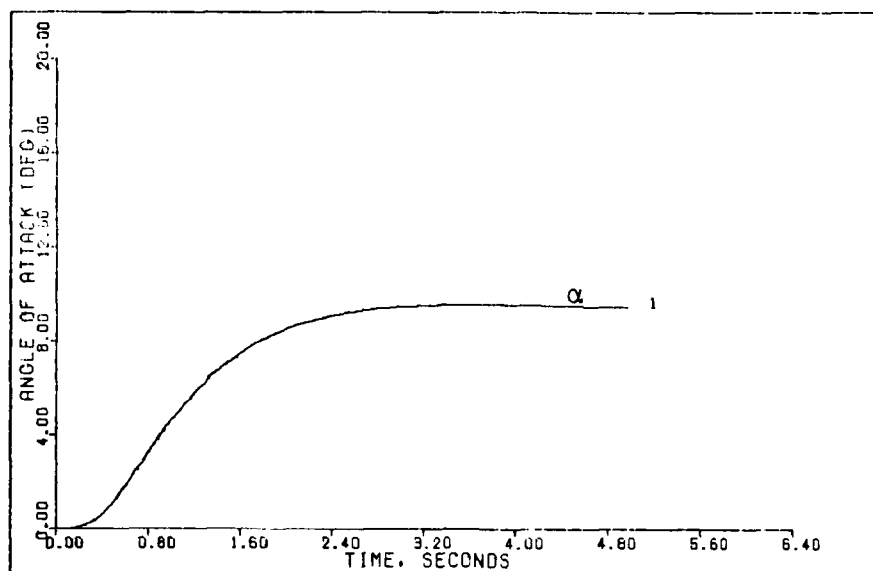(0.9 Mach 20,000 feet)

118

Figure 21. α Response of the Desired Preliminary
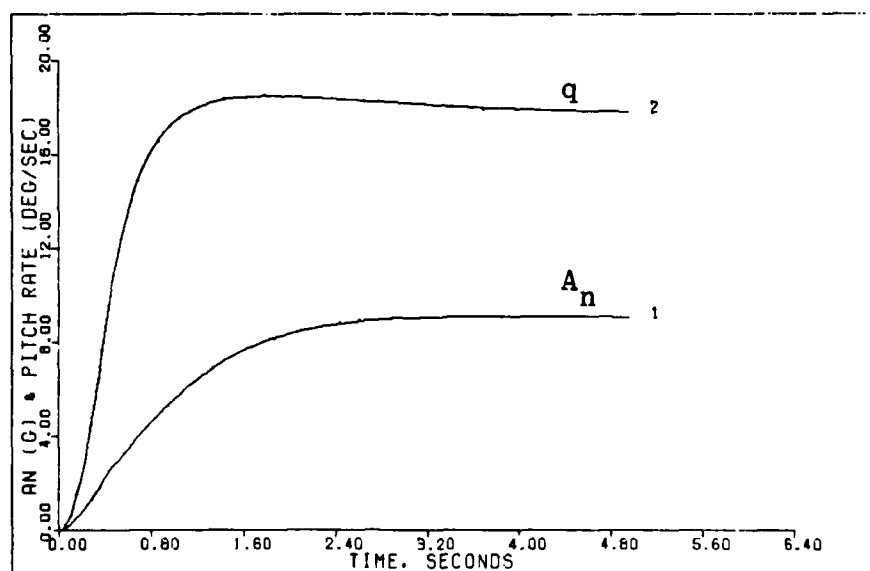Design to a 1g Step Command
(0.9 Mach 20,000 feet)

Figure 22. Pitch Rate and Acceleration Response of
the Desired Preliminary Design to a 1g Step Command
(0.9 Mach 20,000 feet)
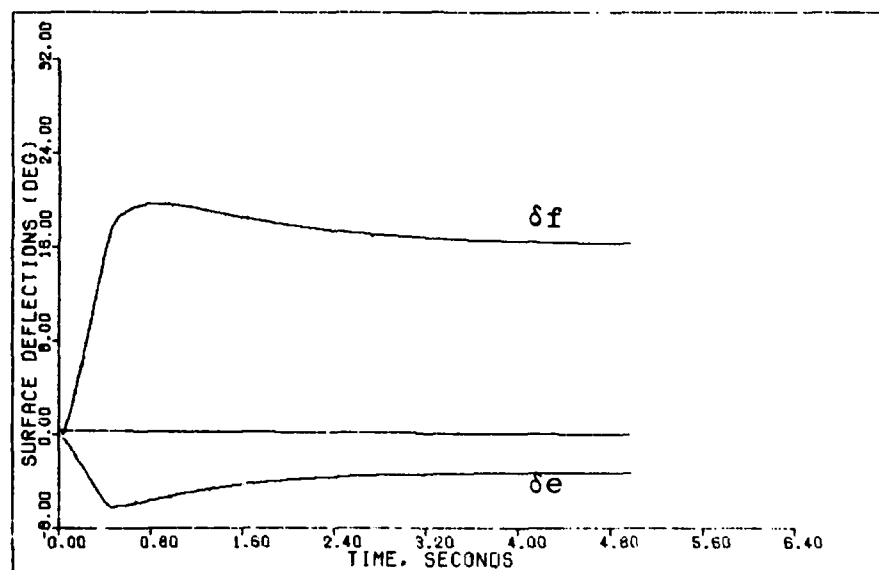
119

Figure 23. Pitch Angle Response of the Desired
Preliminary Design to a 1g Step Command
(0.9 Mach 20,000 feet)

Figure 24. Surface Position Response of the
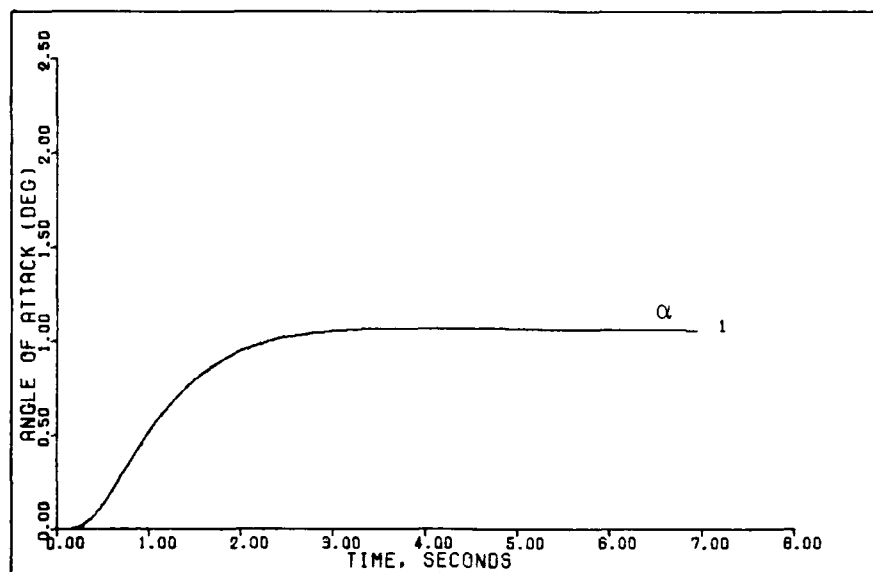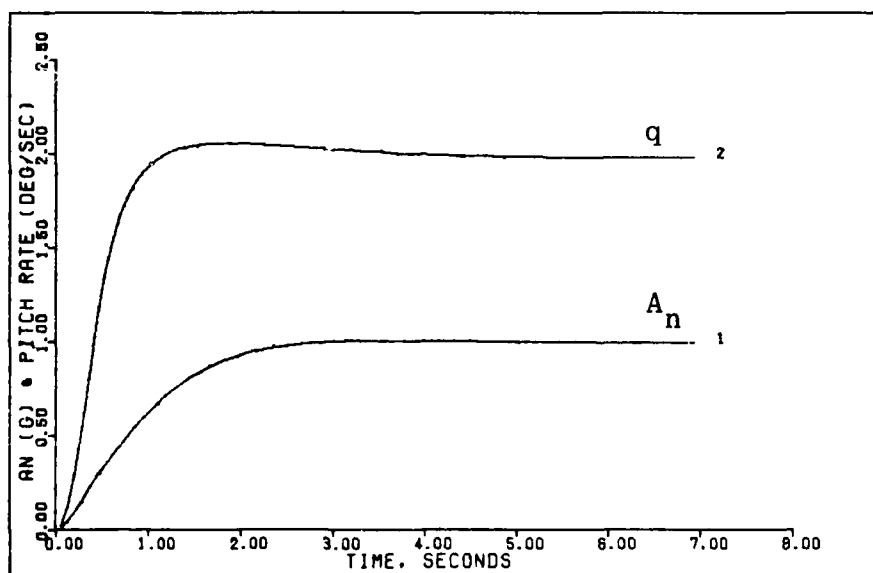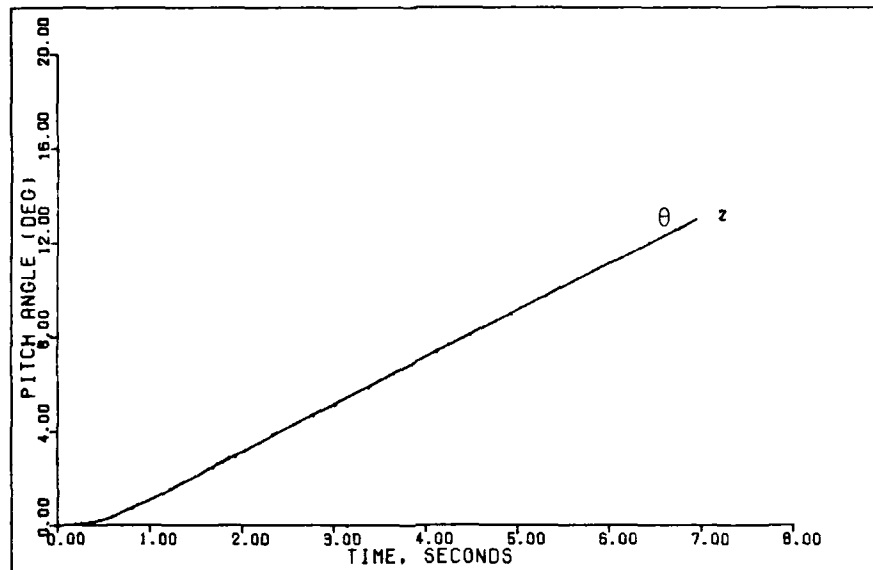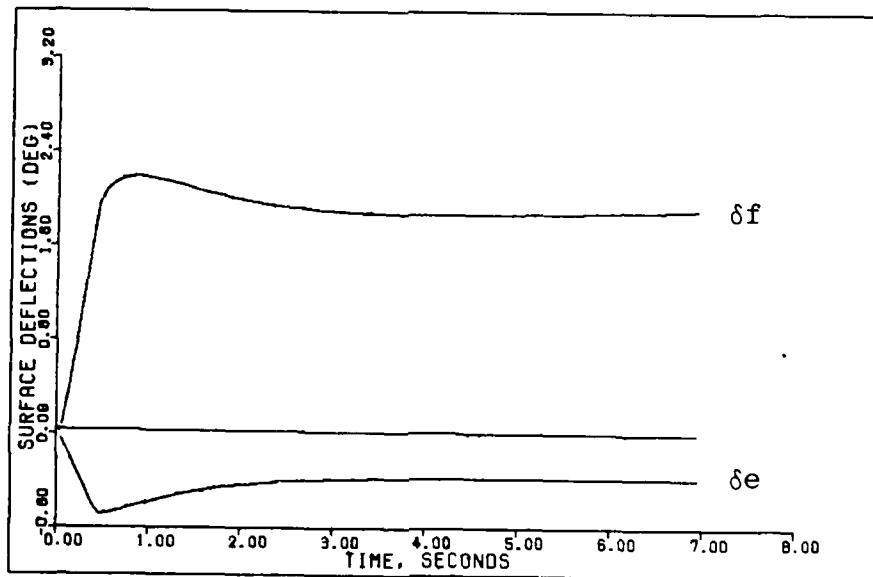Desired Preliminary Design to a 1g Step Command
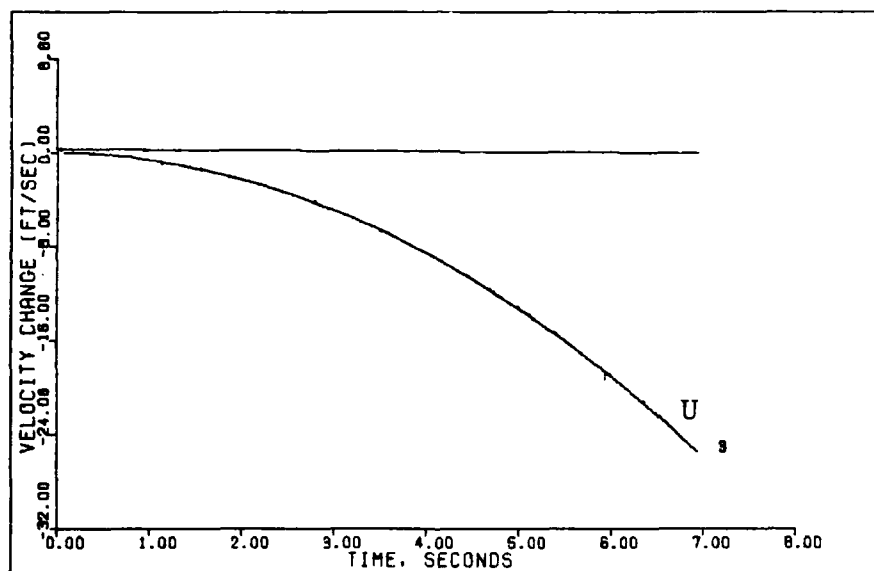(0.9 Mach 20,000 feet)

120

Figure 25.   Forward Velocity Change of the Desired
Preliminary Design to a 1g Step Command
(0.9 Mach 20,000 feet)

121

acceleration command is simultaneously sent to the controller. Pitch rate develops and then reduces to zero, in the steady state, while acceleration is held at zero. The aircraft rotates, developing an angle of attack, without experiencing longitudinal acceleration. The aircraft nose is pointed upward without altering the flight trajectory (Figures 26 through 29).

With the design, pointing can be accomplished while in an accelerated turn. For example, a 4 "g" turn can be commanded with the appropriate acceleration and pitch rate steps. Pointing during the turn can be accomplished by adding a pitch rate pulse on top of the steady-state command while keeping the acceleration command at its steady-state value. This same technique is successfully applied in the lateral-directional axis to develop yaw pointing. A pulse yaw rate command is applied while side acceleration is held constant.

A trade-off exists between speed of response and pureness of the maneuver. As illustrated by Figure 27, the pointing maneuver is not completely decoupled, and a small amount of acceleration is generated. Pointing can be quickened by making the command pulse larger in amplitude while reducing its duration. However, as larger pulses are commanded, more acceleration results. If duration is not reduced, a larger pointing angle is commanded than can be generated. The surfaces then saturate while attempting to

Figure 26. α Response of the Initial Pitch Pointing
System to a 2 deg/sec Pitch Rate Pulse of
0.9 sec Duration
(0.9 Mach 20,000 feet)

Figure 27. Pitch Rate and Acceleration Response of the
Initial Pitch Pointing System to a 2 deg/sec
Pitch Rate Pulse of 0.9 sec Duration
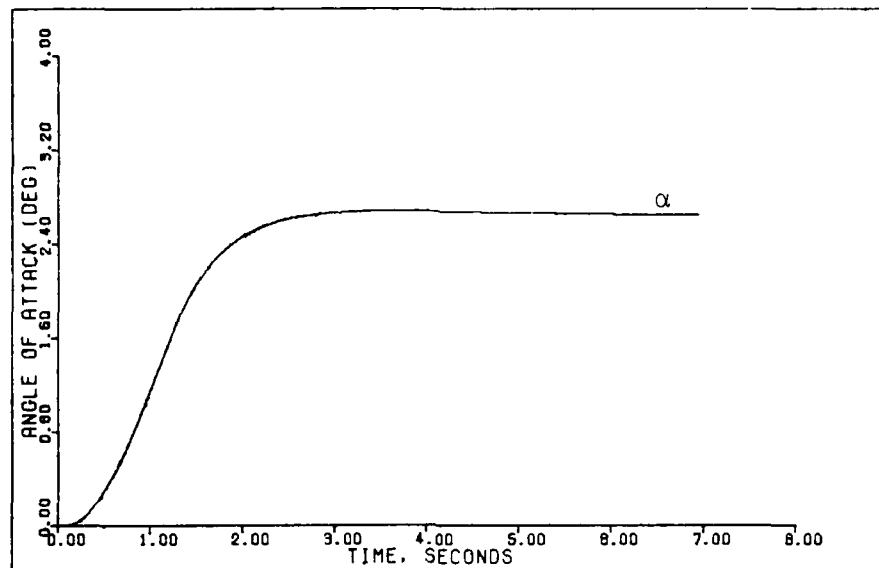(0.9 Mach 20,000 feet)

123
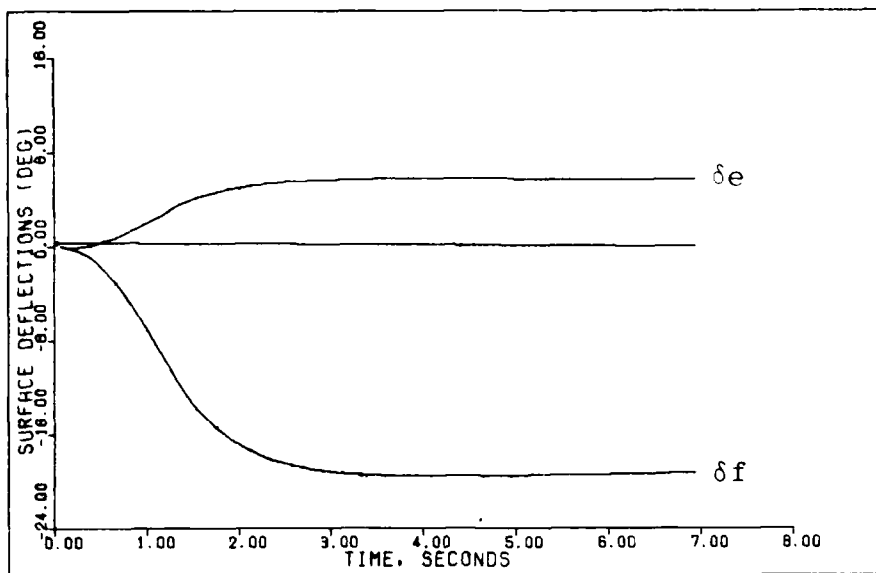
Figure 28.   Surface Response of the Initial Pitch
Pointing System to a 2 deg/sec Pitch Rate
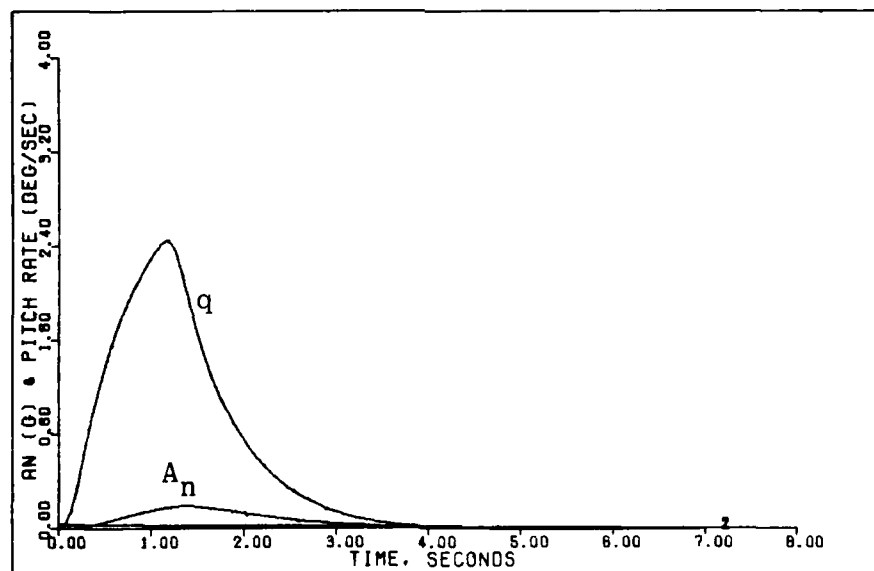Pulse of 0.9 sec Duration
(0.9 Mach 20,000 feet)
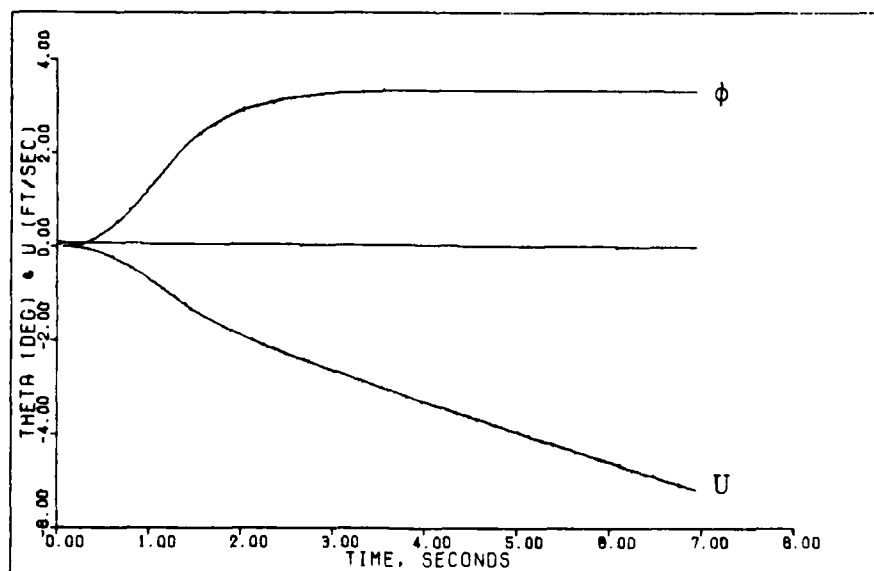
Figure 29.   Pitch Angle and Velocity Change of the
Initial Pitch Pointing System to a 2 deg/sec
Pitch Rate Pulse of 0.9 sec Duration
(0.9 Mach 20,000 feet)

124

satisfy the command, and thus decoupling is lost. If these
surfaces are providing stability augmentation, that is also
lost. As can be seen in Figure 28, surface rate limiting
is not a problem for this design. Maximum Pointing of 2.7
degrees is achieved with a full upward flap deflection of
-20 degrees.

The final design sets the pulse peak at a point
determined by a compromise between quickness and purity.
Pulse duration is selected so that the product of the pulse
peak and pulse duration does not exceed the maximum pointing
capability. Proportional control of pointing is obtained by
varying the pulse value from zero to this peak value while
holding the pulse width constant.

The final lateral-directional design results in a
system in which roll rate, yaw rate, and side acceleration
are commanded. The system provides conventional roll rate
response and direct sideforce control. Lateral pointing
can be accomplished in the same manner as employed for
longitudinal pointing. The roll rate system requires fur-
ther discussion. The equation for side force, including
the gravitational force, can be written as:

$$F_{y_{cg}} = m(\dot{V} + Ur - pW) - gm\cos\theta\sin\phi \qquad (4.19)$$

Dividing by m, multiplying the right hand side by $\frac{U}{U}$, and
letting $A_{y_{cg}} = \frac{F_{y_{cg}}}{m}$ yields:

$$A_{y_{cg}} = U(\dot{\beta} + r - p\alpha - \frac{g}{U}(\sin\phi\cos\theta)) \qquad (4.20)$$

The desire is to roll about the velocity vector without developing a sideslip angle or side acceleration on the aircraft. Conventionally, the method employed is to feed back an estimate of $\dot{\beta}$ to the rudder so that as the aircraft rolls, β is driven to zero. Equation (4.20) is solved for $\dot{\beta}$:

$$\dot{\beta} = \frac{A_{y_{cg}}}{U} - r + p\alpha + \frac{g}{U}\sin\phi\cos\theta \qquad (4.21)$$

Using Equation (2.34):

$$\dot{\beta} = \frac{A_{y_p}}{U} - \frac{(\ell_x)\dot{r}}{U} - r + p\alpha + \frac{g}{U}\sin\phi\cos\theta \qquad (4.22)$$

For steady state rolls, r is a constant and $\dot{r}$ is zero; therefore

$$\dot{\beta} = \frac{A_{y_p}}{U} - r + p\alpha + \frac{g}{U}\sin\phi\cos\theta \qquad (4.23)$$

$$\dot{\beta} \approx \frac{A_{y_p}}{U} - r + p\alpha \qquad (4.24)$$

The approximation comes about in the following way. If the aircraft is simply rolling, the $\frac{g}{U}\sin\phi\cos\theta$ term should be included. Usually, rolling is a means of developing a desired bank angle to develop a turn. In such cases the longitudinal lift force is increased by the pilot to hold altitude constant (assuming a level turn). Thus, the

126

$\frac{g}{U}\sin\phi\cos\theta$ term is exactly cancelled by a portion of the lift force. In the analyses in this thesis, the longitudinal and lateral-directional axes are decoupled. Thus, there is no way of including that portion of the lift force into the lateral-directional equations.

If the aircraft is rolled into a bank without inclusion of the lift force, the rudder is deflected to counter the side acceleration component developed by the gravitational force. This is not desired for a turn. For the investigation at hand, this poses a problem. How to simulate a 360 degree roll and a banked turn with the equations that have been developed? For pure rolling maneuvers, such as 360 degree rolls, the full equations should be used since generally no additional *lift force* is developed to counter the gravity term. However, the assumption that $\sin\phi = \phi$(radians) is used in the equations developed for the aircraft model. This assumption is used to simplify the equations, but above a roll angle of ten degrees, it is invalid. Thus, for both 360 degree rolls and turns, the gravity term is dropped from both the β and sideforce equations.

The controller developed for rolling response commands the acceleration A_{y_p} to zero, roll rate to the desired level, and yaw rate to a value developed by solving Equation (4.23) for r assuming $\dot{\beta}$ is zero.

127

$$r = -\dot{\beta} + p\alpha + \frac{A_{y_p}}{U} + \frac{g}{U}\sin\phi\cos\theta \qquad (4.25)$$

$$r = p\alpha + \frac{A_{y_p}}{U} + \frac{g}{U}\sin\phi\cos\theta \qquad (4.26)$$

For turning flight, this becomes:

$$r = p\alpha + \frac{A_{y_p}}{U} \qquad (4.27)$$

Assuming sideforce is kept close to zero, the A_{y_p} term can be neglected. Figures 30 and 31 are the results of the roll rate design for maximum inputs at 0.9 Mach and 20,000 feet. Responses for a 10 degree per second command at the same flight condition are shown in Figures 32 and 33.

Sideforce is developed by commanding A_{y_p} to a constant value and roll rate to zero. Yaw rate is commanded to the value developed using Equation (4.12)

$$r = \left[\frac{1845}{U}\right] A_{y_p} \qquad (4.28)$$

A maximum sideforce maneuver is commanded at 0.9 Mach 20,000 feet for this design in Figures 34 through 37.

As in the longitudinal axis, sideforce can be developed while the aircraft is in turning flight or during a combat maneuver with the design by superimposing those commands over the normal roll commands.
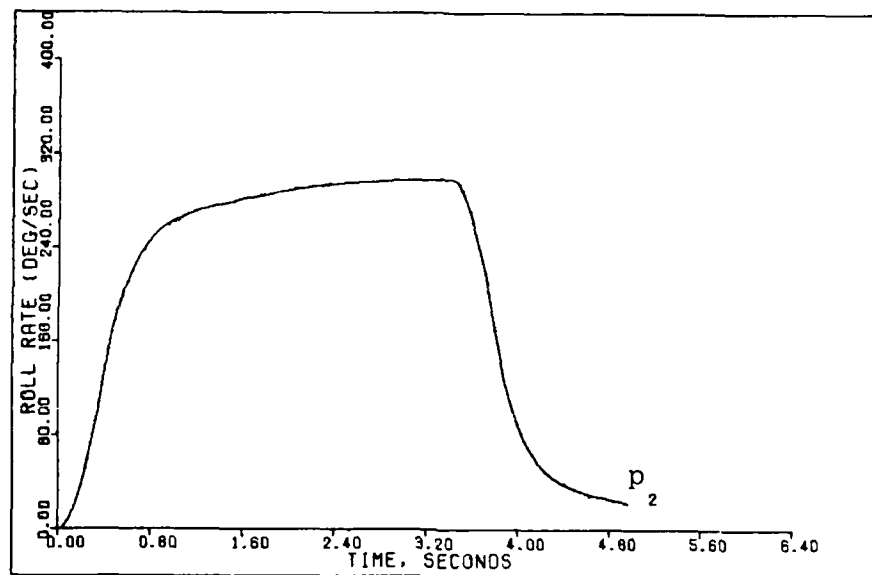
Figure 30.   Roll Rate Response of the Initial Roll Rate
Command System to 308 deg/sec Pulse Command
(0.9 Mach 20,000 feet)
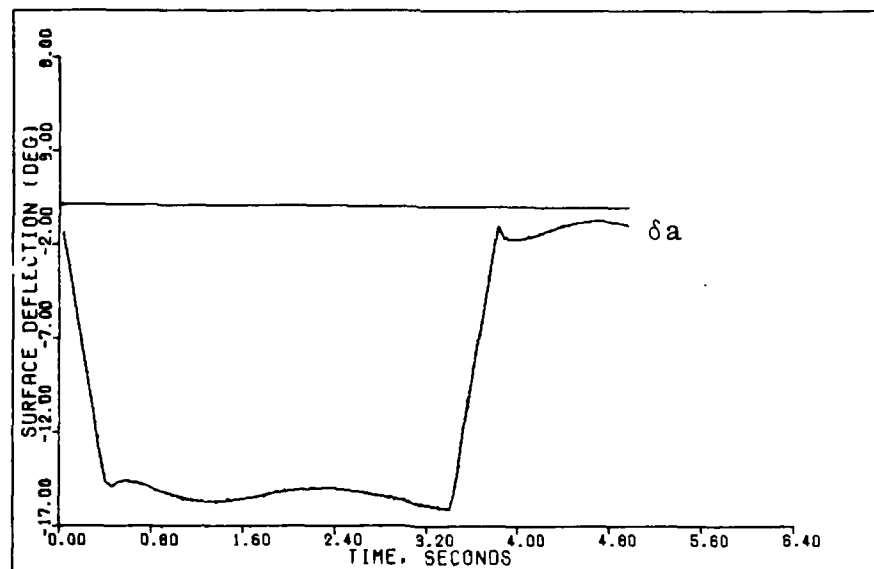
Figure 31.   Aileron Response of the Initial Roll Rate
Command System to a 308 deg/sec Pulse Command
(0.9 Mach 20,000 feet)

129
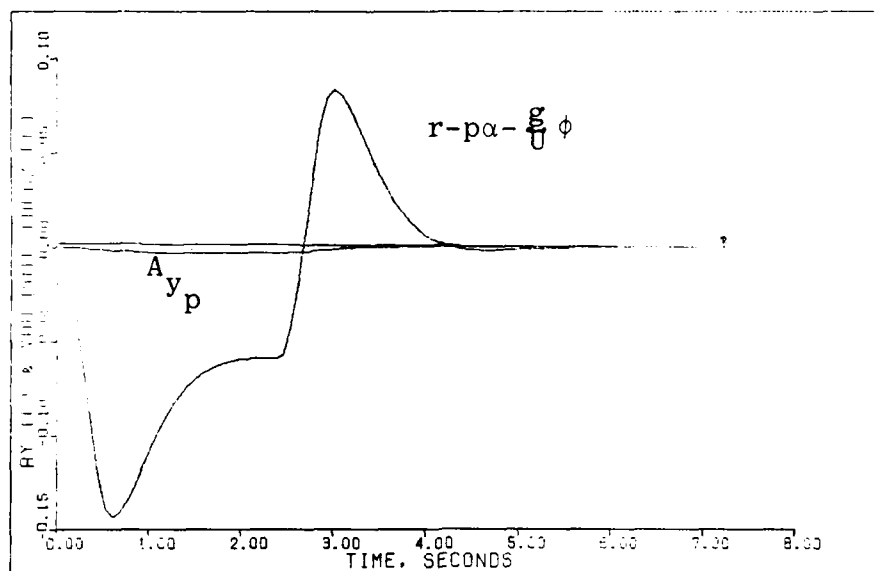
Figure 32. Sideforce and Output Feedback Response of
the Initial Roll Rate Command System to a
10 deg/sec Pulse
(0.9 Mach 20,000 feet)
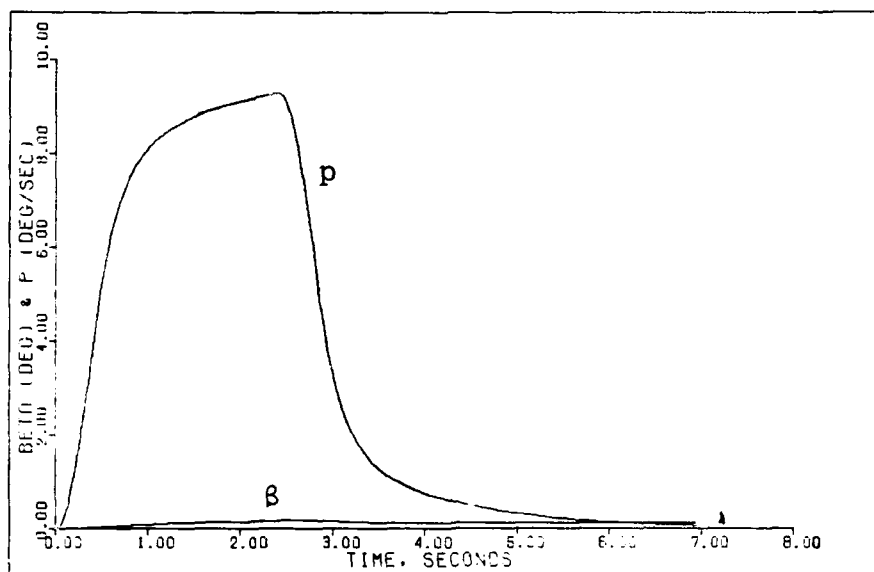
Figure 33. Roll Rate and Sideslip Response of the
Initial Roll Rate Command System to a
10 deg/sec Pulse
(0.9 Mach 20,000 feet)

130
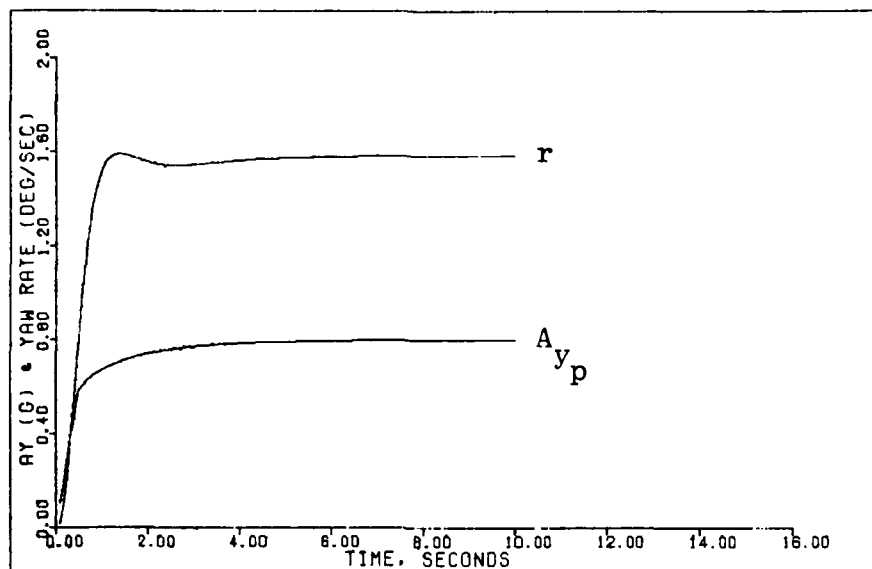
Figure 34. Yaw Rate and Sideforce Responses of the
Sideforce System to a 0.8g Step Command
(0.9 Mach 20,000 feet)
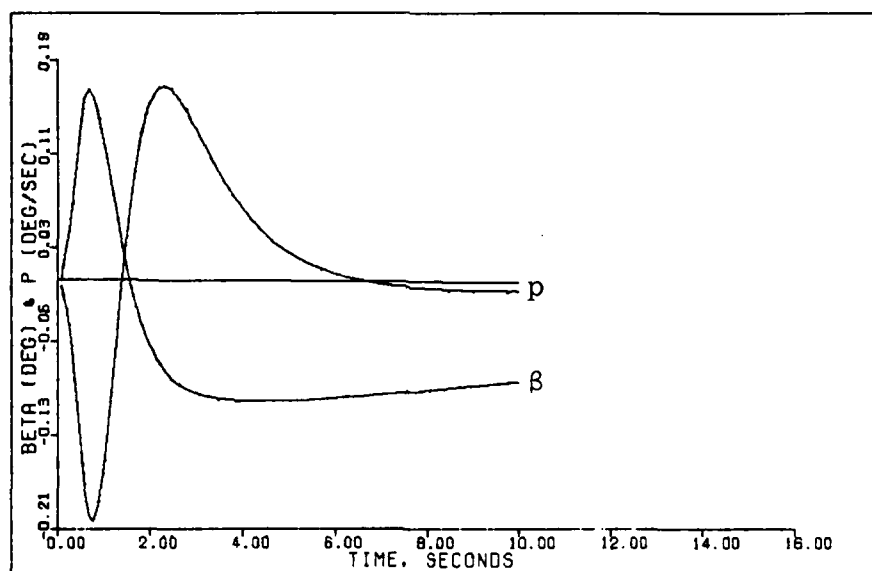
Figure 35. Sideslip and Roll Rate Response of the
Sideforce System to a 0.8g Step Command
(0.9 Mach 20,000 feet)

131
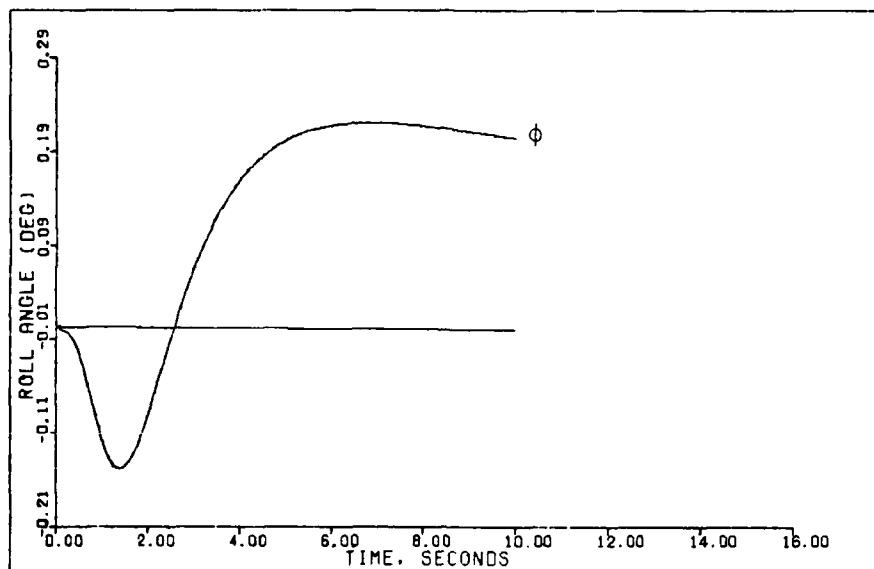
Figure 36. Roll Angle Response of the Sideforce
System to a 0.8g Step Command
(0.9 Mach 20,000 feet)
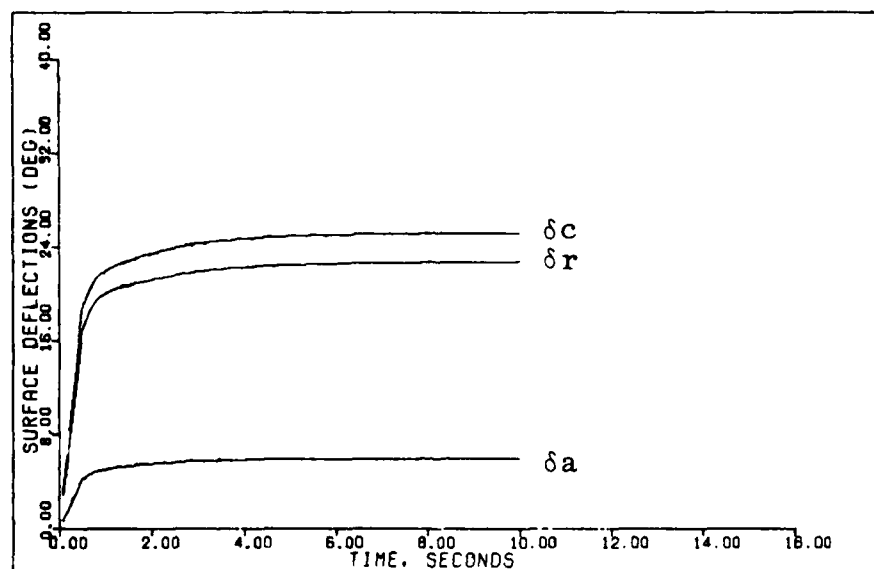
Figure 37. Surface Response of the Sideforce
System to a 0.8g Step Command
(0.9 Mach 20,000 feet)

132

Pilot Interface

A major design consideration for any control system
is the means by which the pilot injects his commands. In
current fighter aircraft, the pilot is usually flying with
one hand on the stick and the other on the throttle.
Because of the highly maneuverable nature of combat with
the associated high workload and the criticality of fast
response, it is important to provide complete control with-
out requiring the pilot to release either stick or throttle.
At last count, the pilot had six functions to perform with
switches on the throttle (not including thrust control
itself) and up to seven functions on the stick in addition
to conventional pitch and roll control. It is not practical
to add extra input devices and expect anything but reduced
performance.

The approach taken in this study is to preserve the
conventional pilot control input methods. This is accom-
plished by an interface computation that provides the digital
controller with the proper inputs for normal operation. In
all cases, these interface computations are kept extremely
simple. Note that in each case, all inputs to the controller
must be specified. Two are required for pitch, while three
are needed for the lateral-directional controller. In pitch
control, the conventional stick input is accepted as a "g"
command, and the two inputs needed by the controller are
developed from Equation (4.11) as shown in Figure 38. In

133

roll, the commands to the controller are developed as illustrated in Figure 39. For sideforce control, the rudder pedal input is used as illustrated in Figure 40. The development of a yaw rate input is from Equation (4.12).

Roll and sideforce command methods can be combined for the lateral-directional system. The zero input to the A_{y_p} command path, needed for a roll rate response system, can be supplied by the rudder pedal transducer when no force is applied by the pilot. The same can be said for the zero roll rate command for the sideforce system. The zero input can be provided by the roll stick transducer.

Pointing is assumed to be commanded from an automated fire control system. However, manual control can be provided using a twist throttle for pitch pointing command and switching the rudder pedal signal so that it provides an input to the lateral pointing system.

The complete control system block diagrams are shown in Figures 41 and 42 with the pilot interface and controller separated by the dot-dash line. The portion in dashed lines indicates the pointing system.

Instabilities

As discussed in Chapter I, because of the need for a controller that commands rates and accelerations, conditional stability is accepted for the designs. However, care is exercised to identify all instabilities encountered in the design process. Two general types of instabilities are
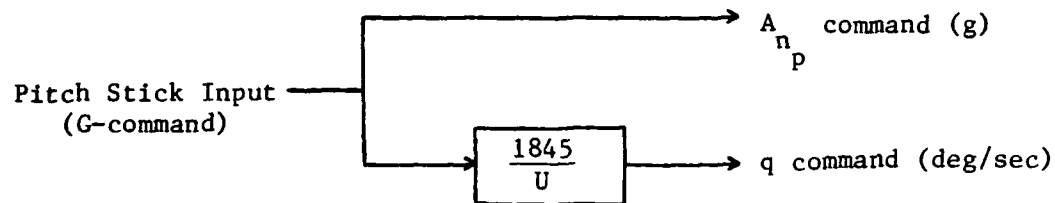
Figure 38.   Pilot Interface for the G-Command System
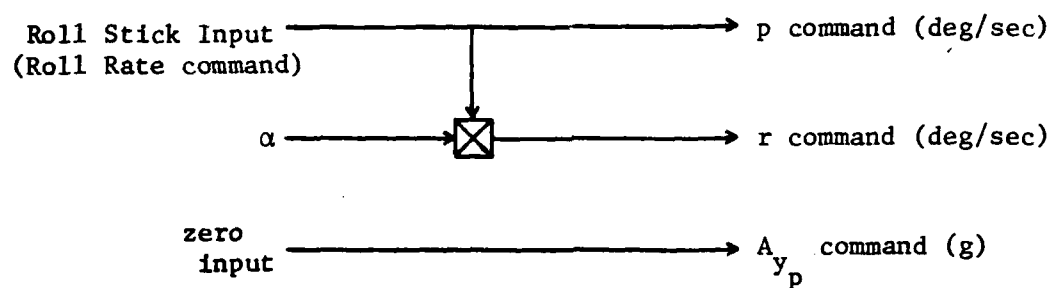
Figure 39.   Pilot Interface for the Roll Rate
Command System
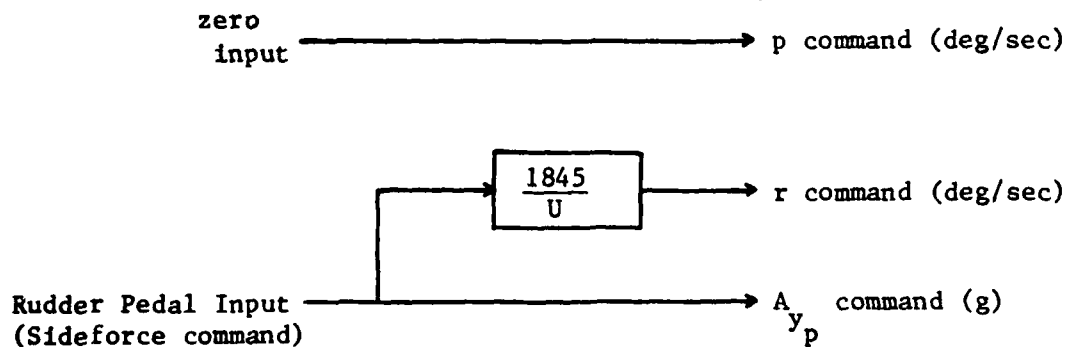
Figure 40.   Pilot Interface for the Sideforce System

135
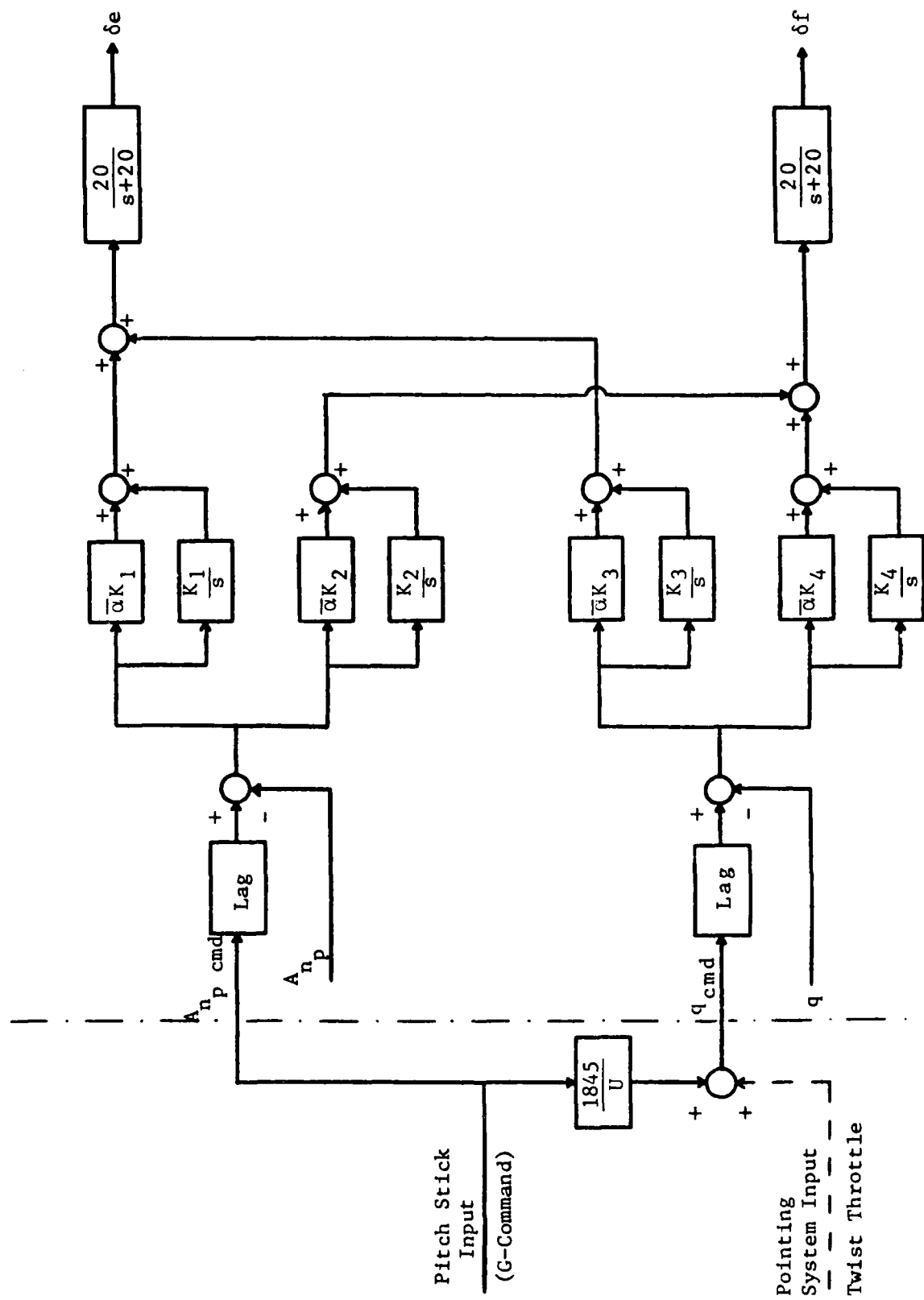
Figure 41. Block Diagram of Longitudinal G-Command System With Pilot Interface Addition and Including the Pitch Pointing System

136
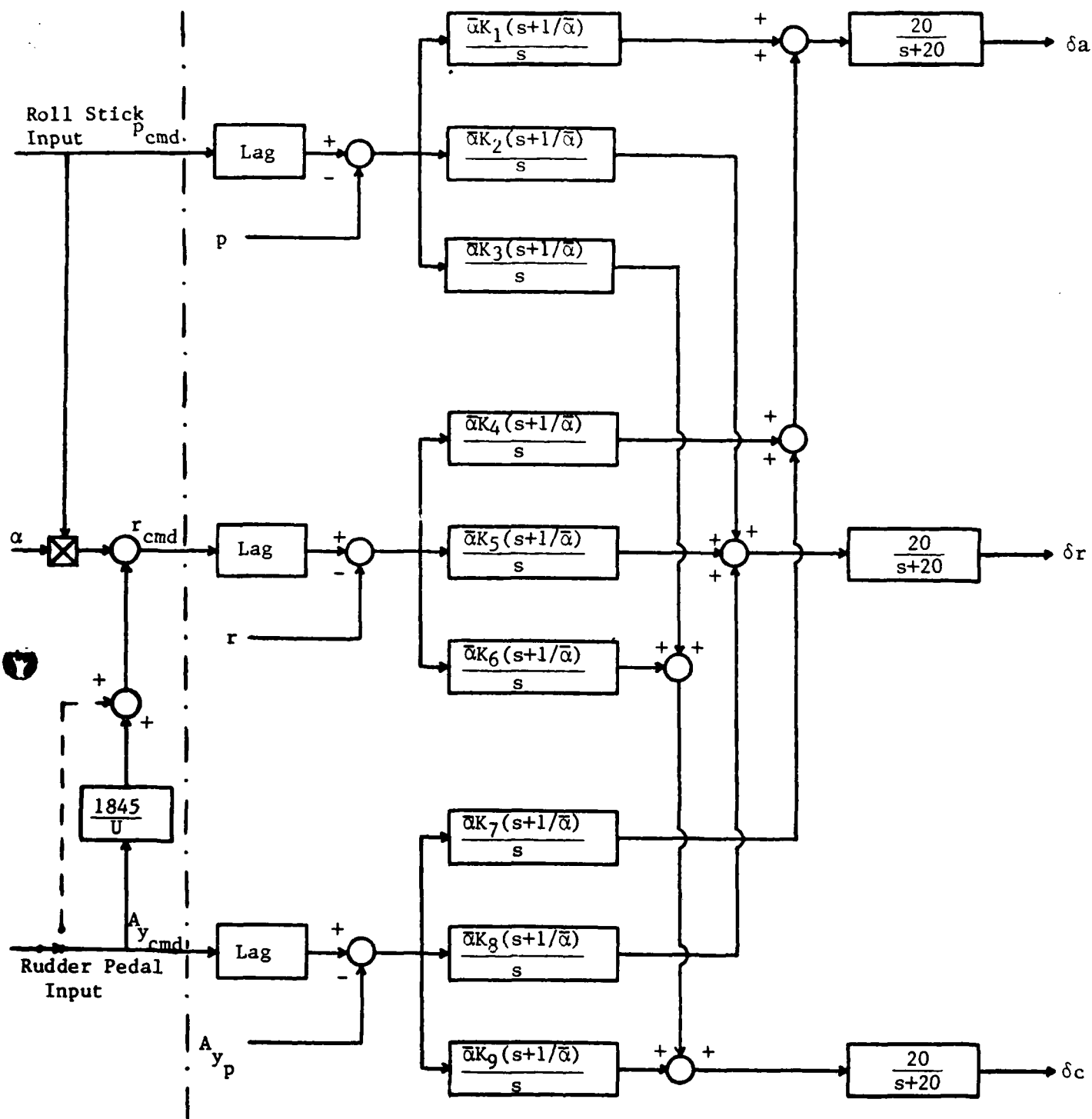
Figure 42. Block Diagram of the Roll Rate Command System
and Direct Sideforce System with Pilot Interface
Addition (Yaw Pointing System is included)

137

found. These consist of a low gain instability and a high gain instability. The low gain stability is seen in the longitudinal designs and is the result of having a statically unstable aircraft. As control system gain is reduced, a point is reached where the unstable aircraft reappears; adequate augmentation is not being provided. This establishes a lower gain boundary for all subsonic longitudinal designs.

In both longitudinal and lateral-directional designs, an oscillation is consistently encountered for high gains. An example is shown in Figures 43 and 44. This is the longitudinal design at 0.9 Mach and 20,000 feet with parameters of $\bar{\alpha} = 1.0$, $\epsilon = 1.0$, and Σ elements equal to one. Figures 11 and 12 illustrate the same high gain instability in the very simple regular design discussed earlier in this chapter. It is apparent that the instability occurs regardless of the inclusion of sensor or actuator dynamics or a measurement matrix. The observed frequency of the oscillation is always a subharmonic of the sampling frequency. Further investigation is warranted to enable the setting of boundaries for such an instability. The system roots are checked and are stable for the system responses shown. The initial attempt of each design generally results in this instability. As gain is reduced, the oscillation dies out. It is fortunate that this high gain limit usually does not compromise performance of the designs. The gain
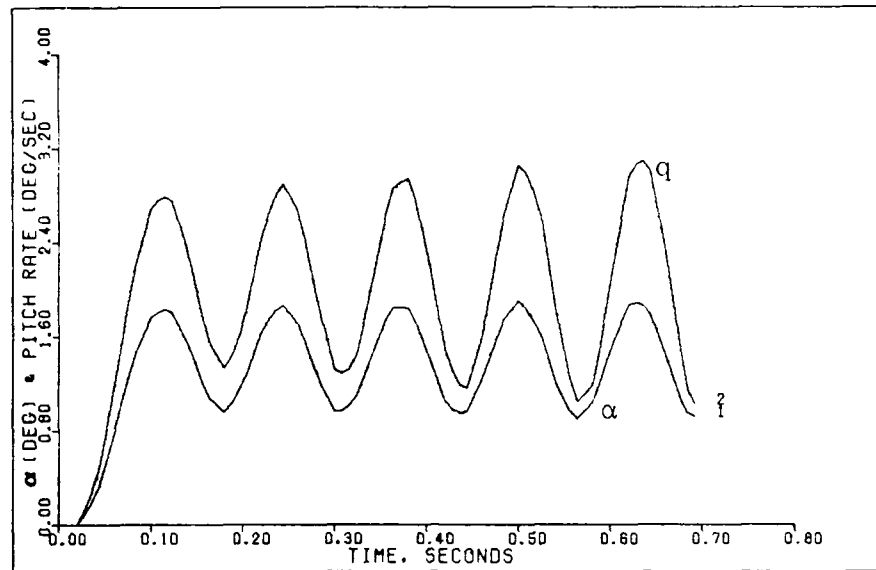
Figure 43. Response Plot for the Rate Controller to
a 2 deg/sec Step Command (0.9 Mach 20,000 feet)
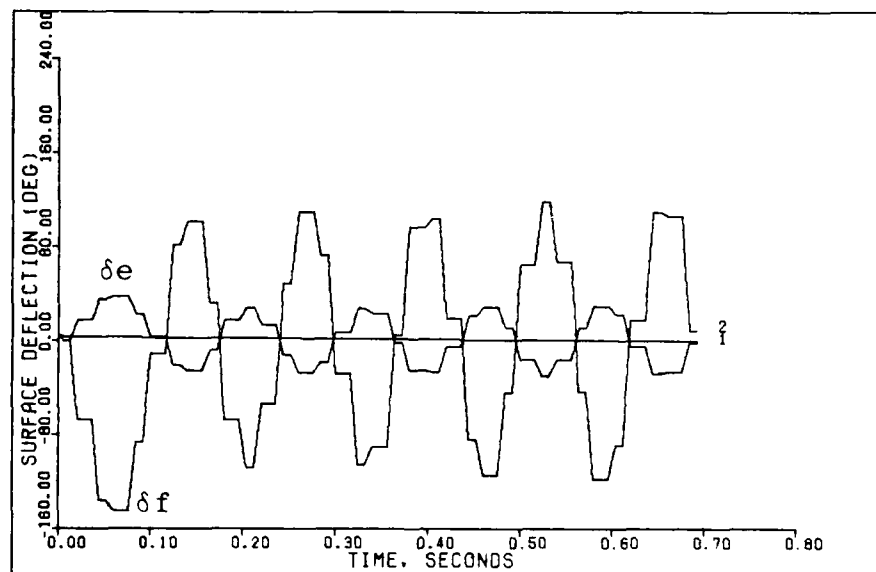
Figure 44. Surface Position Plot for the Rate
Controller to a 2 deg/sec Step Command
(0.9 Mach 20,000 feet)

139

reductions required to meet surface rate limit requirements prevent the instability. However, as faster actuators become available, this should be considered as a limiting condition in design performance.

V. Evaluation

Time Response Analysis

For the longitudinal designs, time responses for 1 g step commands are presented for each flight condition under study. Five degree per second roll rate pulses are used to evaluate the roll rate design. Maximum step commands are used for the sideforce design demonstrations. In addition, fuselage pitch pointing is shown at the 0.9 Mach 20,000 feet condition for a pitch rate step command.

The time responses presented exhibit the properties desired of the design. Stability is adequate, and the system provides proper, fast, well-behaved responses. The outputs are free of ringing or oscillations. Control surface deflections are within both rate and position limits for all maneuvers. Control of body rates and accelerations is provided using reliable feedbacks.

The designs are established using maximum estimated commands for each flight condition to provide system gains which do not exceed surface rate or position limits. Responses for maximum commands are presented in Appendix C. Such maximum maneuvers are not meant to imply that the aircraft model is an adequate representation for such large commands; they are used only to give an indication of the maximum acceptable system gains to prevent exceeding hardware limits.

141

Prior to each set of responses, the design values, controller gains, and measurement matrix elements are specified.

- -

Design Data for the G-Command System

Flight Condition: 0.9 Mach 20,000 feet

$T = 0.02$

$\bar{\alpha} = 1.0$

$$\underline{\Sigma} = \begin{bmatrix} 0.1 & 0.0 \\ 0.0 & 2.35 \end{bmatrix}$$

$\varepsilon = 1.0$

$$\underline{M} = \begin{bmatrix} 0 & 0 & 0 & 0 & 0 \\ 0 & 0 & 0 & 0 & 0.1 \end{bmatrix}$$

$$\underline{K}_0 = \underline{K}_1 = \begin{bmatrix} -0.01299 & -0.03534 \\ 0.04827 & -0.05016 \end{bmatrix}$$

Input ramp time: 0.4 seconds

Input commands: $A_{n_p} = 1g$ step

$$q = \left[\frac{1845}{U} \right] A_{n_p} = 1.977 \text{ deg/sec}$$

NOTE: Step inputs are ramped to steady state over a specified time. This time is designated as the "input ramp time" given above.

142
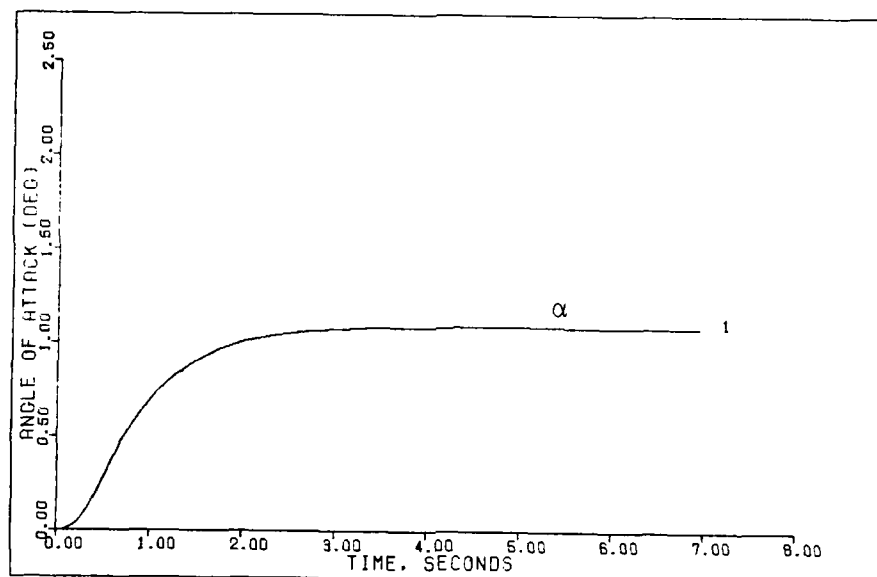
Figure 45a. G-Command System Response to a 1g Step
Command (0.9 Mach 20,000 feet)

Figure 45b. G-Command System Response to a 1g Step
Command (0.9 Mach 20,000 feet)

142a

Figure 45c.   G-Command System Response to a 1g Step
            Command (0.9 Mach 20,000 feet)
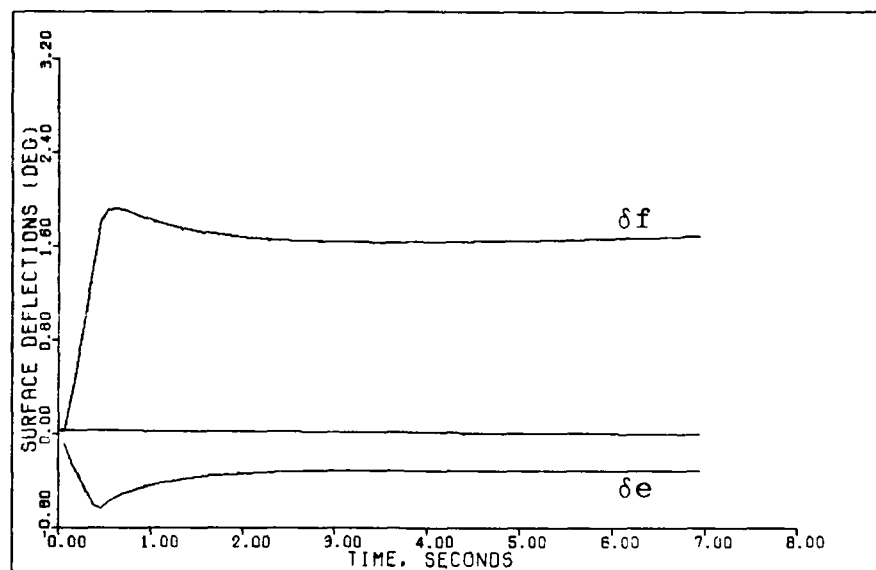
Figure 45d.   G-Command System Response to a 1g Step
            Command (0.9 Mach 20,000 feet)

143

Design Data for the Pitch Pointing System

Flight Condition: 0.9 Mach 20,000 fee'

$T = 0.02$

$\bar{\alpha} = 0.5$

$$\underline{\Sigma} = \begin{bmatrix} 2.5 & 0 \\ 0 & 1.0 \end{bmatrix}$$

$\varepsilon = 1.0$

$$\underline{M} = \begin{bmatrix} 0 & 0 & 0 & 0 & 0 \\ 0 & 0 & 0 & 0 & 0.1 \end{bmatrix}$$

$$\underline{K}_0 = \begin{bmatrix} -0.1623 & -0.007519 \\ 0.6034 & -0.01067 \end{bmatrix}$$

$$\underline{K}_1 = \begin{bmatrix} -0.3247 & -0.01504 \\ 1.207 & -0.02135 \end{bmatrix}$$

Input ramp time: 0.0 seconds

Input command: $A_{n_p} = 0.0$

$q = 1.0$ deg/sec step

NOTE: Step commands are ramped to steady state over a specified time. This time is designated as the "input ramp time" given above.
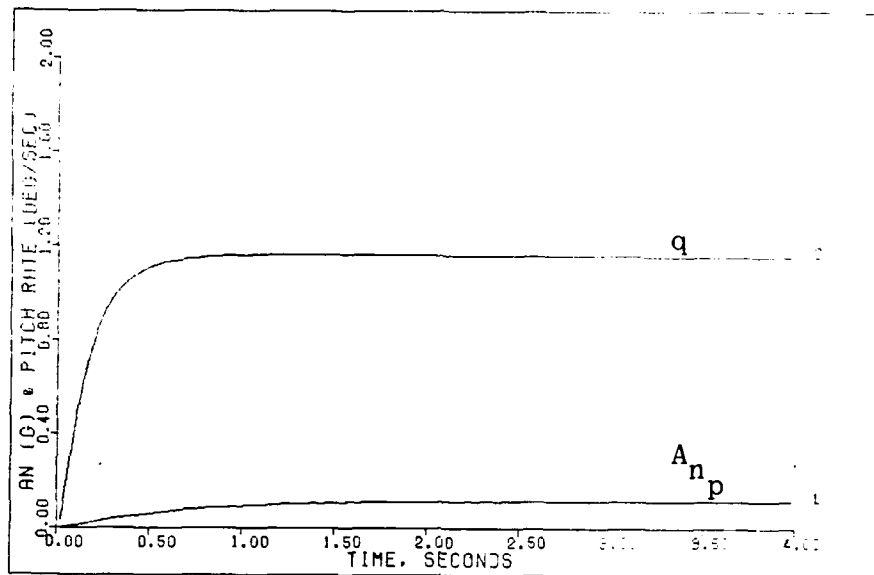
Figure 46a. Pitch Pointing System Response to a
1 deg/sec Step Command (0.9 Mach 20,000 feet)

Figure 46b. Pitch Pointing System Response to a
1 deg/sec Step Command (0.9 Mach 20,000 feet)

145

Design Data for the Roll Rate Command System

Flight Condition: 0.9 Mach   20,000 feet

$T = 0.02$

$\overline{\alpha} = 1.0$

$$\underline{\Sigma} = \begin{bmatrix} 1 & 0 & 0 \\ 0 & 1 & 0 \\ 0 & 0 & 1 \end{bmatrix}$$

$\varepsilon = 1.0$

$$\underline{M} = \begin{bmatrix} 0 & 0 & 0 & 0 & 0 \\ 0 & 0 & 0 & 0.25 & 0 \\ 0 & 0 & 0 & 0 & 0.25 \end{bmatrix}$$

$$\underline{K}_0 = \underline{K}_1 = \begin{bmatrix} 0.377 & -0.0030510 & -0.0120 \\ 1.460 & 0.0008075 & -0.0583 \\ 1.601 & -0.0005162 & -0.0287 \end{bmatrix}$$

Input ramp time: 0.4 seconds

Input command: $A_{y_p} = 0.0$

$p = 5$ deg/sec pulse for 3 sec duration

$r = p\alpha$ where $\alpha = 0.0325$ radians

NOTE: 1. Pulse inputs are ramped to a maximum value over a specified time. This time is designated as the input ramp time given above. The input is held at a maximum value for a duration time and then ramped back to zero. Both ramp times have the same value.
   2. Rolls are performed about the velocity vector.

Figure 47a. Roll Rate Command System Response to a
5 deg/sec Pulse Command (0.9 Mach 20,000 feet)

Figure 47b. Roll Rate Command System Response to a
5 deg/sec Pulse Command (0.9 Mach 20,000 feet)

147

Figure 47c. Roll Rate Command System Response to a
5 deg/sec Pulse Command (0.9 Mach 20,000 feet)

Figure 47d. Roll Rate Command System Response to a
5 deg/sec Pulse Command (0.9 Mach 20,000 feet)

148
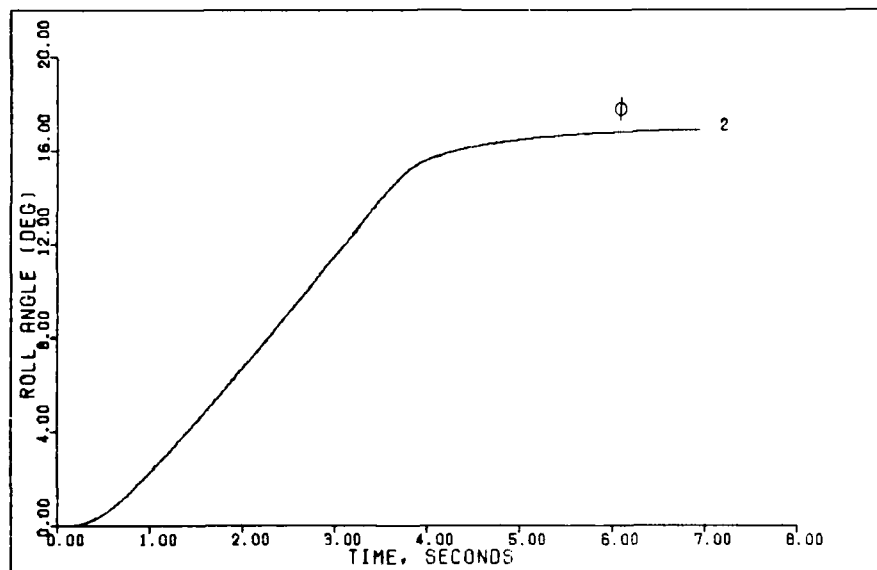
Figure 47e. Roll Rate Command System Response to a
5 deg/sec Pulse Command (0.9 Mach 20,000 feet)

Design Data for the Sideforce System

Flight Condition: 0.9 Mach 20,000 feet

$T = 0.02$

$\overline{\alpha} = 1.0$

$$\underline{\Sigma} = \begin{bmatrix} 1.0 & 0 & 0 \\ 0 & 2.3 & 0 \\ 0 & 0 & 1.0 \end{bmatrix}$$

$\varepsilon = 1.0$

$$\underline{M} = \begin{bmatrix} 0 & 0 & 0 & 0 & 0 \\ 0 & 0 & 0 & 0.25 & 0 \\ 0 & 0 & 0 & 0 & 0.25 \end{bmatrix}$$

$$\underline{K}_0 = \underline{K}_1 = \begin{bmatrix} 0.377 & -0.007018 & -0.0120 \\ 1.460 & 0.001857 & -0.0583 \\ 1.601 & -0.001187 & -0.0287 \end{bmatrix}$$

Input ramp time: 0.5 seconds

Input commands: $A_{y_p} = 0.8g$ step

$p = 0.0$

$r = \left[\dfrac{1845}{U} \right] A_{n_p} = 1.5816$ deg/sec

NOTE: Step inputs are ramped to steady state over a specified time. This time is designated as the input ramp time given above.

15C
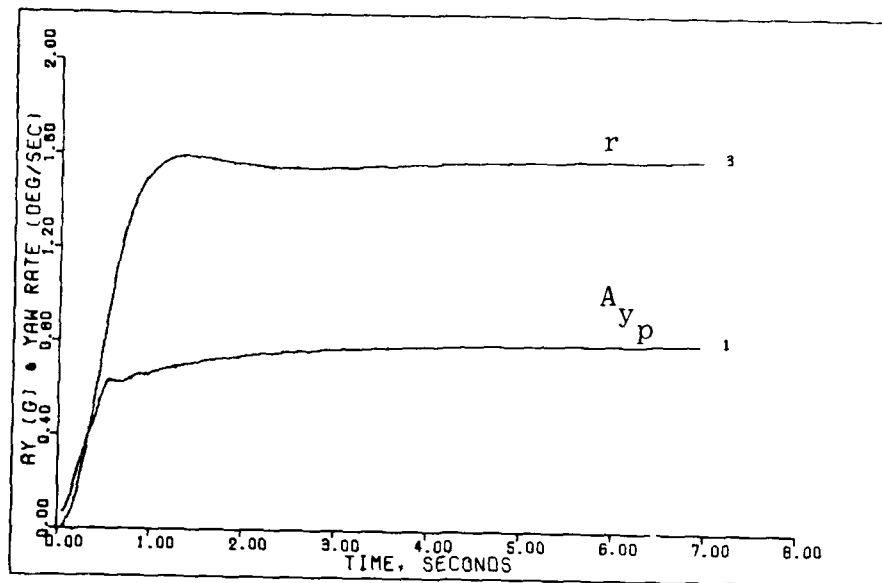
Figure 48a.   Sideforce System Response to a 0.8g Step
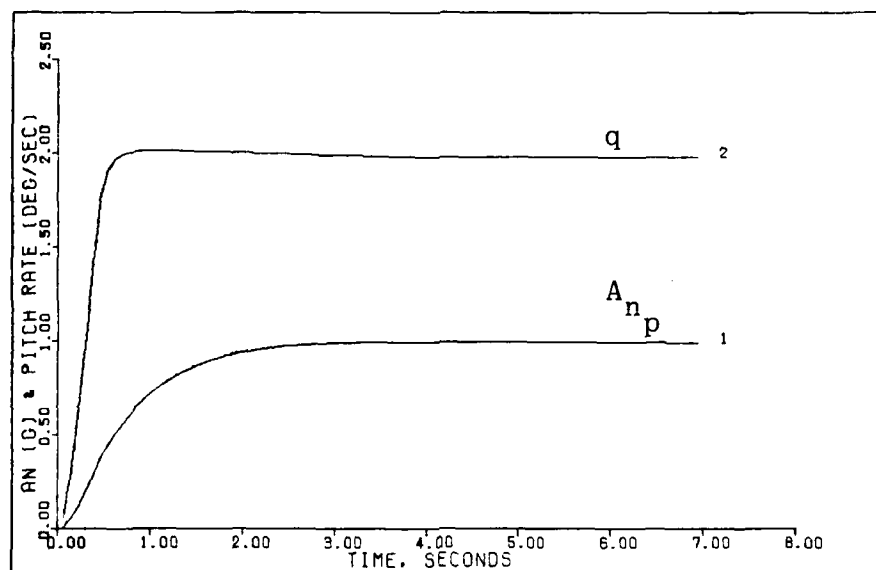Command (0.9 Mach 20,000 feet)

Figure 48b.   Sideforce System Response to a 0.8g Step
Command (0.9 Mach 20,000 feet)
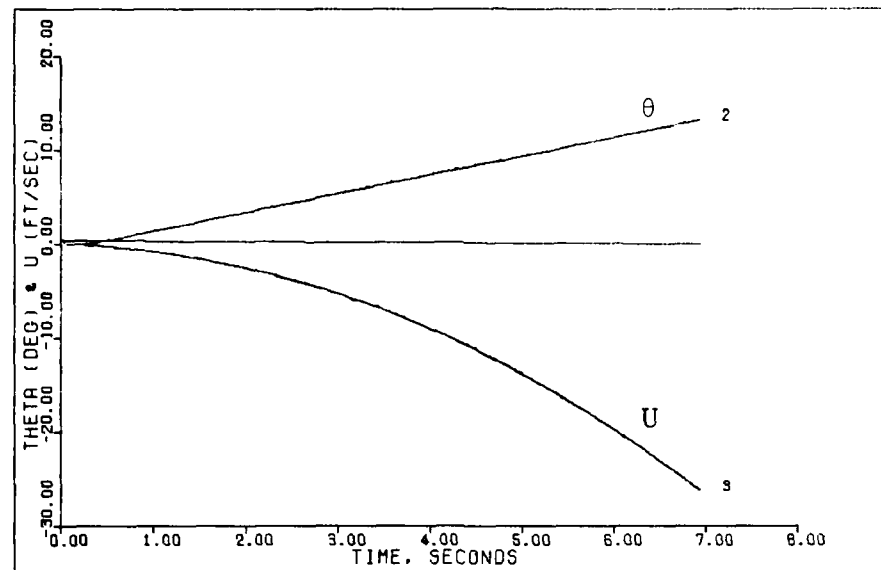
151

Figure 48c. Sideforce System Response to a 0.8g Step
Command (0.9 Mach 20,000 feet)

Figure 48d. Sideforce System Response to a 0.8g Step
Command (0.9 Mach 20,000 feet)

152

Design Data for the G-Command System

Flight Condition: 1.6 Mach   30,000 feet

$T = 0.02$

$\bar{\alpha} = 0.2$

$\underline{\Sigma} = \begin{bmatrix} 0.045 & 0 \\ 0 & 4.5 \end{bmatrix}$

$\epsilon = 2.5$

$\underline{M} = \begin{bmatrix} 0 & 0 & 0 & 0 & 0 \\ 0 & 0 & 0 & 0 & 0.1 \end{bmatrix}$

$\underline{K}_0 = \begin{bmatrix} -0.00425 & -0.01493 \\ 0.02389 & -0.1084 \end{bmatrix}$

$\underline{K}_1 = \begin{bmatrix} -0.02125 & -0.07464 \\ 0.1195 & -0.5419 \end{bmatrix}$

Input ramp time: 0.4 seconds

Input commands: $A_{n_p} = 1g$ step

$q = \left[\dfrac{1845}{U}\right] A_{n_p} = 1.159$ deg/sec

NOTE: Step inputs are ramped to steady state over a speci-
fied time.   This time is designated as the input
ramp time given above.

153
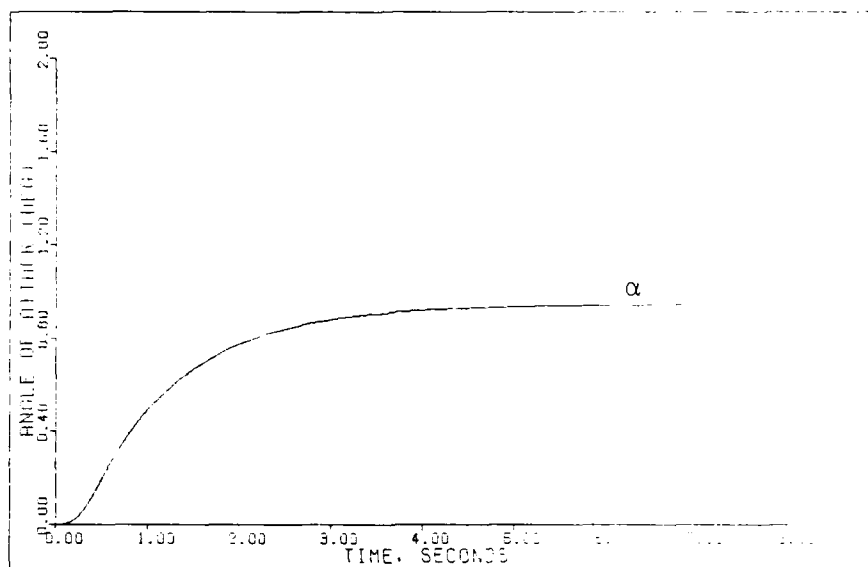
Figure 49a.   G-Command System Response to a 1g Step
Command (1.6 Mach 30,000 feet)
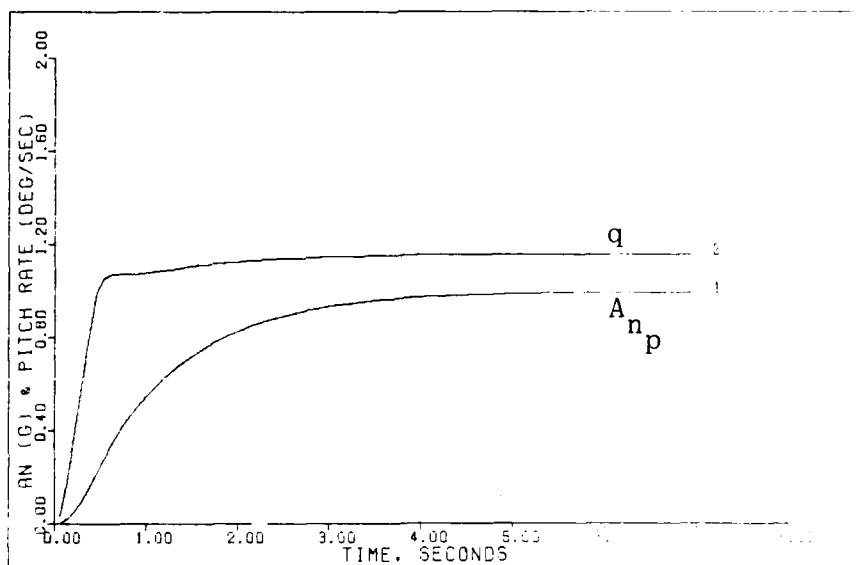
Figure 49b.   G-Command System Response to a 1g Step
Command (1.6 Mach 30,000 feet)

154

Figure 49c.   G-Command System Response to a 1g Step
              Command (1.6 Mach 30,000 feet)

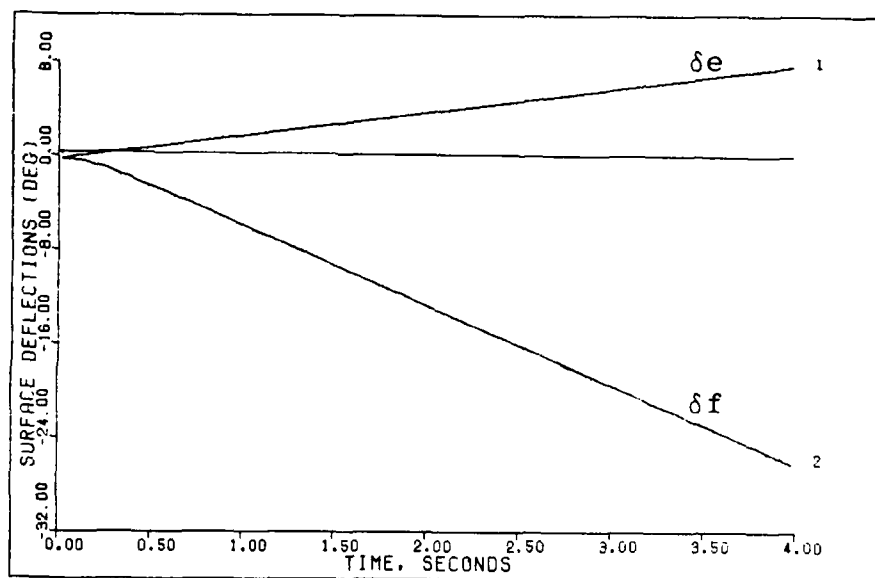Figure 49d.   G-Command System Response to a 1g Step
              Command (1.6 Mach 30,000 feet)

Design Data for the Roll Rate Command System

Flight Condition: 1.6 Mach 30,000 feet

$T = 0.02$

$\bar{\alpha} = 1.0$

$$\underline{\Sigma} = \begin{bmatrix} 1.0 & 0 & 0 \\ 0 & 1.0 & 0 \\ 0 & 0 & 1.0 \end{bmatrix}$$

$\varepsilon = 1.0$

$$\underline{M} = \begin{bmatrix} 0 & 0 & 0 & 0 & 0 \\ 0 & 0 & 0 & 0.25 & 0 \\ 0 & 0 & 0 & 0 & 0.25 \end{bmatrix}$$

$$\underline{K}_0 = \underline{K}_1 = \begin{bmatrix} 0.8775 & -0.006716 & -0.02719 \\ 2.0680 & 0.005948 & -0.09214 \\ 1.0260 & -0.0002461 & -0.02024 \end{bmatrix}$$

Input ramp time: 0.3 seconds

Input commands: $A_{y_p} = 0.0$

p = 5 deg/sec pulse for 3 sec duration

$r = p\alpha$ where $\alpha = 0.02932$ radians

NOTE: 1. Pulse inputs are ramped to a maximum value over a specific time. This time is designated as the input ramp time above. The input is held at a maximum value for a duration time and then ramped back to zero. Both ramp times have the same value.
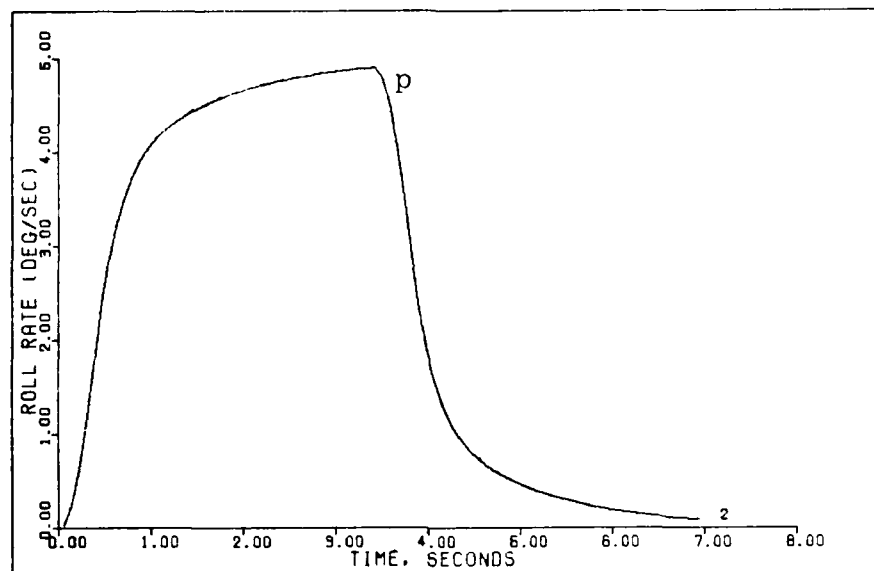2. Rolls are performed about the velocity vector.
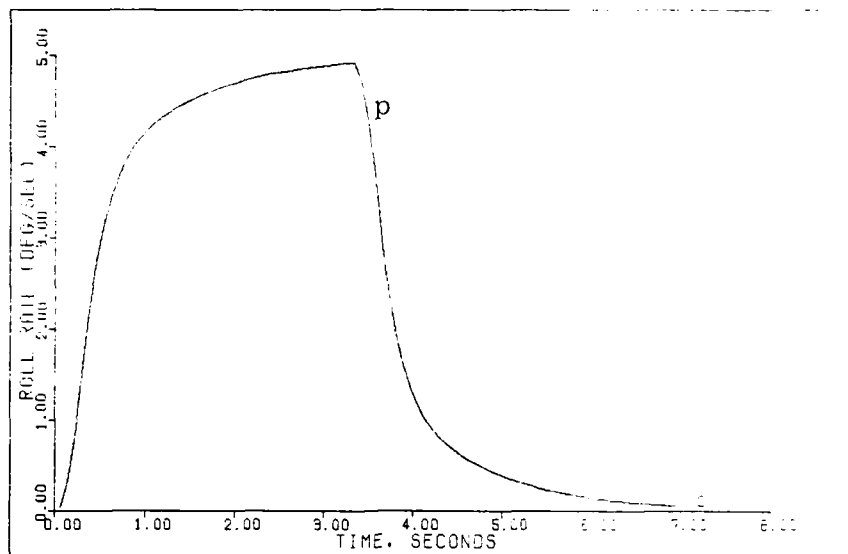
Figure 50a. Roll Rate Command System Response to a
5 deg/sec Pulse Command (1.6 Mach 30,000 feet)
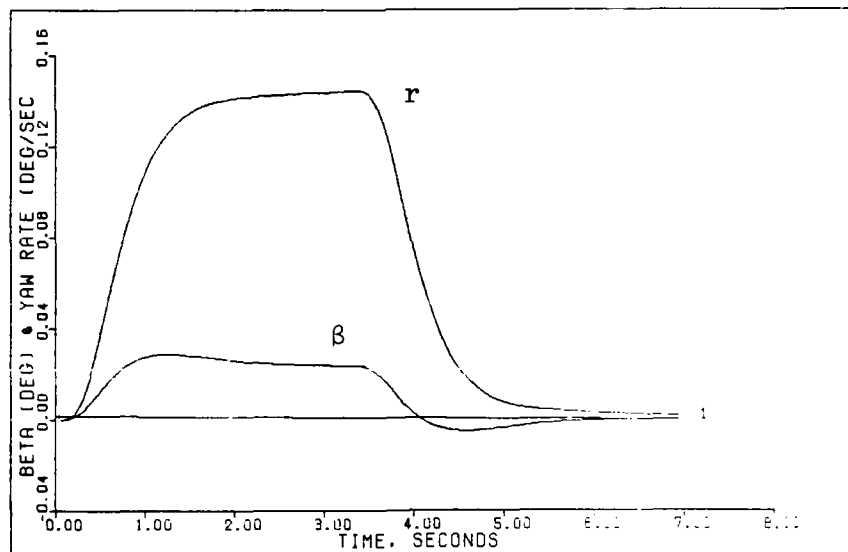
Figure 50b. Roll Rate Command System Response to a
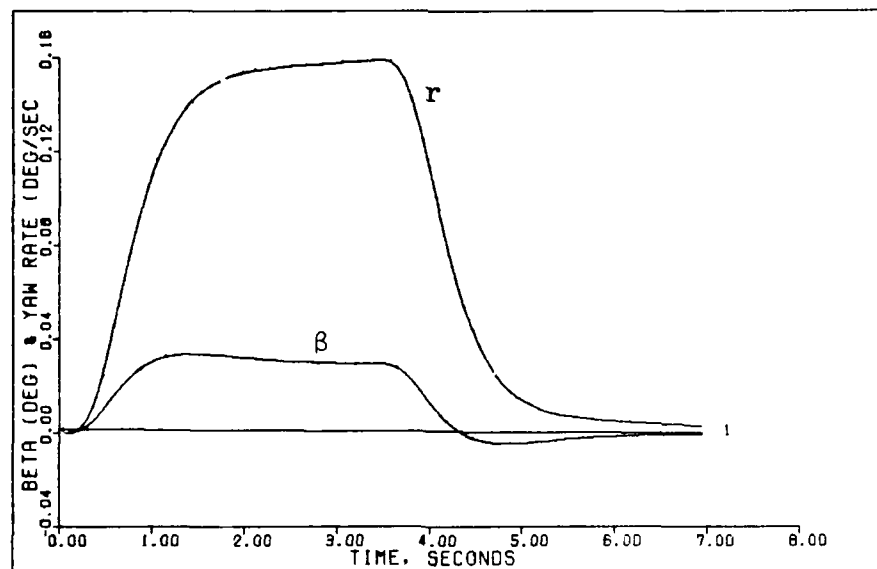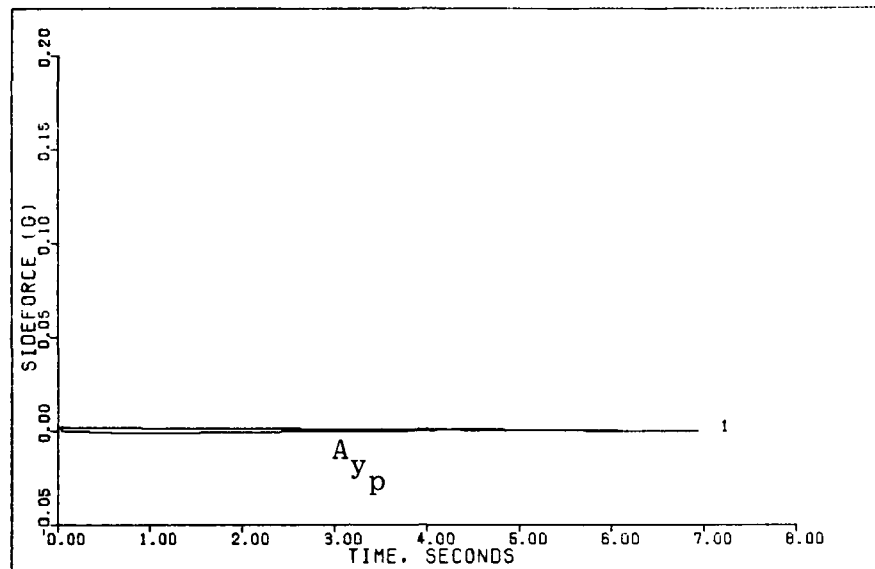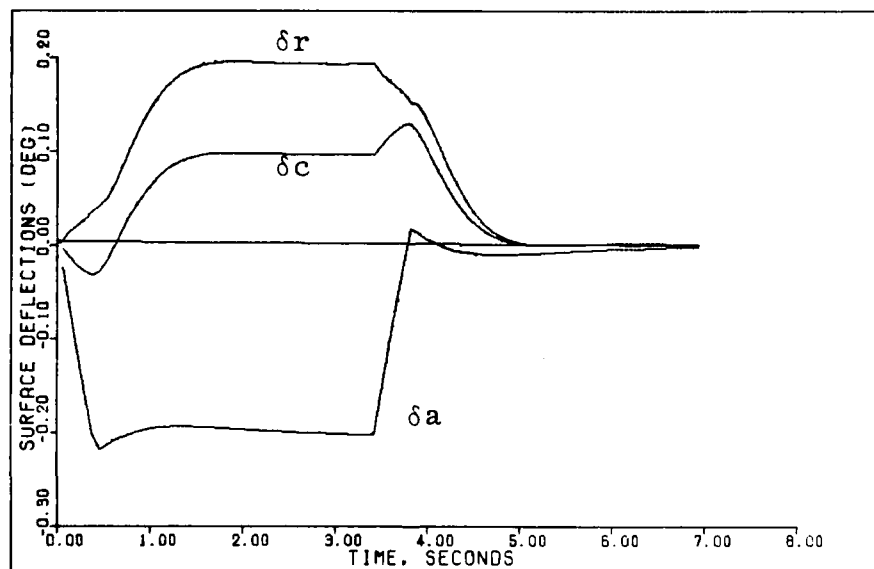5 deg/sec Pulse Command (1.6 Mach 30,000 feet)

157

Figure 50c. Roll Rate Command System Response to a
5 deg/sec Pulse Command (1.6 Mach 30,000 feet)

Figure 50d. Roll Rate Command System Response to a
5 deg/sec Pulse Command (1.6 Mach 30,000 feet)

158

Figure 50e.   Roll Rate Command System Response to a
5 deg/sec Pulse Command (1.6 Mach 30,000 feet)

Design Data for the Sideforce System

Flight Condition: 1.6 Mach 30,000 feet

$T = 0.02$

$\overline{\alpha} = 1.0$

$$\underline{\Sigma} = \begin{bmatrix} 1.0 & 0 & 0 \\ 0 & 1.0 & 0 \\ 0 & 0 & 1.0 \end{bmatrix}$$

$\varepsilon = 1.0$

$$\underline{M} = \begin{bmatrix} 0 & 0 & 0 & 0 & 0 \\ 0 & 0 & 0 & 0.1 & 0 \\ 0 & 0 & 0 & 0 & 0.1 \end{bmatrix}$$

$$\underline{K}_0 = \underline{K}_1 = \begin{bmatrix} 0.8775 & -0.016790 & -0.06799 \\ 2.0680 & 0.014870 & -0.23040 \\ 1.0260 & -0.0006154 & -0.05060 \end{bmatrix}$$

Input ramp time: 0.5 seconds

Input commands: $A_{y_p} = 0.6g$ step

$p = 0.0$

$r = \left[\dfrac{1845}{U} \right] A_{y_p} = 0.7$ deg/sec

NOTE: Step inputs are ramped to steady state over a specific time. This time is designated as the input ramp time given above.

160

Figure 51a.   Sideforce System Response to a 0.6g Step
              Command (1.6 Mach 30,000 feet)

Figure 51b.   Sideforce System Response to a 0.6g Step
              Command (1.6 Mach 30,000 feet)

Figure 51c. Sideforce System Response to a 0.6g Step Command (1.6 Mach 30,000 feet)

Figure 51d. Sideforce System Response to a 0.6g Step Command (1.6 Mach 30,000 feet)

162

Design Data for the G-Command System

Flight Condition: 0.6 Mach   30,000 feet

$T = 0.02$

$\overline{\alpha} = 1.0$

$$\underline{\Sigma} = \begin{bmatrix} 0.02 & 0 \\ 0 & 1.0 \end{bmatrix}$$

$\varepsilon = 1.0$

$$\underline{M} = \begin{bmatrix} 0 & 0 & 0 & 0 & 0 \\ 0 & 0 & 0 & 0 & 0.167 \end{bmatrix}$$

$$\underline{K}_0 = \underline{K}_1 = \begin{bmatrix} -0.00102 & -0.04998 \\ 0.02827 & -0.03316 \end{bmatrix}$$

Input ramp time: 0.4 seconds

Input commands: $A_{n_p} = 1g$ step

$$q = \left[\frac{1845}{U}\right] A_{n_p} = 3.091 \text{ deg/sec}$$

NOTE: Step inputs are ramped to steady state over a speci-
fied time. This time is designated as the input
ramp time given above.
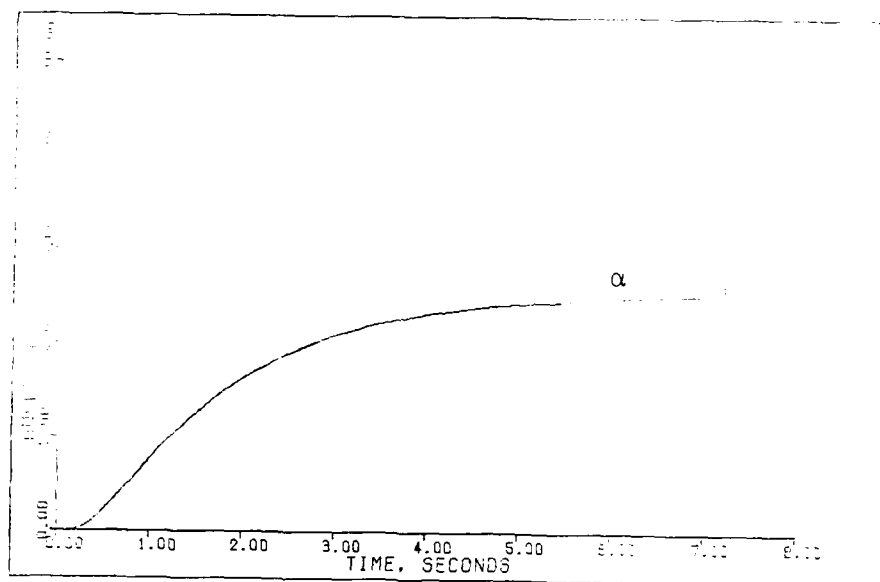
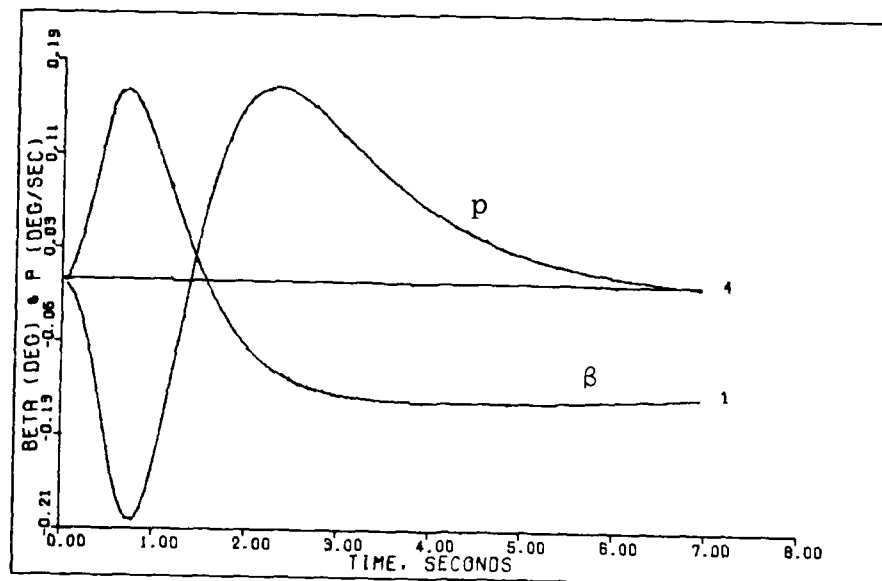Figure 52a. G-Command System Response to a 1g Step
Command (0.6 Mach 30,000 feet)
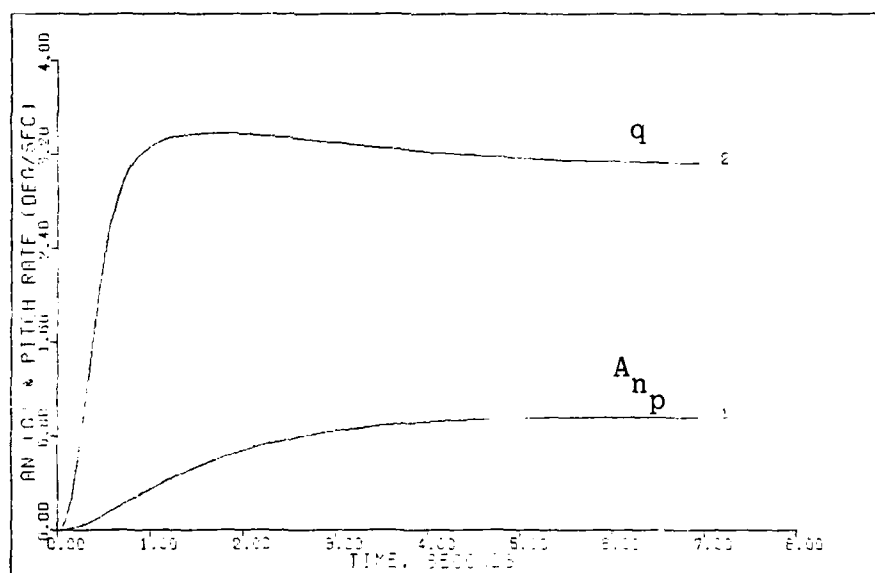
Figure 52b. G-Command System Response to a 1g Step
Command (0.6 Mach 30,000 feet)

164
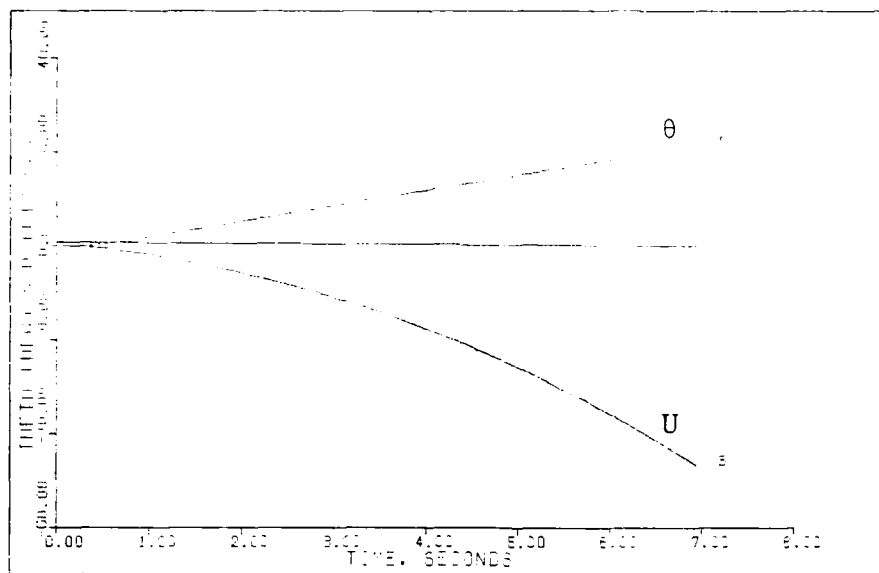
Figure 52c. G-Command System Response to a 1g Step
Command (0.6 Mach 30,000 feet)
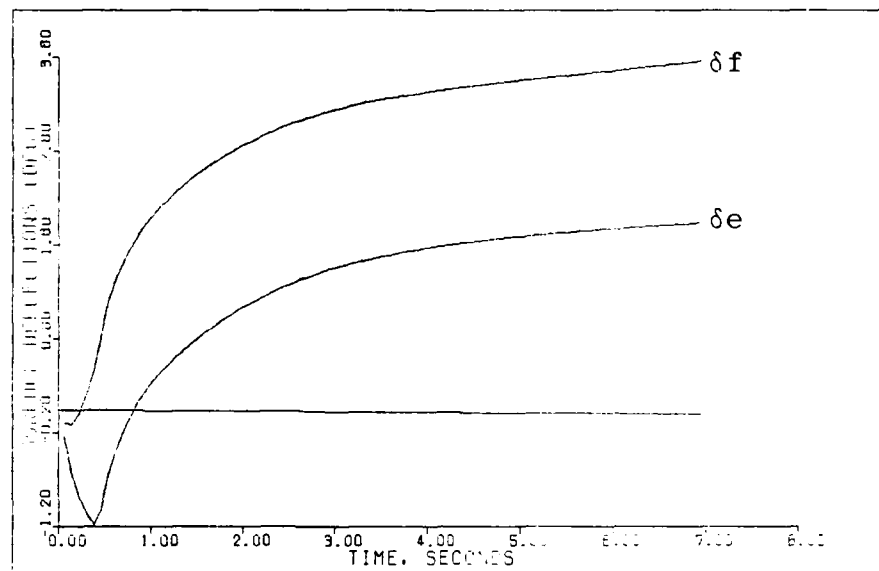
Figure 52d. G-Command System Response to a 1g Step
Command (0.6 Mach 30,000 feet)

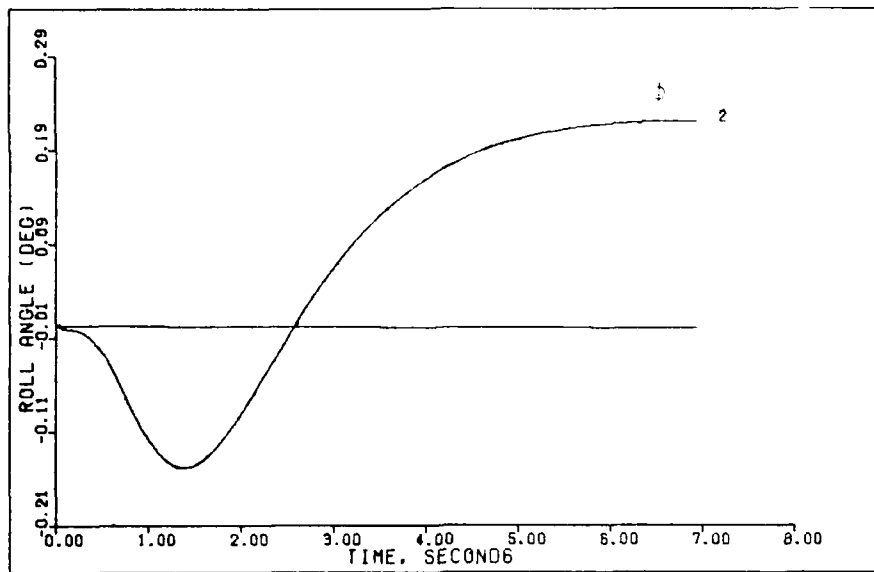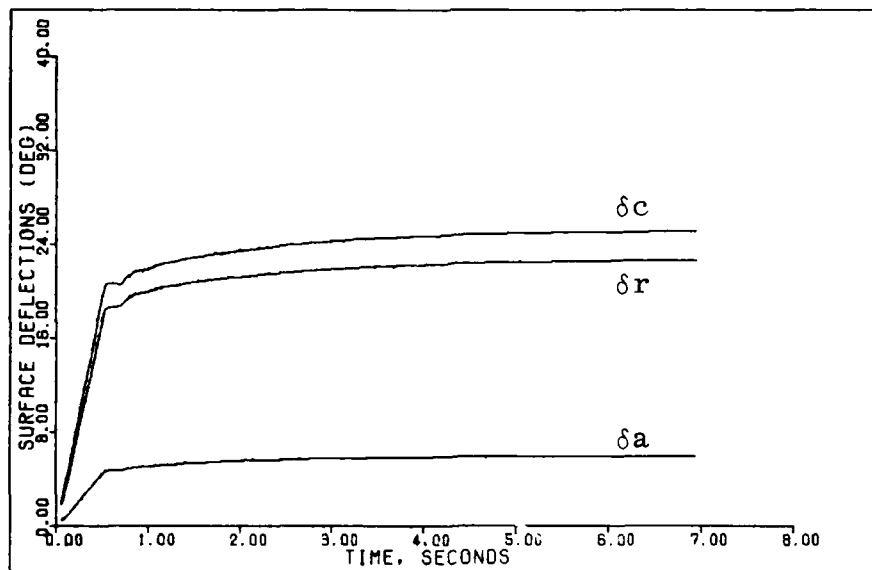Design Data for the Roll Rate Command System

Flight Condition: 0.6 Mach 30,000 feet

$T = 0.02$

$\bar{\alpha} = 1.0$

$$\underline{\Sigma} = \begin{bmatrix} 1.0 & 0 & 0 \\ 0 & 0.24 & 0 \\ 0 & 0 & 0.5 \end{bmatrix}$$

$\varepsilon = 0.25$

$$\underline{M} = \begin{bmatrix} 0 & 0 & 0 & 0 & 0 & 0 \\ 0 & 0 & 0 & 0 & 0.1 & 0 \\ 0 & 0 & 0 & 0 & 0 & 0.1 \end{bmatrix}$$

$$\underline{K}_0 = \underline{K}_1 = \begin{bmatrix} 0.2589 & -0.001383 & -0.01103 \\ 1.19\cdot\cdot & 0.000319 & -0.05492 \\ 1.67\cdot0 & -0.000175 & -0.03482 \end{bmatrix}$$

Input ramp time: 0.3 seconds

Input commands: $A_{y_p} = 0.0$

p = 5 deg/sec pulse for 3 sec duration

$r = p\alpha$ where $\alpha = 0.082115$ radians

NOTE: 1. Pulse inputs are ramped to a maximum value over a specific time. This time is designated as the input ramp time above. The input is held at a maximum value for a duration time and then ramped back to zero. Both ramp times are the same value.

2. Rolls are performed about the velocity vector.
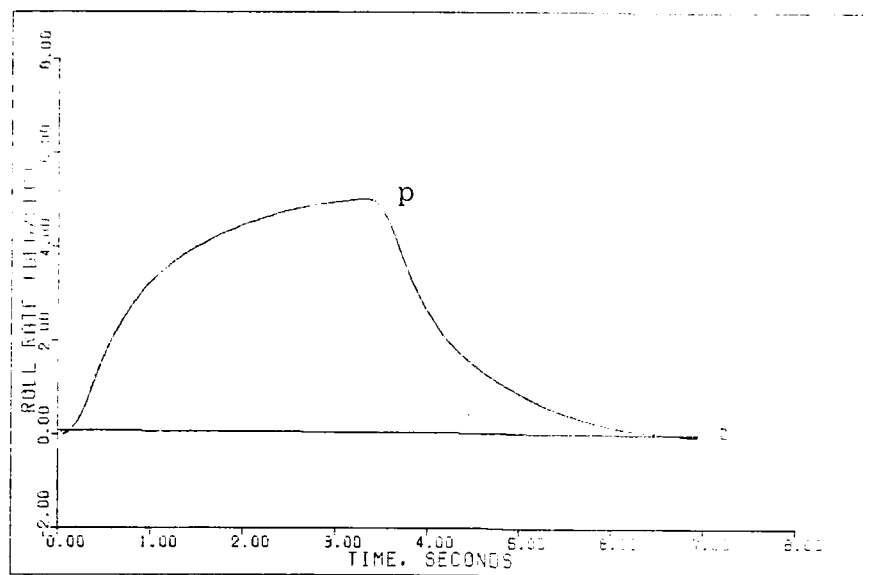
Figure 53a. Roll Rate Command System Response to a
5 deg/sec Pulse Command (0.6 Mach 30,000 feet)
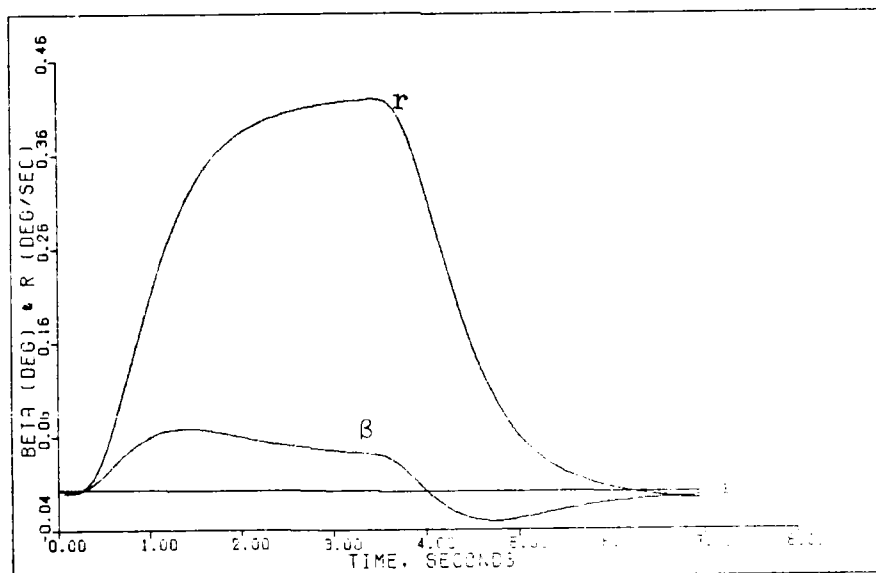
Figure 53b. Roll Rate Command System Response to a
5 deg/sec Pulse Command (0.6 Mach 30,000 feet)

167
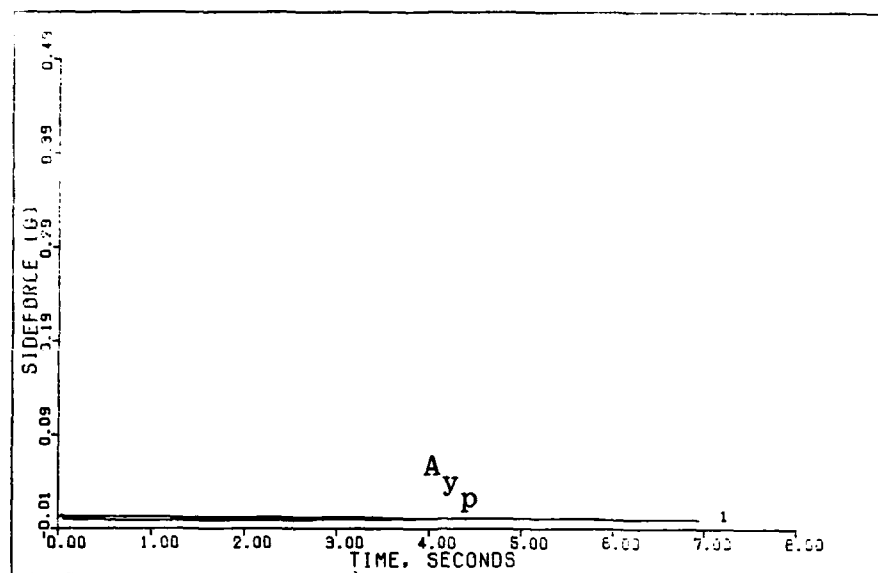
Figure 53c. Roll Rate Command System Responses to a 5 deg/sec Pulse Command (0.6 Mach 30,000 feet)
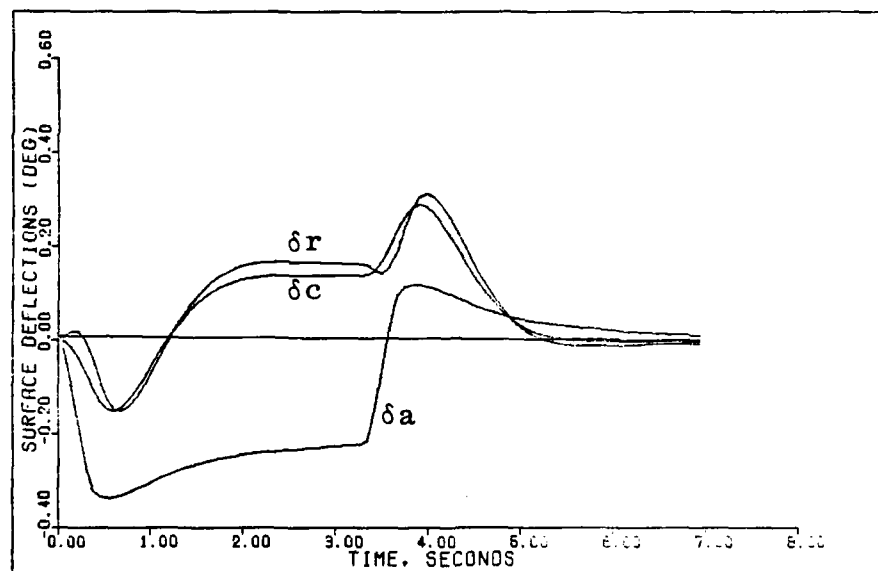
Figure 53d. Roll Rate Command System Response to a 5 deg/sec Pulse Command (0.6 Mach 30,000 feet)

168
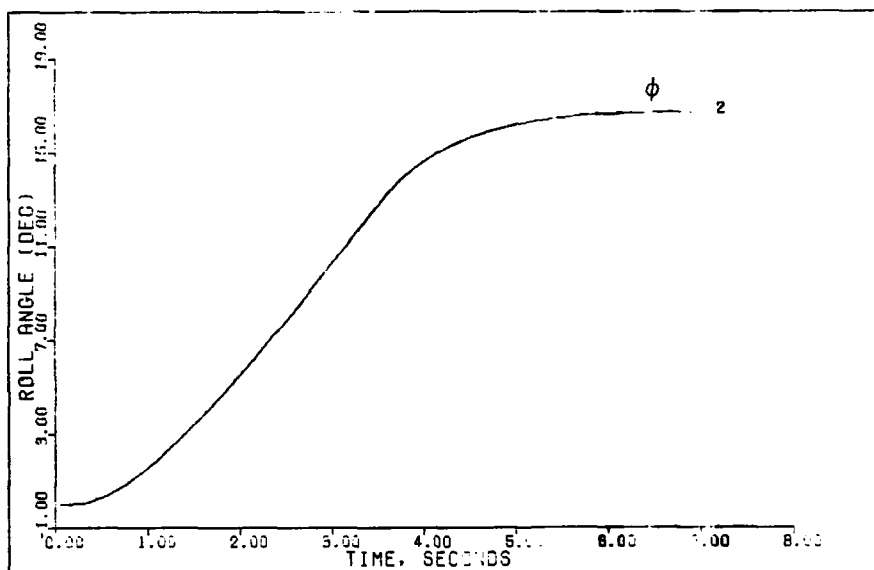
Figure 53e.   Roll Rate Command System Response to a
5 deg/sec Pulse Command (0.6 Mach 30,000 feet)

Design Data for the Sideforce System

Flight Condition: 0.6 Mach   30,000 feet

$T = 0.02$

$\bar{\alpha} = 1.0$

$$\underline{\Sigma} = \begin{bmatrix} 1.0 & 0 & 0 \\ 0 & 1.0 & 0 \\ 0 & 0 & 1.0 \end{bmatrix}$$

$\varepsilon = 1.0$

$$\underline{M} = \begin{bmatrix} 0 & 0 & 0 & 0 & 0 \\ 0 & 0 & 0 & 0.1 & 0 \\ 0 & 0 & 0 & 0 & 0.1 \end{bmatrix}$$

$$\underline{K}_0 = \underline{K}_1 = \begin{bmatrix} 1.036 & -0.02305 & -0.08824 \\ 4.794 & 0.05318 & -0.43930 \\ 6.684 & -0.02917 & -0.27850 \end{bmatrix}$$

Input ramp time: 0.5 seconds

Input commands: $A_{y_p} = 0.2g$ step

$p = 0.0$

$r = \left[\dfrac{1845}{U}\right] A_{y_p} = 0.618$ deg/sec

NOTE: Step inputs are ramped to steady state over a specific time. This time is designated as the input ramp time given above.

170
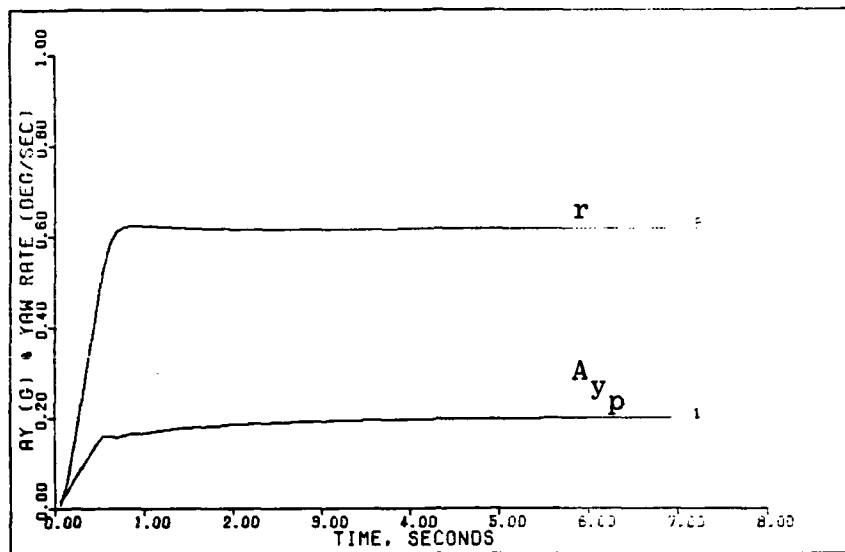
Figure 54a. Sideforce System Response to a 0.2g Step
Command (0.6 Mach 30,000 feet)
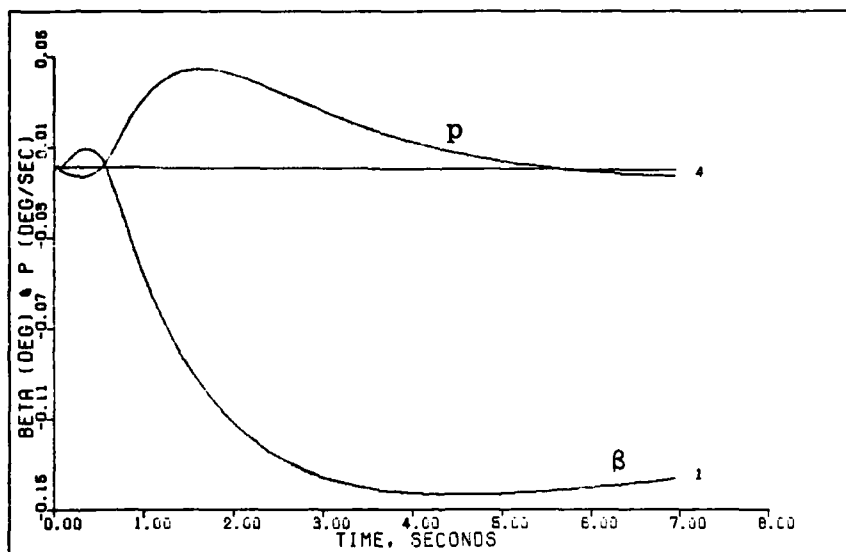
Figure 54b. Sidefor e System Response to a 0.2g Step
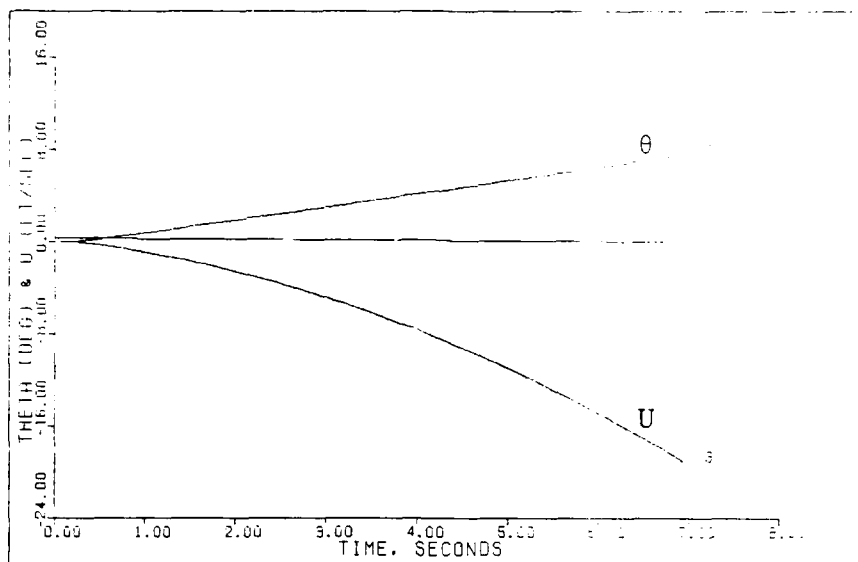Command (0.6 Mach 30,000 feet)

171
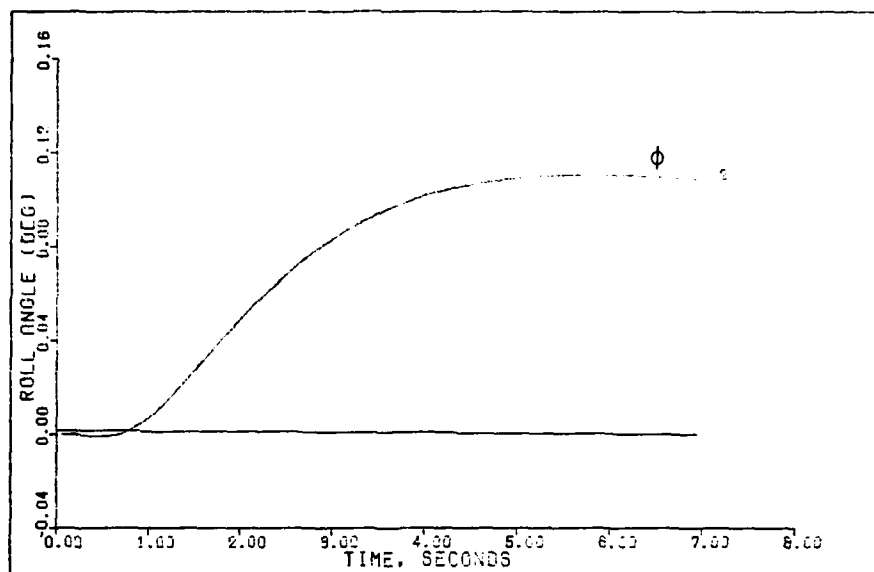
Figure 54c. Sideforce System Response to a 0.2g Step
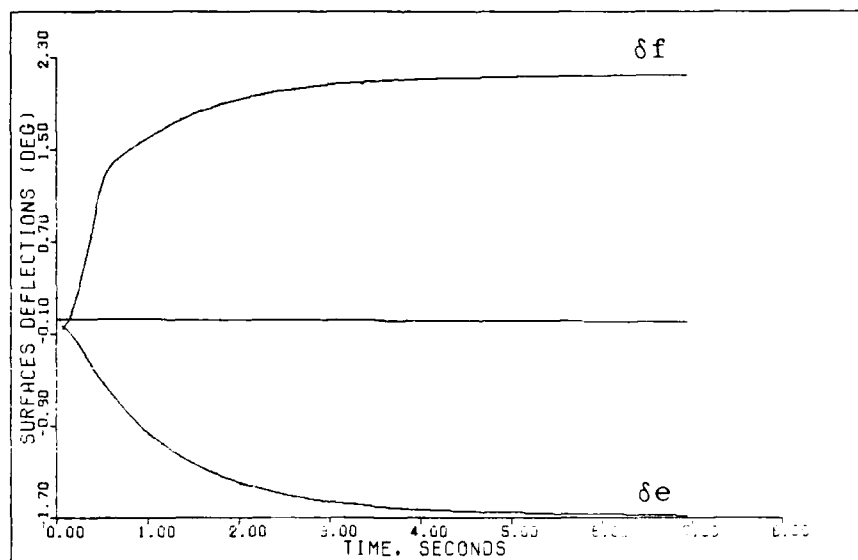Command (0.6 Mach 30,000 feet)
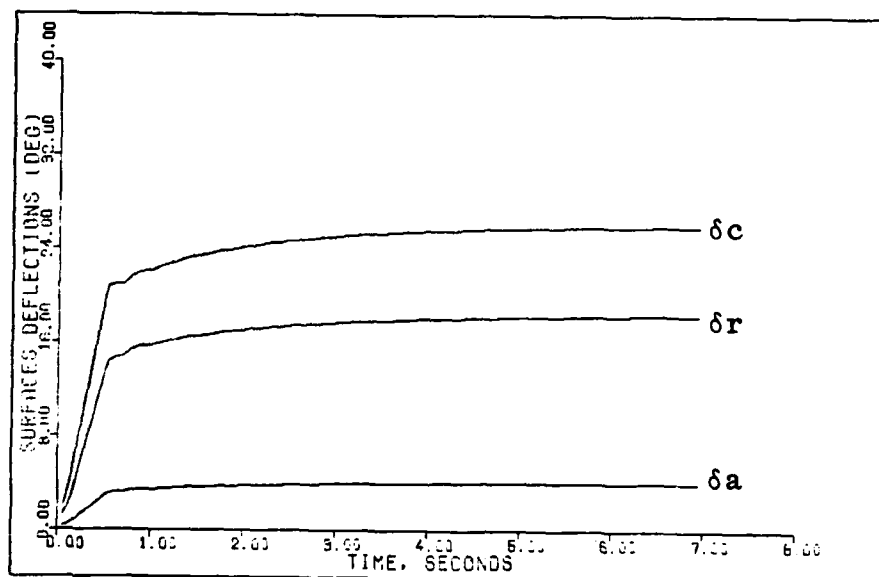
Figure 54d. Sideforce System Response to a 0.2g Step
Command (0.6 Mach 30,000 feet)

172

Design Data for the G-Command System

Flight Condition: 0.2 Mach   30 feet

$T = 0.02$

$\bar{\alpha} = 1.0$

$$\underline{\Sigma} = \begin{bmatrix} 0.1 & 0 \\ 0 & 0.1 \end{bmatrix}$$

$\varepsilon = 1.0$

$$\underline{M} = \begin{bmatrix} 0 & 0 & 0 & 0 & 0 \\ 0 & 0 & 0 & 0 & 0.25 \end{bmatrix}$$

$$\underline{K}_0 = \underline{K}_1 = \begin{bmatrix} 0.06429 & -0.09859 \\ 0.59430 & -0.08450 \end{bmatrix}$$

Input ramp time: 0.4 seconds

Input commands: $A_{n_p} = 0.15g$ step

$q = 1.0$ deg/sec

NOTE: Step inputs are ramped to steady state over a specific time. This time is designated as the input ramp time given above.
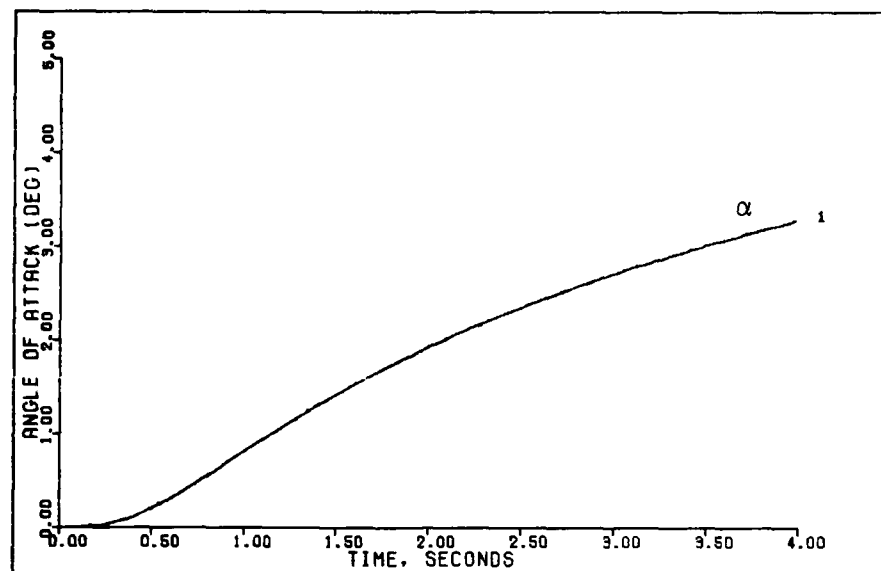
Figure 55a.   G-Command System Response to a 0.15g
Step Command (0.2 Mach 30 feet)
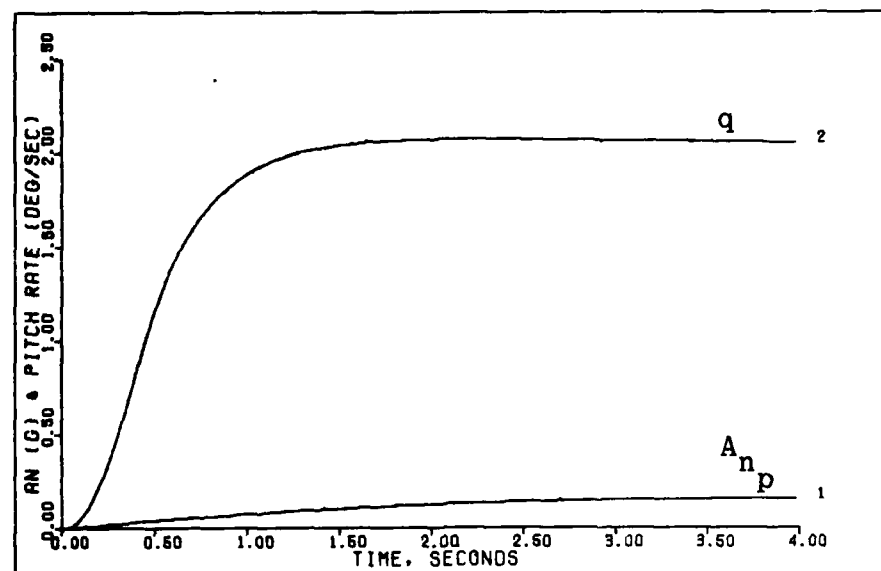
Figure 55b.   G-Command System Response to a 0.15g
Step Command (0.2 Mach 30 feet)

174
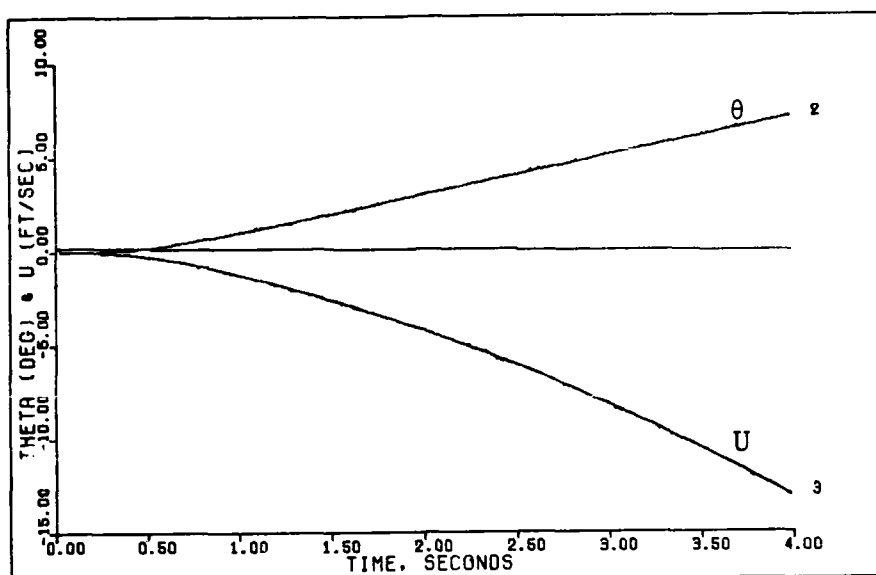
Figure 55c.   G-Command System Response to a 0.15g
Step Command (0.2 Mach 30 feet)
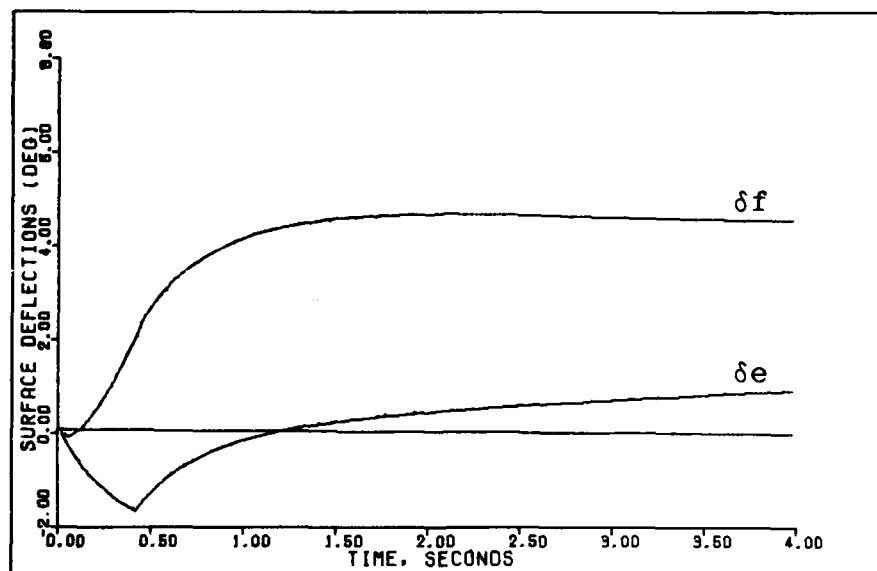
Figure 55d.   G-Command System Response to a 0.15g
Step Command (0.2 Mach 30 feet)

175

Design Data for the Roll Rate Command System

Flight Condition: 0.2 Mach 30 feet

$T = 0.02$

$\bar{\alpha} = 1.0$

$$\underline{\Sigma} = \begin{bmatrix} 1.0 & 0 & 0 \\ 0 & 1.0 & 0 \\ 0 & 0 & 0.6 \end{bmatrix}$$

$\varepsilon = 1.0$

$$\underline{M} = \begin{bmatrix} 0 & 0 & 0 & 0 & 0 \\ 0 & 0 & 0 & 0.25 & 0 \\ 0 & 0 & 0 & 0 & 0.25 \end{bmatrix}$$

$$\underline{K}_0 = \underline{K}_1 = \begin{bmatrix} 1.291 & -0.03368 & -0.04875 \\ 10.520 & 0.01574 & -0.24040 \\ 26.420 & 0.03132 & -0.24260 \end{bmatrix}$$

Input ramp time: 0.3 seconds

Input commands: $A_{y_p} = 0.0$

$p = 5$ deg/sec pulse for 3 sec duration

$r = p\alpha$ where $\alpha = 0.26143$ radians

NOTE: 1. Pulse inputs are ramped to a maximum value over a specific time. This time is designated as the input ramp time above. The input is held at a maximum value for a duration time and then ramped back to zero. Both ramp times are the same value.
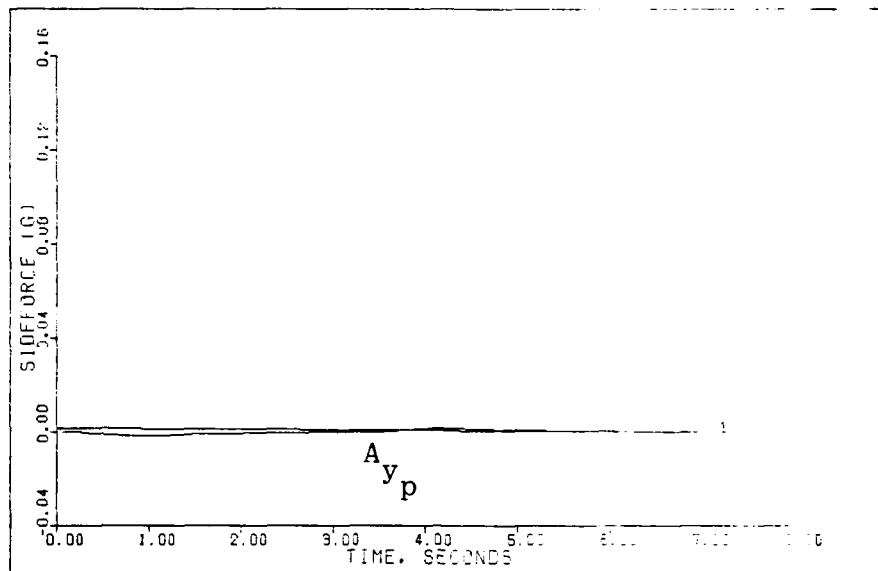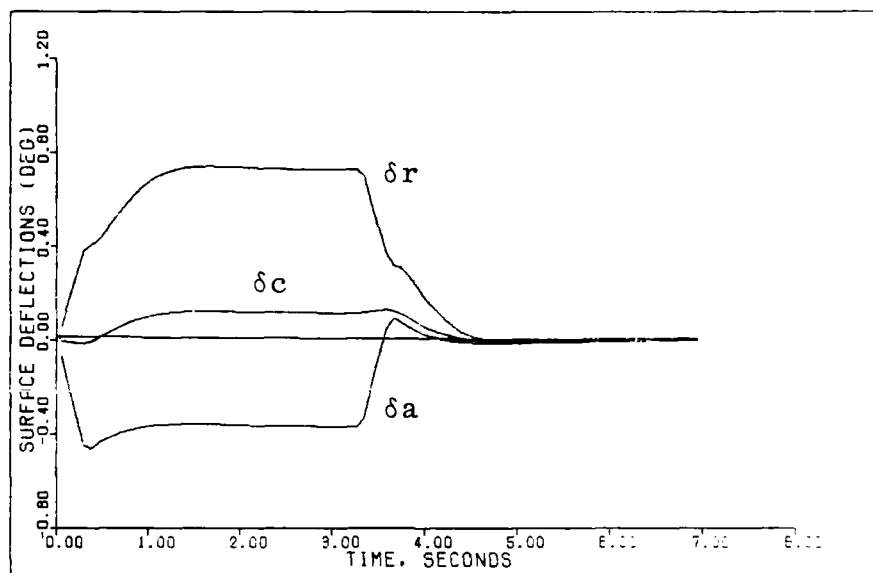
2. Rolls are performed about the velocity vector.
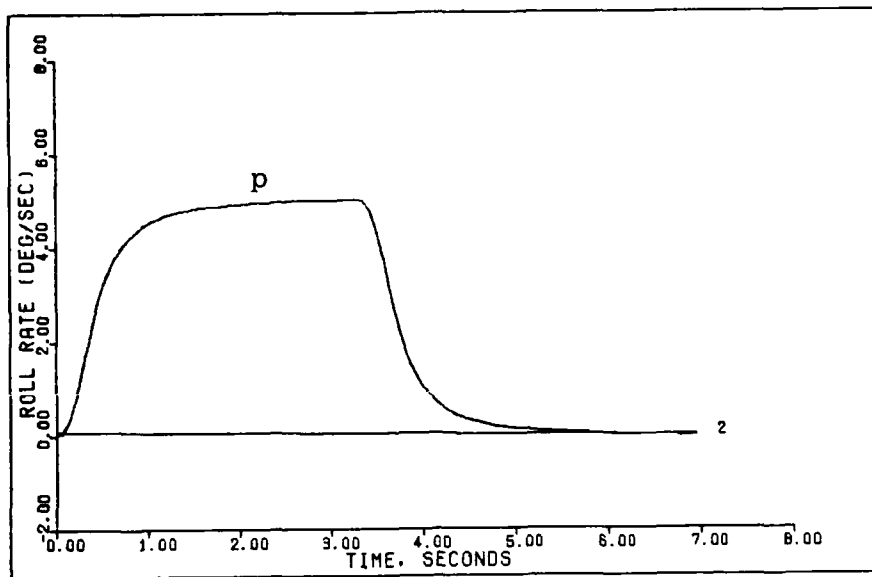
Figure 56a. Roll Rate Command System Response to a
5 deg/sec Pulse Command (0.2 Mach 30 feet)
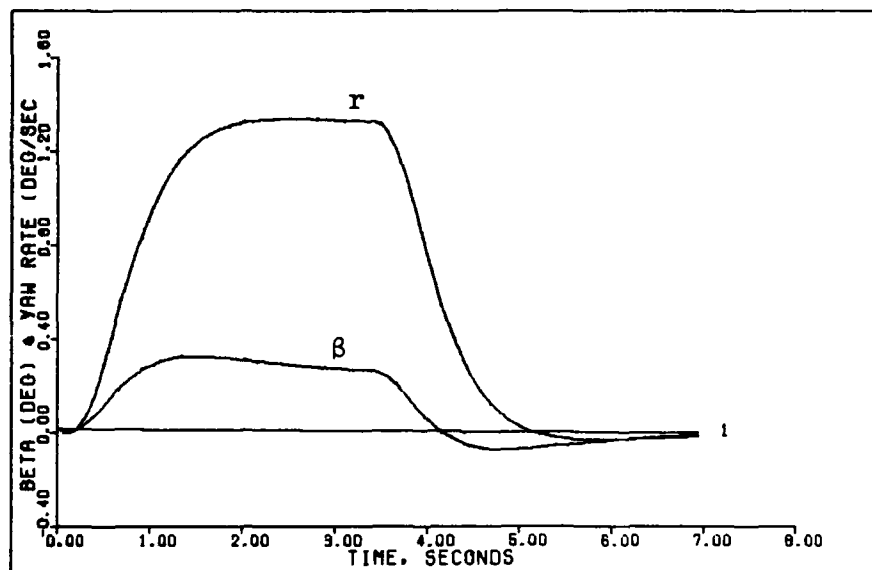
Figure 56b. Roll Rate Command System Response to a
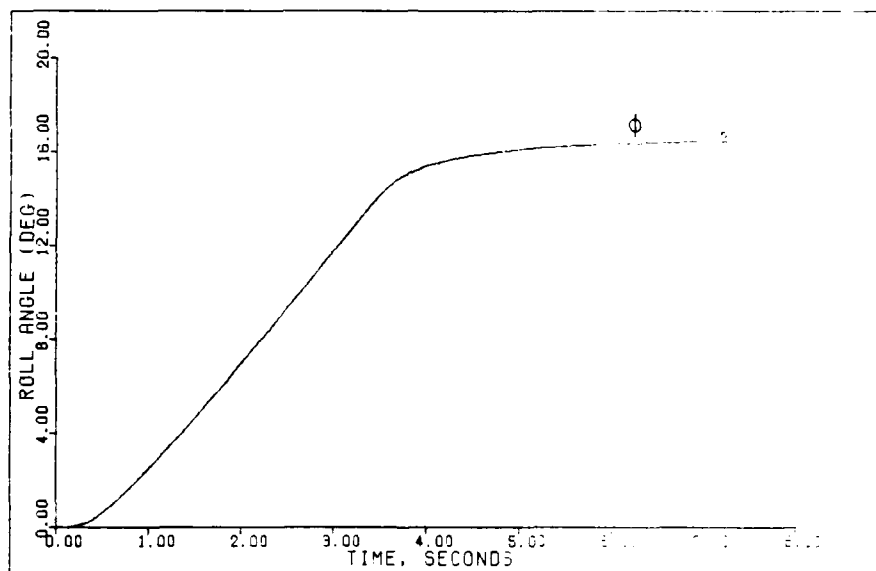5 deg/sec Pulse Command (0.2 Mach 30 feet)

177
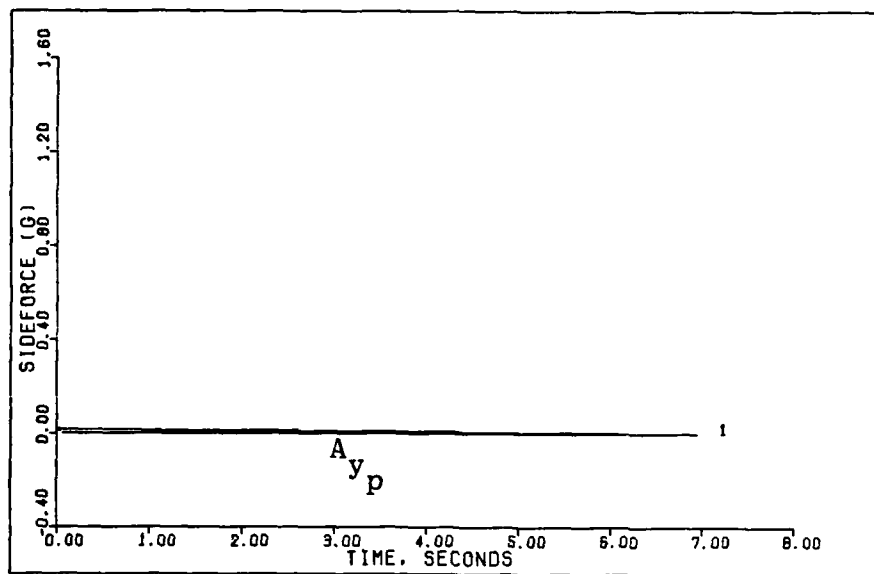
Figure 56c. Roll Rate Command System Response to a
5 deg/sec Pulse Command (0.2 Mach 30 feet)
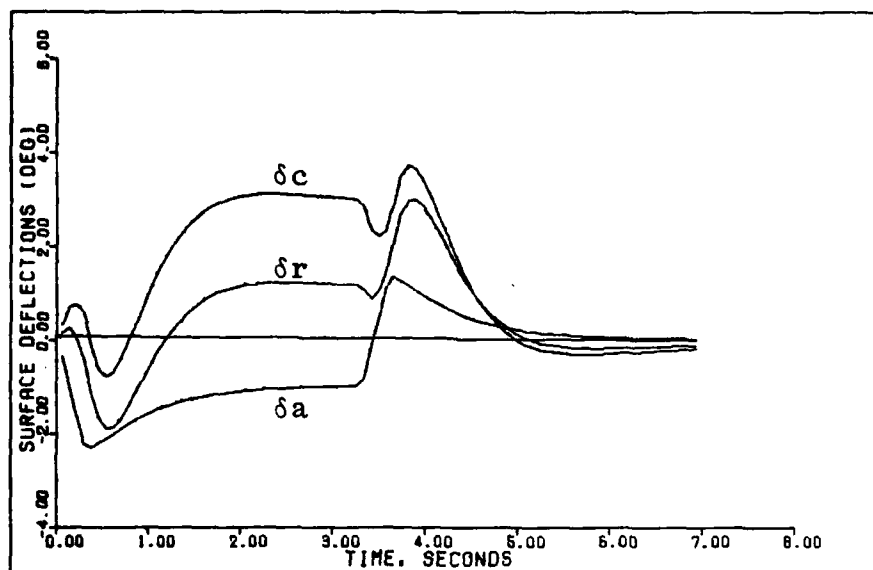
Figure 56d. Roll Rate Command System Response to a
5 deg/sec Pulse Command (0.2 Mach 30 feet)

178
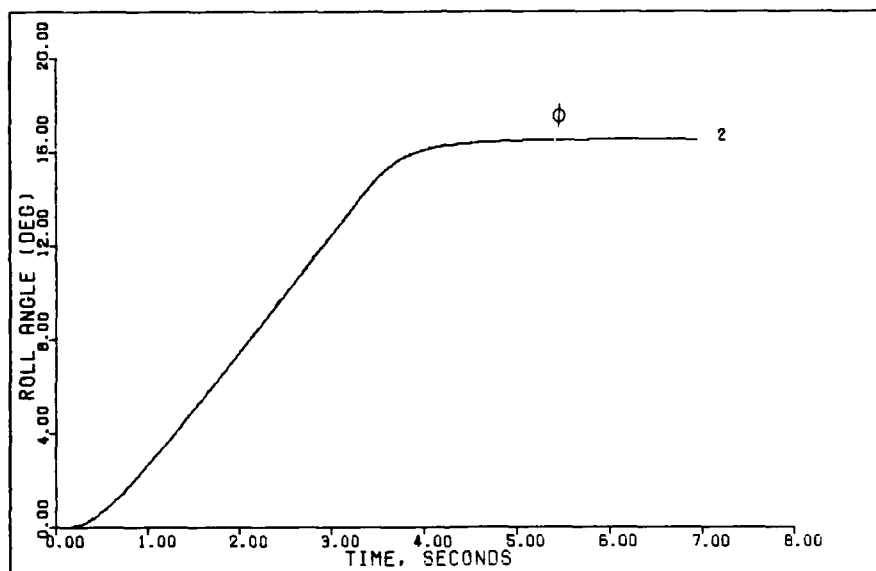
Figure 56e.   Roll Rate Command System Response to a
5 deg/sec Pulse Command (0.2 Mach 30 feet)

Design Data for the Sideforce System

Flight Condition: 0.2 Mach 30 feet

$T = 0.02$

$\overline{\alpha} = 1.0$

$$\underline{\Sigma} = \begin{bmatrix} 1.0 & 0 & 0 \\ 0 & 1.0 & 0 \\ 0 & 0 & 1.0 \end{bmatrix}$$

$\varepsilon = 1.0$

$$\underline{M} = \begin{bmatrix} 0 & 0 & 0 & 0 & 0 \\ 0 & 0 & 0 & 0.1 & 0 \\ 0 & 0 & 0 & 0 & 0.1 \end{bmatrix}$$

$$\underline{K}_0 = \underline{K}_1 = \begin{bmatrix} 1.291 & -0.08420 & -0.2031 \\ 10.520 & 0.03936 & -1.0020 \\ 26.420 & 0.07829 & -1.0110 \end{bmatrix}$$

Input ramp time: 0.3 seconds

Input commands: $A_{y_p} = 0.053g$ step

$p = 0.0$

$r = \left[\dfrac{1845}{U} \right] A_{y_p} = 0.438$ deg/sec

NOTE: Step inputs are ramped to steady state over a specific time. This time is designated as the input ramp time given above.
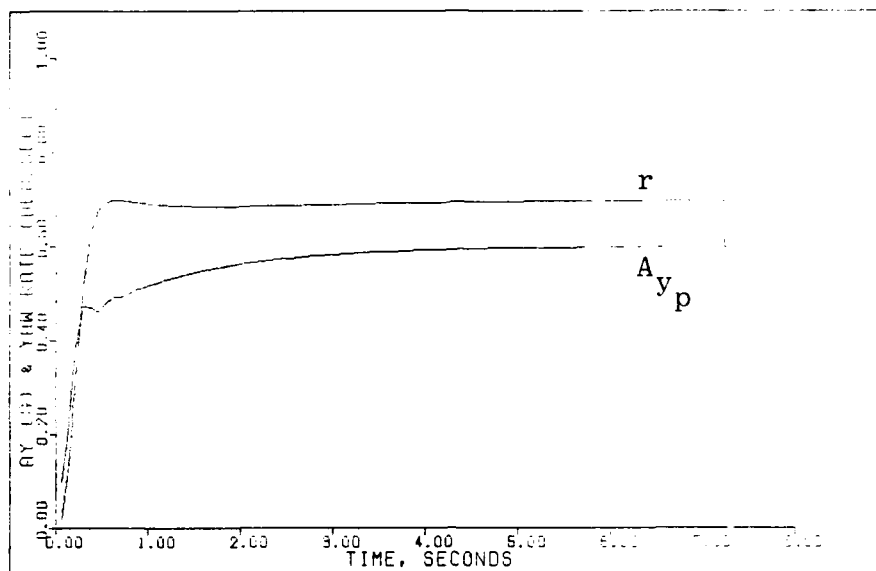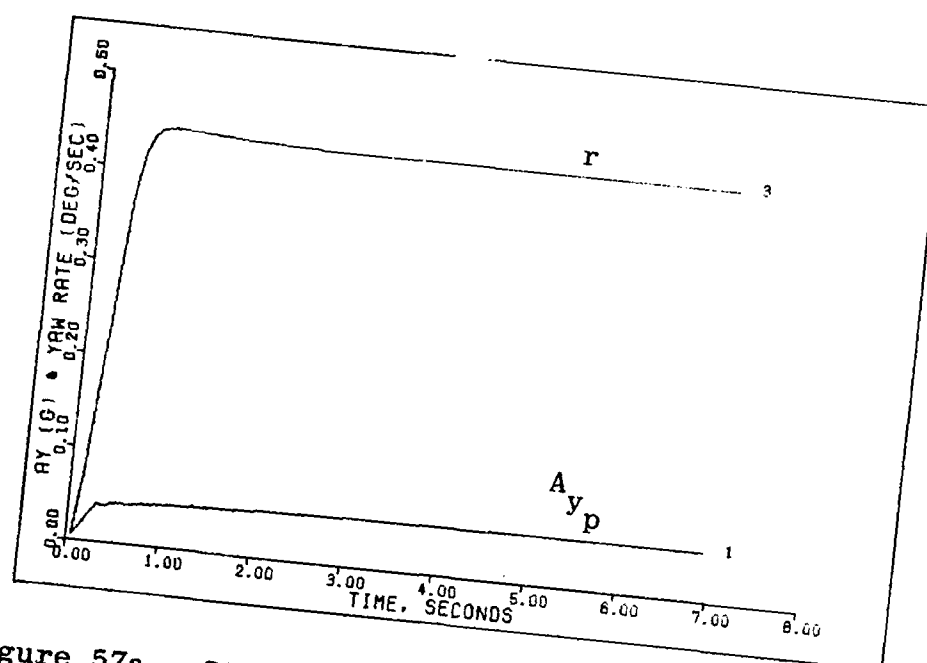
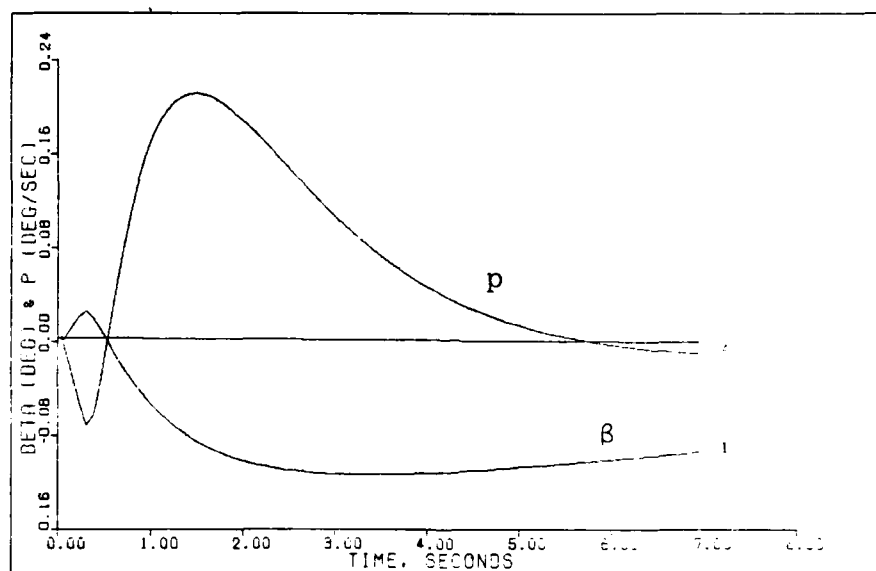Figure 57a. Sideforce System Response to a 0.053g
Step Command (0.2 Mach 30 feet)
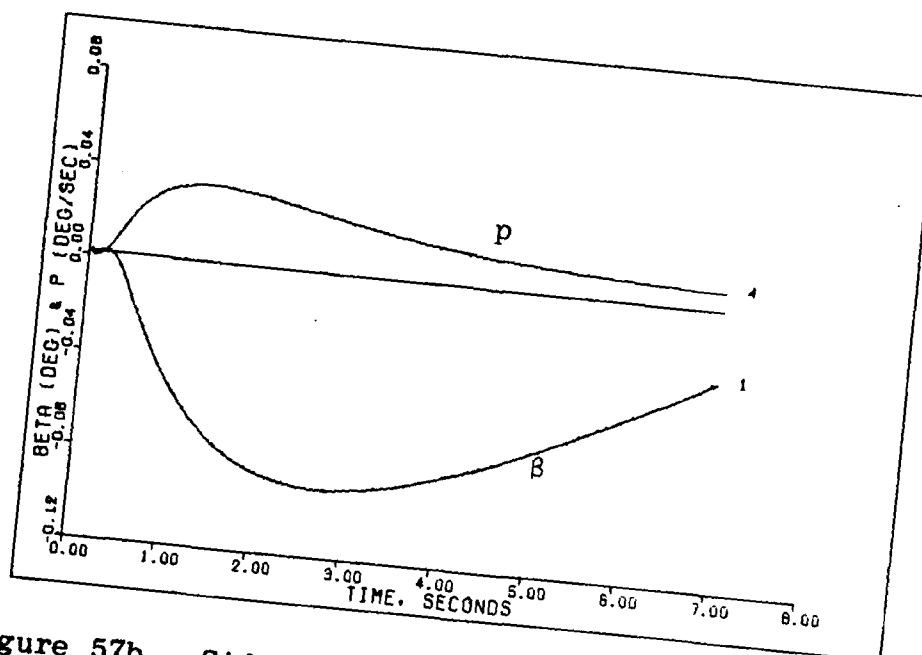
Figure 57b. Sideforce System Response to a 0.053g
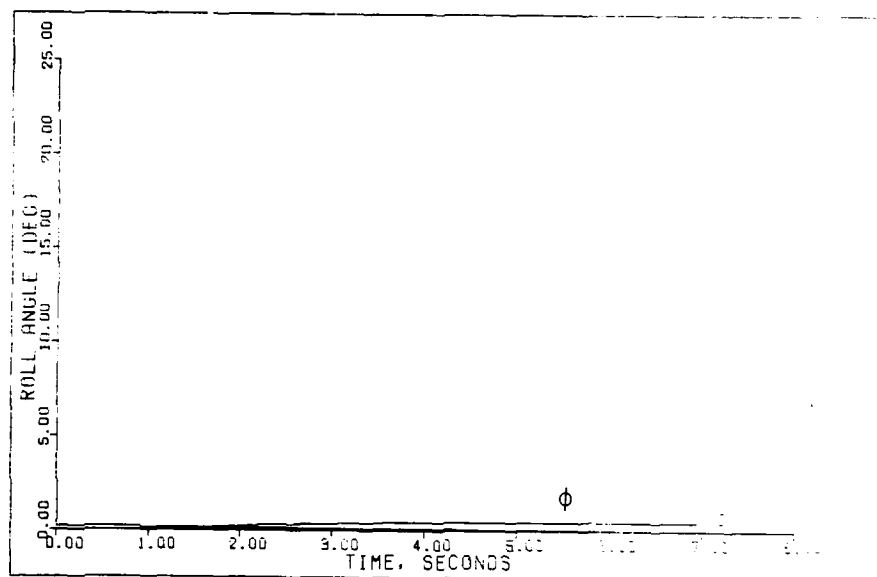Step Command (0.2 Mach 30 feet)

181
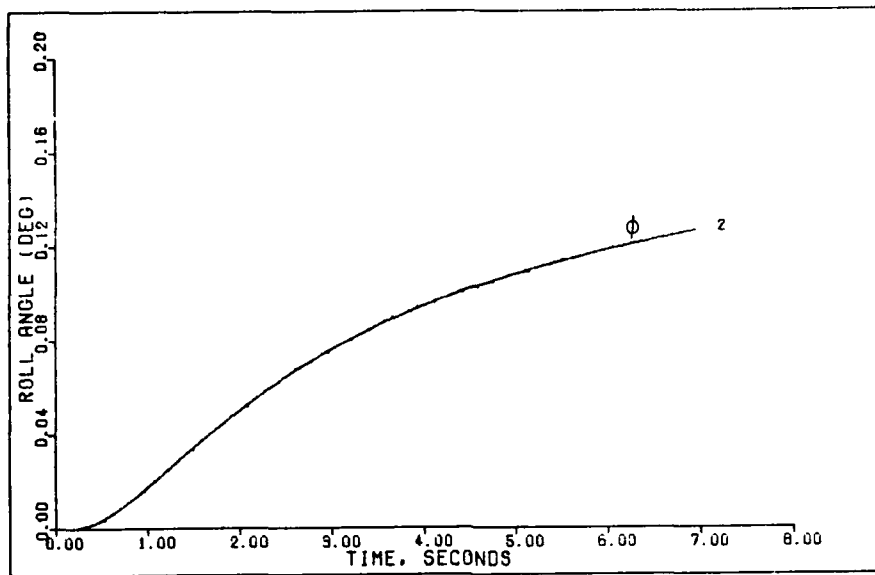
Figure 57c. Sideforce System Response to a 0.053g
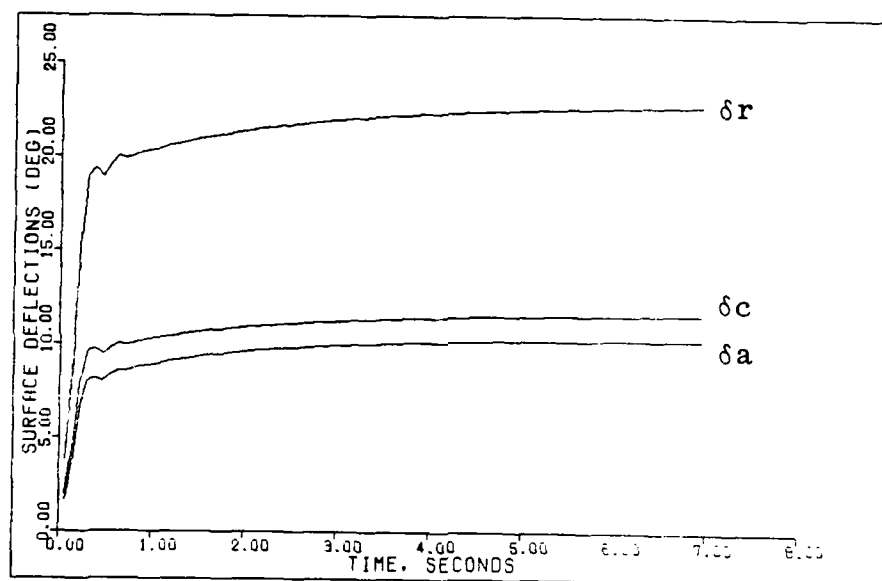Step Command (0.2 Mach 30 feet)
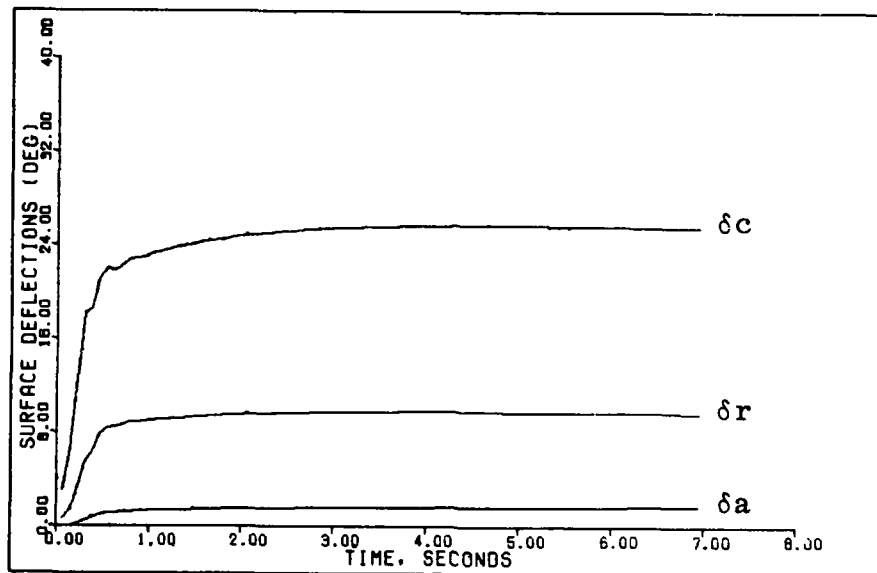
Figure 57d. Sideforce System Response to a 0.053g
Step Command (0.2 Mach 30 feet)

Neal-Smith Criterion

The acceptance of a design by the pilot is always an issue of utmost importance that must be addressed in any flight control work. Professor Porter's method, as applied in this effort, results in a closed-loop system with either all real roots or complex conjugate pairs with very high damping ratios. In light of this fact, a means of assessing pilot acceptance is needed.

One method of predicting pilot ratings for a longitudinal compensatory tracking task was suggested by Peter Neal and Roger Smith in Reference 16. The complete theoretical basis and the data used for the criterion development are provided in the reference. A summary of the technique is presented here. The assumption is made that the acceptability of an aircraft's maneuvering response in performing a specific task can be expressed in terms of the pilot compensation needed to achieve some "minimum standard of performance" with the least tendency to develop a pilot induced oscillation (PIO). The standard of performance is established by the task which is required of the pilot. For the final phase of a fighter's combat maneuvering, precise control of pitch attitude is assumed to be the critical task in the reference. The control of pitch attitude is modelled as shown in Figure 58. This model and the definitions presented are direct extracts from Reference 16.

183
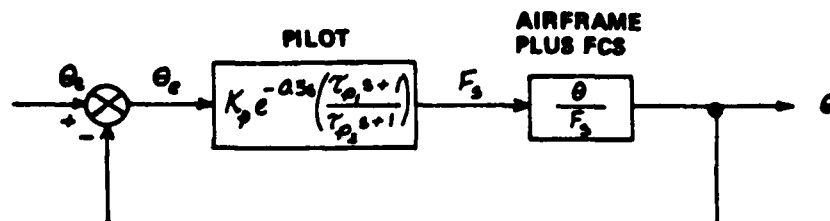
Using this model, the following terms are defined:

Bandwidth (BW): Bandwidth is defined as the frequency for which the closed-loop Bode phase, $\angle \left(\theta/\theta_c \right)$, is equal to -90 degrees. It is a measure of how quickly the pilot can move the airplane's nose toward the target.

Droop: Droop is defined as the maximum excursion of closed-loop Bode amplitude, $\left| \theta/\theta_c \right|$, below the 0 dB line for frequencies less than BW. In the absence of large oscillations, droop is a measure of how slowly the nose settles down on target.

Standard of Performance: A minimum bandwidth, $(BW)_{min}$, of 3.5 rad/sec, and a maximum droop of 3 dB:

$$\left. \begin{array}{l} \angle \left(\theta/\theta_c \right) \text{ greater than } (-90) \text{ degree} \\ \text{and } \left| \theta/\theta_c \right| \text{ greater than } (-3) \text{ dB} \end{array} \right\} \begin{array}{l} \text{for } \omega \text{ less} \\ \text{than 3.5} \end{array}$$

PIO Tendency: The tendency to oscillate or PIO is defined in terms of the Bode magnitude of any closed-loop resonant peak, $\left| \theta/\theta_c \right|_{max}$, that results from the pilot's efforts to achieve the performance standards.

Pilot Compensation: The pilot's physical and mental workload required to achieve the standard of performance is defined in terms of the phase of his compensation at $\omega = (BW)_{min}$:

$$\angle_{pc} = \angle \left(\frac{j\omega\,\tau_{p_1} + 1}{j\omega\,\tau_{p_2} + 1} \right)_{\omega = (BW)_{min}}$$

Figure 58. Neal-Smith Model for Pitch
Attitude Control

184

To evaluate a design, the engineer selects values of K_p, τ_{p1}, and τ_{p2} in the pilot model that yield the smallest maximum value for $|\theta/\theta_c|$ for the closed-loop system while maintaining a minimum bandwidth of 3.5 radians per second and a maximum droop of -3 dB. The method of this selection is covered later.

For each specific selection of pilot model parameters, the maximum value of $|\theta/\theta_c|$ and the phase angle at the 3.5 rad/sec frequency are determined for the closed-loop system using a Nichols chart. These values are plotted in Figure 59 and evaluated against the boundaries in the figure to determine a prediction of a pilot rating (PR) and the acceptability of the design. The PR boundaries in the figure correspond to the Cooper-Harper Pilot Ratings given in Table 7.

To employ this method, the airframe plus flight control system transfer function, θ/F_s, must first be determined for the longitudinal system. With two inputs and two outputs, $\underline{G}(s)$ is a two-by-two transfer function matrix as expressed below.

$$\underline{G}(s) = \begin{bmatrix} \dfrac{A_{n_p}}{v_1} & \dfrac{A_{n_p}}{v_2} \\[2em] \dfrac{q}{v_1} & \dfrac{q}{v_2} \end{bmatrix}$$

$$(5.1)$$
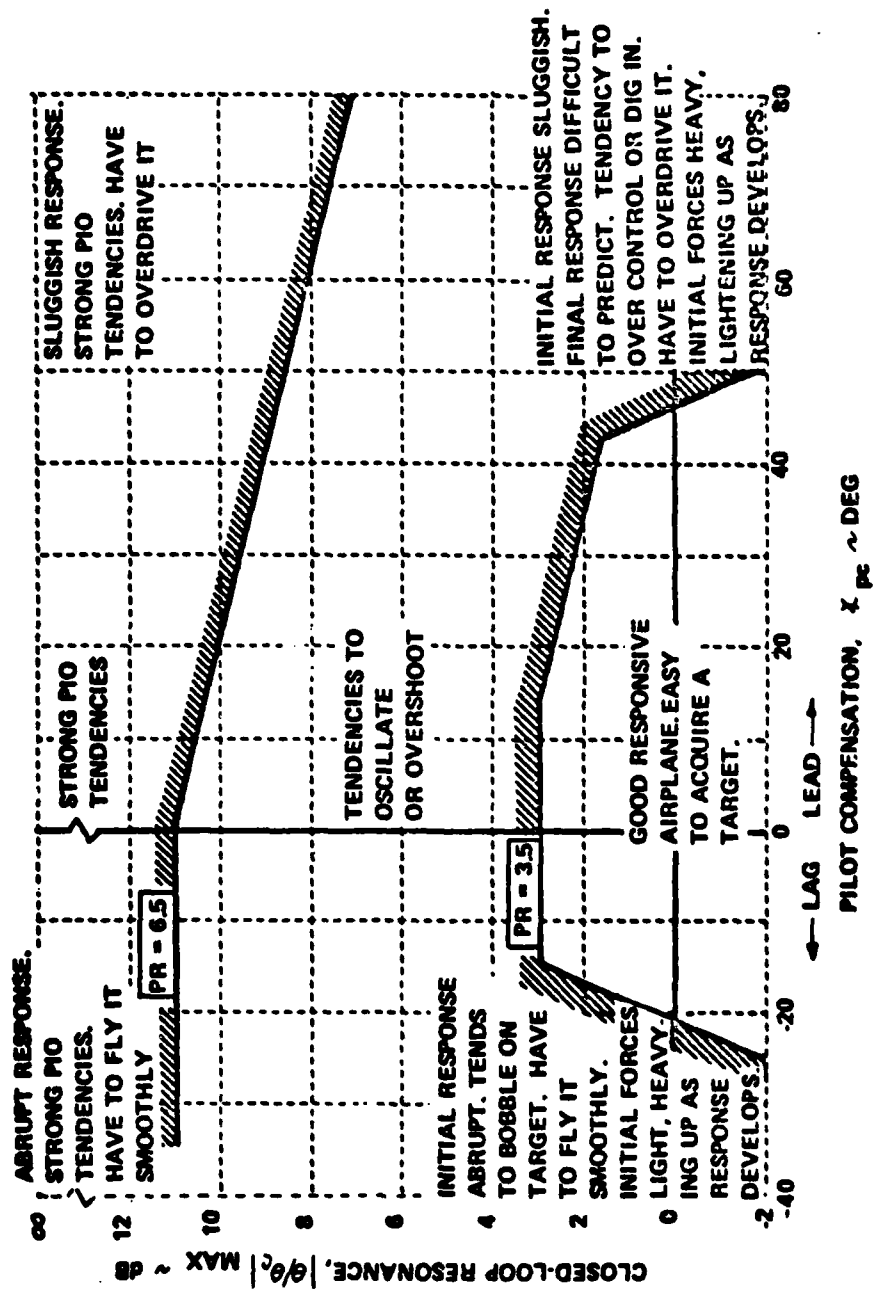
Figure 59. Neal-Smith Criterion for Fighter Maneuvering Dynamics

186

Table 7

Cooper-Harper Handling Qualities Rating Scale

ADEQUACY FOR SELECTED TASK OR REQUIRED OPERATION*	AIRCRAFT CHARACTERISTICS	DEMANDS ON THE PILOT IN SELECTED TASK OR REQUIRED OPERATION*	PILOT RATING
	Excellent Highly desirable	Pilot compensation not a factor for desired performance	1
	Good Negligible deficiencies	Pilot compensation not a factor for desired performance	2
	Fair — Some mildly unpleasant deficiencies	Minimal pilot compensation required for desired performance	3
Is it satisfactory without improvement? — No → Deficiencies warrant improvement	Minor but annoying deficiencies	Desired performance requires moderate pilot compensation	4
	Moderately objectionable deficiencies	Adequate performance requires considerable pilot compensation	5
	Very objectionable but tolerable deficiencies	Adequate performance requires extensive pilot compensation	6
Is adequate performance attainable with a tolerable pilot workload? — No → Deficiencies require improvement	Major deficiencies	Adequate performance not attainable with maximum tolerable pilot compensation. Controllability not in question	7
	Major deficiencies	Considerable pilot compensation is required for control	8
	Major deficiencies	Intense pilot compensation is required to retain control	9
Is it controllable? — No → Improvement mandatory	Major deficiencies	Control will be lost during some portion of required operation	10

Pilot decisions

Cooper-Harper   Ref. NASA TND-5153

* Definition of required operation involves designation of flight phase and/or subphases with accompanying conditions.

The contribution from both inputs must be considered in the pitch attitude output since the aircraft is not completely decoupled. The system mechanization chosen for the longitudinal design shown in Figure 41 of Chapter IV relates stick force input (F_s) to the control commands v_1 and v_2 by

$$v_1 = F_s \qquad \text{and} \qquad v_2 = \left[\frac{1845}{U}\right] F_s \qquad (5.2)$$

thus

$$q = \frac{q}{v_1} v_1 + \frac{q}{v_2} v_2 = \frac{q}{v_1} (F_s) + \frac{q}{v_2} \left[\frac{1845}{U}\right] (F_s) \qquad (5.3)$$

and

$$\frac{q}{F_s} = \frac{q}{v_1} + \frac{q}{v_2} \left[\frac{1845}{U}\right] \qquad (5.4)$$

$$\frac{\theta}{F_s} = \frac{1}{s} \left\{\frac{q}{v_1} + \frac{q}{v_2} \left(\frac{1845}{U}\right)\right\} \qquad (5.5)$$

At the 0.9 Mach 20,000 feet flight condition, this transfer function is

$$\frac{\theta}{F_s} = \frac{929.5(s + 1)(s + 1.4)}{s(s + 1.065 \pm j\ 0.4189)(s + 3.75)(s + 133.8)} \qquad (5.6)$$

Magnitude and phase values are calculated for frequencies between 0.1 and 10 radians per second from this transfer function. The next step is to establish values for the pilot model that allow the standard of performance to be met.

Initially, a check is made to find if varying only K_p, the pilot's gain, can provide a solution. This is accomplished by letting τ_{p1} and τ_{p2} equal zero and setting K_p to one. The phase angle from the exponential term in the pilot model is $(57.3)(0.3)(\omega)$ and is added to the phase values of θ/F_s. This establishes the open-loop θ/θ_e magnitude and phase information.

The standard of performance (closed-loop) boundaries are established on a Nichols chart (Figure 60). The open-loop amplitude-phase plot of θ/θ_e is then overlaid and moved vertically to determine if any value of K_p allows the closed-loop tracking system θ/θ_c to meet the standards.

188
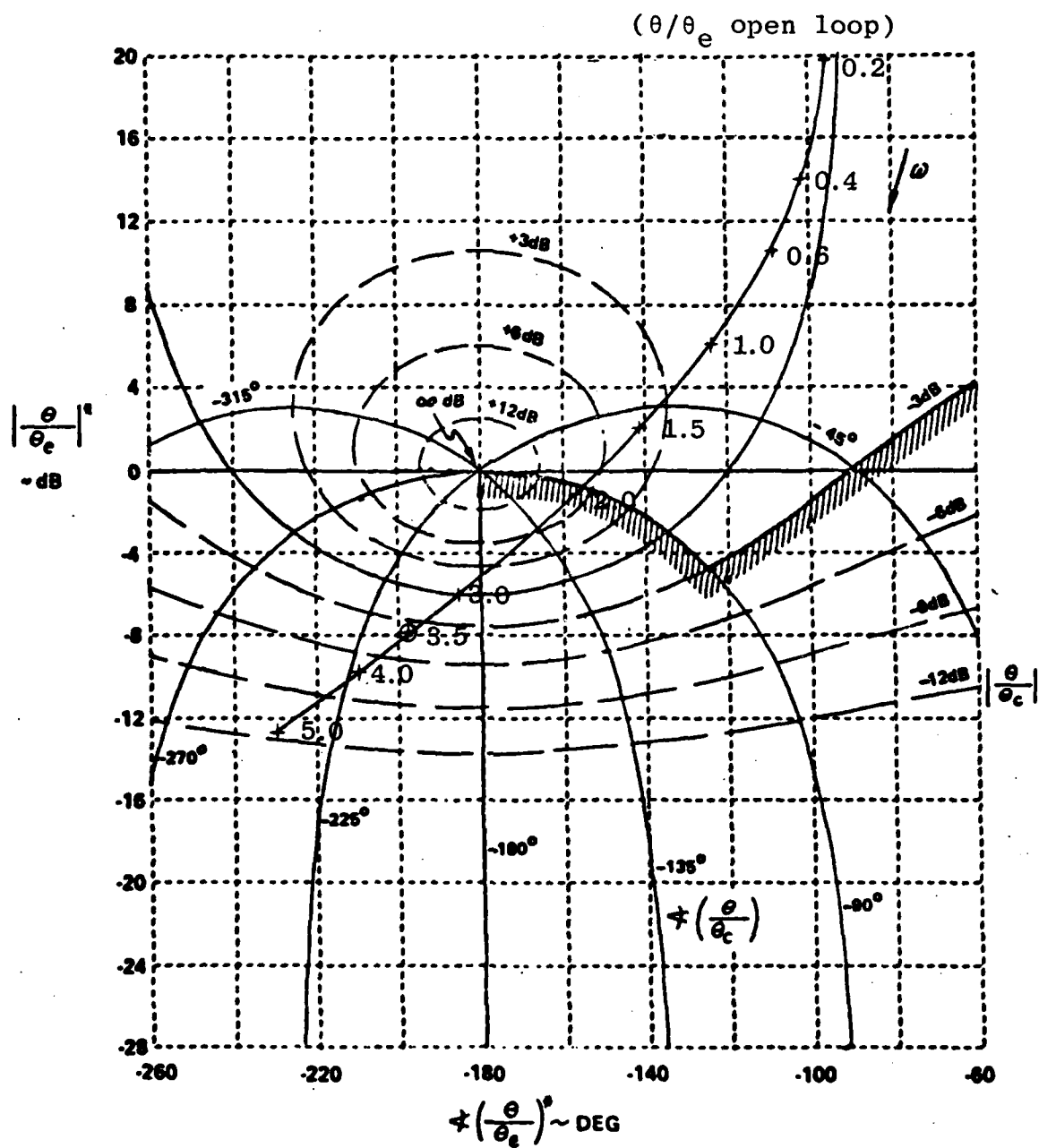
Figure 60. Nichols Chart with Performance Standard
Boundaries and Overlay of Amplitude-Phase
Plot of θ/θ_e with τ_{p_1} and τ_{p_2} Equal to Zero

189

This plot indicates that K_p alone can not satisfy the standard. The 3.5 radian per second point on the amplitude-phase plot needs a reduction in phase angle indicating lead compensation by the pilot.

Reference 16 provides a plot of amplitude-phase curves for optimum pilot compensation which simplifies the selection of τ_{p1} and τ_{p2}. Two pilot models are selected for the design being analyzed. The first with τ_{p1} = 0.94 and τ_{p2} = 0.0 meets both the bandwidth and droop requirements. This means that the pilot must generate over 73 degrees of lead at the 3.5 rad/sec frequency. The resulting $|\theta/\theta_c|$ max is plotted (as a dot) versus pilot compensation angle on the criterion graph in Figure 61. The point falls outside the desired PR = 3.5 boundary. A second pilot compensation is found with τ_{p1} = 0.57 and τ_{p2} = 0.0 that requires the pilot to generate 62 degrees of lead at 3.5 rad/sec and meets the bandwidth requirement while exceeding the droop requirement. This point is also plotted (as a dot) in Figure 61. Although moving closer to the desired region, both are outside the "good response area." The lead angle required by the pilot must be reduced if the design is to receive good pilot ratings from this evaluation technique.

An examination of the transfer function reveals that the root at -3.75 contributes slightly over 45 degrees of phase lag at the 3.5 rad/sec bandwidth frequency used to select the pilot compensation. This root is of interest
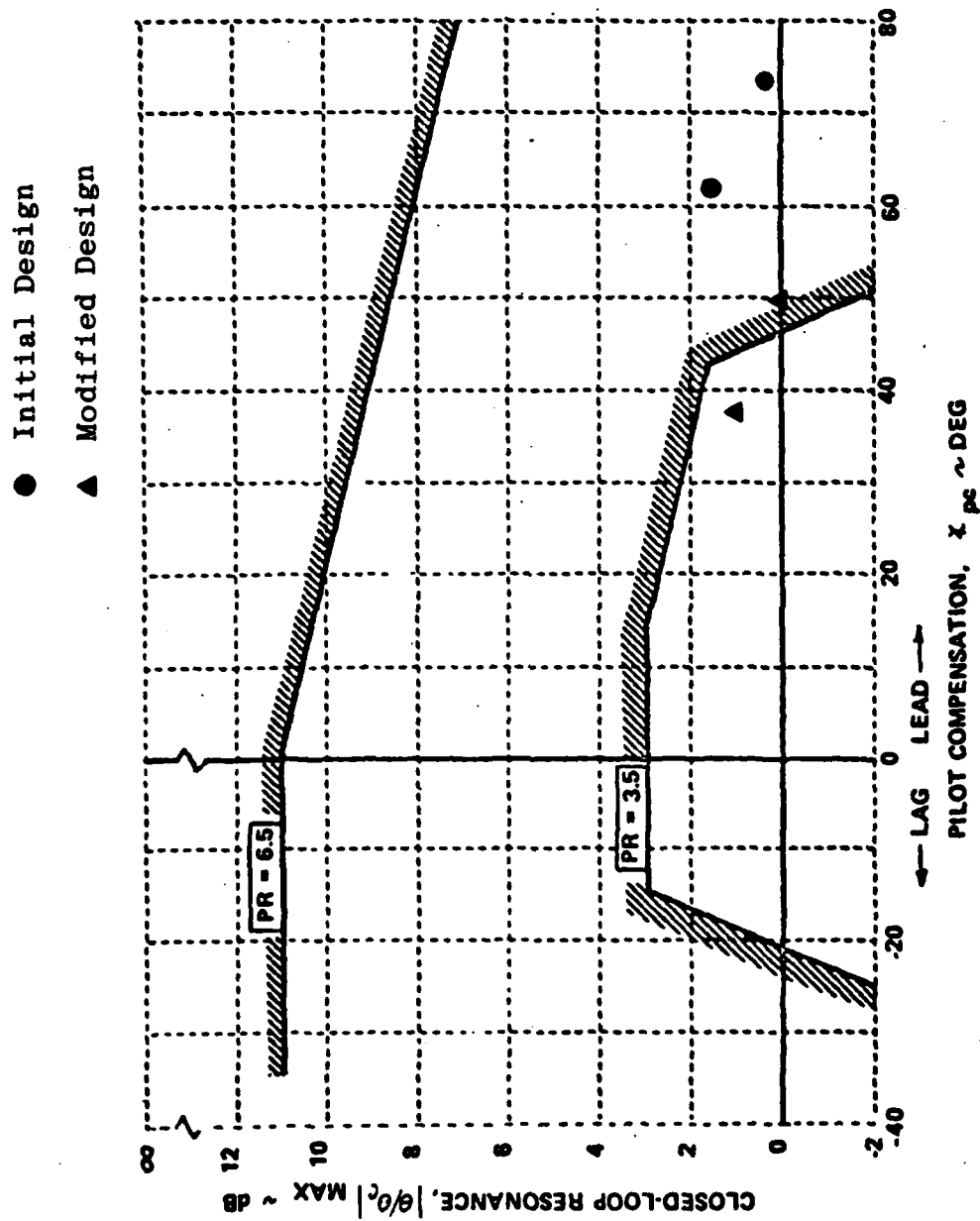
Figure 61. Criterion Graph with Design Evaluation Points

191

because its location is determined by the elements of the measurement matrix. The elements of $\underline{M}$ are changed to 0.1, and the system responses that result are shown in Figure 45. In this case, the first-order root is very close to -10 in the s-plane. Again, two pilot models are chosen and plotted as triangles in Figure 61. The first with τ_{p1} = 0.34 and τ_{p2} = 0.0 meets both constraints. It requires 50 degrees of pilot lead. The second meets the bandwidth condition and exceeds the droop requirement. For this case with τ_{p1} = 0.23 and τ_{p2} = 0.0, a pilot lead of 37 degrees is required.

The last choice yields a design which gives a pilot rating of 3.5 or less. Thus, after several well-placed changes, it appears that this design may be very useful for tracking cases. However, several cautionary notes are provided. The phase lag due to digital computer implementation and the lag from a pilot prefilter have not been included in this evaluation. An estimate for the digital design can be established by using a first-order Padé approximation for a zero-order hold and a factor of (1/T) for the sampling action (Ref 22). This indicates a phase lag of approximately 2 degrees at the 3.5 rad/sec bandwidth. The prefilter is of the order of 7.5/(s + 7.5) and adds as much as 25 degrees to the system. These additions again place the design outside the desired boundary. The prefilter may be increased to 10/(s + 10) or slightly higher depending on the actual surface rates encountered. The current design is conservative

since this is an indirect way to limit such rates, and the ramp times are calculated based on estimated maximum rates. Fine tuning of the prefilter has not been accomplished and can reduce the phase lag considerably.

These additional factors (which are present for any digital controller implementation) tend to cause the design points to fall to the lower right of the 3.5 PR boundary. This may not be a serious deficiency. Review of similar evaluations of both the F-16 and the AFTI/F-16 designs shows they fall in the same general region outside the 3.5 PR boundary.

The Neal-Smith Criterion is only one of several currently being proposed for flight control design evaluations (Refs 17, 18 and 19). Its use has highlighted areas of improvement for the current design; however, its validity in predicting pilot ratings is by no means unquestioned. Thus, further analyses with other criteria are needed to properly evaluate the designs. Ideally, conclusions on the acceptability of the design from these criteria should eventually be validated in a realistic piloted simulation evaluation.

Bandwidth Comparison

Chapter IV includes a discussion of the desirability of limiting the control system bandwidth. The major reason for this is to reduce undesirable effects from structural interaction. Designs with Professor Porter's techniques

can result in extremely fast responses. It is, therefore, important to assess the bandwidth of the designs under consideration. Time permitted only one such assessment in this study. The longitudinal design is compared with the F-16 and AFTI/F-16 control systems. Figures 62 and 63 are plots for the open-loop control system from sensor input to elevator position output. The MULTI Designs (MD) exhibit slightly less bandwidth at high frequencies than either the F-16 or the AFTI/F-16 systems for this path. In the acceleration path the MULTI Design falls between the other two systems and matches AFTI for very high frequencies. The plot for the AFTI design is for the air-to-air mode.

The plots were completed after the design gains had been established. Thus, they illustrate that the Porter design method employing maximum estimated maneuvers and considering limits on surface position and rates results in designs with acceptable bandwidths. The initial designs obtained before such considerations were taken into account had much higher gain values and would indeed have resulted in large bandwidths.

The high gain at low frequencies is due to integral compensation on all MULTI Design feedforward paths. Note that AFTI uses this compensation only in the pitch rate path, and the F-16 uses it only in the normal acceleration path.

A final word of caution must be given. Although the bandwidth of the longitudinal design compares favorably with

194

Note: $\frac{\delta e}{q}$ Transfer Function Comparisons

Gain set for 0.9 Mach 20,000 feet
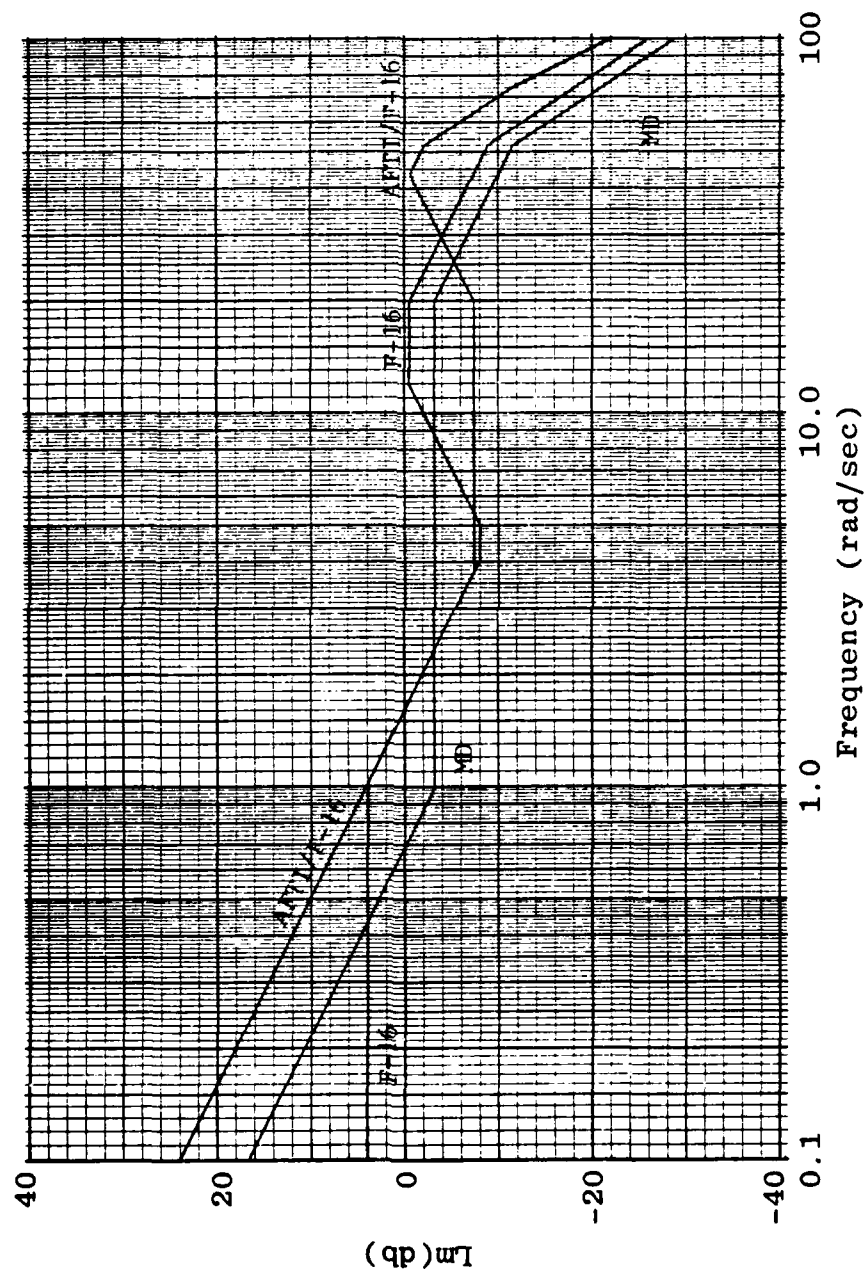
Figure 62. Open-Loop Bandwidth Comparison for the Pitch Rate to Elevator Path

195
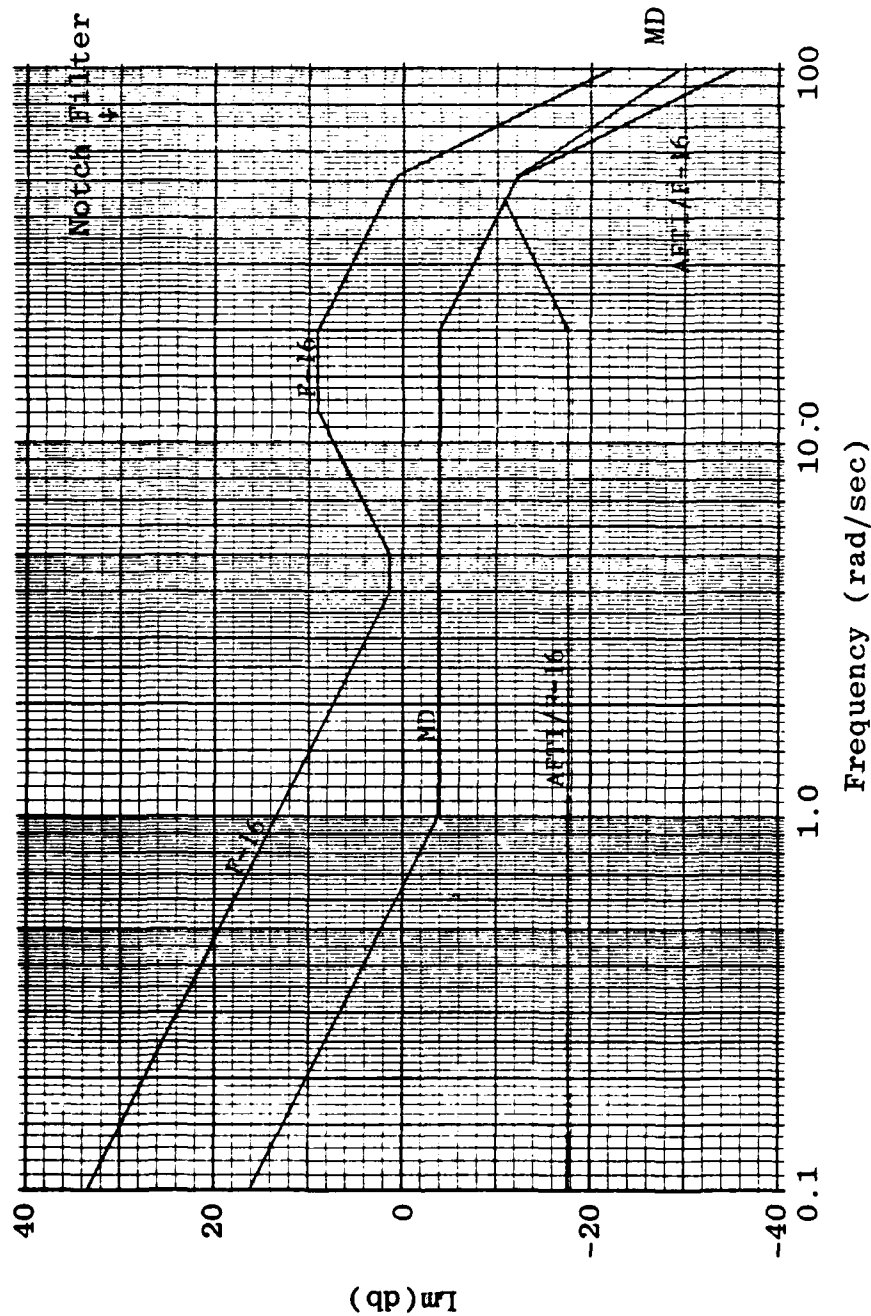
Figure 63. Open-Loop Bandwidth Comparison for the Acceleration to Elevator Path

196

the F-16 and the AFTI/F-16 systems, both of these systems have been modified with notch filters to eliminate structural interaction problems. The center frequency of the AFTI double notch filter is marked on Figure 63. Thus, even with the present system design, notch filters may be required once installation and testing begin. The design must be able to accept such filters without undue degradation. The ability to evaluate such filter additions is needed in the computer-aided design package and is recommended in Chapter VI.

The comparisons are accomplished for only one surface at one flight condition. A complete survey is needed for all sensor-to-surface paths at all flight conditions so that a realistic overall bandwidth assessment can be made. Such an extensive evaluation is recommended for any future efforts with these designs.

Robustness versus Tailoring

One measure of robustness is the ability of a control system design, with fixed gains, to provide acceptable performance over a wide range of flight conditions. However, in this study, emphasis is placed on tailoring the control system design at each flight condition to provide responses that improve the accomplishment of a specific task. The specific task of concern is air-to-air gunnery. To establish one set of gains for all flight conditions results in

197

a compromise in performance for the sake of reduced complexity. Two points need to be considered. First, gain scheduling is easily accomplished with current digital flight hardware. Second, since flight conditions change rather slowly, the update rate for gain scheduling is relatively low. In the AFTI system, the control commands are solved 64 times per second, but the gains are calculated only once a second. Considering both of these points and the desire for improved performance, a compromise in performance is not acceptable.

In this report, a design is considered robust if it can tolerate uncertainties in the aircraft model. A design to give specific performance is based on an aircraft model developed from wind tunnel data with an accuracy of 3 to 5 percent. A test of robustness is the ability of a design to yield acceptable performance for an inaccurate parameter in the aircraft model. Such an ability significantly reduces the fine tuning and redesign at late stages in the development of a new system.

To illustrate the robustness, the design developed for the 0.9 Mach 20,000 feet condition is evaluated with an aircraft model in which the pitching moment coefficient of the elevator ($Cm_{\delta e}$) is decreased by 15 percent. The results are shown in the comparison responses in Figures 64 and 65. The aircraft responses are essentially the same although

some difference in the surface positions are apparent.
Using this measure, these designs are considered robust.
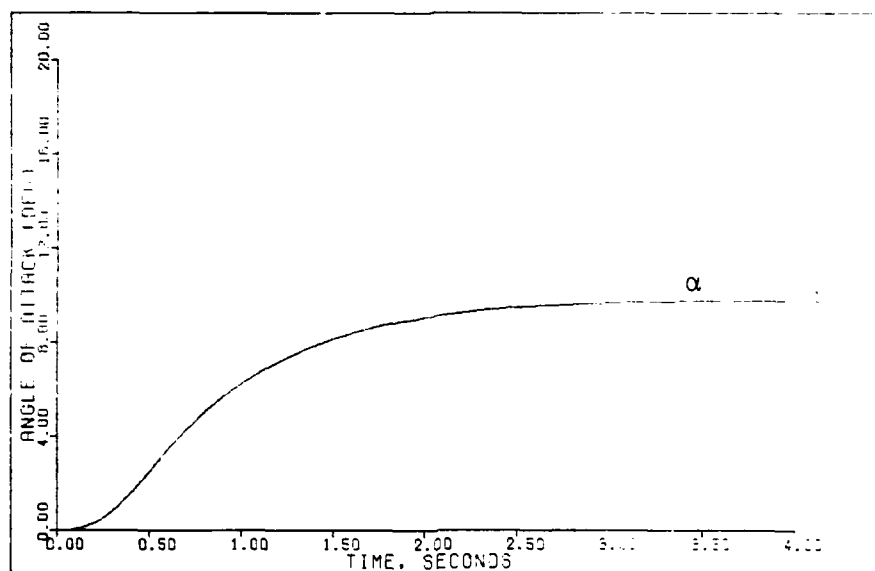
Figure 64a. G-Command System Response to a 9g Step
Command--Nominal $C_{m_{\delta e}}$ (0.9 Mach 20,000 feet)
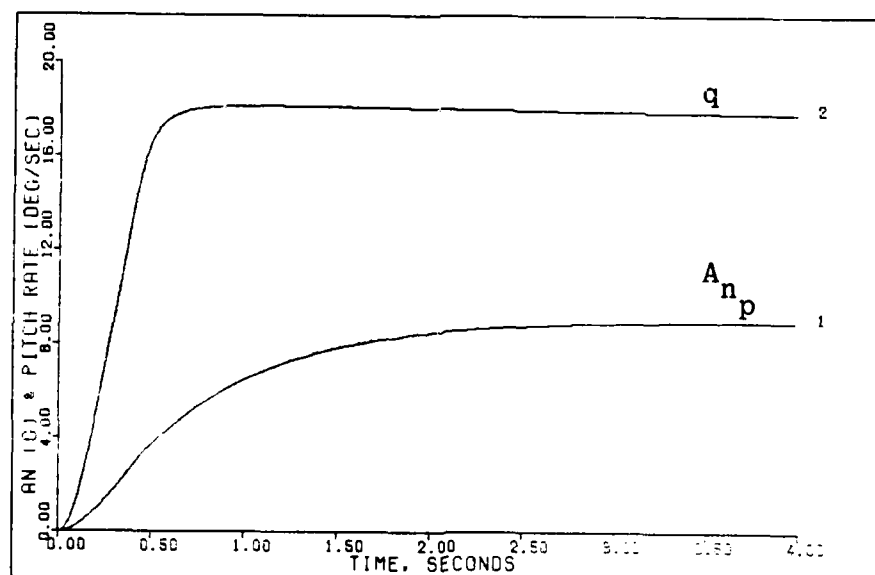
Figure 64b. G-Command System Response to a 9g Step
Command--Nominal $C_{m_{\delta e}}$ (0.9 Mach 20,000 feet)

200
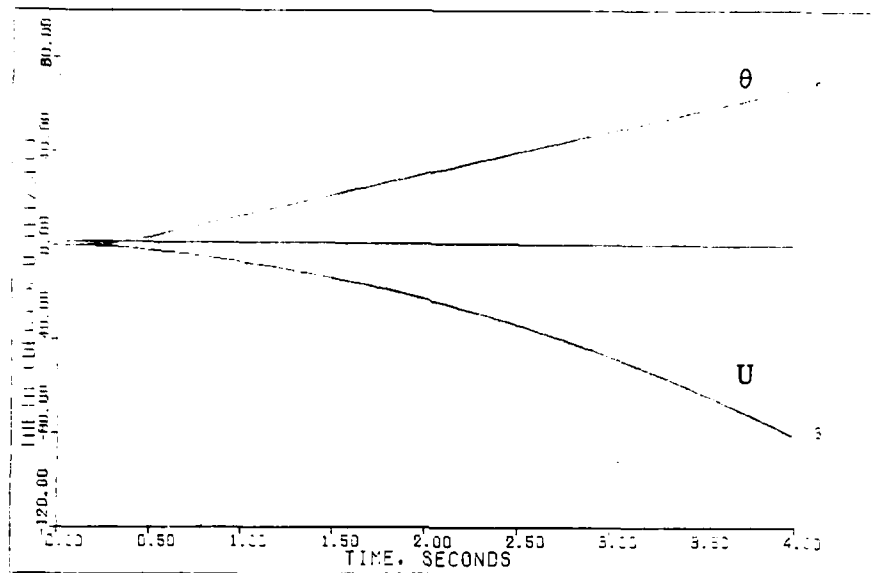
Figure 64c. G-Command System Response to a 9g Step
Command--Nominal $C_{m_{\delta e}}$ (0.9 Mach 20,000 feet)
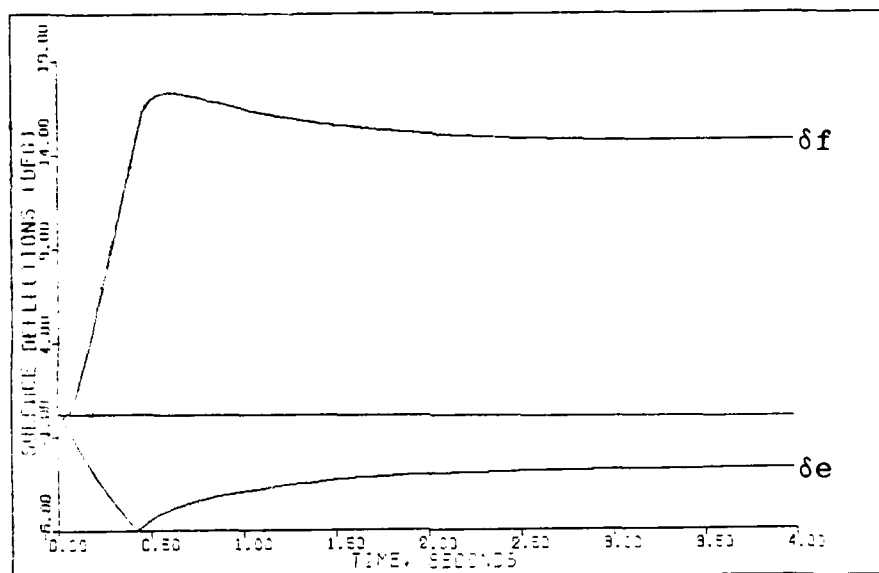
Figure 64d. G-Command System Response to a 9g Step
Command--Nominal $C_{m_{\delta e}}$ (0.9 Mach 20,000 feet)

201
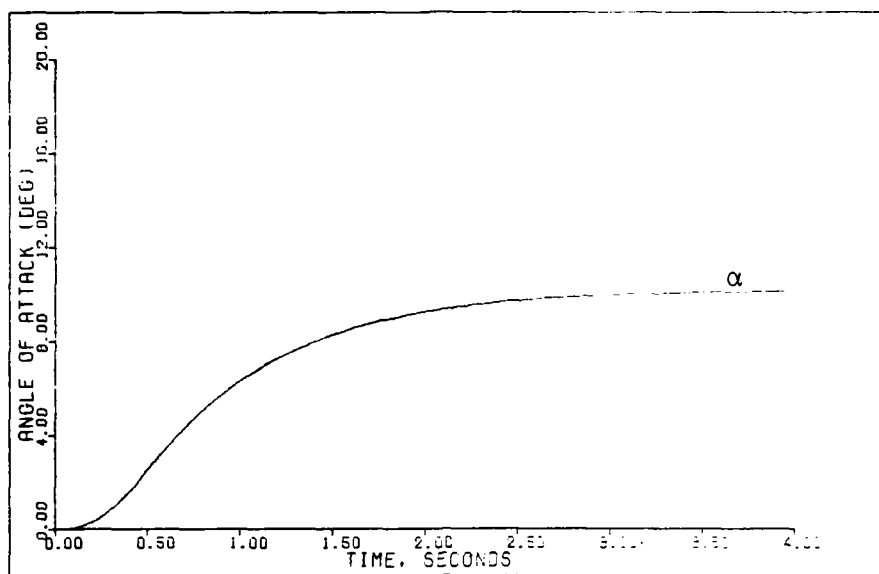
Figure 65a.   G-Command System Response to a 9g Step
Command--Reduced $C_{m_{\delta e}}$ (0.9 Mach 20,000 feet)
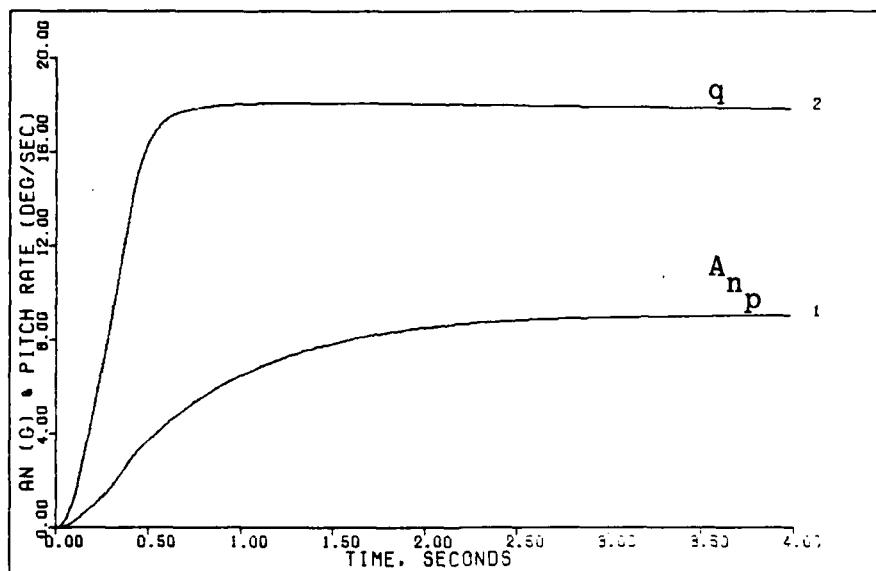
Figure 65b.   G-Command System Response to a 9g Step
Command--Reduced $C_{m_{\delta e}}$ (0.9 Mach 20,000 feet)
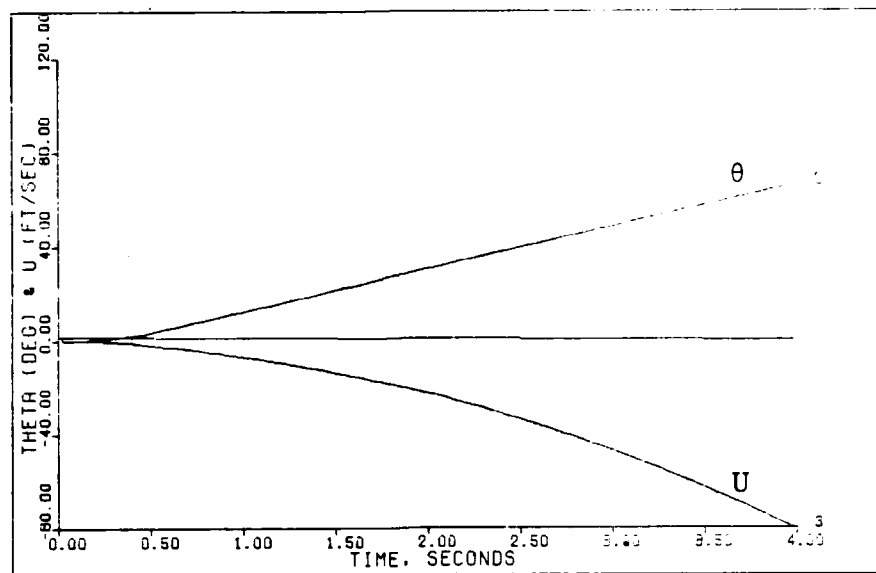
Figure 65c.   G-Command System Response to a 9g Step
     Command--Reduced $C_{m_{\delta e}}$ (0.9 Mach 20,000 feet)
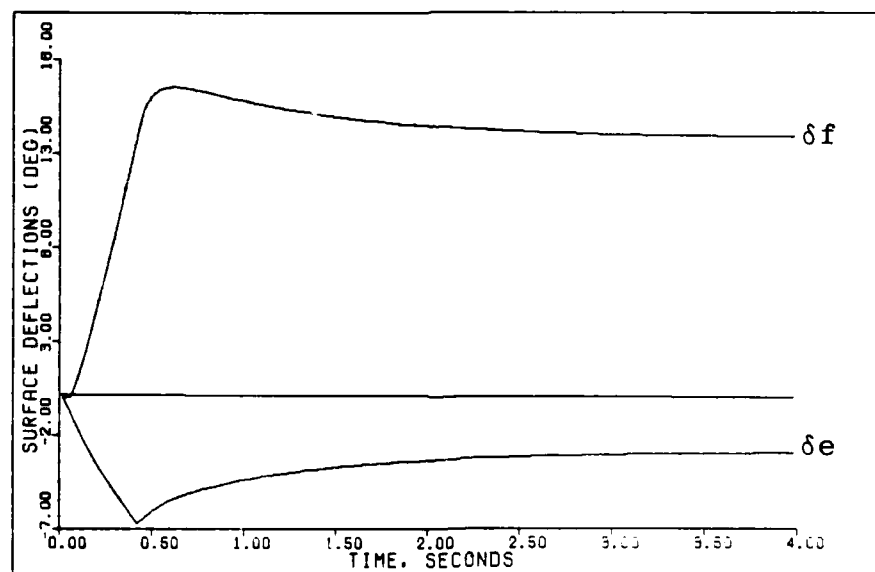
Figure 65d.   G-Command System Response to a 9g Step
     Command--Reduced $C_{m_{\delta e}}$ (0.9 Mach 20,000 feet)

203

VI. Conclusions and Recommendations

Design Results

Very good performance is obtained from the controller
designs developed with Professor Porter's techniques in this
study. The time responses exhibit the desired characteris-
tics and meet the established requirements. The techniques
are found to be extremely flexible. A design method is
formulated that can be used in the synthesis of conventional
multivariable control laws and decoupled (CCV) control laws.
Controllers are developed that provide the pilot with pre-
cise control over aircraft body rates and accelerations
without increasing workload. The interactive capability of
the MULTI program results in an efficient and cost effective
design method.

The flight control design structure consists of a
g-command system in the longitudinal axis. It accepts
inputs in the form of acceleration commands from the pilot's
sidestick and provides a blend of direct lift and conven-
tional aircraft control. In the lateral axis, a roll rate
system accepts pilot commands from lateral forces on the
sidestick and develops the desired roll rate about the air-
craft's velocity vector. For directional control, direct
sideforce is available through the rudder pedals. In addi-
tion, independent fuselage pointing in both the pitch and
yaw axes can be commanded through this same structure.

It is acknowledged that the designs are not *optimum* in every sense; however, the design method is a viable alternative and has many advantages compared with the currently available multivariable techniques. These advantages become more attractive when recognizing that the iterative process of fine tuning is an inherent requirement of any design method. The major advantages are:

1. The ease of design and the ability to fine tune to specific requirements.

2. The use of output feedback without the need of full state information.

3. The high degree of decoupling available.

4. The similarity in developing continuous and discrete designs.

It must be noted that these conclusions are based on a "preliminary design" effort. Because the techniques may result in high gain controllers, caution must be exercised in selecting final design values. It is recommended that surface rate and position limits be considered in the early design work. Use of estimated maximum maneuvers at each design point provides a means of scaling gains to prevent exceeding surface position limits.

Considerable effort is expended in the development of a proper aircraft model for the design. However, this problem is encountered with any design method. Once the modelling is achieved, the designs in this report are

accomplished in a simple, straightforward manner. An under-
standing of the fundamental physics of the aircraft's
response cannot be overemphasized. It is through such an
understanding that a realistic and desirable system design
is established.

Simplifying and Improving the Design Process

From the experience gained in this research, several
changes are suggested to simplify the design process. First,
the use of s-plane closed-loop root migrations and open-loop
frequency response data can reduce trial and error design
time and allow conventional gain and phase margin testing.

Second, the ability to directly observe the influ-
ences of surface rate limits provides valuable insight into
the implementation restrictions imposed on a design. With
such an ability, gain values can be quickly determined which
yield acceptable and practical designs.

Third, a means of including compensation filters in
the design process allows a more realistic assessment to be
made. The ability of a chosen design to accept such filter
additions can then be determined early in the synthesis
process.

Fourth, a way to directly vary the integral gains
without altering proportional gains can simplify the design
process.

Finally, considerable effort and implementation complexity can be saved by designing in a non zero-B_2 format with nonredundant equations.

MULTI Improvements

All of the simplifications and improvements for the design process relate directly to changes in the MULTI package. To be able to use frequency domain techniques in the design, MULTI has been altered to provide both open-loop and closed-loop transfer functions. However, it is necessary at present to go to another program (TOTAL) to obtain frequency response plots. In addition, it will be beneficial to calculate the closed-loop roots for each design iteration. A plot from these iterations will provide a pseudo closed-loop root locus for the system. In this way, the powerful frequency domain techniques can be utilized.

To provide the ability to observe the effects of surface rate limits, the actuator model option must be altered to include these nonlinearities in the same way that position limits are currently provided. In this way, instabilities that might be encountered due to rate limits can be seen immediately. Designs with reduced but practical gains will result.

An option is needed to allow compensation filters to be added at the system inputs and to allow notch filters to be inserted between the controller outputs and the

actuator models. The influence of such filters (that will almost certainly be added during flight test) can be evaluated at this early design stage.

As MULTI is presently configured, changing the $\bar{\alpha}$ parameter varies the proportional gains, directly affecting stability, while holding the integral gains constant. When the integral-to-proportional gain ratio is varied to alter the time to reach steady state, $\bar{\alpha}$ is changed and ε must be adjusted to return the proportional gain to its original value. This unnecessarily complicates the design effort. Only a minor modification to MULTI is needed to eliminate this problem.

The method of calculating gains with $[\underline{F}_2\underline{B}_2]$ requires an additional transformation to zero-B_2 form if a design is to be developed with a minimum number of measurement matrix elements. This transformation results in feedback states that include components of surface deflections for the designs in this study. Although an adequate design can be obtained, this adds complexity to the system. Equivalent performance and decoupling can be achieved without this complication if $[\underline{FB}]$ is used for gain calculations. (Note: This change is currently being made to the MULTI program.)

The use of redundant equations results in unnecessary complexity in the design activity and can cause numerical computation problems. The equations are included so that pertinent aircraft parameters such as angle of attack

and sideslip angle can be evaluated while controlling rates and accelerations. This requires that MULTI be modified to plot any combination of states instead of only those output which are being controlled. In this same light, it will be advantageous to provide a means to plot state derivatives or combinations of state derivatives and states. With such an expanded capability, almost any aircraft parameter of interest can be monitored during the design. Currently, this requires significant modifications to the matrix of system equations.

Proposed Future Work

The major uncertainty with the designs presented in this report concerns their performance in a real world environment. The effects of gust inputs, sensor measurement noise, and structural mode interference need to be evaluated. The system's behavior with digital time delays, quantization effects and nonlinear aerodynamics must be ascertained. It is proposed that the current designs be carried into a nonlinear simulation evaluation where a realistic operational environment can be provided.

The Neal-Smith Criterion is applied to obtain an indication of pilot rating in a compensatory tracking task for one longitudinal design. This is only a cursory check with one of several methods. Recent work has been accomplished on a modified flying qualities evaluation method (Ref 19). Several other evaluation methods such as the step

target tracking technique and the bandwidth criteria are also available (Ref 17 and 18). The current designs should be evaluated using these methods.

The high gain instabilities illustrated in Figures 43 and 44 of Chapter IV should be examined in detail and a method developed to accurately predict the stability boundaries. This work can be a part of the simulation evaluation discussed previously.

References

1. Rubertus, Duane P. "TWEAD Control Augmentation System." Paper presented at the National Aerospace Electronics Conference, Dayton, Ohio, 15-17 May 1972.

2. Sutherland, J.P. "Fly-by-Wire Flight Control System." Paper given at the Joint Meeting of Flight Mechanics and Guidance Control Panels of AGARD, Oslo, Norway, September 1968.

3. Whitmoyer, Robert A., and James K. Ramage. "The Fighter Control Configured Vehicle (CCV) Program Development and Flight Test Summary." Paper presented at the Eighth Annual Symposium of the Society of Flight Test Engineers, Washington, D.C., 10-12 August 1977.

4. McAllister, J.D. Task Oriented CCV Control Modes. (Phase VIII Report), FZM-620-058, General Dynamics, Fort Worth, Texas, 28 September 1979.

5. Barfield, A. Finley. "Flight Experience with Manually Controlled Unconventional Aircraft Motions." Paper presented at the 14th Annual Conference on Manual Control, Los Angeles, California, April 1978.

6. Porter, B. Design of High Performance Tracking Systems. USAME/DC/120/81. Air Force Flight Dynamics Laboratory, Wright-Patterson AFB, Ohio.

7. Johannes, Robert P., and Robert A. Whitmoyer. "AFFDL Experience in Active Control Technology." AGARD Conference Proceedings No. CP262 on Aerodynamic Characteristics of Control, Pozzuoli, Italy, 14-17 May 1979.

8. Rosenbrock, H.H. "The Zeros of a System," International Journal of Control, 18 (2): 297-299 (1973).

9. Ridgely, D. Brett, Siva S. Banda, and John J. D'Azzo. "Decoupling of High Gain Multivariable Tracking Systems." Paper No. 83-0280 presented at the AIAA 21st Aerospace Sciences Conference, Reno, Nevada, 10-13 January 1983.

10. Porter, Douglas S. Design and Analysis of a Multivariable Digital Controller for the A-7D DIGITAC II Aircraft and the Development of an Interactive Computer Design Program. MS Thesis. Air Force Institute of Technology, Wright-Patterson AFB OH, December 1981.

11. D'Azzo, John J., and Constantine H. Houpis. Linear Control Systems Analysis and Design (Second Edition). New York: McGraw-Hill Book Company, 1981.

12. Kennedy, Thomas A. The Design of Digital Controllers for the C-141 Aircraft Using Entire Eigenstructure Assignment and the Development of an Inter-Active Computer Design Program. MS Thesis. Air Force Institute of Technology, Wright-Patterson AFB OH, March 1979.

13. Lewis, Tom. High-Gain Error Actuated Flight Control Systems for Continuous Multivariable Plants. MS Thesis. Air Force Institute of Technology, Wright-Patterson AFB OH, December 1982.

14. Bauschlicher, Jon M. Design of a Complete Multivariable Digital Flight Control System. MS Thesis. Air Force Institute of Technology, Wright-Patterson AFB OH, December 1982.

15. Townsend, James L., and Eugene T. Raymond. Background Information and User Guide for Mil-F-9490D Flight Control Systems - Design, Installation and Test of Piloted Aircraft, General Specification for. AFFDL-TR-74-116, Air Force Flight Dynamics Laboratory, Wright-Patterson AFB, Ohio, January 1975.

16. Neal, Peter T., and Rogers E. Smith. An In-Flight Investigation to Develop Control System Design Criteria for Fighter Aircraft. AFFDL-TR-70-74, Volume 1. Air Force Flight Dynamics Laboratory, Wright-Patterson AFB, Ohio, December 1970.

17. Hoh, Roger H., Thomas T. Myers, Irving L. Ashkenas, Robert F. Ringland, and Samual J. Craig. Development of Handling Quality Criteria for Aircraft With Independent Control of Six Degrees of Freedom. AFWAL-TR-81-3027. Flight Dynamics Laboratory, Wright-Patterson AFB, Ohio, April 1981.

18. Onstott, E.D., and W.H. Faulkner. Prediction, Evaluation, and Specification of Closed Loop and Multiaxis Flying Qualities. AFFDL-TR-78-3. Air Force Flight Dynamics Laboratory, Wright-Patterson AFB, Ohio, February 1978.

19. Smith, Ralph H., and Norman D. Geddes. Handling Quality Requirements for Advanced Aircraft Design: Longitudinal Mode. AFFDL-TR-78-154. Air Force Flight Dynamics Laboratory, Wright-Patterson AFB, Ohio, August 1979.

20. Roskam, J. Airplane Flight Dynamics and Automatic Flight Controls. Lawerence, Kansas: Roskam Aviation and Engineering Corporation, 1976.

21. Barfield, A. Finley, and Larry R. Felt. "Aeroservoelasticity - A Merging of Technologies." Paper presented at the 7th Annual Symposium of the Society of Flight Test Engineers, Eastsound, Washington, 4-6 August 1976.

22. Lamont, Gary B., and Constantine H. Houpis. Digital Control System: Theory, Hardware, Software. McGraw-Hill Book Company, to be published.

Appendix A

Aircraft Aerodynamic Data

At each design flight condition, three types of data are presented for the aircraft.

1. Aircraft parameters and stability axis aerodynamic coefficients are provided in table form.

2. Body axis primed dimensional derivatives from the CAT program (see Appendix D) for use in setting up a state-space model are listed. Chapter II and Appendix B describe the primed derivatives. The units are radians for angles, radians per second for angular rates, feet per second for velocity, and feet per second squared for acceleration.

3. Aircraft model files used for input to the MULTI program are given. (These have been converted to yield acceleration at the pilot's station as a state, and they are in convenient units.) The units are degrees for angular quantities, degrees per second for angular rates, feet per second for velocity, and g's for acceleration. The states are augmented with an actuator model of $20/(s+20)$ for all control surfaces.

In the data for the lateral-directional axis, δ_{DT} represents the differential deflection of the horizontal tail used to augment roll control. For this study, the ratio of aileron to differential tail is set to 0.25; thus when

214

an aileron deflection is shown, it is a combination of the two surfaces.

$$\delta_a = \delta_{aileron} + 0.25\ \delta_{DT}$$

For all designs, an actuator model on all control surfaces and a sensor model on all feed back signals of $500/(s + 500)$ is used.

Aircraft Data for the 0.9 Mach and 20,000 Feet
Flight Condition

Aircraft Parameters

$\bar{q}$ (dynamic pressure - lbs/ft^2) = 552.11295

S (wing reference area - ft^2) = 300.0

c (wing mean aerodynamic cord - ft) = 11.32

b (wing span - ft) = 30.0

V_T (trim velocity - ft/sec) = 933.23

W (weight - lbs) = 21,018.0

Inertias: I_{xx} (slug - ft^2) = 10,033.4

$\qquad\qquad$ I_{yy} (slug - ft^2) = 53,876.3

$\qquad\qquad$ I_{zz} (slug - ft^2) = 61,278.4

$\qquad\qquad$ I_{xz} (slug - ft^2) = 282.132

Aircraft Aerodynamic Coefficients in the Stability Axis

α(deg) = 1.86

C_L = 0.126186	C_m = 0.0	C_D = 0.023766
$C_{L_\alpha}(\frac{1}{deg})$ = 0.094812	$C_{m_\alpha}(\frac{1}{deg})$ = 0.001938	$C_{D_\alpha}(\frac{1}{deg})$ = 0.002636
$C_{L_{\delta_e}}(\frac{1}{deg})$ = 0.009578	$C_{m_{\delta_e}}(\frac{1}{deg})$ = -0.012086	$C_{D_{\delta_e}}(\frac{1}{deg})$ = 0.000173
$C_{L_{\delta_f}}(\frac{1}{deg})$ = 0.015718	$C_{m_{\delta_f}}(\frac{1}{deg})$ = -0.003280	$C_{D_{\delta_f}}(\frac{1}{deg})$ = 0.000351

$C_{L_q}(\frac{1}{rad})$ = 3.161717	$C_{m_q}(\frac{1}{rad})$ = -2.382199	
$C_{L_{\dot{\alpha}}}(\frac{1}{rad})$ = -1.357762	$C_{m_{\dot{\alpha}}}(\frac{1}{rad})$ = -1.307597	
$C_{L_u}(\frac{1}{ft/sec})$ = -0.000442	$C_{m_u}(\frac{1}{ft/sec})$ = -0.000060	$C_{D_u}(\frac{1}{ft/sec})$ = 0.000160
$C_{y_\beta}(\frac{1}{deg})$ = -0.022052	$C_{n_\beta}(\frac{1}{deg})$ = 0.001675	$C_{\ell_\beta}(\frac{1}{deg})$ = -0.001901
$C_{y_p}(\frac{1}{rad})$ = 0.057563	$C_{n_p}(\frac{1}{rad})$ = -0.005541	$C_{\ell_p}(\frac{1}{rad})$ = -0.351217
$C_{y_r}(\frac{1}{rad})$ = 0.557635	$C_{n_r}(\frac{1}{rad})$ = -0.279120	$C_{\ell_r}(\frac{1}{rad})$ = 0.021937
$C_{y_{\delta_r}}(\frac{1}{deg})$ = 0.002377	$C_{n_{\delta_r}}(\frac{1}{deg})$ = -0.001272	$C_{\ell_{\delta_r}}(\frac{1}{deg})$ = 0.000331
$C_{y_{\delta_a}}(\frac{1}{deg})$ = -0.000088	$C_{n_{\delta_a}}(\frac{1}{deg})$ = -0.00016	$C_{\ell_{\delta_a}}(\frac{1}{deg})$ = -0.001804
$C_{y_{\delta_{DT}}}(\frac{1}{deg})$ = 0.001708	$C_{n_{\delta_{DT}}}(\frac{1}{deg})$ = -0.000997	$C_{\ell_{\delta_{DT}}}(\frac{1}{deg})$ = -0.001816
$C_{y_{\delta_c}}(\frac{1}{deg})$ = 0.001716	$C_{n_{\delta_c}}(\frac{1}{deg})$ = 0.001256	$C_{\ell_{\delta_c}}(\frac{1}{deg})$ = 0.000230

0.9 Mach 20,000 Feet Flight Condition

Longitudinal Body Axis Primed Dimensional Derivatives

$Z_\alpha' = -1.48446$ $\qquad$ $M_\alpha' = 4.27171$ $\qquad$ $X_\alpha' = 38.2906$

$Z_{\delta_e}' = -0.149227$ $\qquad$ $M_{\delta_e}' = -24.0581$ $\qquad$ $X_{\delta_e}' = 2.00593$

$Z_{\delta_f}' = -0.244924$ $\qquad$ $M_{\delta_f}' = -6.47269$ $\qquad$ $X_{\delta_f}' = 2.31681$

$Z_q' = 0.994789$ $\qquad$ $M_q' = -0.777221$ $\qquad$ $X_q' = -30.1376$

$Z_u' = -0.000022$ $\qquad$ $M_u' = -0.000130$ $\qquad$ $X_u' = -0.012075$

$Z_\theta' = -0.001120$ $\qquad$ $M_\theta' = 0.000309$ $\qquad$ $X_\theta' = -32.1830$

Lateral-Directional Body Axis Primed Dimensional Derivatives

$N_\beta' = 7.2370$ $\qquad$ $L_\beta' = -55.2526$ $\qquad$ $Y_\beta' = -0.343554$

$N_p' = -0.023184$ $\qquad$ $L_p' = -2.80004$ $\qquad$ $Y_p' = 0.032636$

$N_r' = -0.362530$ $\qquad$ $L_r' = 0.145674$ $\qquad$ $Y_r' = -0.997556$

$N_{\delta_r}' = -5.80890$ $\qquad$ $L_{\delta_r}' = 10.3955$ $\qquad$ $Y_{\delta_r}' = 0.037032$

$N_{\delta_a}' = -1.25006$ $\qquad$ $L_{\delta_a}' = -51.0502$ $\qquad$ $Y_{\delta_a}' = -0.001371$

$N_{\delta_{DT}}' = -5.13710$ $\qquad$ $L_{\delta_{DT}}' = -50.7290$ $\qquad$ $Y_{\delta_{DT}}' = 0.026609$

$N_{\delta_c}' = 5.89254$ $\qquad$ $L_{\delta_c}' = 5.53185$ $\qquad$ $Y_{\delta_c}' = 0.026734$

Longitudinal Axis (0.9 Mach 20,000 Feet)

```
100=1
110=7 2 2
120=0 -.1123E-2 -.1596E-3 -1.896 .9886 -.1492 -.2449
130=0 0 0 0 1 0 0
140=0 -.5617 -.01258 .8522 -.5232 .03492 .0403
150=0 -.1211E-2 -.0782E-4 -1.502 .7764 -.03891 -.1706
160=0 .3213E-3 -.01068 5.455 -.7595 -24.06 -6.473
170=0 0 0 0 0 -20 0
180=0 0 0 0 0 0 -20
190=0 0
200=0 0
210=0 0
220=0 0
230=0 0
240=20 0
250=0 20
260=0 0 0 1 0 -.1064 .07496
270=0 0 0 0 1 0 0
280=NO
290=NO
300=NO
```

The state vector is:

$$
x = \begin{bmatrix}
\alpha(\text{deg}) \\
\theta(\text{deg}) \\
u(\text{ft/sec}) \\
A_{n_p} + 0.1064\ \delta_e - 0.07496\ \delta_f\ (\text{g}) \\
q(\text{deg/sec}) \\
\delta_e(\text{deg}) \\
\delta_f(\text{deg})
\end{bmatrix}
$$

Lateral-Directional Axis (0.9 Mach   20,000 Feet)


```
100=1
110=8,3,3
120=0,.3449E-1,2.886,.3285E-1,-.0032,.5281E-2,.3703E-1,.2673E-1
130=0,0,0,1,0,0,0,0
140=0,-.4105E-2,-.2929,-.3625E-2,.1188,.8796E-2,.3426E-2,-.1254F-1
150=0,0,464.1,-2.759,.8441,-63.73,10.39,5.533
160=0,0,-60.79,-.02853,-.454,-2.534,-5.809,5.802
170=0,0,0,0,0,-20,0,0
180=0,0,0,0,0,0,-20,0
190=0,0,0,0,0,0,0,-20
200=0,0,0
210=0,0,0
220=0,0,0
230=0,0,0
240=0,0,0
250=20,0,0
260=0,20,0
270=0,0,20
280=0,0,1,0,0,-.01649,-.02519,.05807
290=0,0,0,1,0,0,0,0
300=0,0,0,0,1,0,0,0
310=NO
320=NO
330=NO
```

The state vector is:

$$
x = \begin{bmatrix}
\beta(\text{deg}) \\
\phi(\text{deg}) \\
A_{y_p} + 0.01649\ \delta_a + 0.02519\ \delta_r - 0.05807\ \delta_c\ (\text{g}) \\
p(\text{deg/sec}) \\
r(\text{deg/sec}) \\
\delta_a(\text{deg}) \\
\delta_r(\text{deg}) \\
\delta_c(\text{deg})
\end{bmatrix}
$$

NOTE: For the Roll Rate System, the gravity term in the β and A_y equations is dropped, and the yaw rate command drives $r-p\alpha$ to zero. To accomplish this, the 2nd term in lines 120 and 140 must be set to zero, and the fourth term in line 300 is changed from zero to a value of -0.0325 to account for the $p\alpha$ expression.

Aircraft Data for the 1.6 Mach and 30,000 Feet
Flat Condition

<div style="text-align:center;">

$\overline{\overline{}}$

</div>

Aircraft Parameters

$\overline{q}$ (dynamic pressure - lbs/ft^2) = 1129.3126

S (wing reference area - ft^2) = 300.0

c (wing mean aerodynamic cord - ft) = 11.32

b (wing span - ft) = 30.0

V_T (trim velocity - ft/sec) = 1591.75

W (weight - lbs) = 21,018.0

Inertias: I_{xx} (slug - ft^2) = 10,033.4

I_{yy} (slug - ft^2) = 53,876.3

I_{zz} (slug - ft^2) = 61,278.5

I_{xz} (slug - ft^2) = 282.132

Aircraft Aerodynamic Coefficients in the Stability Axis

α(deg) = 1.68

C_L	= 0.060695	C_m	= 0.0	C_D	= 0.046574
$C_{L_\alpha}(\frac{1}{deg})$	= 0.066129	$C_{m_\alpha}(\frac{1}{deg})$	= -0.010705	$C_{D_\alpha}(\frac{1}{deg})$	= 0.001457
$C_{L_{\delta_e}}(\frac{1}{deg})$	= 0.006180	$C_{m_{\delta_e}}(\frac{1}{deg})$	= -0.008061	$C_{D_{\delta_e}}(\frac{1}{deg})$	= -0.000135
$C_{L_{\delta_f}}(\frac{1}{deg})$	= 0.004004	$C_{m_{\delta_f}}(\frac{1}{deg})$	= -0.001432	$C_{D_{\delta_f}}(\frac{1}{deg})$	= 0.000565

$C_{L_q}(\frac{1}{rad})$ $\quad = \quad 3.458724$	$C_{m_q}(\frac{1}{rad})$ $\quad = -1.889366$	
$C_{L_{\dot{\alpha}}}(\frac{1}{rad})$ $\quad = -2.974699$	$C_{m_{\dot{\alpha}}}(\frac{1}{rad})$ $\quad = \quad 0.501981$	
$C_{L_u}(\frac{1}{ft/sec}) = \quad 0.000027$	$C_{m_u}(\frac{1}{ft/sec}) = -0.000046$	$C_{D_u}(\frac{1}{ft/sec}) = \quad 0.000002$
$C_{y_\beta}(\frac{1}{deg})$ $\quad = -0.019192$	$C_{n_\beta}(\frac{1}{deg})$ $\quad = \quad 0.00088$	$C_{\ell_\beta}(\frac{1}{deg})$ $\quad = -0.001702$
$C_{y_p}(\frac{1}{rad})$ $\quad = \quad 0.026463$	$C_{n_p}(\frac{1}{rad})$ $\quad = \quad 0.004371$	$C_{\ell_p}(\frac{1}{rad})$ $\quad = -0.257331$
$C_{y_r}(\frac{1}{rad})$ $\quad = \quad 0.516864$	$C_{n_r}(\frac{1}{rad})$ $\quad = -0.246367$	$C_{\ell_r}(\frac{1}{rad})$ $\quad = \quad 0.018261$
$C_{y_{\delta_r}}(\frac{1}{deg})$ $\quad = \quad 0.000552$	$C_{n_{\delta_r}}(\frac{1}{deg})$ $\quad = -0.000349$	$C_{\ell_{\delta_r}}(\frac{1}{deg})$ $\quad = \quad 0.000077$
$C_{y_{\delta_a}}(\frac{1}{deg})$ $\quad = \quad 0.000362$	$C_{n_{\delta_a}}(\frac{1}{deg})$ $\quad = -0.000236$	$C_{\ell_{\delta_a}}(\frac{1}{deg})$ $\quad = -0.000250$
$C_{y_{\delta_{DT}}}(\frac{1}{deg}) = \quad 0.000281$	$C_{n_{\delta_{DT}}}(\frac{1}{deg}) = -0.000317$	$C_{\ell_{\delta_{DT}}}(\frac{1}{deg}) = -0.000811$
$C_{y_{\delta_c}}(\frac{1}{deg})$ $\quad = \quad 0.001541$	$C_{n_{\delta_c}}(\frac{1}{deg})$ $\quad = \quad 0.000973$	$C_{\ell_{\delta_c}}(\frac{1}{deg})$ $\quad = \quad 0.000232$

222

1.6 Mach 30,000 Feet Flight Condition

Longitudinal Body Axis Primed Dimensional Derivatives

$Z_\alpha{}' = -1.25100$ $M_\alpha{}' = -43.8012$ $X_\alpha{}' = 45.1941$

$Z_{\delta_e}{}' = -0.115337$ $M_{\delta_e}{}' = -32.8919$ $X_{\delta_e}{}' = 9.40431$

$Z_{\delta_f}{}' = -0.075084$ $M_{\delta_f}{}' = -5.85004$ $X_{\delta_f}{}' = -13.3021$

$Z_q{}' = 0.995991$ $M_q{}' = -0.351737$ $X_q{}' = -46.5132$

$Z_u{}' = -0.000002$ $M_u{}' = 0.000802$ $X_u{}' = -0.030046$

$Z_\theta{}' = -0.000593$ $M_\theta{}' = -0.000075$ $X_\theta{}' = -32.1861$

Lateral-Directional Body Axis Primed Dimensional Derivatives

$N_\beta{}' = 7.42422$ $L_\beta{}' = -100.032$ $Y_\beta{}' = -0.358564$

$N_p{}' = -0.005040$ $L_p{}' = -2.46287$ $Y_p{}' = 0.029374$

$N_r{}' = -0.383316$ $L_r{}' = 0.160287$ $Y_r{}' = -0.998410$

$N_{\delta_r}{}' = -3.27086$ $L_{\delta_r}{}' = 4.96942$ $Y_{\delta_r}{}' = 0.010313$

$N_{\delta_a}{}' = -2.37673$ $L_{\delta_a}{}' = -14.1689$ $Y_{\delta_a}{}' = 0.006763$

$N_{\delta_{DT}}{}' = -3.45190$ $L_{\delta_{DT}}{}' = -46.6078$ $Y_{\delta_{DT}}{}' = 0.005250$

$N_{\delta_c}{}' = 9.36290$ $L_{\delta_c}{}' = 12.0662$ $Y_{\delta_c}{}' = 0.028790$

Longitudinal Axis (1.6 Mach   30,000 Feet)

```
100=1
110=7 2 2
120=0 -.5944E-3 .6413E-3 -1.672 .9973 -.1153 -.07509
130=0 0 0 0 1 0 0
140=0 -.5617 -.03054 1.054 -.8126 .1641 -.2321
150=0 -.7057E-3 .524E-3 -1.297 .7455 -.1125 -.06093
160=0 -.1087E-3 .07318 -58.55 -.305 -32.89 -5.85
170=0 0 0 0 0 -20 0
180=0 0 0 0 0 0 -20
190=0 0
200=0 0
210=0 0
220=0 0
230=0 0
240=20 0
250=0 20
260=0 0 0 1 0 -.149182 .020547
270=0 0 0 0 1 0 0
280=NO
290=NO
300=NO
```

The state vector is:

$$
x = \begin{bmatrix}
\alpha(\text{deg}) \\
\theta(\text{deg}) \\
u(\text{ft/sec}) \\
A_{n_p} + 0.149182\,\delta_e - 0.020547\,\delta_f\ (\text{g}) \\
q(\text{deg/sec}) \\
\delta_e(\text{deg}) \\
\delta_f(\text{deg})
\end{bmatrix}
$$

Lateral-Directional Axis (1.6 Mach 30,000 Feet)

```
100=1
110=8 3 3
120=0 .02022 1.416 .02039 -.0962 .008076 .01031 .0288
130=0 0 0 1 0 0 0 0
140=0 -.00512 -.3170 -.007417 .2529 .003112 .00232 -.02157
150=0 0 305.1 -2.46 .7634 -25.82 4.969 12.07
160=0 0 -29.32 -.00528 -.4281 -3.24 -3.271 9.363
170=0 0 0 0 0 -20 0 0
180=0 0 0 0 0 0 -20 0
190=0 0 0 0 0 0 0 -20
200=0 0 0
210=0 0 0
220=0 0 0
230=0 0 0
240=0 0 0
250=20 0 0
260=0 20 0
270=0 0 20
280=0 0 1 0 0 -.0175279853 -.0158341734 .0956337463
290=0 0 0 1 0 0 0 0
300=0 0 0 0 1 0 0 0
310=NO
320=NO
330=NO
```

The state vector is:

$$
x = \begin{bmatrix}
\beta(\text{deg}) \\
\phi(\text{deg}) \\
A_{y_p} + 0.017528\,\delta_a + 0.015834\,\delta_r - 0.095634\,\delta_c\ (\text{g}) \\
p(\text{deg/sec}) \\
r(\text{deg/sec}) \\
\delta_a(\text{deg}) \\
\delta_r(\text{deg}) \\
\delta_c(\text{deg})
\end{bmatrix}
$$

NOTE: For the Roll Rate System, the gravity term in the β and A_y equations is dropped, and the yaw rate command drives $r-p\alpha$ to zero. To accomplish this, the 2nd term in lines 120 and 140 must be set to zero, and the fourth term in line 300 is changed from zero to a value of -0.02932 to account for the $p\alpha$ expression.

225

Table A-3

Aircraft Data for the 0.6 Mach and 30,000 Feet
Flight Condition

Aircraft Parameters

$\bar{q}$ (dynamic pressure - lbs/ft^2) = 158.81

S (wing reference area - ft^2) = 300.0

c (wing mean aerodynamic cord - ft) = 11.32

b (wing span - ft) = 30.0

V_T (trim velocity - ft/sec) = 596.91

W (weight - lbs) = 21,018.0

Inertias: I_{xx} (slug - ft^2) = 10,033.4

I_{yy} (slug - ft^2) = 53,876.3

I_{zz} (slug - ft^2) = 61,278.5

I_{xz} (slug - ft^2) = 282.132

Aircraft Aerodynamic Coefficients in the
Stability Axis

α(deg) = 4.705

C_L	= 0.439013	C_m	= 0.0	C_D	= 0.044151
$C_{L_\alpha} (\frac{1}{deg})$	= 0.073559	$C_{m_\alpha} (\frac{1}{deg})$	= 0.004356	$C_{D_\alpha} (\frac{1}{deg})$	= 0.008210
$C_{L_{\delta_e}} (\frac{1}{deg})$	= 0.009473	$C_{m_{\delta_e}} (\frac{1}{deg})$	= -0.010229	$C_{D_{\delta_e}} (\frac{1}{deg})$	= 0.000019
$C_{L_{\delta_f}} (\frac{1}{deg})$	= 0.015850	$C_{m_{\delta_f}} (\frac{1}{deg})$	= -0.000383	$C_{D_{\delta_f}} (\frac{1}{deg})$	= 0.001808

$C_{L_q}(\frac{1}{\text{rad}})$ = 2.437286	$C_{m_q}(\frac{1}{\text{rad}})$ = -2.859448	
$C_{L_{\dot{\alpha}}}(\frac{1}{\text{rad}})$ = -1.029896	$C_{m_{\dot{\alpha}}}(\frac{1}{\text{rad}})$ = -0.747194	
$C_{L_u}(\frac{1}{\text{ft/sec}})$ = 0.000158	$C_{m_u}(\frac{1}{\text{ft/sec}})$ = -0.000106	$C_{D_u}(\frac{1}{\text{ft/sec}})$ = 0.000050
$C_{y_{\beta}}(\frac{1}{\text{deg}})$ = -0.021995	$C_{n_{\beta}}(\frac{1}{\text{deg}})$ = 0.001972	$C_{\ell_{\beta}}(\frac{1}{\text{deg}})$ = -0.002209
$C_{y_p}(\frac{1}{\text{rad}})$ = 0.132102	$C_{n_p}(\frac{1}{\text{rad}})$ = -0.013813	$C_{\ell_p}(\frac{1}{\text{rad}})$ = -0.243246
$C_{y_r}(\frac{1}{\text{rad}})$ = 0.536904	$C_{n_r}(\frac{1}{\text{rad}})$ = -0.484330	$C_{\ell_r}(\frac{1}{\text{rad}})$ = 0.071941
$C_{y_{\delta_r}}(\frac{1}{\text{deg}})$ = 0.003021	$C_{n_{\delta_r}}(\frac{1}{\text{deg}})$ = -0.001520	$C_{\ell_{\delta_r}}(\frac{1}{\text{deg}})$ = 0.000364
$C_{y_{\delta_a}}(\frac{1}{\text{deg}})$ = 0.000051	$C_{n_{\delta_a}}(\frac{1}{\text{deg}})$ = 0.000035	$C_{\ell_{\delta_a}}(\frac{1}{\text{deg}})$ = -0.002141
$C_{y_{\delta_{DT}}}(\frac{1}{\text{deg}})$ = 0.002055	$C_{n_{\delta_{DT}}}(\frac{1}{\text{deg}})$ = -0.000940	$C_{\ell_{\delta_{DT}}}(\frac{1}{\text{deg}})$ = -0.001742
$C_{y_{\delta_c}}(\frac{1}{\text{deg}})$ = 0.001047	$C_{n_{\delta_c}}(\frac{1}{\text{deg}})$ = 0.001121	$C_{\ell_{\delta_c}}(\frac{1}{\text{deg}})$ = 0.000138

0.6 Mach   30,000 Feet Flight Condition

Longitudinal Body Axis Primed Dimensional Derivatives

$Z_\alpha' = -0.526422$	$M_\alpha' = 2.52708$	$X_\alpha' = 23.0402$
$Z_{\delta_e}' = -0.066156$	$M_{\delta_e}' = -5.86214$	$X_{\delta_e}' = 3.17035$
$Z_{\delta_f}' = -0.111711$	$M_{\delta_f}' = -0.211773$	$X_{\delta_f}' = -2.09855$
$Z_q' = 0.997184$	$M_q' = -0.341902$	$X_q' = -48.8785$
$Z_u' = -0.000109$	$M_u' = -0.000337$	$X_u' = -0.005142$
$Z_\theta' = -0.004425$	$M_\theta' = 0.000313$	$X_\theta' = -32.0915$

Lateral-Directional Body Axis Primed Dimensional Derivatives

$N_\beta' = 2.29583$	$L_\beta' = -19.2246$	$Y_\beta' = -0.154099$
$N_p' = -0.000888$	$L_p' = -0.893601$	$Y_p' = 0.082387$
$N_r' = -0.278676$	$L_r' = 0.318845$	$Y_r' = -0.998322$
$N_{\delta_r}' = -1.96651$	$L_{\delta_r}' = 3.92325$	$Y_{\delta_r}' = 0.021165$
$N_{\delta_a}' = -0.268403$	$L_{\delta_a}' = -17.4468$	$Y_{\delta_a}' = 0.000357$
$N_{\delta_{DT}}' = -1.50547$	$L_{\delta_{DT}}' = -13.5832$	$Y_{\delta_{DT}}' = 0.014398$
$N_{\delta_c}' = 1.51008$	$L_{\delta_c}' = 0.414519$	$Y_{\delta_c}' = 0.007335$

Longitudinal Axis (0.6 Mach   30,000 Feet)

```
100=1
110=7 2 2
120=0 -.004418 -.001035 -2.779 .9925 -.06615 -.1117
130=0 0 0 0 1 0 0
140=0 -.5601 -.000114 2.123 -.8495 .05533 -.0366
150=0 -.001885 -.000139 -.5448 .1869 -.00264 -.02064
160=0 .0002812 -.04429 13.34 -.3196 -5.862 -.2116
170=0 0 0 0 0 -20 0
180=0 0 0 0 0 0 -20
190=0 0
200=0 0
210=0 0
220=0 0
230=0 0
240=20 0
250=0 20
260=0 0 0 1 0 -.0229207 0.0345517
270=0 0 0 0 1 0 0
280=NO
290=NO
300=NO
```

The state vector is:

$$
x = \begin{bmatrix}
\alpha(\text{deg}) \\
\theta(\text{deg}) \\
u(\text{ft/sec}) \\
A_{n_p} + 0.022921\ \delta_e - 0.034552\ \delta_f\ (\text{g}) \\
q(\text{deg/sec}) \\
\delta_e(\text{deg}) \\
\delta_f(\text{deg})
\end{bmatrix}
$$

MULTI Input File

Lateral-Directional Axis (0.6 Mach   30,000 Feet)

```
100=1
110=8 3 3
120=0 .05376 4.742 .08201 -.0909 .003951 .02116 .007338
130=0 0 0 1 0 0 0 0
140=0 -.001747 .003976 -.002748 .0321 -.00082 .002693 -.002558
150=0 0 591.6 -.9412 1.244 -20.94 3.923 .4149
160=0 0 -70.65 .004791 -.3802 -.6447 -1.966 1.51
170=0 0 0 0 0 -20 0 0
180=0 0 0 0 0 0 -20 0
190=0 0 0 0 0 0 0 -20
200=0 0 0
210=0 0 0
220=0 0 0
230=0 0 0
240=0 0 0
250=20 0 0
260=0 20 0
270=0 0 20
280=0 0 1 0 0 -.0035961 -.00802142 .0137009
290=0 0 0 1 0 0 0 0
300=0 0 0 0 1 0 0 0
310=NO
320=NO
330=NO
```

The state vector is:

$$
x = \begin{bmatrix}
\beta(\text{deg}) \\
\phi(\text{deg}) \\
A_{y_p} + 0.003596\, \delta_a + 0.008021\, \delta_r - 0.013791\, \delta_c \ (\text{g}) \\
p(\text{deg/sec}) \\
r(\text{deg/sec}) \\
\delta_a(\text{deg}) \\
\delta_r(\text{deg}) \\
\delta_c(\text{deg})
\end{bmatrix}
$$

NOTE: For the Roll Rate System, the gravity term in the β and A_y equations is dropped, and the yaw rate command drives $r-p\alpha$ to zero. To accomplish this, the 2nd term in lines 120 and 140 must be set to zero, and the fourth term in line 300 is changed from zero to a value of -0.082115 to account for the $p\alpha$ expression.

Aircraft Data for the 0.2 Mach and 30 Feet
Flight Condition

Aircraft Parameters

$\bar{q}$ (dynamic pressure - lbs/ft^2) = 59.18

S (wing reference area - ft^2) = 300.0

c (wing mean aerodynamic cord - ft) = 11.32

b (wing span - ft) = 30.0

V_T (trim velocity - ft/sec) = 223.26

W (weight - lbs) = 21,018.0

Inertias: I_{xx} (slug - ft^2) = 10,033.4

$\quad\quad\quad\quad$ I_{yy} (slug - ft^2) = 53,876.3

$\quad\quad\quad\quad$ I_{zz} (slug - ft^2) = 61,278.5

$\quad\quad\quad\quad$ I_{xz} (slug - ft^2) = 282.132

Aircraft Aerodynamic Coefficients in the Stability Axis

α(deg) = 14.98

C_L	= 1.161817	C_m	= 0.0	C_D	= 0.237224
$C_{L_\alpha} (\frac{1}{deg})$	= 0.053031	$C_{m_\alpha} (\frac{1}{deg})$	= 0.002630	$C_{D_\alpha} (\frac{1}{deg})$	= 0.027636
$C_{L_{\delta_e}} (\frac{1}{deg})$	= 0.010306	$C_{m_{\delta_e}} (\frac{1}{deg})$	= -0.010462	$C_{D_{\delta_e}} (\frac{1}{deg})$	= 0.002519
$C_{L_{\delta_f}} (\frac{1}{deg})$	= 0.008187	$C_{m_{\delta_f}} (\frac{1}{deg})$	= 0.001132	$C_{D_{\delta_f}} (\frac{1}{deg})$	= 0.003501

231

$C_{L_q}(\frac{1}{rad})$ $\quad = \quad 1.428587$	$C_{m_q}(\frac{1}{rad})$ $\quad = -6.716322$	
$C_{L_{\dot{\alpha}}}(\frac{1}{rad})$ $\quad = -0.775892$	$C_{m_{\dot{\alpha}}}(\frac{1}{rad})$ $\quad = \quad 0.017115$	
$C_{L_u}(\frac{1}{ft/sec}) = -0.000178$	$C_{m_u}(\frac{1}{ft/sec}) = \quad 0.000030$	$C_{D_u}(\frac{1}{ft/sec}) = 0.000063$
$C_{y_\beta}(\frac{1}{deg})$ $\quad = -0.020613$	$C_{n_\beta}(\frac{1}{deg})$ $\quad = \quad 0.002824$	$C_{\ell_\beta}(\frac{1}{deg})$ $\quad = -0.003015$
$C_{y_p}(\frac{1}{rad})$ $\quad = \quad 0.214209$	$C_{n_p}(\frac{1}{rad})$ $\quad = -0.065499$	$C_{\ell_p}(\frac{1}{rad})$ $\quad = -0.201582$
$C_{y_r}(\frac{1}{rad})$ $\quad = \quad 0.640146$	$C_{n_r}(\frac{1}{rad})$ $\quad = -0.509547$	$C_{\ell_r}(\frac{1}{rad})$ $\quad = \quad 0.224680$
$C_{y_{\delta_r}}(\frac{1}{deg})$ $\quad = \quad 0.003103$	$C_{n_{\delta_r}}(\frac{1}{deg})$ $\quad = -0.001716$	$C_{\ell_{\delta_r}}(\frac{1}{deg})$ $\quad = \quad 0.000033$
$C_{y_{\delta_a}}(\frac{1}{deg})$ $\quad = \quad 0.001493$	$C_{n_{\delta_a}}(\frac{1}{deg})$ $\quad = -0.000566$	$C_{\ell_{\delta_a}}(\frac{1}{deg})$ $\quad = -0.001373$
$C_{y_{\delta_{DT}}}(\frac{1}{deg})$ $\quad = \quad 0.003154$	$C_{n_{\delta_{DT}}}(\frac{1}{deg})$ $\quad = -0.000769$	$C_{\ell_{\delta_{DT}}}(\frac{1}{deg}) = -0.001658$
$C_{y_{\delta_c}}(\frac{1}{deg})$ $\quad = \quad 0.000893$	$C_{n_{\delta_c}}(\frac{1}{deg})$ $\quad = \quad 0.000665$	$C_{\ell_{\delta_c}}(\frac{1}{deg})$ $\quad = \quad 0.000074$

0.2 Mach   30 Feet Flight Condition

Longitudinal Body Axis Primed Dimensional Derivatives

$Z_\alpha' = -0.459802$ $M_\alpha' = 0.542375$ $X_\alpha' = 12.5375$

$Z_{\delta_e}' = -0.074045$ $M_{\delta_e}' = -2.23634$ $X_{\delta_e}' = 0.357830$

$Z_{\delta_f}' = -0.061526$ $M_{\delta_f}' = 0.241866$ $X_{\delta_f}' = -1.97404$

$Z_q' = 0.995737$ $M_q' = -0.633651$ $X_q' = -58.0974$

$Z_u' = -0.000786$ $M_u' = -0.000651$ $X_u' = 0.002886$

$Z_\theta' = -0.037268$ $M_\theta' = -0.000058$ $X_\theta' = -31.1064$

Lateral-Directional Body Axis Primed Dimensional Derivatives

$N_\beta' = 0.919806$ $L_\beta' = -11.0532$ $Y_\beta' = -0.143895$

$N_p' = -0.003864$ $L_p' = -0.934188$ $Y_p' = 0.261703$

$N_r' = -0.257624$ $L_r' = 1.03044$ $Y_r' = -0.994485$

$N_{\delta_r}' = -0.814818$ $L_{\delta_r}' = 1.42280$ $Y_{\delta_r}' = 0.021662$

$N_{\delta_a}' = 0.075009$ $L_{\delta_a}' = -4.47725$ $Y_{\delta_a}' = 0.010422$

$N_{\delta_{DT}}' = -0.603086$ $L_{\delta_{DT}}' = -4.28449$ $Y_{\delta_{DT}}' = 0.022018$

$N_{\delta_c}' = 0.328110$ $L_{\delta_c}' = -0.296006$ $Y_{\delta_c}' = 0.006234$

Longitudinal Axis (0.2 Mach   30 Feet)

```
100=1
110=7 2 2
120=0 -.03727 -.005265 -7.697 .9628 -.07405 -.06152
130=0 0 0 0 1 0 0
140=0 -.5429 -.01605 3.663 -.9983 .006246 -.03445
150=0 -.005033 -.00003727 -.4797 .05490 .005177 -.004891
160=0 -.00005428 -.08426 9.079 -.5948 -2.236 .2419
170=0 0 0 0 0 -20 0
180=0 0 0 0 0 0 -20
190=0 0
200=0 0
210=0 0
220=0 0
230=0 0
240=20 0
250=0 20
260=0 0 0 1 0 -.007948251 .0092734112
270=0 0 0 0 1 0 0
280=NO
290=NO
300=NO
```

The state vector is:

$$
x = \begin{bmatrix}
\alpha(\deg) \\
\theta(\deg) \\
A_{n_p} + 0.007948\ \delta_e - 0.009273\ \delta_f\ (g) \\
q(\deg/\sec) \\
\delta_e(\deg) \\
\delta_f(\deg)
\end{bmatrix}
$$

234

Lateral-Directional Axis (0.2 Mach   30 Feet)

```
100=1
110=8 3 3
120=0 .1393 13.76 .2615 -.0769 .01593 .02167 .006242
130=0 0 0 1 0 0 0 0
140=0 -.001457 -.01868 -.002743 .01072 -.0001345 .0008309 -.0004769
150=0 0 1057 -.0468 2.384 -5.548 1.423 -.2954
160=0 0 -87.96 -.002817 -.3702 -.07577 -.8148 .3281
170=0 0 0 0 0 -20 0 0
180=0 0 0 0 0 0 -20 0
190=0 0 0 0 0 0 0 -20
200=0 0 0
210=0 0 0
220=0 0 0
230=0 0 0
240=0 0 0
250=20 0 0
260=0 20 0
270=0 0 20
280=0 0 1 0 0 .00135443 -.00353018 .00323567
290=0 0 0 1 0 0 0 0
300=0 0 0 0 1 0 0 0
310=NO
320=NO
330=NO
```

The state vector is:

$$
x = \begin{bmatrix}
\beta(\text{deg}) \\
\phi(\text{deg}) \\
A_{y_p} - 0.001354\,\delta_a + 0.003539\,\delta_r - 0.003236\,\delta_c\ (\text{g}) \\
p\ (\text{deg/sec}) \\
r(\text{deg/sec}) \\
\delta_a(\text{deg}) \\
\delta_r(\text{deg}) \\
\delta_c(\text{deg})
\end{bmatrix}
$$

NOTE: For the Roll Rate System, the gravity term in the β and A_y equations is dropped and the yaw rate command drives $r - p\alpha$ to zero. To accomplish this, the 2nd term in lines 120 and 140 must be set to zero, and the fourth term in line 300 is changed from zero to a value of -0.26143 to account for the $p\alpha$ expression.

Appendix B

Aircraft Equations of Motion

Longitudinal Equations - Body Axes

$$F_{z_{cg}} = m(\dot{W} + pV - qU) - mg\cos\theta\cos\phi \qquad \text{(B-1)}$$

thus

$$\dot{W} = \frac{F_{z_{cg}}}{m} - pV + qU + g\cos\theta\cos\phi \qquad \text{(B-2)}$$

$$\frac{F_{z_{cg}}}{m} = \frac{\bar{q}s}{m}\left[C_{z_o} + C_{z_\alpha}\alpha + \{C_{z_{\dot\alpha}}\dot\alpha + C_{z_q}q\}\frac{c}{2V_T} + C_{z_u}\frac{\Delta U}{V_T} \right.$$
$$\left. + C_{z_{\delta e}}\delta e + C_{z_{\delta f}}\delta f \right] \qquad \text{(B-3)}$$

Substituting Eq. (B-3) into (B-2) gives:

$$\dot{W} = \frac{\bar{q}s}{m}\left[C_{z_o} + C_{z_\alpha}\alpha + \{C_{z_{\dot\alpha}}\dot\alpha + C_{z_q}q\}\frac{c}{2V_T} + C_{z_u}\frac{\Delta U}{V_T} \right.$$
$$\left. + C_{z_{\delta e}}\delta e + C_{z_{\delta f}}\delta f \right] - pV + qU + g\cos\theta\cos\phi \qquad \text{(B-4)}$$

To develop perturbation equations, a 1g wings level trim flight condition is examined where $\phi=0$, $\dot\alpha=0$, $q=0$, $\delta f=0$, $\Delta U=0$, $p=0$, and $\cos\theta$ is approximately one. The trim angle of attack and elevator position are α_T and δe_T respectively.

236

$$\dot{W} = 0 = \frac{\bar{q}S}{m}\left[C_{z_o} + C_{z_\alpha}\alpha_T + C_{z_{\delta e}}\delta e_T\right] + g \qquad (B-5)$$

Thus, the aerodynamic forces balance the vehicle's weight. To account for small variations from this trim condition, perturbation angle of attack α_p and elevator position δe_p are added to the equation. A term for small changes in sensed g is also included.

$$\dot{W} = \frac{\bar{q}S}{m}\left[C_{z_o} + C_{z_\alpha}(\alpha_T + \alpha_p) + C_{z_{\delta e}}(\delta e_T + \delta e_p)\right]$$
$$+ g - (g\sin\theta_T)\theta \qquad (B-6)$$

Cancelling the terms that are equal from Eq. (B-5) yields:

$$\dot{W} = \frac{\bar{q}S}{m}\left[C_{z_\alpha}\alpha_p + C_{z_{\delta e}}\delta e_p\right] - (g\sin\theta_T)\theta \qquad (B-7)$$

The equation is expanded to include perturbations in $\dot{\alpha}$, q, U and δf by referring to Eq. (B-4).

$$\dot{W} = \frac{\bar{q}S}{m}\left[C_{z_\alpha}\alpha_p + \{C_{z_\alpha}\dot{\alpha} + C_{z_q}q\}\frac{c}{2V_T} + C_{z_u}\frac{\Delta U}{V_T} + C_{z_{\delta e}}\delta e_p\right.$$
$$\left. + C_{z_{\delta f}}\delta f\right] + qU - (g\sin\theta_T)\theta \qquad (B-8)$$

The p subscript is dropped and $U = V_T$. ΔU is expressed as u. Thus, the perturbation equation is:

$$\dot{w} = (\frac{\bar{q}S}{m})C_{z_\alpha}\alpha + (\frac{\bar{q}Sc}{m2U})C_{z_{\dot{\alpha}}}\dot{\alpha} + (\frac{\bar{q}Sc}{m2U})C_{z_q}q + (\frac{\bar{q}S}{mU})C_{z_u}u$$

$$+ (\frac{\bar{q}S}{m})C_{z_{\delta e}}\delta e + (\frac{\bar{q}S}{m})C_{z_{\delta f}}\delta f + qU - (g \sin\theta_T)\theta \quad \text{(B-9)}$$

or

$$\dot{w} = (Z_\alpha)\alpha + (Z_{\dot{\alpha}})\dot{\alpha} + (Z_q)q + (Z_u)u + (Z_{\delta e})\delta e$$

$$+ (Z_{\delta f})\delta f + qU - (g \sin\theta_T)\theta \quad \text{(B-10)}$$

Dividing by U, letting $\dot{\alpha} = \frac{\dot{w}}{U}$, and gathering the $\dot{\alpha}$ terms on the left-hand side of the equation gives:

$$\dot{\alpha}(1 - \frac{Z_{\dot{\alpha}}}{U}) = (\frac{Z_\alpha}{U})\alpha + (\frac{Z_q}{U})q + (\frac{Z_u}{U})u + (\frac{Z_{\delta e}}{U})\delta e$$

$$+ (\frac{Z_{\delta f}}{U})\delta f + q - (\frac{g \sin\theta_T}{U})\theta \quad \text{(B-11)}$$

$\frac{Z_{\dot{\alpha}}}{U}$ is very small and is ignored. Using the primed notation and noting that all states are perturbations from the trim condition, the equation can be expressed as:

$$\dot{\alpha} = (Z_\alpha{}')\alpha + (Z_q{}')q + (Z_u{}')u + (Z_{\delta e}{}')\delta e$$

$$+ (Z_{\delta f}{}')\delta f + (Z_\theta{}')\theta \quad \text{(B-12)}$$

where
$$Z_\alpha{}' = \frac{Z_\alpha}{U} = \frac{\bar{q}S}{mU} C_{z_\alpha} \quad \text{(B-13)}$$

$$Z_q{}' = 1 + \frac{Z_q}{U} = 1 + \frac{\bar{q}Sc}{m2U^2} C_{z_q} \quad \text{(B-14)}$$

$$Z_u{}' = \frac{Z_u}{U} = \frac{\bar{q}S}{mU^2} C_{z_u} \quad \text{(B-15)}$$

238

$$Z_{\delta e}' = \frac{Z_{\delta e}}{U} = \frac{\overline{q}S}{mU}\, C_{z_{\delta e}} \tag{B-16}$$

$$Z_{\delta f}' = \frac{Z_{\delta f}}{U} = \frac{\overline{q}S}{mU}\, C_{z_{\delta f}} \tag{B-17}$$

$$Z_{\theta}' = \frac{Z_{\theta}}{U} = -\frac{g}{U}\, \sin\theta_T \tag{B-18}$$

In a similar manner, the force equation in the x-axis is reduced to a perturbation equation.

$$F_{x_{cg}} = m(\dot{U} + qW - rV) + mg\, \sin\theta \tag{B-19}$$

thus

$$\dot{U} = \frac{F_{x_{cg}}}{m} - qW + rV - g\, \sin\theta \tag{B-20}$$

$$\frac{F_{x_{cg}}}{m} = \frac{\overline{q}S}{m}\left[C_{x_0} + C_{x_\alpha}\alpha + \{C_{x_q}q\}\frac{c}{2V_T} + C_{x_u}\frac{\Delta U}{V_T} \right.$$
$$\left. + C_{x_{\delta e}}\delta e + C_{x_{\delta f}}\delta f \right] \tag{B-21}$$

$$\dot{U} = \frac{\overline{q}S}{m}\left[C_{x_0} + C_{x_\alpha}\alpha + \{C_{x_q}q\}\frac{c}{2V_T} + C_{x_u}\frac{\Delta U}{V_T} \right.$$
$$\left. + C_{x_{\delta e}}\delta e + C_{x_{\delta f}}\delta f \right] - qW + rV - g\, \sin\theta \tag{B-22}$$

For trimmed flight, thrust exactly equals the drag forces.

$$T = \overline{q}S\left[C_{x_0} + C_{x_\alpha}\alpha_T + C_{x_{\delta e}}\delta e_T \right] \tag{B-23}$$

239

The perturbation equation is:

$$\dot{u} = \frac{\bar{q}S}{m} C_{x_\alpha} \alpha + \frac{\bar{q}Sc}{m2U} C_{x_q} q + \frac{\bar{q}S}{mU} C_{x_u} u + \frac{\bar{q}S}{m} C_{x_{\delta e}} \delta e$$

$$+ \frac{\bar{q}S}{m} C_{x_{\delta f}} \delta f - qW \frac{U}{U} + rV \frac{U}{U} - (g \cos\theta_T)\theta \quad \text{(B-24)}$$

By letting $\alpha_T = \frac{W}{U}$ and $\beta = \frac{V}{U}$, the equation can be written as:

$$\dot{u} = (X_\alpha)\alpha + (X_q)q + (X_u)u + (X_{\delta e})\delta e + (X_{\delta f})\delta f$$

$$- q\alpha_T U + r\beta U + X_\theta \theta \quad \text{(B-25)}$$

Assuming only longitudinal motion, β and r are zero and noting that all states are perturbations from trim conditions, the equation is expressed as:

$$\dot{u} = (X_\alpha{}')\alpha + (X_u{}')u + (X_{\delta e}{}')\delta e + (X_{\delta f}{}')\delta f$$

$$+ (X_q{}')q + (X_\theta{}')\theta \quad \text{(B-26)}$$

where

$$X_\alpha{}' = X_\alpha = \frac{\bar{q}S}{m} C_{x_\alpha} \quad \text{(B-27)}$$

$$X_u{}' = X_u = \frac{\bar{q}S}{mU} C_{x_u} \quad \text{(B-28)}$$

$$X_{\delta e}{}' = X_{\delta e} = \frac{\bar{q}S}{m} C_{x_{\delta e}} \quad \text{(B-29)}$$

$$X_{\delta f} = X_{\delta f} = \frac{\bar{q}S}{m} C_{x_{\delta f}} \quad \text{(B-30)}$$

$$X_q{}' = X_q - U\alpha_T = \frac{\bar{q}Sc}{m2U} C_{x_q} - U\alpha_T \tag{B-31}$$

$$X_\theta{}' = X_\theta = -g\, \cos\theta_T \tag{B-32}$$

The pitching moment equation is used to develop the perturbation $\dot{q}$ equation.

$$M_y = \dot{q}\, I_{yy} + pr(I_{xx} - I_{zz}) - (r^2 - p^2)I_{xz} \tag{B-33}$$

$$\dot{q}\, I_{yy} = M_y - pr(I_{xx} - I_{zz}) + (r^2 - p^2)I_{xz} \tag{B-34}$$

For longitudinal motion only, r and p are zero and the equation becomes:

$$\dot{q} = \frac{M_y}{I_{yy}} \tag{B-35}$$

and

$$M_y = \bar{q}Sc \left[C_{m_o} + C_{m_\alpha}\alpha + \{C_{m_{\dot\alpha}}\dot\alpha + C_{m_q}q\} \frac{c}{2V_T} \right.$$
$$\left. + C_{m_u} \frac{\Delta U}{V_T} + C_{m_{\delta e}}\delta e + C_{m_{\delta f}}\delta f \right] \tag{B-36}$$

In trimmed flight, the moments are assumed to be zero.

$$M_y = \bar{q}Sc \left[C_{m_o} + C_{m_\alpha}\alpha_T + C_{m_{\delta e}}\delta e_T \right] = 0 \tag{B-37}$$

Letting $V_T = U$, introducing perturbation angle of attack and elevator position variables, and cancelling the above

241

terms that add to zero, gives the perturbation equation:

$$M_y = \bar{q}Sc \left[C_{m_\alpha}\alpha + \{C_{m_{\dot\alpha}}\dot\alpha + C_{m_q}q\}\frac{c}{2U} + \frac{C_{m_u}}{U}\Delta U \right.$$

$$\left. + C_{m_{\delta e}}\delta e + C_{m_{\delta f}}\delta f \right] \qquad (B-38)$$

Substituting Eq. (B-38) into (B-35)

$$\dot{q} = \frac{\bar{q}Sc}{I_{yy}}C_{m_\alpha}\alpha + \frac{\bar{q}Sc^2}{2UI_{yy}}C_{m_{\dot\alpha}}\dot\alpha + \frac{\bar{q}Sc^2}{2UI_{yy}}C_{m_q}q + \frac{\bar{q}Sc}{UI_{yy}}C_{m_u}\Delta U$$

$$+ \frac{\bar{q}Sc}{I_{yy}}C_{m_{\delta e}}\delta e + \frac{\bar{q}Sc}{I_{yy}}C_{m_{\delta f}}\delta f \qquad (B-39)$$

In dimensional form, this is written as follows:

$$\dot{q} = (M_\alpha)\alpha + (M_{\dot\alpha})\dot\alpha + (M_q)q + (M_u)\Delta U$$

$$+ (M_{\delta e})\delta e + (M_{\delta f})\delta f \qquad (B-40)$$

Substituting Eq (B-12) for $\dot\alpha$ into Eq. (B-40) and letting ΔU
be represented by perturbation u yields:

$$\dot{q} = (M_\alpha + M_{\dot\alpha}Z_\alpha{}')\alpha + (M_q + M_{\dot\alpha}Z_q{}')q + (M_u + M_{\dot\alpha}Z_u{}')u$$

$$+ (M_{\delta e} + M_{\dot\alpha}Z_{\delta e}{}')\delta e + (M_{\delta f} + M_{\dot\alpha}Z_{\delta f}{}')\delta f$$

$$+ (M_{\dot\alpha}Z_\theta{}')\theta \qquad (B-41)$$

Using the primed notation, the equation is represented as:

$$\dot{q} = (M_\alpha{}')\alpha + (M_q{}')q + (M_u{}')u + (M_{\delta e}{}')\delta e$$

$$+ (M_{\delta f}{}')\delta f + (M_\theta{}')\theta \qquad (B-42)$$

where

$$M_\alpha{}' = \frac{\bar{q}Sc}{I_{yy}} (C_{m_\alpha})_b + \left[\frac{\bar{q}Sc^2}{2UI_{yy}} (C_{m_{\dot\alpha}})_b\right] Z_\alpha{}' \qquad \text{(B-43)}$$

$$M_q{}' = \frac{\bar{q}Sc^2}{2UI_{yy}} \left[(C_{m_q})_b + (C_{m_{\dot\alpha}})_b \, Z_q{}'\right] \qquad \text{(B-44)}$$

$$M_u{}' = \frac{\bar{q}Sc}{UI_{yy}} (C_{m_u})_b + \left[\frac{\bar{q}Sc^2}{2UI_{yy}} (C_{m_{\dot\alpha}})_b\right] Z_u{}' \qquad \text{(B-45)}$$

$$M_{\delta e}{}' = \frac{\bar{q}Sc}{I_{yy}} (C_{m_{\delta e}})_b + \left[\frac{\bar{q}Sc^2}{2UI_{yy}} (C_{m_{\dot\alpha}})_b\right] Z_{\delta e}{}' \qquad \text{(B-46)}$$

$$M_{\delta f}{}' = \frac{\bar{q}Sc}{I_{yy}} (C_{m_{\delta f}})_b + \left[\frac{\bar{q}Sc^2}{2UI_{yy}} (C_{m_{\dot\alpha}})_b\right] Z_{\delta f}{}' \qquad \text{(B-47)}$$

$$M_\theta{}' = \left[\frac{\bar{q}Sc^2}{2UI_{yy}} (C_{m_{\dot\alpha}})_b\right] Z_\theta{}' \qquad \text{(B-48)}$$

Note: $(\ )_b$ denotes coefficients that are expressed in the body axes.

Lateral-Directional Equation - Body Axes

The sideforce equation is:

$$F_{y_{cg}} = m(\dot{V} + rU - pW) - mg \cos\theta\sin\phi \qquad \text{(B-49)}$$

thus

$$\dot{V} = \frac{F_{y_{cg}}}{m} - rU + pW + g \cos\theta\sin\phi \qquad \text{(B-50)}$$

243

$$\frac{F_{y_{cg}}}{m} = \frac{\bar{q}S}{m} \left[C_{y_\beta}\beta + \{C_{y_p}p + C_{y_r}r\} \frac{b}{2V_T} + C_{y_{\delta a}}\delta a \right.$$
$$\left. + C_{y_{\delta r}}\delta r + C_{y_{\delta c}}\delta c \right] \qquad (B-51)$$

Substituting Eq. (B-51) into (B-50) and letting $U = V_T$ yields:

$$\dot{V} = \frac{\bar{q}S}{m} C_{y_\beta}\beta + \frac{\bar{q}Sb}{m2U} C_{y_p}p + \frac{\bar{q}Sb}{m2U} C_{y_r}r + \frac{\bar{q}S}{m} C_{y_{\delta a}}\delta a$$
$$+ \frac{\bar{q}S}{m} C_{y_{\delta r}}\delta r + \frac{\bar{q}S}{m} C_{y_{\delta c}}\delta c$$
$$- rU + pW + g\cos\theta\sin\phi \qquad (B-52)$$

Written with dimensional derivatives, this becomes:

$$\dot{V} = (Y_\beta)\beta + (Y_p)p + (Y_r)r + (Y_{\delta a})\delta a + (Y_{\delta r})\delta r$$
$$+ (Y_{\delta c})\delta c - rU + pW + g\cos\theta\sin\phi \qquad (B-53)$$

Dividing by U, letting $\dot{\beta} = \frac{\dot{V}}{U}$, $\beta = \frac{V}{U}$, $\alpha = \frac{W}{U}$, $\sin\phi = \phi$ in radians, and gathering terms together yields:

$$\dot{\beta} = (\frac{Y_\beta}{U})\beta + (\frac{Y_p}{U} + \alpha)p + (\frac{Y_r}{U} - 1)r + (\frac{Y_{\delta a}}{U})\delta a$$
$$+ (\frac{Y_{\delta r}}{U})\delta r + (\frac{Y_{\delta c}}{U})\delta c + (\frac{g\cos\theta_T}{U})\phi \qquad (B-54)$$

Using the primed notation, the equation is represented as:

$$\dot{\beta} = (Y_\beta{}')\beta + (Y_p{}')p + (Y_r{}')r + (Y_{\delta a}{}')\delta a + (Y_{\delta r}{}')\delta r$$
$$+ (Y_{\delta c}{}')\delta c + (Y\phi{}')\phi \qquad (B-55)$$

244

where

$$Y_{\beta}{}' = \frac{\bar{q}S}{mU} \, (C_{y_{\beta}})_b \qquad\qquad \text{(B-56)}$$

$$Y_{p}{}' = \frac{\bar{q}Sb}{m2U^2} \, (C_{y_p})_b + \alpha_T \qquad\qquad \text{(B-57)}$$

$$Y_{r}{}' = \frac{\bar{q}Sb}{m2U^2} \, (C_{y_r})_b - 1 \qquad\qquad \text{(B-58)}$$

$$Y_{\delta a}{}' = \frac{\bar{q}S}{mU} \, (C_{y_{\delta a}})_b \qquad\qquad \text{(B-59)}$$

$$Y_{\delta r}{}' = \frac{\bar{q}S}{mU} \, (C_{y_{\delta r}})_b \qquad\qquad \text{(B-60)}$$

$$Y_{\delta c}{}' = \frac{\bar{q}S}{mU} \, (C_{y_{\delta c}})_b \qquad\qquad \text{(B-61)}$$

$$Y_{\theta}{}' = \frac{g \, \cos\theta_T}{U} \qquad\qquad \text{(B-62)}$$

The yawing moment equation can be expressed as:

$$M_z = \dot{r} \, I_{zz} + qp(I_{yy} - I_{xx}) - (\dot{p} - qr)I_{xz} \qquad \text{(B-63)}$$

Assuming $q = 0$, this reduces to:

$$\dot{r} \, I_{zz} = M_z + \dot{p} \, I_{xz} \qquad\qquad \text{(B-64)}$$

$$M_z = \bar{q}Sb \left[C_{n_\beta}\beta + \{C_{n_p}p + C_{n_r}r\} \frac{b}{2V_T} + C_{n_{\delta a}}\delta a \right.$$
$$\left. + C_{n_{\delta r}}\delta r + C_{n_{\delta c}}\delta c \right] \qquad \text{(B-65)}$$

245

Combining Eqs. (B-64) and (B-65) and solving for $\dot{r}$ with $U = V_T$ gives:

$$\dot{r} = \frac{\bar{q}Sb}{I_{zz}} C_{n_\beta}\beta + \frac{\bar{q}Sb^2}{I_{zz}2U} C_{n_p}p + \frac{\bar{q}Sb^2}{I_{zz}2U} C_{n_r}r + \frac{\bar{q}Sb}{I_{zz}} C_{n_{\delta a}}\delta a$$

$$+ \frac{\bar{q}Sb}{I_{zz}} C_{n_{\delta r}}\delta r + \frac{\bar{q}Sb}{I_{zz}} C_{n_{\delta c}}\delta c + \dot{p}\frac{I_{xz}}{I_{zz}} \quad \text{(B-66)}$$

In dimensional derivative notation, this is:

$$\dot{r} = (N_\beta)\beta + (N_p)p + (N_r)r + (N_{\delta a})\delta a + (N_{\delta r})\delta r$$

$$+ (N_{\delta c})\delta c + \dot{p}\frac{I_{xz}}{I_{zz}} \quad \text{(B-67)}$$

The rolling moment equation is written as:

$$M_x = \dot{p}\, I_{xx} + qr(I_{zz} - I_{yy}) - (pq + \dot{r})I_{xz} \quad \text{(B-68)}$$

Assuming $q = 0$, the equation reduces to:

$$\dot{p}\, I_{xx} = M_x + \dot{r}\, I_{xz} \quad \text{(B-69)}$$

$$M_x = \bar{q}Sb \left[C_{\ell_\beta}\beta + \{C_{\ell_p}p + C_{\ell_r}r\}\frac{b}{2V_T} + C_{\ell_{\delta a}}\delta a \right.$$

$$\left. + C_{\ell_{\delta r}}\delta r + C_{\ell_{\delta c}}\delta c \right] \quad \text{(B-70)}$$

Combining Eqs. (B-69) and (B-70) and solving for $\dot{p}$ with $U = V_T$ gives:

$$\dot{p} = \frac{\bar{q}Sb}{I_{xx}} C_{\ell_\beta} \beta + \frac{\bar{q}Sb^2}{I_{xx}2U} C_{\ell_p} p + \frac{\bar{q}Sb^2}{I_{xx}2U} C_{\ell_r} r + \frac{\bar{q}Sb}{I_{xx}} C_{\ell_{\delta a}} \delta a$$

$$+ \frac{\bar{q}Sb}{I_{xx}} C_{\ell_{\delta r}} \delta r + \frac{\bar{q}Sb}{I_{xx}} C_{\ell_{\delta c}} \delta c + \dot{r} \frac{I_{xz}}{I_{xx}} \quad \text{(B-71)}$$

$$\dot{p} = (L_\beta)\beta + (L_p)p + (L_r)r + (L_{\delta a})\delta a + (L_{\delta r})\delta r$$

$$+ (L_{\delta c})\delta c + \dot{r} \frac{I_{xz}}{I_{xx}} \quad \text{(B-72)}$$

Equations (B-67) and (B-72) are solved to give expressions
for $\dot{r}$ and $\dot{p}$. Written in primed derivatives, these are:

$$\dot{r} = (N_\beta{}')\beta + (N_p{}')p + (N_r{}')r + (N_{\delta a}{}')\delta a$$

$$+ (N_{\delta r}{}')\delta r + (N_{\delta c}{}')\delta c \quad \text{(B-73)}$$

where

$$N_i{}' = \frac{N_i + \dfrac{I_{xz}}{I_{zz}} L_i}{1 - \dfrac{I_{xz}^2}{(I_{xx})(I_{zz})}} \quad \text{for } i = \beta, \; p, \; r, \; \delta a, \; \delta r, \; \delta c \quad \text{(B-74)}$$

and

$$\dot{p} = (L_\beta{}')\beta + (L_p{}')p + (L_r{}')r + (L_{\delta a}{}')\delta a$$

$$+ (L_{\delta r}{}')\delta r + (L_{\delta c}{}')\delta c \quad \text{(B-75)}$$

where

$$L_i{}' = \frac{L_i + \dfrac{I_{xz}}{I_{xx}} N_i}{1 + \dfrac{(I_{xz})^2}{(I_{xx})(I_{zz})}} \qquad \text{for } i = \beta,\ p,\ r,\ \delta a,\ \delta r,\ \delta c$$

(B-76)

The State Equations

Equations (B-12), (B-26) and (B-42) are combined with an expression for $\dot{\theta}$ and first-order actuator models (developed in Chapter II) to form the longitudinal state equations.

$$\dot{\theta} = q \cos\phi - r \sin\phi \qquad \text{(B-77)}$$

Assuming ϕ is small and r is zero, this becomes:

$$\dot{\theta} \approx q \qquad \text{(B-78)}$$

Thus, the longitudinal state equations are:

$$
\begin{bmatrix} \dot{\theta} \\ \dot{u} \\ \dot{\alpha} \\ \dot{q} \\ \dot{\delta e} \\ \dot{\delta f} \end{bmatrix}
=
\begin{bmatrix}
0 & 0 & 0 & 1 & 0 & 0 \\
X_\theta{}' & X_u{}' & X_\alpha{}' & X_q{}' & X_{\delta e}{}' & X_{\delta f}{}' \\
Z_\theta{}' & Z_u{}' & Z_\alpha{}' & Z_q{}' & Z_{\delta e}{}' & Z_{\delta f}{}' \\
M_\theta{}' & M_u{}' & M_\alpha{}' & M_q{}' & M_{\delta e}{}' & M_{\delta f}{}' \\
0 & 0 & 0 & 0 & -20 & 0 \\
0 & 0 & 0 & 0 & 0 & -20
\end{bmatrix}
\begin{bmatrix} \theta \\ u \\ \alpha \\ q \\ \delta e \\ \delta f \end{bmatrix}
+
\begin{bmatrix} 0 & 0 \\ 0 & 0 \\ 0 & 0 \\ 0 & 0 \\ 20 & 0 \\ 0 & 20 \end{bmatrix}
\begin{bmatrix} \delta e_{cmd} \\ \delta f_{cmd} \end{bmatrix}
$$

(B-79)

Units are radians, feet per second, and radians per second.

248

Equations (B-55), (B-73) and (B-75) are combined with an expression for $\dot{\phi}$ and first-order actuator models to form the lateral-directional state equations.

$$\dot{\phi} = p + q \sin\phi \tan\theta + r \cos\phi \tan\theta \qquad (B-80)$$

Assuming $\theta = 0$, this becomes:

$$\dot{\phi} = p \qquad (B-81)$$

Thus, the lateral-directional state equations are:

$$
\begin{bmatrix} \dot{\phi} \\ \dot{\beta} \\ \dot{p} \\ \dot{r} \\ \dot{\delta a} \\ \dot{\delta r} \\ \dot{\delta c} \end{bmatrix}
=
\begin{bmatrix}
0 & 0 & 1 & 0 & 0 & 0 & 0 \\
Y_\phi{}' & Y_\beta{}' & Y_p{}' & Y_r{}' & Y_{\delta a}{}' & Y_{\delta r}{}' & Y_{\delta c}{}' \\
0 & L_\beta{}' & L_p{}' & L_r{}' & L_{\delta a}{}' & L_{\delta r}{}' & L_{\delta c}{}' \\
0 & N_\beta{}' & N_p{}' & N_r{}' & N_{\delta a}{}' & N_{\delta r}{}' & N_{\delta c}{}' \\
0 & 0 & 0 & 0 & -20 & 0 & 0 \\
0 & 0 & 0 & 0 & 0 & -20 & 0 \\
0 & 0 & 0 & 0 & 0 & 0 & -20
\end{bmatrix}
\begin{bmatrix} \phi \\ \beta \\ p \\ r \\ \delta a \\ \delta r \\ \delta c \end{bmatrix}
+
\begin{bmatrix}
0 & 0 & 0 \\
0 & 0 & 0 \\
0 & 0 & 0 \\
0 & 0 & 0 \\
20 & 0 & 0 \\
0 & 20 & 0 \\
0 & 0 & 20
\end{bmatrix}
\begin{bmatrix} \delta a_{cmd} \\ \delta r_{cmd} \\ \delta c_{cmd} \end{bmatrix}
$$

$$(B-82)$$

These state equations must still be transformed as shown in Chapter II to obtain longitudinal and lateral accelerations as states. The stability axes coefficients must be converted to body axes coefficients for use in the equations previously developed. The conversion equations are:

$$C_{Z_\alpha} = (-C_{L_\alpha} - C_D) \cos^2 \alpha_T + (-C_{D_u} - 2C_D) \sin^2 \alpha_T$$

$$+ (-C_{L_u} - C_L - C_{D_\alpha}) \cos\alpha_T \sin\alpha_T \qquad (\text{B}-83)$$

$$C_{Z_{\dot{\alpha}}} = -C_{L_{\dot{\alpha}}} \cos^2 \alpha_T \qquad\qquad (B-83a)$$

$$C_{Z_q} = -C_{L_q} \cos\alpha_T \qquad\qquad (B-84)$$

$$C_{Z_u} = (-C_{L_u} - 2C_L) \cos^2 \alpha_T + (C_{D_\alpha} - C_L) \sin^2 \alpha_T$$

$$+ (C_{L_\alpha} - C_{D_u} - C_D) \cos\alpha_T \sin\alpha_T \qquad (B-85)$$

$$C_{Z_\delta} = -C_{L_\delta} \cos\alpha_T - C_{D_\delta} \sin\alpha_T \qquad\qquad (B-86)$$

$$C_{X_\alpha} = (-C_{D_\alpha} + C_L) \cos^2 \alpha_T + (C_{L_u} + 2C_L) \sin^2 \alpha_T$$

$$+ (-C_{D_u} - C_D + C_{L_\alpha}) \cos\alpha_T \sin\alpha_T \qquad (B-87)$$

$$C_{X_q} = C_{L_q} \sin\alpha_T \qquad\qquad (B-88)$$

$$C_{X_u} = (-C_{D_u} - 2C_D) \cos^2 \alpha_T + (-C_{L_\alpha} - C_D) \sin^2 \alpha_T$$

$$+ (C_{D_\alpha} + C_{L_u} + C_L) \cos\alpha_T \sin\alpha_T \qquad (B-89)$$

$$C_{X_\delta} = -C_{D_\delta} \cos\alpha_T + C_{L_\delta} \sin\alpha_T \qquad\qquad (B-90)$$

$$(C_{M_\alpha})_b = C_{M_\alpha} \cos\alpha_T + (C_{M_u} + 2C_M) \sin\alpha_T \qquad\qquad (B-91)$$

$$(C_{M_{\dot{\alpha}}})_b = C_{M_{\dot{\alpha}}} \cos\alpha_T \qquad\qquad (B-92)$$

$$(C_{M_u})_b = (C_{M_u} + 2C_M) \cos\alpha_T - C_{M_\alpha} \sin\alpha_T \qquad\qquad (B-93)$$

250

$$(C_{M_q})_b = C_{M_q} \tag{B-94}$$

$$(C_{M_\delta})_b = C_{M_\delta} \tag{B-95}$$

where $(\ )_b$ is used to distinguish body axes from stability axes when necessary.

The equations for converting the lateral derivatives to body axes are:

$$(C_{\ell_\beta})_b = C_{\ell_\beta} \cos\alpha_T - C_{n_\beta} \sin\alpha_T \tag{B-96}$$

$$(C_{\ell_p})_b = C_{\ell_p} \cos^2\alpha_T + C_{n_r} \sin^2\alpha_T$$
$$- (C_{\ell_r} + C_{n_p}) \sin\alpha_T \cos\alpha_T \tag{B-97}$$

$$(C_{\ell_r})_b = C_{\ell_r} \cos^2\alpha_T - (C_{n_r} - C_{\ell_p}) \sin\alpha_T \cos\alpha_T$$
$$- C_{n_p} \sin^2\alpha_T \tag{B-98}$$

$$(C_{\ell_\delta})_b = C_{\ell_\delta} \cos\alpha_T - C_{n_\delta} \sin\alpha_T \tag{B-99}$$

$$(C_{n_\beta})_b = C_{n_\beta} \cos\alpha_T + C_{\ell_\beta} \sin\alpha_T \tag{B-100}$$

$$(C_{n_p})_b = C_{n_p} \cos^2\alpha_T - (C_{n_r} - C_{\ell_p}) \sin\alpha_T \cos\alpha_T$$
$$- C_{\ell_r} \sin^2\alpha_T \tag{B-101}$$

$$(C_{n_r})_b = C_{n_r} \cos^2\alpha_T + (C_{\ell_r} + C_{n_p}) \sin\alpha_T \cos\alpha_T$$
$$+ C_{\ell_p} \sin^2\alpha_T \qquad \text{(B-102)}$$

$$(C_{n_\delta})_b = C_{n_\delta} \cos\alpha_T + C_{\ell_\delta} \sin\alpha_T \qquad \text{(B-103)}$$

$$(C_{y_\beta})_b = C_{y_\beta} \qquad \text{(B-104)}$$

$$(C_{y_p})_b = C_{y_p} \cos\alpha_T - C_{y_r} \sin\alpha_T \qquad \text{(B-105)}$$

$$(C_{y_r})_b = C_{y_r} \cos\alpha_T + C_{y_p} \sin\alpha_T \qquad \text{(B-106)}$$

$$(C_{y_\delta})_b = C_{y_\delta} \qquad \text{(B-107)}$$

All of the computations to develop the body axes primed derivatives from stability axes coefficients are performed by the CAT program (see Appendix D).

Miscellaneous Equations

To convert inertias from the body axes to the stability axes, the following equations are used.

$$(I_{xx})_S = (I_{xx})_B \cos^2\alpha_T + (I_{zz})_B \sin^2\alpha_T$$
$$- 2(I_{xz})_B \cos\alpha_T \sin\alpha_T \qquad \text{(B-108)}$$

$$(I_{zz})_S = (I_{xx})_B \sin^2\alpha_T + (I_{zz})_B \cos^2\alpha_T$$
$$+ 2(I_{xz})_B \cos\alpha_T \sin\alpha_T \qquad \text{(B-109)}$$

$$(I_{xz})_S = [(I_{xx})_B - (I_{zz})_B] \cos\alpha_T \sin\alpha_T$$

$$+ (I_{xz})_B [\cos^2\alpha_T - \sin^2\alpha_T] \qquad \text{(B-110)}$$

where $(\ )_S$ is used to denote the stability axes.

Accelerations at points other than the center of gravity are calculated using:

$$A_x = A_{x_{cg}} - (\frac{\ell_x}{1845})(\frac{q^2 + r^2}{57.3}) + (\frac{\ell_y}{1845})(\frac{pq}{57.3} - \dot{r})$$

$$+ (\frac{\ell_z}{1845})(\frac{pr}{57.3} + \dot{q}) \qquad \text{(B-111)}$$

$$A_y = A_{y_{cg}} + (\frac{\ell_x}{1845})(\frac{pq}{57.3} + \dot{r}) - (\frac{\ell_y}{1845})(\frac{p^2 + r^2}{57.3})$$

$$+ (\frac{\ell_z}{1845})(\frac{qr}{57.3} - \dot{p}) \qquad \text{(B-112)}$$

$$A_n = A_{n_{cg}} - (\frac{\ell_x}{1845})(\frac{pr}{57.3} - \dot{q}) - (\frac{\ell_y}{1845})(\frac{rq}{57.3} + \dot{p})$$

$$+ (\frac{\ell_z}{1845})(\frac{p^2 + q^2}{57.3}) \qquad \text{(B-113)}$$

Accelerations are in units of g, angular rates are in units of degrees per second, and angular accelerations are in degrees per second^2. The distances ℓ_x, ℓ_y, ℓ_z are measured in feet. The ℓ_x distance is positive moving forward from the CG along the x-axis. The ℓ_y distance is positive along the y-axis moving out the right wing from the center of gravity. The ℓ_z distance is positive along the z-axis or down from the CG.

Angle of attack and angle of sideslip are expressed as:

$$\alpha = \tan^{-1}(\frac{W}{U}) \qquad \text{and} \qquad \beta = \sin^{-1}(\frac{V}{V_T}) \qquad \text{(B-114)}$$

where $V_T = (U^2 + V^2 + W^2)^{\frac{1}{2}}$ \qquad\qquad\qquad\qquad (B-115)

Appendix C
Maximum Command Responses

This appendix contains responses to maximum estimated commands used to select system gains that do not cause control surface position or rate limits to be exceeded. Pointing and sideforce system plots are not included since the maximum commanded responses are presented in Chapter V.

The responses in this appendix are not intended to indicate adequacy of the aircraft model in properly representing such large maneuvers. They are simply used as a guideline in establishing realistic gains.

The design parameters given in Chapter V for each flight condition and system apply to these responses with the exception that the inputs have been appropriately increased.
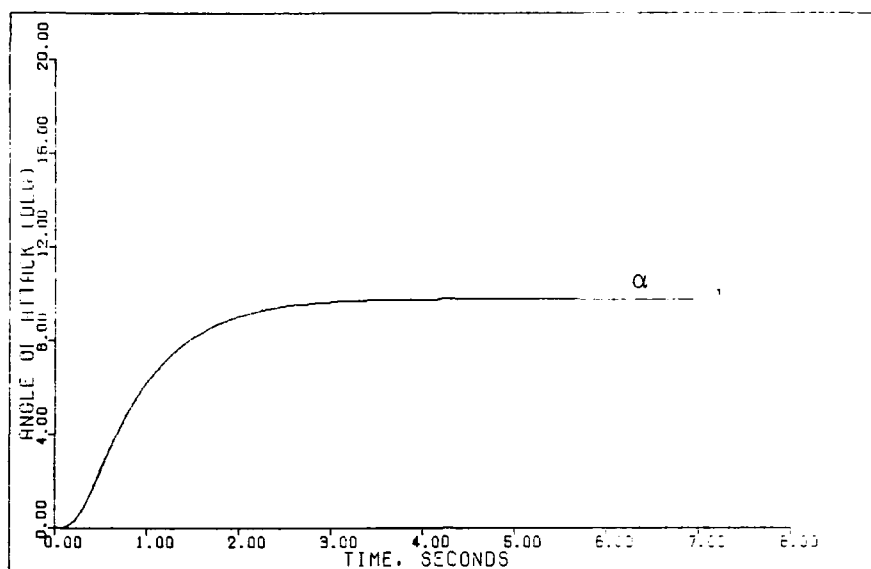
Figure C-1a. G-Command System Response to a 9g Step
Command (0.9 Mach 20,000 feet)
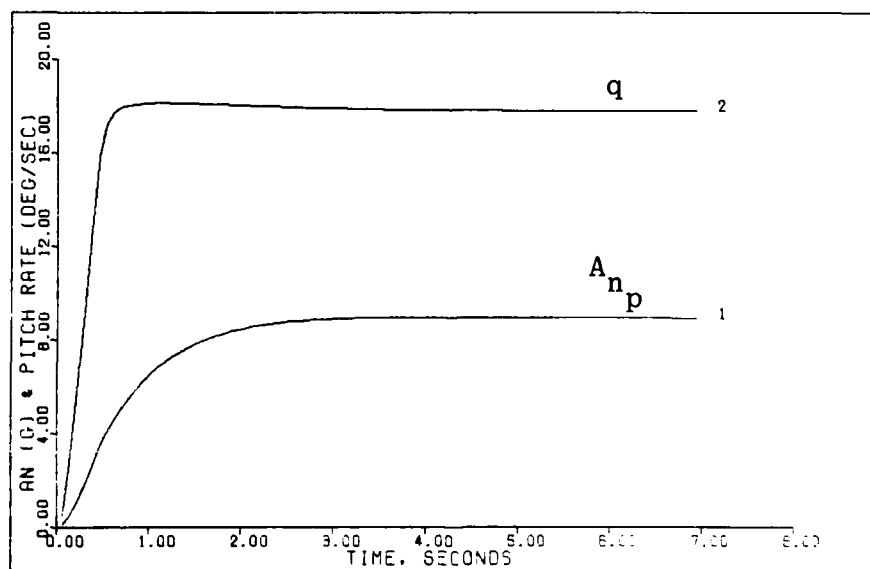
Figure C-1b. G-Command System Response to a 9g Step
Command (0.9 Mach 20,000 feet)
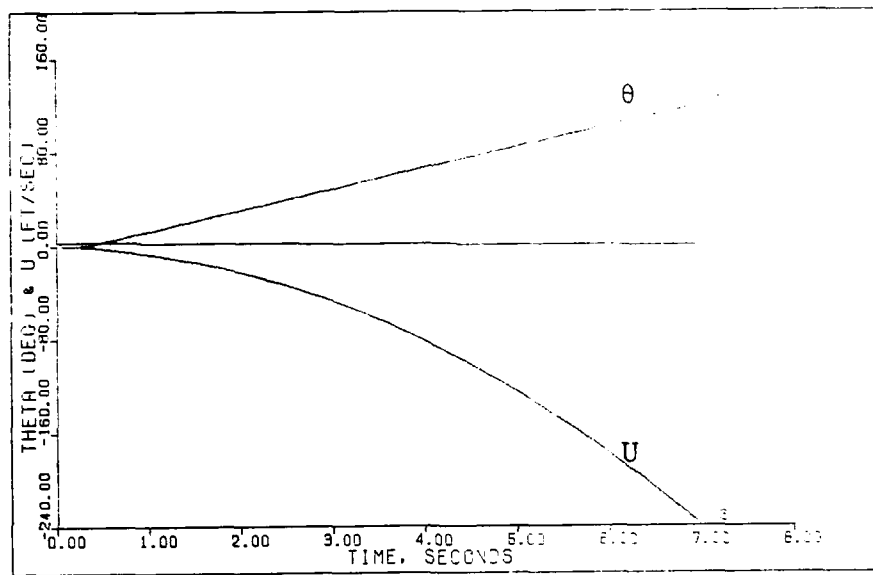
Figure C-1c.   G-Command System Response to a 9g Step
Command (0.9 Mach 20,000 feet)
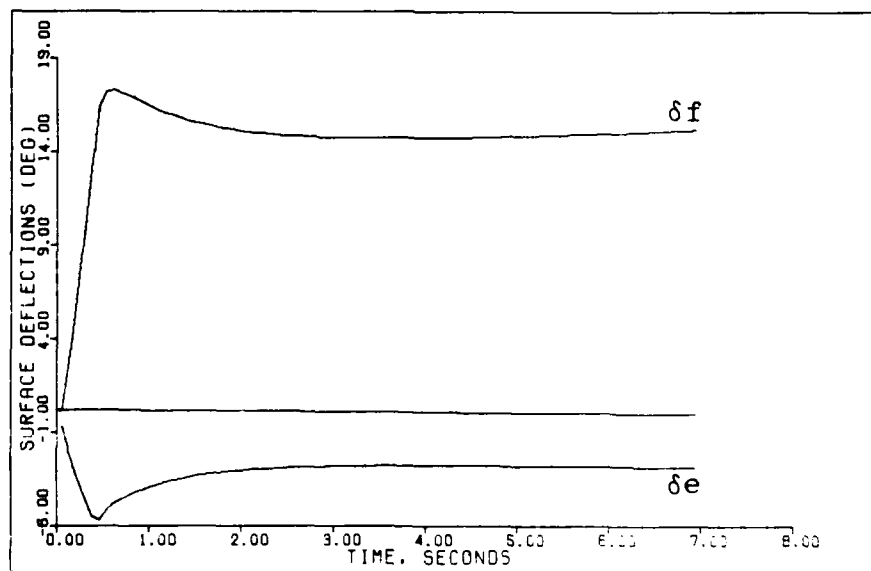
Figure C-1d.   G-Command System Response to a 9g Step
Command (0.9 Mach 20,000 feet)

257
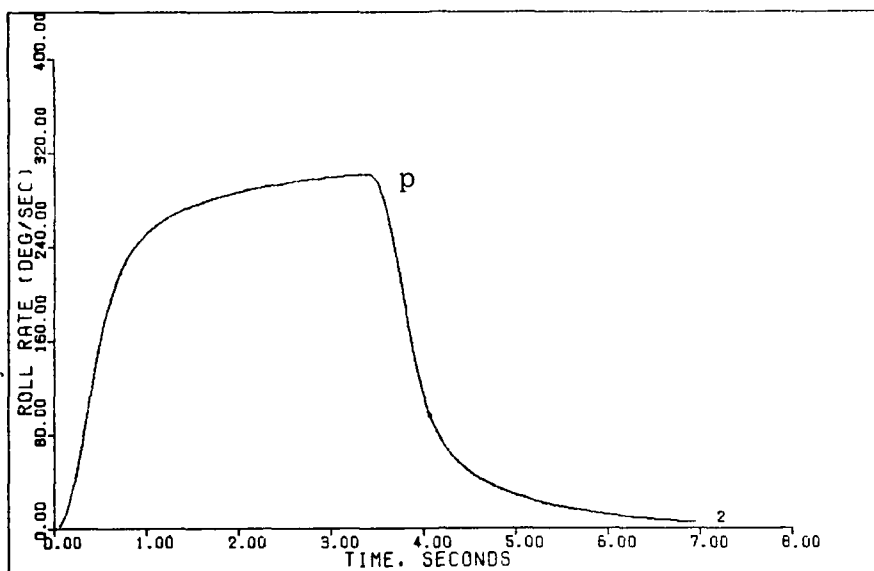
Figure C-2a.   Roll Rate Command System Response to a
308 deg/sec Pulse Command (0.9 Mach 20,000 feet)
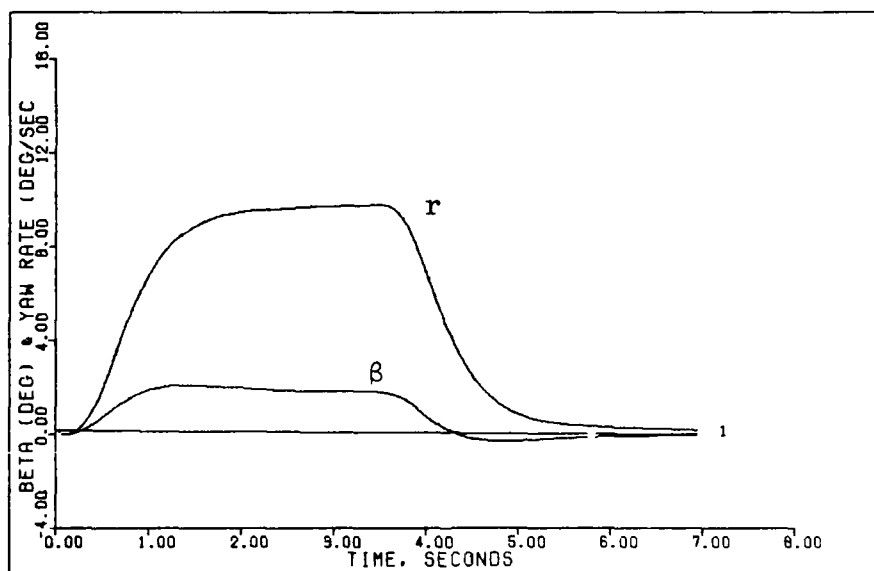
Figure C-2b.   Roll Rate Command System Response to a
308 deg/sec Pulse Command (0.9 Mach 20,000 feet)

258
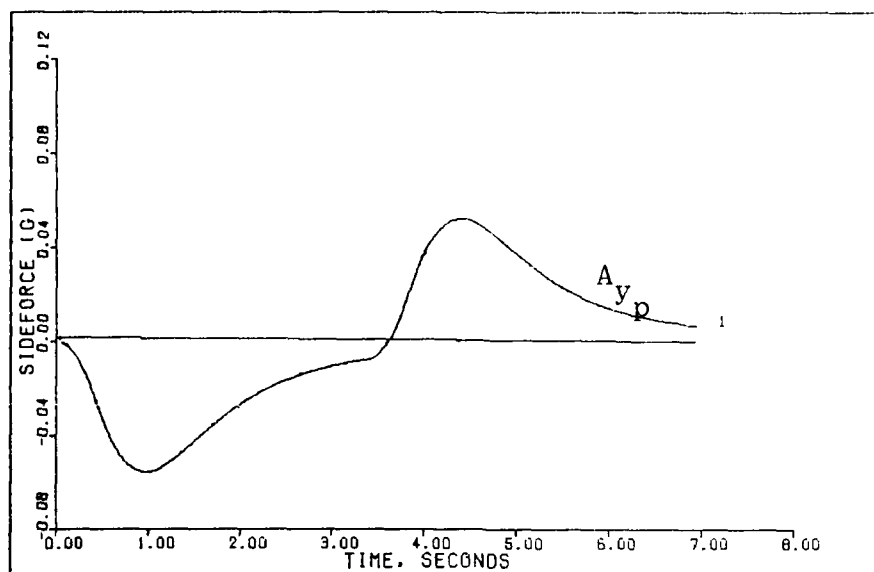
Figure C-2c.   Roll Rate Command System Response to a
308 deg/sec Pulse Command (0.9 Mach 20,000 feet)
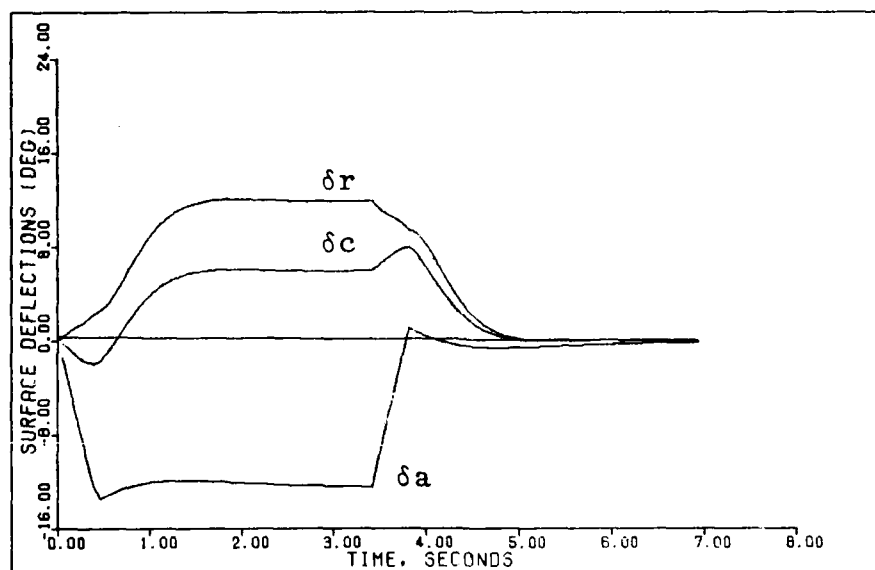
Figure C-2d.   Roll Rate Command System Response to a
308 deg/sec Pulse Command (0.9 Mach 20,000 feet)

259
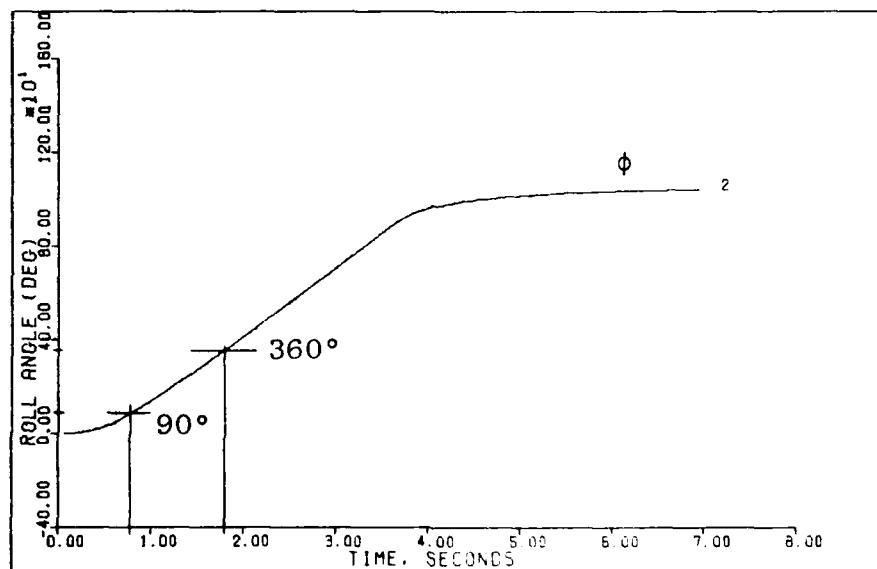
Figure C-2e. Roll Rate Command System Response to a
308 deg/sec Pulse Command (0.9 Mach 20,000 feet)

NOTE: Points in the figure indicate the time to roll
        to 90° and time to roll to 360° for a maximum
        command input.
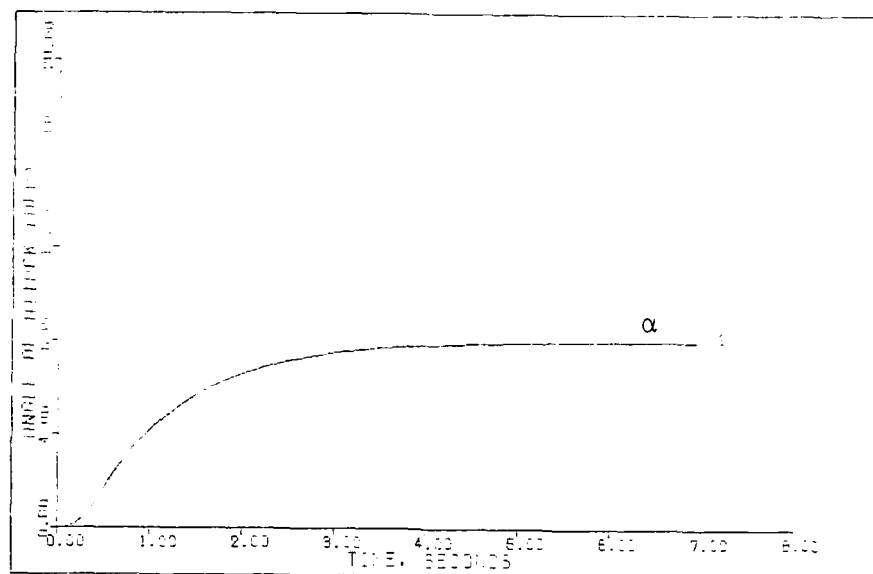
Figure C-3a.   G-Command System Response to a 8.5g
Step Command (1.6 Mach 30,000 feet)
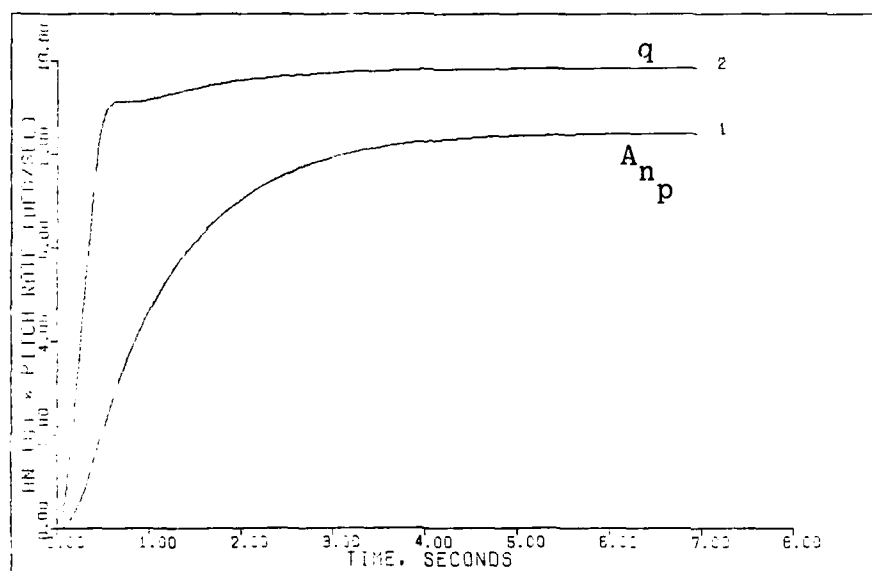
Figure C-3b.   G-Command System Response to a 8.5g
Step Command (1.6 Mach 30,000 feet)

261
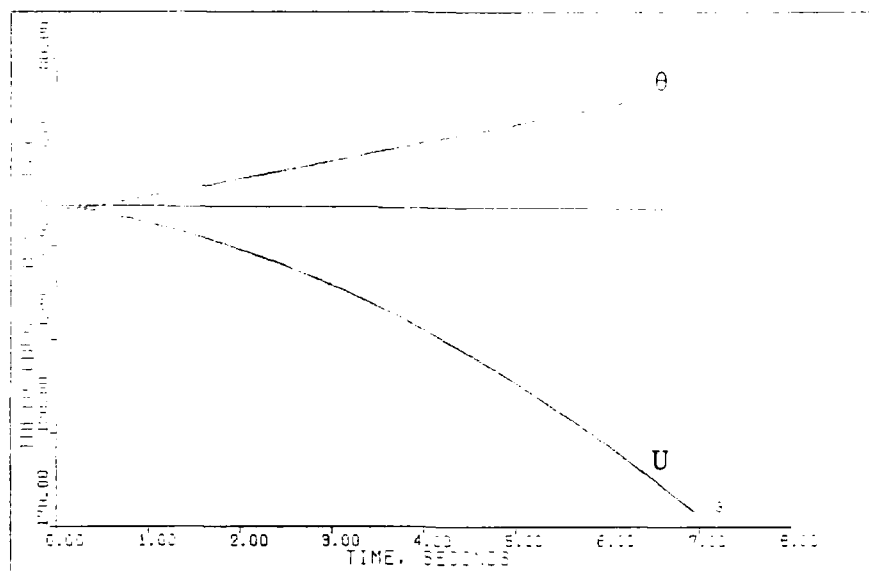
Figure C-3c.   G-Command System Response to a 8.5g
          Step Command (1.6 Mach 30,000 feet)
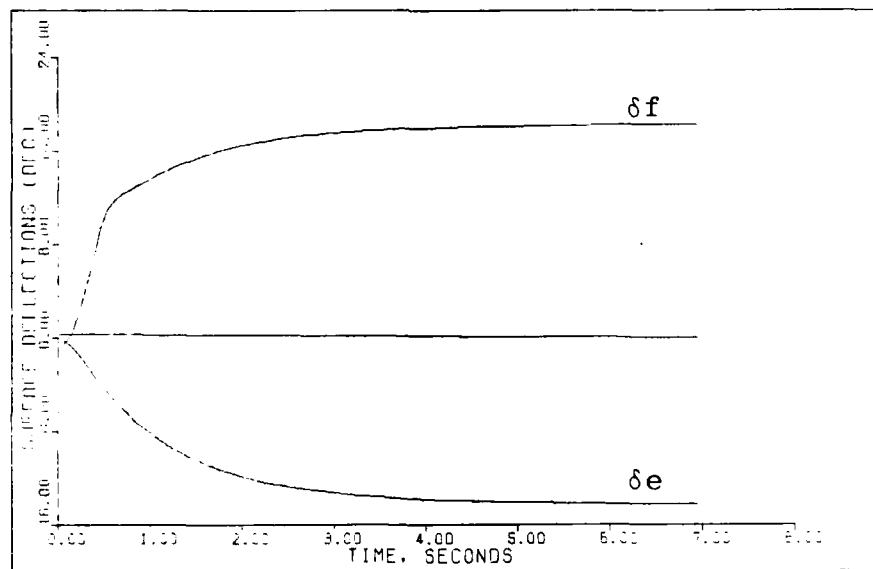
Figure C-3d.   G-Command System Response to a 8.5g
          Step Command (1.6 Mach 30,000 feet)

262
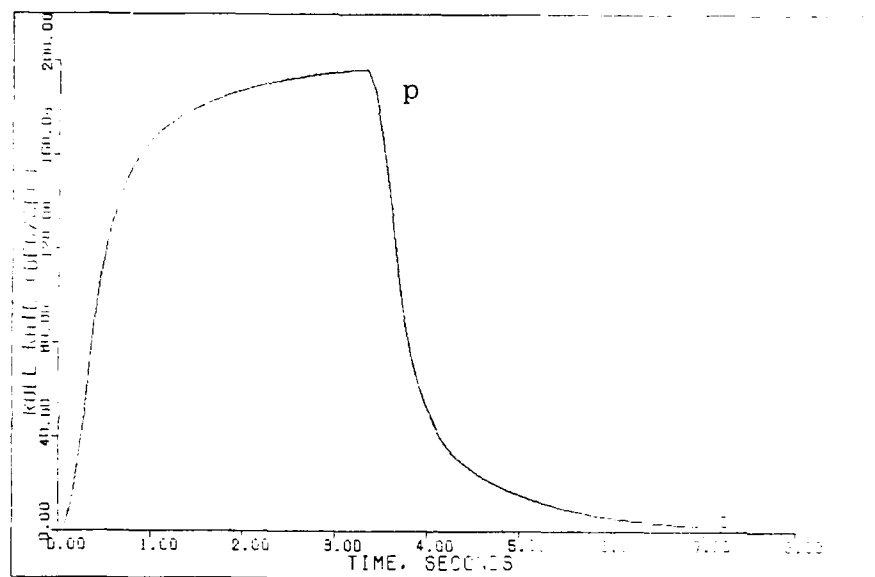
Figure C-4a.   Roll Rate Command System Response to a
200 deg/sec Pulse Command (1.6 Mach 30,000 feet)
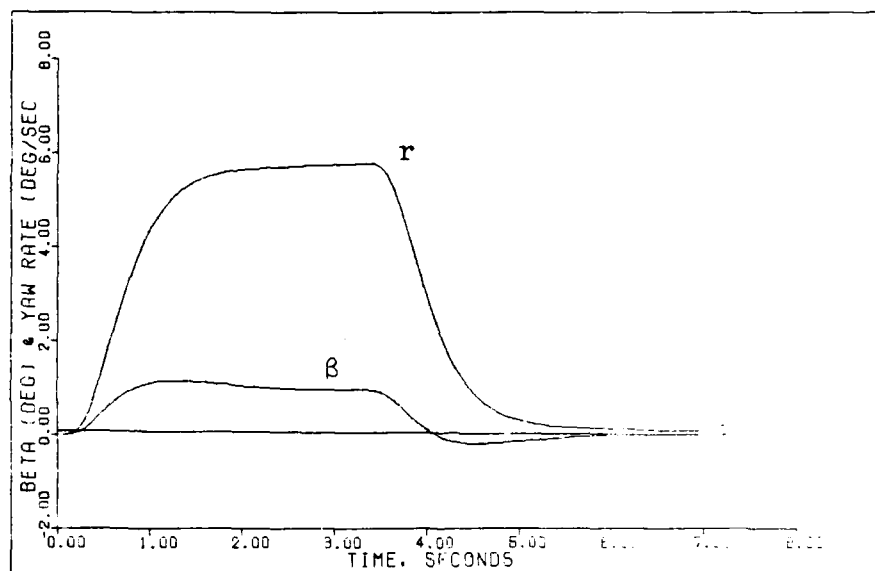
Figure C-4b.   Roll Rate Command System Response to a
200 deg/sec Pulse Command (1.6 Mach 30,000 feet)
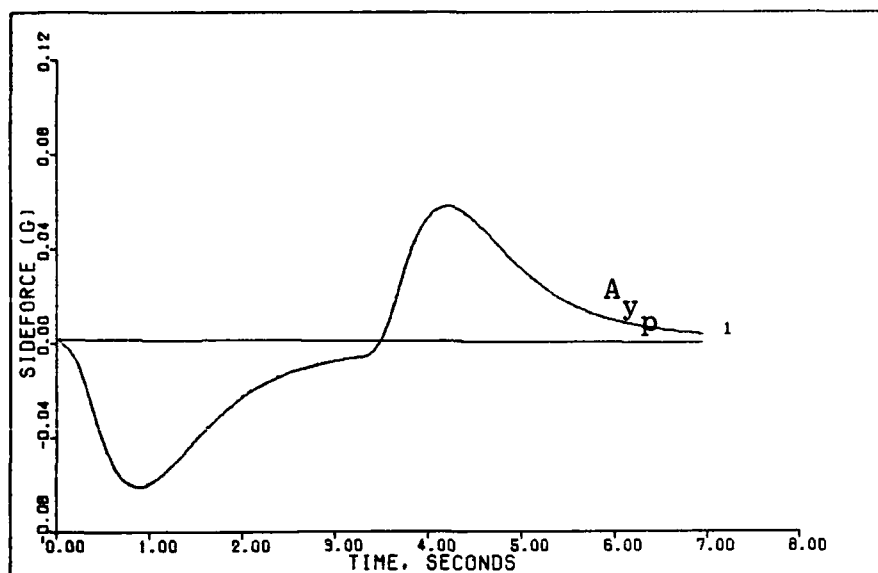
Figure C-4c.   Roll Rate Command System Response to a
200 deg/sec Pulse Command (1.6 Mach 30,000 feet)
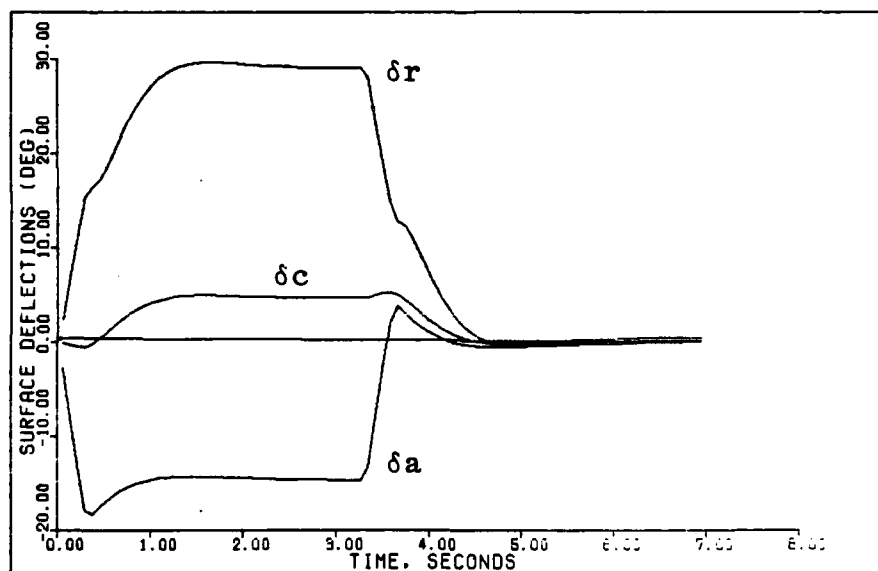
Figure C-4d.   Roll Rate Command System Response to a
200 deg/sec Pulse Command (1.6 Mach 30,000 feet)
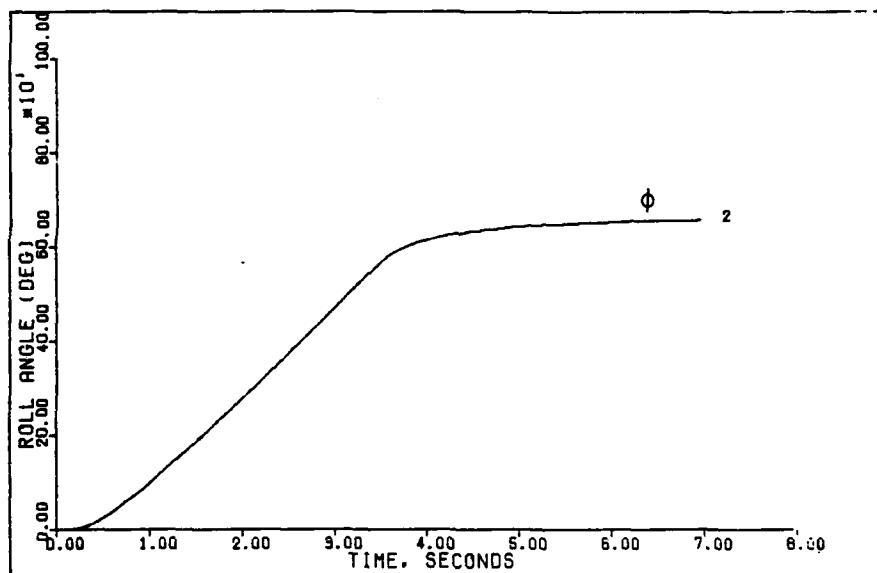
Figure C-4e.   Roll Rate Command System Response to a
200 deg/sec Pulse Command (1.6 Mach 30,000 feet)
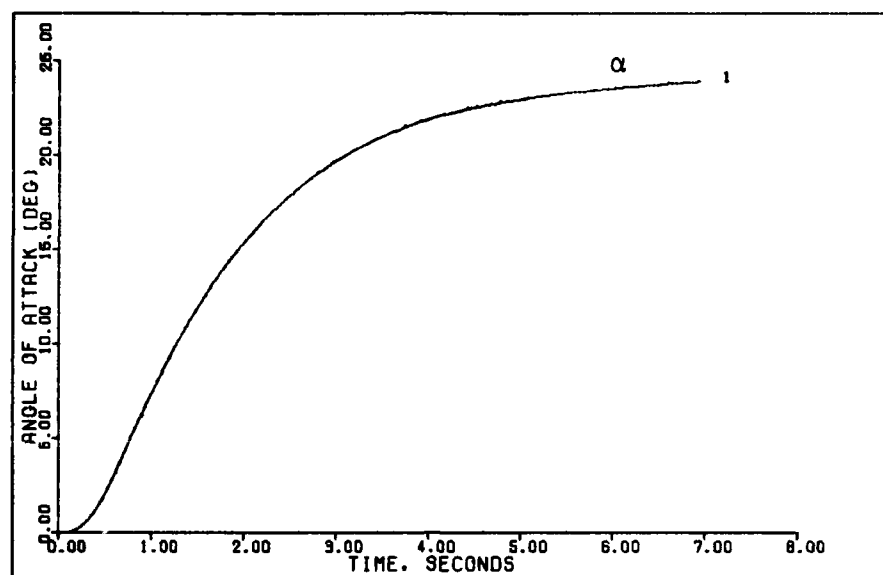
Figure C-5a.   G-Command System Response to a 4.7g
Step Command (0.6 Mach 30,000 feet)
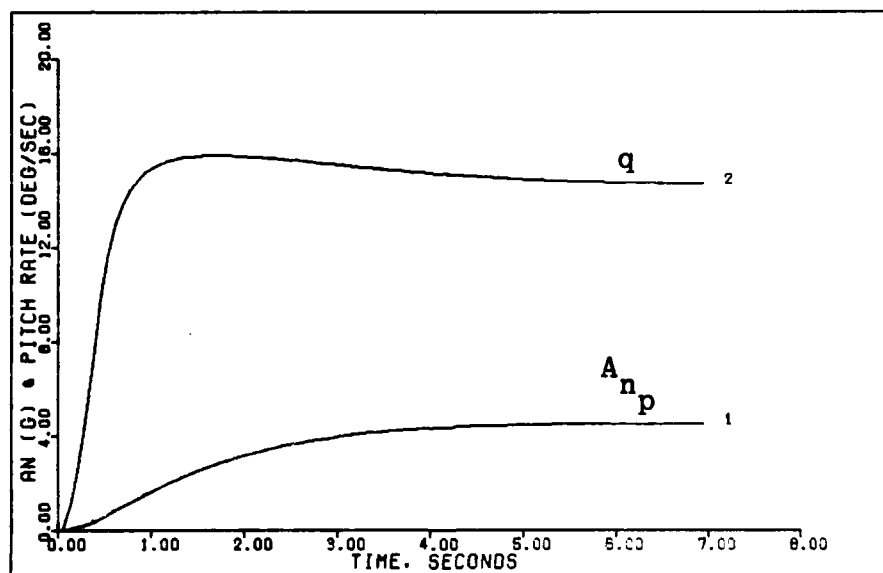
Figure C-5b.   G-Command System Response to a 4.7g
Step Command (0.6 Mach 30,000 feet)

266
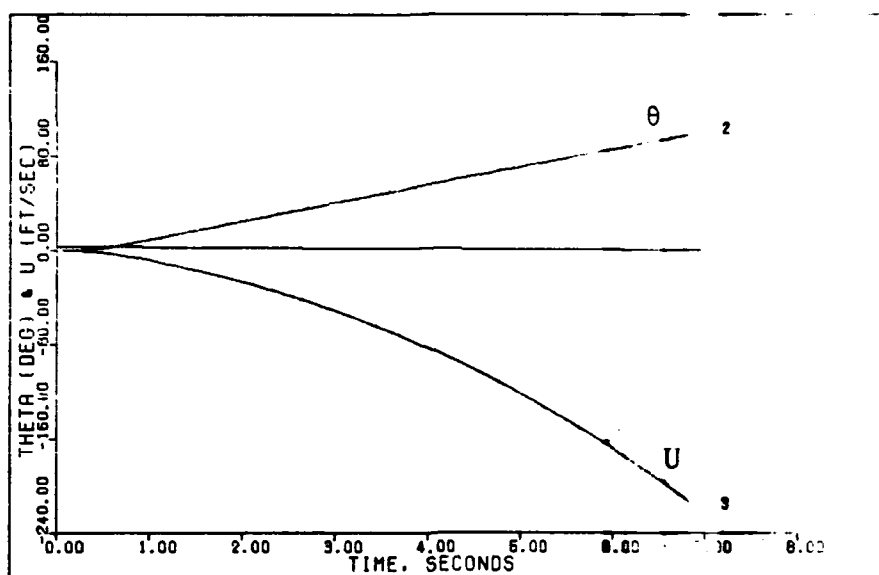
Figure C-5c.   G-Command System Response to a 4.7g
Step Command (0.6 Mach 30,000 feet)
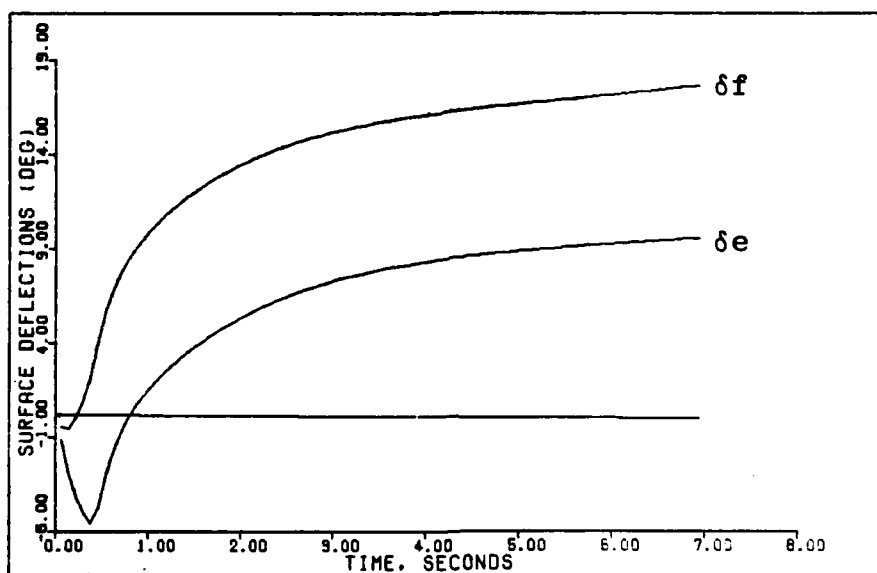
Figure C-5d.   G-Command System Response to a 4.7g
Step Command (0.6 Mach 30,000 feet)

267
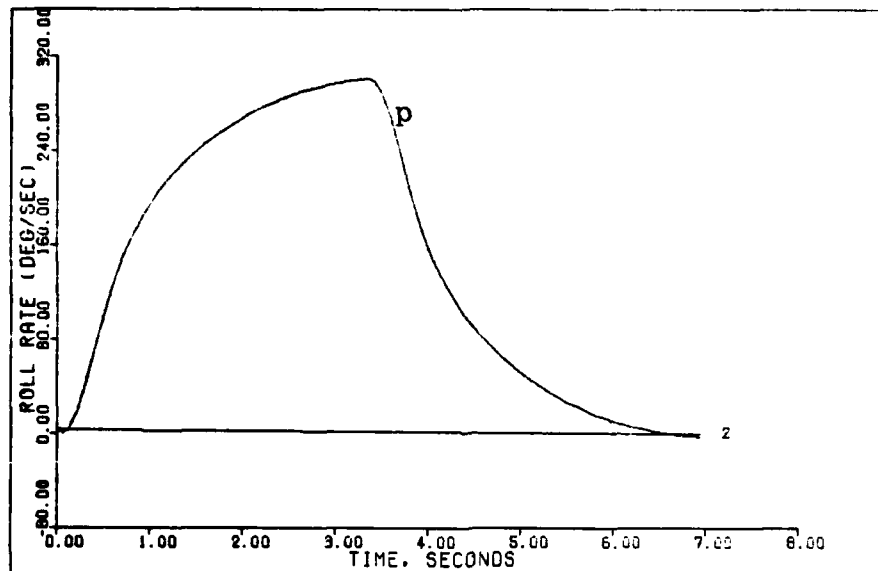
Figure C-6a. Roll Rate Command System Response to a 300 deg/sec Pulse Command (0.6 Mach 30,000 feet)
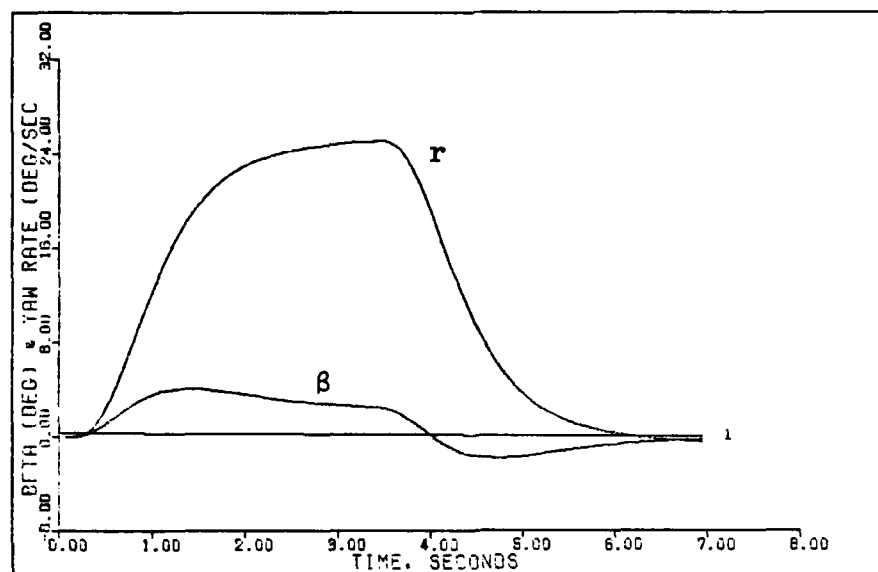
Figure C-6b. Roll Rate Command System Response to a 300 deg/sec Pulse Command (0.6 Mach 30,000 feet)
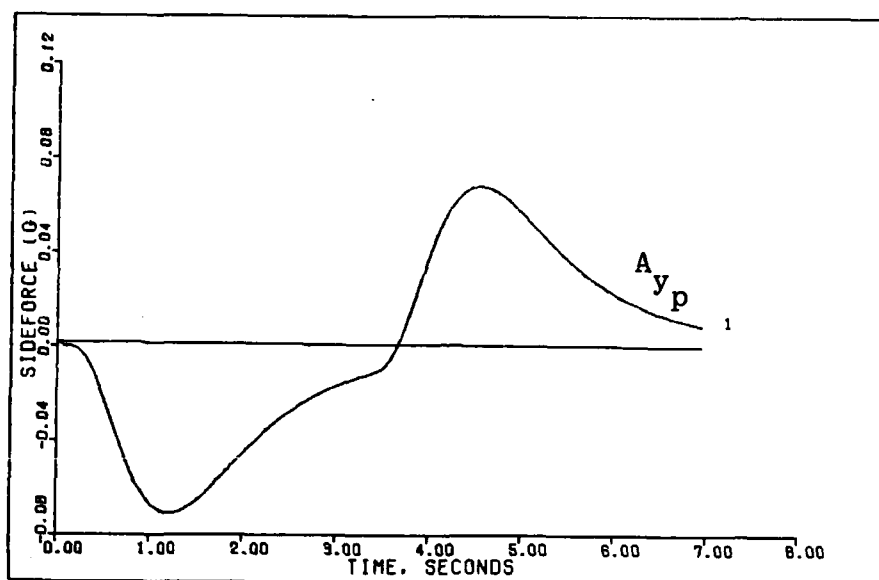
Figure C-6c.   Roll Rate Command System Response to a
300 deg/sec Pulse Command (0.6 Mach 30,000 feet)
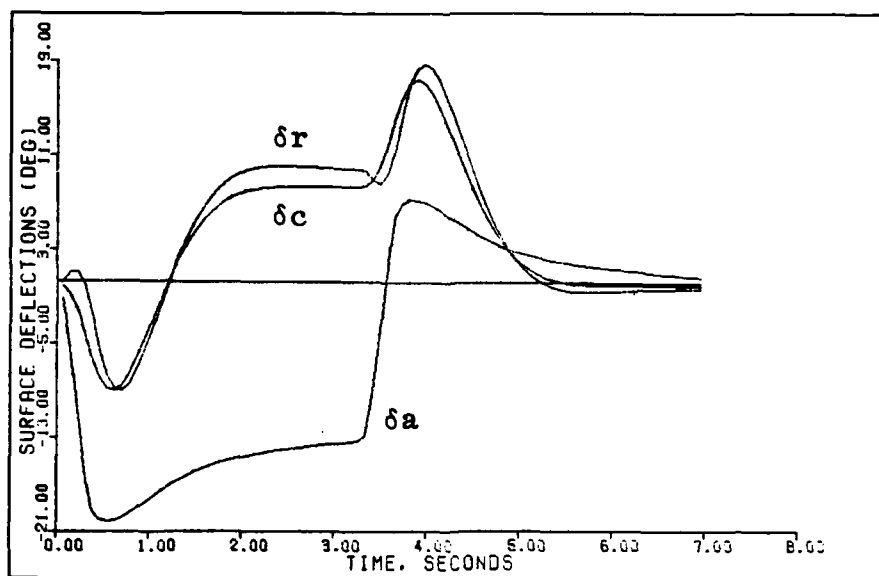
Figure C-6d.   Roll Rate Command System Response to a
300 deg/sec Pulse Command (0.6 Mach 30,000 feet)

269
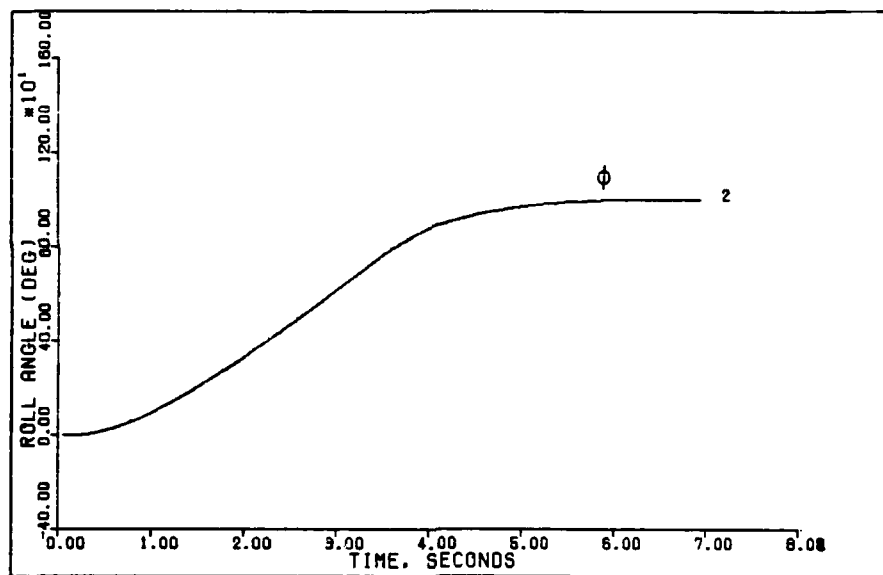
Figure C-6e. Roll Rate Command System Response to a
300 deg/sec Pulse Command (0.6 Mach 30,000 feet)
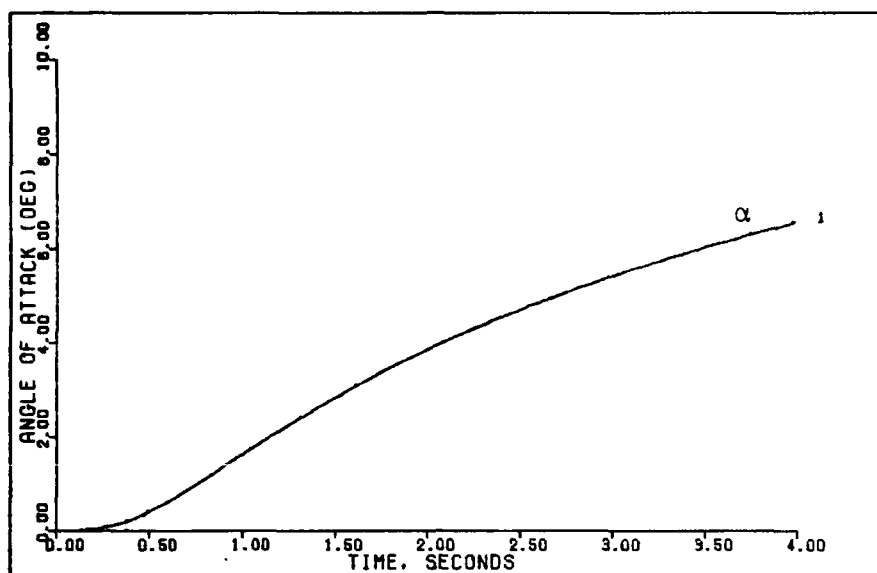
Figure C-7a.   G-Command System Response to a 0.3g
                Step Command (0.2 Mach 30 feet)
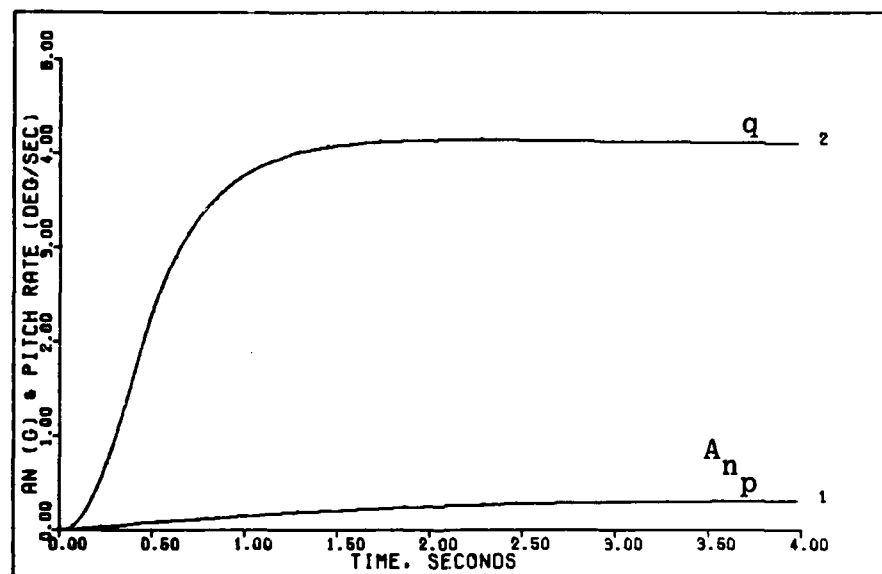
Figure C-7b.   G-Command System Response to a 0.3g
                Step Command (0.2 Mach 30 feet)

271
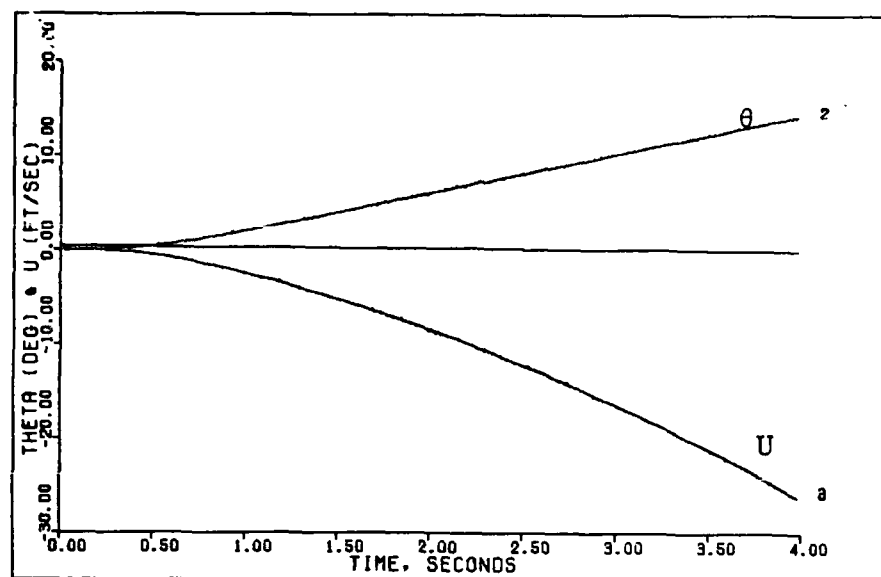
Figure C-7c.   G-Command System Response to a 0.3g
Step Command (0.2 Mach 30 feet)
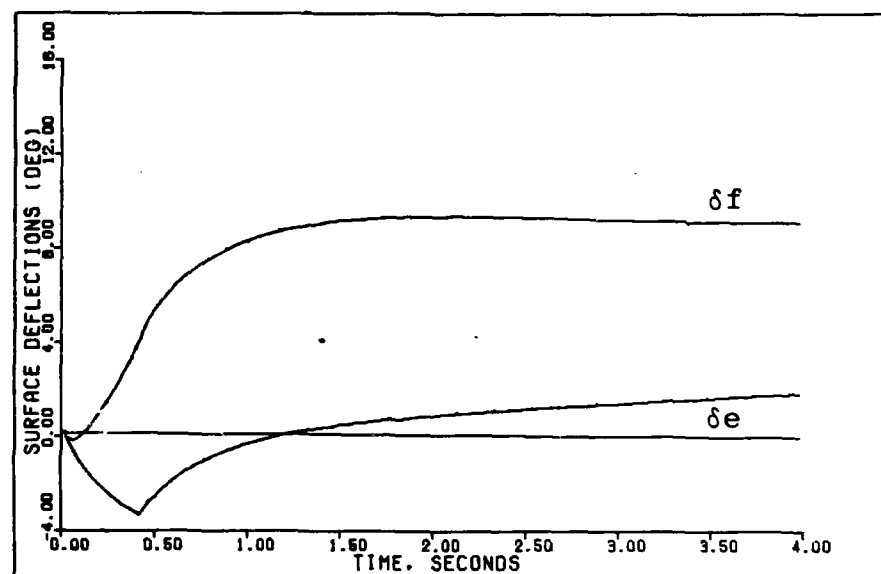
Figure C-7d.   G-Command System Response to a 0.3g
Step Command (0.2 Mach 30 feet)

272
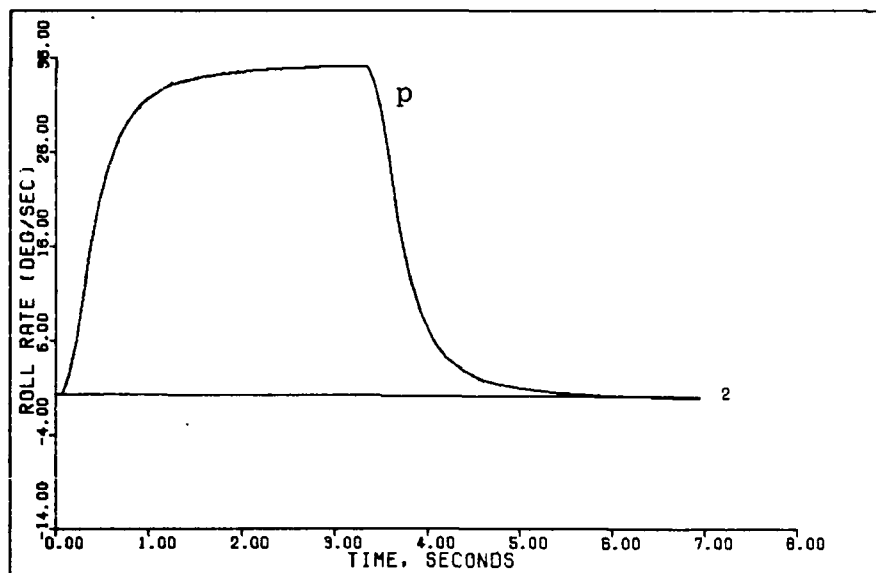
Figure C-8a. Roll Rate Command System Response to a
35 deg/sec Pulse Command (0.2 Mach 30 feet)
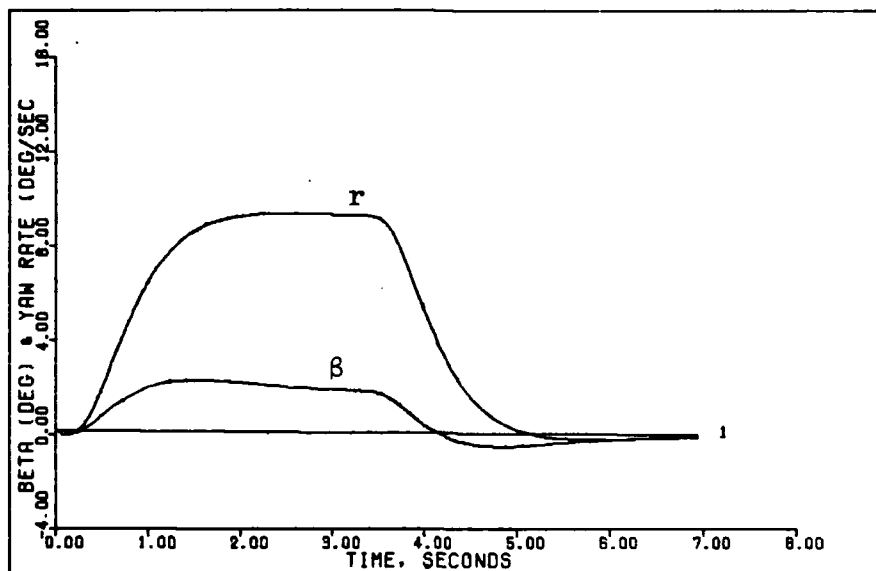
Figure C-8b. Roll Rate Command System Response to a
35 deg/sec Pulse Command (0.2 Mach 30 feet)

273
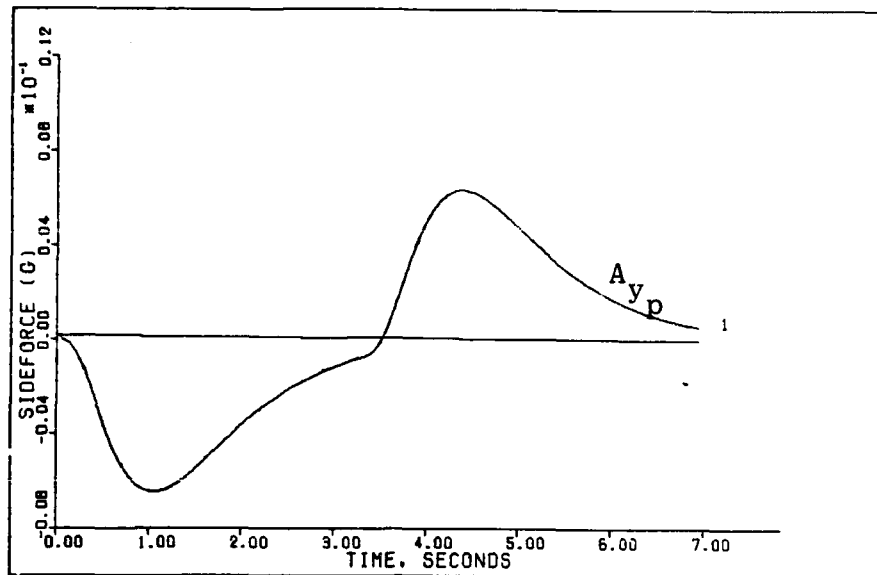
Figure C-8c.   Roll Rate Command System Respc ᴢ to a
35 deg/sec Pulse Command (0.2 Mach 30 feet)
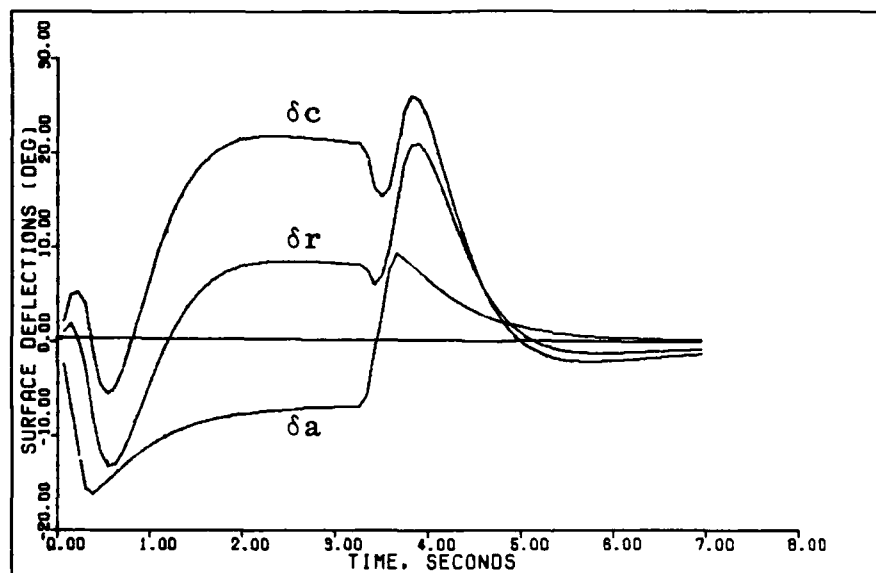
Figure C-8d.   Roll Rate Command System Response to a
35 deg/sec Pulse Command (0.2 Mach 30 feet)

274
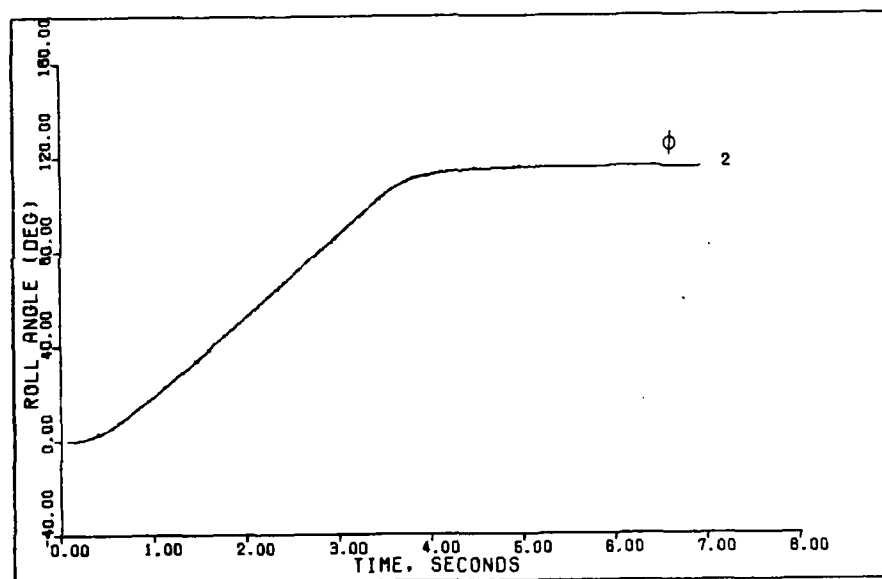
Figure C-8e.   Roll Rate Command System Response to a
35 deg/sec Pulse Command (0.2 Mach 30 feet)

Appendix D

Conversion And Transformation (CAT) Program

Results of the CAT program for the 0.9 Mach 20,000 feet flight condition are given as a sample of the program's output. A listing of the program is also included in this appendix.

CAT is an interactive program requiring 27K of computer memory and 0.16 seconds of CP time for execution. The program performs an axis transformation on nondimensional aircraft data from the stability to the body axis. If requested it also dimensionalizes the data and converts it to primed body axis derivatives for direct use in a state-space model representation for the aircraft. (Refer to Chapter II or Appendix B for an explanation of the primed derivatives.) The program can perform these calculations on longitudinal data, lateral-directional data, or both simultaneously as specified by the user in answer to questions at the beginning of the program.

It should be noted that aerodynamic data are entered in terms of the stability axis and inertias are entered in body axis by convention. The proper units for each input are specified when the input is requested by the program. Theta is requested as an input. For trimmed level flight, theta should be set equal to the trim angle of attack.

Sample Run for the CAT Program

```
**********************************************************
******** AXIS TRANSFORMATION PROGRAM ****************
**********************. .*************************
ENTER STABILITY AXIS COEFFICIENTS FOR TRANSFORMATION
TO BODY AXIS.  TRIM ALPHA IS NEEDED FOR CONVERSION.
MOMENT COEFFICIENTS AND SIDEFORCE COEFFICIENTS NOT
REQUESTED REMAIN UNCHANGED.
NOTE:  ALL COEFFICIENTS ARE REQUESTED WHEN COMPUTING
DIMENSIONAL DERIVATIVES.
**********************************************************
TO TRANSFORM ONLY LONGITUDINAL DATA - TYPE LONG
TO TRANSFORM ONLY LATERAL-DIRECTIONAL DATA - TYPE LAT
TO TRANSFORM BOTH LONG AND LAT-DIR DATA - TYPE BOTH
KEYWORD =BOTH
ARE DIMENSIONAL BODY AXIS DERIVATIVES REQUIRED ?  (YES/NO)YES
**********************************************************
Q  (DYNAMIC PRESSURE - LBS/FT2) = 552.11295
S  (WING REFERENCE AREA - FT2) = 300.0
C  (WING MEAN AERODYNAMIC CORD - FT) = 11.32
B  (WING SPAN - FT) = 30.0
VT (TRIM VELOCITY - FT/SEC) = 933.23
THETA (PITCH ANGLE - DEGS) = 1.86
W  (WEIGHT - LBS) = 21018.0
INERTIAS MUST BE INPUT IN BODY AXIS.
IXX  (SLUG-FT2) = 10033.429
IYY  (SLUG-FT2) = 53876.269
IZZ  (SLUG-FT2) = 61278.452
IXZ  (SLUG-FT2) = 282.13217
**********************************************************
                AIRCRAFT PARAMETERS
Q  (DYNAMIC PRESSURE - LBS/FT2) =   552.113
S  (WING REFERENCE AREA - FT2) =   300.000
C  (WING MEAN AERODYNAMIC CORD - FT) =   11.3200
B  (WING SPAN - FT) =   30.0000
VT (TRIM VELOCITY - FT/SEC) =   933.230
THETA =   1.86000
W  (WEIGHT - LBS) =   21018.0
IXX  (SLUG-FT2) =   10033.4
IYY  (SLUG-FT2) =   53876.3
IZZ  (SLUG-FT2) =   61278.5
IXZ  (SLUG-FT2) =   282.132
**********************************************************
IS THE ENTERED DATA CORRECT ?  (YES/NO)YES
**********************************************************
ALPHA (DEG) = 1.86
CL = 0.12618613
CLA (1/DEG) = 0.094812
CLDE (1/DEG) = 0.009578
CLDF (1/DEG) = 0.015718
CLQ (1/RAD) = 3.161717
CLAD (1/RAD) = -1.357762
CLU (1/(FT/SEC)) = -0.000442
```

```
CD = 0.023765548
CDA (1/DEG) = 0.002636
CDDE (1/DEG) = 0.000173
CDDF (1/DEG) = 0.000351
CDU (1/(FT/SEC)) = 0.00016
CM = 0.0
CMA (1/DEG) = 0.001938
CMDE (1/DEG) = -0.012086
CMDF (1/DEG) = -0.00328
CMQ (1/RAD) = -2.382199
CMAD (1/RAD) = -1.307597
CMU (1/(FT/SEC)) = -0.00006
*****************************************************
        LONGITUDINAL STABILITY AXIS COEFFICIENTS
                ALPHA =   1.86000
    CL =   .126186          CM =  0.              CD =    .237655E-01
    CLA =   .948120E-01      CMA =   .193800E-02   CDA =    .263600E-02
    CLDE =   .957800E-02     CMDE = -.120860E-01   CDDE =    .173000E-03
    CLDF =   .157180E-01     CMDF = -.328000E-02   CDDF =    .351000E-03
    CLQ =  3.16172          CMQ = -2.38220
    CLAD = -1.35776         CMAD = -1.30760
    CLU = -.442000E-03      CMU = -.600000E-04   CDU =    .160000E-03
*****************************************************
IS THE ENTERED DATA CORRECT ?   (YES/NO)YES
*****************************************************
        LONGITUDINAL BODY AXIS COEFFICIENTS   (1/RAD)
    CZ = -.126891                              CX = -.196573E-01
    CZA = -5.45937          CMA =    .110979    CXA =    .150896
    CZDE = -.548812                            CXDE =    .790500E-02
    CZDF = -.900753                            CXDF =    .913012E-02
    CZQ = -3.16005                            CXQ =    .102621
    CZAD =  1.35633         CMAD = -1.30691    CXAD = -.440462E-01
    CZU = -.761884E-01      CMU = -.366402E-02   CXU = -.444101E-01
*****************************************************
    LONG BODY AXIS DIMENSIONAL DERIVATIVES
    Z = -21017.5           M = 0.              X = -3255.92
    ZA = -1385.34          MA =  3.86223        XA =   38.2906
    ZDE = -139.263         MDE = -24.0992       XDE =   2.00593
    ZDF = -228.570         MDF = -6.54025       XDF =   2.31681
    ZQ = -4.86335          MQ = -.502810       XQ =   .157935
    ZAD =  2.08741         MAD = -.275849       XAD = -.677876E-01
    ZU = -.207164E-01      MU = -.136636E-03    XU = -.120755E-01
*****************************************************
    LONG BODY AXIS PRIMED DIMENSONAL DERIVATIVES
    ZA' = -1.48446         MA' =  4.27171       XA' =   38.2906
    ZDE' = -.149227        MDE' = -24.0581      XDE' =   2.00593
    ZDF' = -.244924        MDF' = -6.47269      XDF' =   2.31681
    ZQ' =  .994789         MQ' = -.777221       XQ' = -30.1376
    ZU' = -.221986E-04     MU' = -.130513E-03   XU' = -.120755E-01
ZTHETA' = -.111991E-02     MTHETA' =  .308924E-03   XTHETA' = -32.1830
*****************************************************
```

```
**********************************************************
CNB  (1/DEG) = 0.001675
CNP  (1/RAD) = -0.005541
CNR  (1/RAD) = -0.27912
CNDR (1/DEG) = -0.001272
CNDA (1/DEG) = -0.00016
CNDDT (1/DEG) = -0.000997
CNDC (1/DEG) = 0.001256
CLB  (1/DEG) = -0.001901
CLP  (1/RAD) = -0.351217
CLR  (1/RAD) = 0.021937
CLDR (1/DEG) = 0.000331
CLDA (1/DEG) = -0.001804
CLDDT (1/DEG) = -0.001816
CLDC (1/DEG) = 0.00023
CYB  (1/DEG) = -0.022052
CYP  (1/RAD) = 0.057563
CYR  (1/RAD) = 0.557635
CYDR (1/DEG) = 0.002377
CYDA (1/DEG) = -0.000088
CYDDT (1/DEG) = 0.001708
CYDC (1/DEG) = 0.001716
**********************************************************
        LAT-DIR STABILITY AXIS COEFFICIENTS
  CNB  =   .167500E-02      CLB  = -.190100E-02      CYB  = -.220520E-01
  CNP  = -.554100E-02       CLP  = -.351217          CYP  =  .575630E-01
  CNR  = -.279120           CLR  =  .219370E-01      CYR  =  .557635
  CNDR = -.127200E-02       CLDR =  .331000E-03      CYDR =  .237700E-02
  CNDA = -.160000E-03       CLDA = -.180400E-02      CYDA = -.880000E-04
  CNDDT = -.997000E-03      CLDDT = -.181600E-02     CYDDT =  .170800E-02
  CNDC =  .125600E-02       CLDC =  .230000E-03      CYDC =  .171600E-02
**********************************************************
IS THE ENTERED DATA CORRECT ?   (YES/NO)YES
**********************************************************
        LAT-DIR BODY AXIS COEFFICIENTS
  CNB  =   .923846E-01      CLB  = -.111977          CYB  = -1.26349
  CNP  = -.789712E-02       CLP  = -.351673          CYP  =  .394333E-01
  CNR  = -.278664           CLR  =  .195809E-01      CYR  =  .559210
  CNDR = -.722263E-01       CLDR =  .213204E-01      CYDR =  .136192
  CNDA = -.125173E-01       CLDA = -.103010          CYDA = -.504203E-02
  CNDDT = -.604710E-01      CLDDT = -.102140         CYDDT =  .978612E-01
  CNDC =  .723533E-01       CLDC =  .108353E-01      CYDC =  .983196E-01
**********************************************************
    LAT-DIR BODY AXIS DIMENSIONAL DERIVATIVES
   NB  =  7.49139       LB  = -55.4561       YB  = -320.615
   NP  = -.102928E-01   LP  = -2.79938       YP  =  .160834
   NR  = -.363200       LR  =  .155868       YR  =  2.28082
  NDR  = -5.85677       LDR =  10.5589       YDR =  34.5593
  NDA  = -1.01502       LDA = -51.0151       YDA = -1.27944
  NDDT = -4.90354       LDDT = -50.5845      YDDT =  24.8327
  NDC  =  5.86707       LDC =  5.36616       YDC =  24.9490
**********************************************************
```

```
LAT-DIR BODY AXIS PRIMED DIMENSIONAL DERIVATIVES
  NB'  =    7.23700             LB'  =  -55.2526         YB'  =   -.343554
  NP'  =  -.231845E-01          LP'  =   -2.80004        YP'  =    .326355E-01
  NR'  =  -.362530              LR'  =    .145674        YR'  =   -.997556
 NDR'  =  -5.80890             LDR'  =   10.3955        YDR'  =    .370320E-01
 NDA'  =  -1.25006             LDA'  =  -51.0502        YDA'  =   -.137098E-02
NDDT'  =  -5.13710            LDDT'  =  -50.7290       YDDT'  =    .266094E-01
 NDC'  =   5.89254             LDC'  =    5.53185       YDC'  =    .267341E-01
******************************************************
IS ANOTHER PROGRAM RUN DESIRED ?   (YES/NO)NO
******************************************************
     END   CAT
     027000 MAXIMUM EXECUTION FL.
     0.242 CP SECONDS EXECUTION TIME.
COMMAND-
```

280

```
100=        PROGRAM CAT (INPUT,OUTPUT,TAPE5=INPUT,TAPE6=OUTPUT)
110=        REAL ALPHA,CL,CLA,CLDE,CLDF,CLQ,CLAD,CLU,
120=       1CD,CDA,CDDE,CDDF,CDU,
130=       2CZ,CZA,CZDE,CZDF,CZQ,CZAD,CZU,
140=       3CX,CXA,CXDE,CXDF,CXU,DALPHA,DPR,
150=       4CNB,CNP,CNR,
160=       5CNDR,CNDA,CNDDT,CNDC,
170=       6CLB,CLP,CLR,
180=       7CLDR,CLDA,CLDDT,CLDC,
190=       8CYP,CYR,L,N,
200=       9M,M1,MA,MAD,MQ,MU,MDE,MDF
210=        DPR = 57.2957795
220=        WRITE(6,5)
230= 5      FORMAT(1X,"***********************************************")
240=        WRITE(6,10)
250= 10     FORMAT(1X,"******** AXIS TRANSFORMATION PROGRAM ***************")
260=        WRITE(6,20)
270= 20     FORMAT(1X,"***********************************************")
280=        WRITE(6,100)
290= 100    FORMAT(1X,*ENTER STABILITY AXIS COEFFICIENTS FOR TRANSFORMATION*)
300=        WRITE(6,101)
310= 101    FORMAT(1X,*TO BODY AXIS.  TRIM ALPHA IS NEEDED FOR CONVERSION.*)
320=        WRITE(6,102)
330= 102    FORMAT(1X,*MOMENT COEFFICIENTS AND SIDEFORCE COEFFICIENTS NOT*)
340=        WRITE(6,40)
350= 40     FORMAT(1X,*REQUESTED REMAIN UNCHANGED.*)
360=        WRITE(6,41)
370= 41     FORMAT(1X,*NOTE:  ALL COEFFICIENTS ARE REQUESTED WHEN COMPUTING*)
380=        WRITE(6,42)
390= 42     FORMAT(1X,*DIMENSIONAL DERIVATIVES.*)
400= 103    CONTINUE
410=        WRITE(6,30)
420= 30     FORMAT(1X,"***********************************************")
430=        WRITE(6,106)
440= 106    FORMAT(1X,*TO TRANSFORM ONLY LONGITUDINAL DATA - TYPE LONG*)
450=        WRITE(6,107)
460= 107    FORMAT(1X,*TO TRANSFORM ONLY LATERAL-DIRECTIONAL DATA - TYPE LAT*)
470=        WRITE(6,108)
480= 108    FORMAT(1X,*TO TRANSFORM BOTH LONG AND LAT-DIR DATA - TYPE BOTH*)
490=        WRITE(6,111)
500= 111    FORMAT(1X,*KEYWORD =   *)
510=        READ(5,109) KEY
520= 109    FORMAT(A3)
530=        IF(KEY .EQ. 3HLAT) GO TO 104
540=        IF(KEY .EQ. 3HLON) GO TO 104
550=        IF(KEY .EQ. 3HBOT) GO TO 104
560=        GO TO 103
570= 104    CONTINUE
580= 2000   CONTINUE
590=        WRITE(6,2010)
```

```
600= 2010 FORMAT(1X,*ARE DIMENSIONAL BODY AXIS DERIVATIVES REQUIRED ?  (YES/
610=      1NO)*)
620=      READ(5,2020) KEY1
630= 2020 FORMAT(A3)
640=      WRITE(6,2030)
650= 2030 FORMAT(1X,"*********************************************")
660=      IF (KEY1 .EQ. 3HYES) GO TO 2040
670=      IF (KEY1 .EQ. 3HNO ) GO TO 2150
680=      GO TO 2000
690= 2040 CONTINUE
700=      WRITE(6,2050)
710= 2050 FORMAT(1X,*Q  (DYNAMIC PRESSURE - LBS/FT**2) = *)
720=      READ(5,*) Q
730=      WRITE(6,2060)
740= 2060 FORMAT(1X,*S  (WING REFERENCE AREA - FT**2) = *)
750=      READ(5,*) S
760=      WRITE(6,2065)
770= 2065 FORMAT(1X,*C  (WING MEAN AERODYNAMIC CORD - FT) = *)
780=      READ(5,*) C
790=      WRITE(6,2070)
800= 2070 FORMAT(1X,*B  (WING SPAN - FT) = *)
810=      READ(5,*) B
820=      WRITE(6,2080)
830= 2080 FORMAT(1X,*VT (TRIM VELOCITY - FT/SEC) = *)
840=      READ (5,*) U
850=      WRITE(6,2081)
860= 2081 FORMAT(1X,*THETA (PITCH ANGLE - DEGS) = *)
870=      READ(5,*) DTHETA
880=      WRITE(6,2085)
890= 2085 FORMAT(1X,*W  (WEIGHT - LBS) = *)
900=      READ(5,*) W
910=      WRITE(6,2090)
920= 2090 FORMAT(1X,*INERTIAS MUST BE INPUT IN BODY AXIS.*)
930=      WRITE(6,2100)
940= 2100 FORMAT(1X,*IXX  (SLUG-FT**2) = *)
950=      READ(5,*) BIXX
960=      WRITE(6,2110)
970= 2110 FORMAT(1X,*IYY  (SLUG-FT**2) = *)
980=      READ(5,*) BIYY
990=      WRITE(6,2120)
1000= 2120 FORMAT(1X,*IZZ  (SLUG-FT**2) = *)
1010=      READ(5,*) BIZZ
1020=      WRITE(6,2130)
1030= 2130 FORMAT(1X,*IXZ  (SLUG-FT**2) = *)
1040=      READ(5,*) BIXZ
1050=      WRITE(6,2140)
1060= 2140 FORMAT(1X,"*********************************************")
1070=      WRITE(6,3030)
1080= 3030 FORMAT(16X,*AIRCRAFT PARAMETERS*)
1090=      WRITE(6,3050) Q
1100= 3050 FORMAT(1X,*Q  (DYNAMIC PRESSURE - LBS/FT**2) = *,G13.6)
1110=      WRITE(6,3060) S
```

```
1120= 3060 FORMAT(1X,*S  (WING REFERENCE AREA - FT**2) = *,G13.6)
1130=      WRITE(6,3065) C
1140= 3065 FORMAT(1X,*C  (WING MEAN AERODYNAMIC CORD - FT) = *,G13.6)
1150=      WRITE(6,3070) B
1160= 3070 FORMAT(1X,*B  (WING SPAN - FT) = *,G13.6)
1170=      WRITE(6,3080) U
1180= 3080 FORMAT(1X,*VT (TRIM VELOCITY - FT/SEC) = *,G13.6)
1190=      WRITE(6,3081) DTHETA
1200= 3081 FORMAT(1X,*THETA = *,G13.6)
1210=      WRITE(6,3085) W
1220= 3085 FORMAT(1X,*W  (WEIGHT - LBS) = *,G13.6)
1230=      WRITE(6,3100) BIXX
1240= 3100 FORMAT(1X,*IXX  (SLUG-FT**2) = *,G13.6)
1250=      WRITE(6,3110) BIYY
1260= 3110 FORMAT(1X,*IYY  'SLUG-FT**2) = *,G13.6)
1270=      WRITE(6,3120) BIZZ
1280= 3120 FORMAT(1X,*IZZ  (SLUG-FT**2) = *,G13.6)
1290=      WRITE(6,3130) BIXZ
1300= 3130 FORMAT(1X,*IXZ  (SLUG-FT**2) = *,G13.6)
1310=      WRITE(6,3140)
1320= 3140 FORMAT(1X,"*****************************************************")
1330= 3000 CONTINUE
1340=      WRITE(6,3010)
1350= 3010 FORMAT(1X,*IS THE ENTERED DATA CORRECT ?  (YES/NO) *)
1360=      READ(5,3020) DATA3
1370= 3020 FORMAT(A3)
1380=      WRITE(6,3025)
1390= 3025 FORMAT(1X,"*****************************************************")
1400=      IF(DATA3 .EQ. 3HNO ) GO TO 2040
1410=      IF(DATA3 .EQ. 3HYES) GO TO 2150
1420=      GO TO 3000
1430= 2150 CONTINUE
1440=      WRITE(6, 105)
1450= 105  FORMAT(1X,*ALPHA (DEG) = *)
1460=      READ(5,*) DALPHA
1470=      ALPHA = DALPHA/DPR
1480=      IF(KEY .EQ. 3HLAT)GO TO 460
1490=      WRITE(6, 110)
1500= 110  FORMAT (1X,*CL = *)
1510=      READ(5,*) CL
1520=      WRITE(6, 120)
1530= 120  FORMAT(1X,*CLA (1/DEG) = *)
1540=      READ(5,*) CLA
1550=      WRITE(6, 130)
1560= 130  FORMAT(1X,*CLDE (1/DEG) = *)
1570=      READ(5,*) CLDE
1580=      WRITE(6, 140)
1590= 140  FORMAT(1X,*CLDF (1/DEG) = *)
1600=      READ(5,*) CLDF
1610=      WRITE(6, 150)
1620= 150  FORMAT(1X,*CLQ (1/RAD) = *)
1630=      READ(5,*) CLQ
```

```
1640=         WRITE(6, 160)
1650= 160   FORMAT(1X,*CLAD (1/RAD) = *)
1660=         READ(5,*) CLAD
1670=         WRITE(6, 170)
1680= 170   FORMAT(1X,*CLU (1/(FT/SEC)) = *)
1690=         READ(5,*) CLU
1700=         WRITE(6, 180)
1710= 180   FORMAT(1X,*CD = *)
1720=         READ(5,*) CD
1730=         WRITE(6, 190)
1740= 190   FORMAT(1X,*CDA (1/DEG) = *)
1750=         READ(5,*) CDA
1760=         WRITE(6,200)
1770= 200   FORMAT(1X,*CDDE (1/DEG) = *)
1780=         READ(5,*) CDDE
1790=         WRITE(6,210)
1800= 210   FORMAT(1X,*CDDF (1/DEG) = *)
1810=         READ(5,*) CDDF
1820=         WRITE(6,220)
1830= 220   FORMAT(1X,*CDU (1/(FT/SEC)) = *)
1840=         READ(5,*) CDU
1850=         WRITE(6, 1000)
1860= 1000  FORMAT(1X,*CM = *)
1870=         READ(5,*) CM
1880=         WRITE(6, 1010)
1890= 1010  FORMAT(1X,*CMA (1/DEG) = *)
1900=         READ(5,*) CMA
1910=         IF (KEY1 .EQ. 3HNO ) GO TO 1005
1920=         WRITE(6, 1030)
1930= 1030  FORMAT(1X,*CMDE (1/DEG) = *)
1940=         READ(5,*) CMDE
1950=         WRITE(6, 1040)
1960= 1040  FORMAT(1X,*CMDF (1/DEG) = *)
1970=         READ(5,*) CMDF
1980=         WRITE(6, 1050)
1990= 1050  FORMAT(1X,*CMQ (1/RAD) = *)
2000=         READ(5,*) CMQ
2010= 1005  CONTINUE
2020=         WRITE(6, 1060)
2030= 1060  FORMAT(1X,*CMAD (1/RAD) = *)
2040=         READ(5,*) CMAD
2050=         WRITE(6, 1020)
2060= 1020  FORMAT(1X,*CMU (1/(FT/SEC)) = *)
2070=         READ(5,*) CMU
2080=         WRITE(6,225)
2090= 225   FORMAT(1X,"***************************************************")
2100=         WRITE(6,226)
2110= 226   FORMAT(6X,*LONGITUDINAL STABILITY AXIS COEFFICIENTS*)
2120=         WRITE(6,230) DALPHA
2130= 230   FORMAT(15X,*ALPHA =*,G13.6)
2140=         IF (KEY1 .EQ. 3HYES) GO TO 1080
2150=         WRITE(6,240) CL,CD
```

284

```
2160= 240   FORMAT(1X,*CL =      *,G13.6,6X,*CD = *,G13.6)
2170=        WRITE(6,250) CLA,CDA
2180= 250   FORMAT(1X,*CLA =    *,G13.6,5X,*CDA = *,G13.6)
2190=        WRITE(6,260) CLDE,CDDE
2200= 260   FORMAT(1X,*CLDE =  *,G13.6,4X,*CDDE = *,G13.6)
2210=        WRITE(6,270) CLDF,CDDF
2220= 270   FORMAT(1X,*CLDF =  *,G13.6,4X,*CDDF = *,G13.6)
2230=        WRITE(6,280) CLQ
2240= 280   FORMAT(1X,*CLQ =    *,G13.6)
2250=        WRITE(6,290) CLAD
2260= 290   FORMAT(1X,*CLAD =   *,G13.6)
2270=        WRITE(6,300) CLU,CDU
2280= 300   FORMAT(1X,*CLU =    *,G13.6,5X,*CDU = *,G13.6)
2290= 1080  CONTINUE
2300=        IF(KEY1 .EQ. 3HNO ) GO TO 1170
2310=        WRITE(6,1090) CL,CM,CD
2320= 1090  FORMAT(4X,*CL = *,G13.6,9X,*CM = *,G13.6,6X,*CD = *,G13.6)
2330=        WRITE(6,1100) CLA,CMA,CDA
2340= 1100  FORMAT(3X,*CLA = *,G13.6,8X,*CMA = *,G13.6,5X,*CDA = *,G13.6)
2350=        WRITE(6,1110) CLDE,CMDE,CDDE
2360= 1110  FORMAT(2X,*CLDE = *,G13.6,7X,*CMDE = *,G13.6,4X,*CDDE = *,G13.6)
2370=        WRITE(6,1120) CLDF,CMDF,CDDF
2380= 1120  FORMAT(2X,*CLDF = *,G13.6,7X,*CMDF = *,G13.6,4X,*CDDF = *,G13.6)
2390=        WRITE(6,1130) CLQ,CMQ
2400= 1130  FORMAT(3X,*CLQ = *,G13.6,8X,*CMQ = *,G13.6)
2410=        WRITE(6,1150) CLAD,CMAD
2420= 1150  FORMAT(2X,*CLAD = *,G13.6,7X,*CMAD = *,G13.6)
2430=        WRITE(6,1140) CLU,CMU,CDU
2440= 1140  FORMAT(3X,*CLU = *,G13.6,8X,*CMU = *,G13.6,5X,*CDU = *,G13.6)
2450= 1170  CONTINUE
2460=        WRITE(6,310)
2470= 310   FORMAT(1X,"***********************************************************")
2480= 315   CONTINUE
2490=        WRITE(6,320)
2500= 320   FORMAT(1X,*IS THE ENTERED DATA CORRECT ?    (YES/NO)*)
2510=        READ(5,330) DATA1
2520= 330   FORMAT(A3)
2530=        WRITE(6,335)
2540= 335   FORMAT(1X,"***********************************************************")
2550=        IF(DATA1 .EQ. 3HNO ) GO TO 2150
2560=        IF(DATA1 .EQ. 3HYES) GO TO 340
2570=        GO TO 315
2580= 340   CONTINUE
2590=        WRITE(6,345)
2600= 345   FORMAT(6X,*LONGITUDINAL BODY AXIS COEFFICIENTS  (1/RAD)*)
2610=C
2620=        CLA = CLA*DPR
2630=        CLDE = CLDE*DPR
2640=        CLDF = CLDF*DPR
2650=        CDA = CDA*DPR
2660=        CDDE = CDDE*DPR
2670=        CDDF = CDDF*DPR
```

285

```
2680=        CMA = CMA*DPR
2690=C
2700=        IF (KEY1 .EQ. 3HNO ) GO TO 346
2710=C
2720=        CMDE = CMDE*DPR
2730=        CMDF = CMDF*DPR
2740=C
2750= 346  CONTINUE
2760=C
2770=        SCZA = -CLA - CD
2780=        SCZAD = -CLAD
2790=        SCZQ = -CLQ
2800=        SCZU = -CLU - 2.0*CL
2810=        SCZDE = -CLDE
2820=        SCZDF = -CLDF
2830=        SCXA = -CDA + CL
2840=        SCXU = -CDU - 2.0*CD
2850=        SCXDE = -CDDE
2860=        SCXDF = -CDDF
2870=C
2880=        CAL = COS(ALPHA)
2890=        SAL = SIN(ALPHA)
2900=        COSSQ = CAL**2
2910=        SINSQ = SAL**2
2920=        COSSIN = CAL*SAL
2930=C
2940=        CZ = -CL*CAL - CD*SAL
2950=        CZA = SCZA*COSSQ +(SCZU+SCXA)*COSSIN + SCXU*SINSQ
2960=        CZAD = SCZAD*COSSQ
2970=        CZQ = SCZQ*CAL
2980=        CZU = SCZU*COSSQ - (SCZA-SCXU)*COSSIN - SCXA*SINSQ
2990=        CZDE = SCZDE*CAL + SCXDE*SAL
3000=        CZDF = SCZDF*CAL + SCXDF*SAL
3010=C
3020=        CX = -CD*CAL + CL*SAL
3030=        CXA = SCXA*COSSQ + (SCXU-SCZA)*COSSIN - SCZU*SINSQ
3040=        CXAD = CLAD*COSSIN
3050=        CXQ = CLQ*SAL
3060=        CXU = SCXU*COSSQ - (SCXA+SCZU)*COSSIN + SCZA*SINSQ
3070=        CXDE = SCXDE*CAL - SCZDE*SAL
3080=        CXDF = SCXDF*CAL - SCZDF*SAL
3090=C
3100=        BCMA = CMA*CAL + (CMU + 2.0*CM)*SAL
3110=        BCMAD = CMAD*CAL
3120=        BCMU = (CMU + 2.0*CM)*CAL - CMA*SAL
3130=C
3140=        WRITE(6,350) CZ,CX
3150= 350  FORMAT(4X,*CZ = *,G13.6,33X,*CX = *,G13.6)
3160=        WRITE(6,360) CZA,BCMA,CXA
3170= 360  FORMAT(3X,*CZA = *,G13.6,8X,*CMA = *,G13.6,5X,*CXA = *,G13.6)
3180=        WRITE(6,370) CZDE,CXDE
3190= 370  FORMAT(2X,*CZDE = *,G13.6,31X,*CXDE = *,G13.6)
```

286

```
3200=        WRITE(6,380) CZDF,CXDF
3210= 380    FORMAT(2X,*CZDF = *,G13.6,31X,*CXDF = *,G13.6)
3220=        WRITE(6,390) CZQ,CXQ
3230= 390    FORMAT(3X,*CZQ = *,G13.6,32X,*CXQ = *,G13.6)
3240=        WRITE(6,400) CZAD,BCMAD,CXAD
3250= 400    FORMAT(2X,*CZAD = *,G13.6,7X,*CMAD = *,G13.6,4X,*CXAD = *,G13.6)
3260=        WRITE(6,410) CZU,BCMU,CXU
3270= 410    FORMAT(3X,*CZU = *,G13.6,8X,*CMU = *,G13.6,5X,*CXU = *,G13.6)
3280=        WRITE(6,420)
3290= 420    FORMAT(1X,"***************************************************")
3300=        IF (KEY1 .EQ. 3HNO ) GO TO 1360
3310=        Z1 = (Q*S*32.2)/W
3320=        A = C/(2.0*U)
3330=        THETA = DTHETA/DPR
3340=C
3350=      · Z = Q*S*CZ
3360=        ZA = Z1*CZA
3370=        ZAD = Z1*A*CZAD
3380=        ZQ = Z1*A*CZQ
3390=        ZU = (Z1/U)*CZU
3400=        ZDE = Z1*CZDE
3410=        ZDF = Z1*CZDF
3420=C
3430=        X = Q*S*CX
3440=        XA = Z1*CXA
3450=        XAD = Z1*A*CXAD
3460=        XQ = Z1*A*CXQ
3470=        XU = (Z1/U)*CXU
3480=        XDE = Z1*CXDE
3490=        XDF = Z1*CXDF
3500=C
3510=        M1 = (Q*S*C)/BIYY
3520=C
3530=        M = Q*S*C*CM
3540=        MA = M1*BCMA
3550=        MAD = M1*A*BCMAD
3560=        MQ = M1*A*CMQ
3570=        MU = (M1/U)*BCMU
3580=        MDE = M1*CMDE
3590=        MDF = M1*CMDF
3600=C
3610=        WRITE(6,1180)
3620= 1180   FORMAT(5X,*LONG BODY AXIS DIMENSIONAL DERIVATIVES*)
3630=        WRITE(6,1190) Z,M,X
3640= 1190   FORMAT(5X,*Z = *,G13.6,10X,*M = *,G13.6,7X,*X = *,G13.6)
3650=        WRITE(6,1200) ZA,MA,XA
3660= 1200   FORMAT(4X,*ZA = *,G13.6,9X,*MA = *,G13.6,6X,*XA = *,G13.6)
3670=        WRITE(6,1210) ZDE,MDE,XDE
3680= 1210   FORMAT(3X,*ZDE = *,G13.6,8X,*MDE = *,G13.6,5X,*XDE = *,G13.6)
3690=        WRITE(6,1220) ZDF,MDF,XDF
3700= 1220   FORMAT(3X,*ZDF = *,G13.6,8X,*MDF = *,G13.6,5X,*XDF = *,G13.6)
3710=        WRITE(6,1230) ZQ,MQ,XQ
```

287

```
3720=  1230 FORMAT(4X,*ZQ = *,G13.6,9X,*MQ = *,G13.6,6X,*XQ = *,G13.6)
3730=       WRITE(6,1250) ZAD,MAD,XAD
3740=  1250 FORMAT(3X,*ZAD = *,G13.6,8X,*MAD = *,G13.6,5X,*XAD = *,G13.6)
3750=       WRITE(6,1240) ZU,MU,XU
3760=  1240 FORMAT(4X,*ZU = *,G13.6,9X,*MU = *,G13.6,6X,*XU = *,G13.6)
3770=       WRITE(6,1260)
3780=  1260 FORMAT(1X,"*******************************************************")
3790=C
3800=       PZA = ZA/U
3810=       PZQ = (ZQ/U) + 1.0
3820=       PZU = ZU/U
3830=       PZDE = ZDE/U
3840=       PZDF = ZDF/U
3850=       PZTHETA = -(32.2/U)*SIN(THETA)
3860=C
3870=       PMA = MA + MAD*PZA
3880=       PMQ = MQ + MAD*PZQ
3890=       PMU = MU + MAD*PZU
3900=       PMDE = MDE + MAD*PZDE
3910=       PMDF = MDF + MAD*PZDF
3920=       PMTHETA = MAD*PZTHETA
3930=C
3940=       PXQ = XQ - U*ALPHA
3950=       PXTHETA = -32.2*COS(THETA)
3960=       WRITE(6,1280)
3970=  1280 FORMAT(5X,*LONG BODY AXIS PRIMED DIMENSONAL DERIVATIVES*)
3980=       WRITE(6,1290) PZA,PMA,XA
3990=  1290 FORMAT(3X,*ZA' = *,G13.6,8X,*MA' = *,G13.6,5X,*XA' = *,G13.6)
4000=       WRITE(6,1300) PZDE,PMDE,XDE
4010=  1300 FORMAT(2X,*ZDE' = *,G13.6,7X,*MDE' = *,G13.6,4X,*XDE' = *,G13.6)
4020=       WRITE(6,1310) PZDF,PMDF,XDF
4030=  13100FORMAT(2X,*ZDF' = *,G13.6,7X,*MDF' = *,G13.6,4X,*XDF' = *,G13.6)
4040=       WRITE(6,1320) PZQ,PMQ,PXQ
4050=  1320 FORMAT(3X,*ZQ' = *,G13.6,8X,*MQ' = *,G13.6,5X,*XQ' = *,G13.6)
4060=       WRITE(6,1330) PZU,PMU,XU
4070=  1330 FORMAT(3X,*ZU' = *,G13.6,8X,*MU' = *,G13.6,5X,*XU' = *,G13.6)
4080=       WRITE(6,1340) PZTHETA,PMTHETA,PXTHETA
4090=  1340 FORMAT(1X,*ZTHETA' = *,G12.6,4X,*MTHETA' = *,G12.6,3X,*XTHETA' = *
4100=      +,G12.6)
4110=       WRITE(6,1350)
4120=  1350 FORMAT(1X,"*******************************************************")
4130=  1360 CONTINUE
4140=       IF(KEY .EQ. 3HBOT) GO TO 446
4150=  421  CONTINUE
4160=       WRITE(6,430)
4170=  430  FORMAT(1X,*IS ANOTHER PROGRAM RUN DESIRED ?  (YES/NO)*)
4180=       READ(5,440) RUN
4190=  440  FORMAT(A3)
4200=       WRITE(6,445)
4210=  445  FORMAT(1X,"*******************************************************")
4220=       IF(RUN .EQ. 3HNO ) GO TO 450
4230=       IF(RUN .EQ. 3HYES) GO TO 103
```

```
4240=          GO TO 421
4250= 446   CONTINUE
4260=          WRITE(6,447)
4270= 447   FORMAT(1X,"**************************************************")
4280= 460   CONTINUE
4290=          WRITE(6,455)
4300= 455   FORMAT(1X,*CNB (1/DEG) = *)
4310=          READ(5,*) CNB
4320=          WRITE(6,470)
4330= 470   FORMAT(1X,*CNP (1/RAD) = *)
4340=          READ(5,*) CNP
4350=          WRITE(6,480)
4360= 480   FORMAT(1X,*CNR (1/RAD) = *)
4370=          READ(5,*) CNR
4380=          WRITE(6,490)
4390= 490   FORMAT(1X,*CNDR (1/DEG) = *)
4400=          READ(5,*) CNDR
4410=          WRITE(6,500)
4420= 500   FORMAT(1X,*CNDA (1/DEG) = *)
4430=          READ(5,*) CNDA
4440=          WRITE(6,510)
4450= 510   FORMAT(1X,*CNDDT (1/DEG) = *)
4460=          READ(5,*) CNDDT
4470=          WRITE(6,520)
4480= 520   FORMAT(1X,*CNDC (1/DEG) = *)
4490=          READ(5,*) CNDC
4500=          WRITE(6,530)
4510= 530   FORMAT(1X,*CLB (1/DEG) = *)
4520=          READ(5,*) CLB
4530=          WRITE(6,540)
4540= 540   FORMAT(1X,*CLP (1/RAD) = *)
4550=          READ(5,*) CLP
4560=          WRITE(6,550)
4570= 550   FORMAT(1X,*CLR (1/RAD) = *)
4580=          READ(5,*) CLR
4590=          WRITE(6,560)
4600= 560   FORMAT(1X,*CLDR (1/DEG) = *)
4610=          READ(5,*) CLDR
4620=          WRITE(6,570)
4630= 570   FORMAT(1X,*CLDA (1/DEG) = *)
4640=          READ(5,*) CLDA
4650=          WRITE(6,580)
4660= 580   FORMAT(1X,*CLDDT (1/DEG) = *)
4670=          READ(5,*) CLDDT
4680=          WRITE(6,590)
4690= 590   FORMAT(1X,*CLDC (1/DEG) = *)
4700=          READ(5,*) CLDC
4710=          IF (KEY1 .EQ. 3HNO ) GO TO 609
4720=          WRITE(6,611)
4730= 611   FORMAT(1X,*CYB (1/DEG) = *)
4740=          READ(5,*) CYB
4750= 609   CONTINUE
```

289

```
4760=        WRITE(6,600)
4770= 600   FORMAT(1X,*CYP (1/RAD) = *)
4780=        READ(5,*) CYP
4790=        WRITE(6,610)
4800= 610   FORMAT(1X,*CYR (1/RAD) = *)
4810=        READ(5,*) CYR
4820=        IF(KEY1 .EQ. 3HNO ) GO TO 616
4830=        WRITE(6,612)
4840= 612   FORMAT(1X,*CYDR (1/DEG) = *)
4850=        READ(5,*) CYDR
4860=        WRITE(6,613)
4870= 613   FORMAT(1X,*CYDA (1/DEG) = *)
4880=        READ(5,*) CYDA
4890=        WRITE(6,614)
4900= 614   FORMAT(1X,*CYDDT (1/DEG) = *)
4910=        READ(5,*) CYDDT
4920=        WRITE(6,615)
4930= 615   FORMAT(1X,*CYDC (1/DEG) = *)
4940=        READ(5,*) CYDC
4950= 616   CONTINUE
4960=        WRITE(6,620)
4970= 620   FORMAT(1X,"*************************************************")
4980=        WRITE(6,630)
4990= 630   FORMAT(8X,*LAT-DIR STABILITY AXIS COEFFICIENTS*)
5000=        IF(KEY .EQ. 3HLON) GO TO 635
5010=        IF(KEY .EQ. 3HBOT) GO TO 635
5020=        WRITE(6,631) DALPHA
5030= 631   FORMAT(15X,*ALPHA = *,G13.6)
5040= 635   CONTINUE
5050=        IF(KEY1 .EQ. 3HYES) GO TO 711
5060=        WRITE(6,640) CNB,CLB
5070= 640   FORMAT(3X,*CNB = *,G13.6,8X,*CLB = *,G13.6)
5080=        WRITE(6,650) CNP,CLP,CYP
5090= 650   FORMAT(3X,*CNP = *,G13.6,8X,*CLP = *,G13.6,5X,*CYP = *,G13.6)
5100=        WRITE(6,660) CNR,CLR,CYR
5110= 660   FORMAT(3X,*CNR = *,G13.6,8X,*CLR = *,G13.6,5X,*CYR = *,G13.6)
5120=        WRITE(6,670) CNDR,CLDR
5130= 670   FORMAT(2X,*CNDR = *,G13.6,7X,*CLDR = *,G13.6)
5140=        WRITE(6,680) CNDA,CLDA
5150= 680   FORMAT(2X,*CNDA = *,G13.6,7X,*CLDA = *,G13.6)
5160=        WRITE(6,690) CNDDT,CLDDT
5170= 690   FORMAT(1X,*CNDDT = *,G13.6,6X,*CLDDT = *,G13.6)
5180=        WRITE(6,700) CNDC,CLDC
5190= 700   FORMAT(2X,*CNDC = *,G13.6,7X,*CLDC = *,G13.6)
5200=        WRITE(6,710)
5210= 710   FORMAT(1X,"*************************************************")
5220=        IF(KEY1 .EQ. 3HNO ) GO TO 720
5230= 711   CONTINUE
5240=        WRITE(6,712) CNB,CLB,CYB
5250= 712   FORMAT(3X,*CNB = *,G13.6,8X,*CLB = *,G13.6,5X,*CYB = *,G13.6)
5260=        WRITE(6,713) CNP,CLP,CYP
5270= 713   FORMAT(3X,*CNP = *,G13.6,8X,*CLP = *,G13.6,5X,*CYP = *,G13.6)
```

```
5280=          WRITE(6,714) CNR,CLR,CYR
5290= 714   FORMAT(3X,*CNR = *,G13.6,8X,*CLR = *,G13.6,5X,*CYR = *,G13.6)
5300=          WRITE(6,715) CNDR,CLDR,CYDR
5310= 715   FORMAT(2X,*CNDR = *,G13.6,7X,*CLDR = *,G13.6,4X,*CYDR = *,G13.6)
5320=          WRITE(6,716) CNDA,CLDA,CYDA
5330= 716   FORMAT(2X,*CNDA = *,G13.6,7X,*CLDA = *,G13.6,4X,*CYDA = *,G13.6)
5340=          WRITE(6,717) CNDDT,CLDDT,CYDDT
5350= 717   FORMAT(1X,*CNDDT = *,G13.6,6X,*CLDDT = *,G13.6,3X,*CYDDT = *,G13.6
5360=      +)
5370=          WRITE(6,718) CNDC,CLDC,CYDC
5380= 718   FORMAT(2X,*CNDC = *,G13.6,7X,*CLDC = *,G13.6,4X,*CYDC = *,G13.6)
5390=          WRITE(6,719)
5400= 719   FORMAT(1X,"****************************************************")
5410= 720   CONTINUE
5420=          WRITE(6,730)
5430= 730   FORMAT(1X,*IS THE ENTERED DATA CORRECT ?    (YES/NO)*)
5440=          READ(5,740) DATA2
5450= 740   FORMAT(A3)
5460=          WRITE(6,750)
5470= 750   FORMAT(1X,"****************************************************")
5480=          IF(KEY .EQ. 3HBOT) GO TO 755
5490=          IF(DATA2 .EQ. 3HNO ) GO TO 2150
5500=          IF(DATA2 .EQ. 3HYES) GO TO 760
5510=          GO TO 720
5520= 755   CONTINUE
5530=          IF(DATA2 .EQ. 3HNO ) GO TO 460
5540=          IF(DATA2 .EQ. 3HYES) GO TO 760
5550=          GO TO 720
5560= 760   CONTINUE
5570=          CNB=CNB*DPR
5580=          CNDR=CNDR*DPR
5590=          CNDA =CNDA*DPR
5600=          CNDDT=CNDDT*DPR
5610=          CNDC=CNDC*DPR
5620=          CLB=CLB*DPR
5630=          CLDR=CLDR*DPR
5640=          CLDA=CLDA*DPR
5650=          CLDDT=CLDDT*DPR
5660=          CLDC=CLDC*DPR
5670=          IF(KEY1 .EQ. 3HNO ) GO TO 765
5680=          CYB = CYB*DPR
5690=          CYDR = CYDR*DPR
5700=          CYDA = CYDA*DPR
5710=          CYDDT = CYDDT*DPR
5720=          CYDC = CYDC*DPR
5730=  765 CONTINUE
5740=          BCLB = CLB*COS(ALPHA)-CNB*SIN(ALPHA)
5750=          BCLP=CLP*COS(ALPHA)**2-(CLR+CNP)*SIN(ALPHA)*COS(ALPHA)+CNR*SIN(ALP
5760=      1HA)**2
5770=          BCLR=CLR*COS(ALPHA)**2-(CNR-CLP)*SIN(ALPHA)*COS(ALPHA)-CNP*SIN(ALP
5780=      1HA)**2
5790=          BCLDA = CLDA*COS(ALPHA)-CNDA*SIN(ALPHA)
```

291

```
5800=        BCLDR = CLDR*COS(ALPHA)-CNDR*SIN(ALPHA)
5810=        BCLDC = CLDC*COS(ALPHA)-CNDC*SIN(ALPHA)
5820=        BCLDDT = CLDDT*COS(ALPHA)-CNDDT*SIN(ALPHA)
5830=        BCNB = CNB*COS(ALPHA)+CLB*SIN(ALPHA)
5840=        BCNP = CNP*COS(ALPHA)**2-(CNR-CLP)*SIN(ALPHA)*COS(ALPHA)-CLR*SIN(A
5850=       1LPHA)**2
5860=        BCNR = CNR*COS(ALPHA)**2+(CLR+CNP)*SIN(ALPHA)*COS(ALPHA)+CLP*SIN(A
5870=       1LPHA)**2
5880=        BCNDA = CNDA*COS(ALPHA)+CLDA*SIN(ALPHA)
5890=        BCNDR = CNDR*COS(ALPHA)+CLDR*SIN(ALPHA)
5900=        BCNDC = CNDC*COS(ALPHA)+CLDC*SIN(ALPHA)
5910=        BCNDDT = CNDDT*COS(ALPHA)+CLDDT*SIN(ALPHA)
5920=        BCYR = CYR*COS(ALPHA)+CYP*SIN(ALPHA)
5930=        BCYP = CYP*COS(ALPHA)-CYR*SIN(ALPHA)
5940=        WRITE(6,770)
5950= 770    FORMAT(9X,*LAT-DIR BODY AXIS COEFFICIENTS*)
5960=        WRITE(6,780) BCNB,BCLB,CYB
5970= 780    FORMAT(3X,*CNB = *,G13.6,8X,*CLB = *,G13.6,5X,*CYB = *,G13.6)
5980=        WRITE(6,790) BCNP,BCLP,BCYP
5990= 790    FORMAT(3X,*CNP = *,G13.6,8X,*CLP = *,G13.6,5X,*CYP = *,G13.6)
6000=        WRITE(6,800) BCNR,BCLR,BCYR
6010= 800    FORMAT(3X,*CNR = *,G13.6,8X,*CLR = *,G13.6,5X,*CYR = *,G13.6)
6020=        WRITE(6,810) BCNDR,BCLDR,CYDR
6030= 810    FORMAT(2X,*CNDR = *,G13.6,7X,*CLDR = *,G13.6,4X,*CYDR = *,G13.6)
6040=        WRITE(6,820) BCNDA,BCLDA,CYDA
6050= 820    FORMAT(2X,*CNDA = *,G13.6,7X,*CLDA = *,G13.6,4X,*CYDA = *,G13.6)
6060=        WRITE(6,830) BCNDDT,BCLDDT,CYDDT
6070= 830    FORMAT(1X,*CNDDT = *,G13.6,6X,*CLDDT = *,G13.6,3X,*CYDDT = *,G13.6
6080=       +)
6090=        WRITE(6,840) BCNDC,BCLDC,CYDC
6100= 840    FORMAT(2X,*CNDC = *,G13.6,7X,*CLDC = *,G13.6,4X,*CYDC = *,G13.6)
6110=        WRITE(6,850)
6120= 850    FORMAT(1X,"**********************************************************")
6130=        IF (KEY1 .EQ. 3HNO ) GO TO 421
6140=        N = (Q*S*B)/BIZZ
6150=        L = (Q*S*B)/BIXX
6160=        B = B/(2.0*U)
6170=        Y = (Q*S*32.2)/W
6180=        BNB = N*BCNB
6190=        BNP = N*B*BCNP
6200=        BNR = N*B*BCNR
6210=        BNDR = N*BCNDR
6220=        BNDA = N*BCNDA
6230=        BNDDT = N*BCNDDT
6240=        BNDC = N*BCNDC
6250=        BLB = L*BCLB
6260=        BLP = L*B*BCLP
6270=        BLR = L*B*BCLR
6280=        BLDR = L*BCLDR
6290=        BLDA = L*BCLDA
6300=        BLDDT = L*BCLDDT
6310=        BLDC = L*BCLDC
```

```
6320=        YB = Y*CYB
6330=        BYR = Y*B*BCYR
6340=        BYP = Y*B*BCYP
6350=        YDR = Y*CYDR
6360=        YDA = Y*CYDA
6370=        YDDT = Y*CYDDT
6380=       . YDC = Y*CYDC
6390=        WRITE(6,2160)
6400= 2160 FORMAT(5X,*LAT-DIR BODY AXIS DIMENSIONAL DERIVATIVES*)
6410=        WRITE(6,2170) BNB,BLB,YB
6420= 2170 FORMAT(4X,*NB = *,G13.6,9X,*LB = *,G13.6,5X,*YB = *,G13.6)
6430=        WRITE(6,2180) BNP,BLP,BYP
6440= 2180 FORMAT(4X,*NP = *,G13.6,9X,*LP = *,G13.6,5X,*YP = *,G13.6)
6450=        WRITE(6,2190) BNR,BLR,BYR
6460= 2190 FORMAT(4X,*NR = *,G13.6,9X,*LR = *,G13.6,5X,*YR = *,G13.6)
6470=        WRITE(6,2200) BNDR,BLDR,YDR
6480= 2200 FORMAT(3X,*NDR = *,G13.6,8X,*LDR = *,G13.6,4X,*YDR = *,G13.6)
6490=        WRITE(6,2210) BNDA,BLDA,YDA
6500= 2210 FORMAT(3X,*NDA = *,G13.6,8X,*LDA = *,G13.6,4X,*YDA = *G13.6)
6510=        WRITE(6,2220) BNDDT,BLDDT,YDDT
6520= 2220 FORMAT(2X,*NDDT = *,G13.6,7X,*LDDT = *,G13.6,3X,*YDDT = *,G13.6)
6530=        WRITE(6,2230) BNDC,BLDC,YDC
6540= 2230 FORMAT(3X,*NDC = *,G13.6,8X,*LDC = *,G13.6,4X,*YDC = *,G13.6)
6550=        WRITE(6,2240)
6560= 2240 FORMAT(1X,"*********************************************************")
6570=        D = 1.0 - ((BIXZ*BIXZ)/(BIXX*BIZZ))
6580=        R1 = BIXZ/BIZZ
6590=        R2 = BIXZ/BIXX
6600=        PBNB = (BNB + R1*BLB)/D
6610=        PBNP = (BNP + R1*BLP)/D
6620=        PBNR = (BNR + R1*BLR)/D
6630=        PBNDR = (BNDR + R1*BLDR)/D
6640=        PBNDA = (BNDA + R1*BLDA)/D
6650=        PBNDDT = (BNDDT + R1*BLDDT)/D
6660=        PBNDC = (BNDC + R1*BLDC)/D
6670=        PBLB = (BLB + R2*BNB)/D
6680=        PBLP = (BLP + R2*BNP)/D
6690=        PBLR = (BLR + R2*BNR)/D
6700=        PBLDR = (BLDR + R2*BNDR)/D
6710=        PBLDA = (BLDA + R2*BNDA)/D
6720=        PBLDDT = (BLDDT + R2*BNDDT)/D
6730=        PBLDC = (BLDC + R2*BNDC)/D
6740=        PYB = YB/U
6750=        PBYP = BYP/U + ALPHA
6760=        PBYR = BYR/U - 1.0
6770=        PYDR = YDR/U
6780=        PYDA = YDA/U
6790=        PYDDT = YDDT/U
6800=        PYDC = YDC/U
6810=        WRITE(6,2250)
6820= 2250 FORMAT(3X,*LAT-DIR BODY AXIS PRIMED DIMENSIONAL DERIVATIVES*)
6830=        WRITE(6,2260) PBNB,PBLB,PYB
```

293

```
6840= 2260 FORMAT(3X,*NB' = *,G13.6,8X,*LB' = *,G13.6,4X,*YB' = *,G13.6)
6850=      WRITE(6,2270) PBNP,PBLP,PBYP
6860= 2270 FORMAT(3X,*NP' = *,G13.6,8X,*LP' = *,G13.6,4X,*YP' = *,G13.6)
6870=      WRITE(6,2280) PBNR,PBLR,PBYR
6880= 2280 FORMAT(3X,*NR' = *,G13.6,8X,*LR' = *,G13.6,4X,*YR' = *,G13.6)
6890=      WRITE(6,2290) PBNDR,PBLDR,PYDR
6900= 2290 FORMAT(2X,*NDR' = *,G13.6,7X,*LDR' = *,G13.6,3X,*YDR' = *,G13.6)
6910=      WRITE(6,2300) PBNDA,PBLDA,PYDA
6920= 2300 FORMAT(2X,*NDA' = *,G13.6,7X,*LDA' = *,G13.6,3X,*YDA' = *,G13.6)
6930=      WRITE(6,2310) PBNDDT,PBLDDT,PYDDT
6940= 2310 FORMAT(1X,*NDDT' = *,G13.6,6X,*LDDT' = *,G13.6,2X,*YDDT' = *,G13.6
6950=     +)
6960=      WRITE(6,2320) PBNDC,PBLDC,PYDC
6970= 2320 FORMAT(2X,*NDC' = *,G13.6,7X,*LDC' = *,G13.6,3X,*YDC' = *,G13.6)
6980=      WRITE(6,2340)
6990= 2340 FORMAT(1X,"******************************************************")
7000=      GO TO 421
7010=  450 CONTINUE
7020=      END
```

TOTAL Macro Program to Calculate
Transmission Zeros

The TOTAL interactive design program written by
Stanley J. Larimer is programmable. Using the CREATE com-
mand, a user can define a Macro program that automatically
runs options of TOTAL. Such a Macro program must be labeled
either AKEY, BKEY, or CKEY. Each is limited to 50 instruc-
tions which can do anything allowed in the Option mode of
TOTAL. These instructions are executed like a subprogram
anytime the key name is typed. A more detailed explanation
can be found on page A-70 of the TOTAL User's Manual.

Once in the TOTAL program, the sequences in this
appendix are input. After typing the AKEY and BKEY sequences
given, TOTAL is capable of calculating transmission zeros of
a system once it is converted to zero-B_2 form. Using the
matrix partitions from the zero-B_2 form, $\underline{A}_{11}$ is input into
HMAT, and $\underline{A}_{12}$ is input into IMAT. $\underline{C}_1$ is input into JMAT,
and $\underline{C}_2$ is input into LMAT. This is easily accomplished by
using Option 11 to place each matrix into AMAT and then
employing a copy command to transfer it to the appropriate
storage matrix location. The proposed $\underline{M}$ matrix is input
into AMAT using Option 11, and AKEY is typed. The AKEY
Macro program stores the $\underline{M}$ matrix that is entered and calcu-
lates $\underline{F}_1$ and $\underline{F}_2$. (These are stored in NMAT and OMAT

respectively.) It then automatically calls BKEY. BKEY

calculates the matrix $\underline{Z}t = \lambda \underline{I}_{n-m} - \underline{A}_{11} + \underline{A}_{12}\underline{F}_2^{-1}\underline{F}_1$ and

obtains eigenvalues which are the transmission zeros.

The operator has only to input a new $\underline{M}$ matrix into

AMAT using Option 11 and type AKEY again to obtain the

transmission zeros for this new measurement matrix.

Upon exit from TOTAL, the user finds that local

files AKEY and BKEY have been created as unformatted files.

These can be stored and retrived for use each time trans-

mission zeros must be calculated. TOTAL requires that these

local files be attached and have the names AKEY and BKEY

before it is started. Note that $\underline{A}_{11}$, $\underline{A}_{12}$, $\underline{C}_1$, and $\underline{C}_2$ must be

entered on each new entry into the TOTAL program unless

Memaux is also saved and attached as a local file prior to

entering TOTAL.

```
CREATE, AKEY, COPY, AMAT, MMAT,
              COPY, HMAT, BMAT, 74,
              COPY, CMAT, BMAT,
              COPY, JMAT, AMAT, 72,
              COPY, CMAT, NMAT,
              COPY, MMAT, AMAT,
              COPY, IMAT, BMAT, 74,
              COPY, CMAT, BMAT,
              COPY, LMAT, AMAT, 72,
              COPY, CMAT, OMAT, BKEY




CREATE, BKEY, COPY, OMAT, AMAT, 75,
              COPY, CMAT, AMAT,
              COPY, NMAT, BMAT, 74,
              COPY, CMAT, BMAT,
              COPY, IMAT, AMAT, 74,
              COPY, CMAT, BMAT,
              COPY, HMAT, AMAT, 73,
              COPY, CMAT, AMAT, 71,
              COPY, AMAT, EMAT,
              COPY, MMAT, AMAT
```

In this example, AKEY and BKEY have been created previously and saved. They are attached as local files prior to starting TOTAL.

```
--LOCAL FILES--
 $INPUT     $OUTPUT     AKEY       BKEY
COMMAND- ATTACH,TOTAL,ID=AFIT,SN=AFIT
 PFN IS
 TOTAL
 AT CY= 194 SN=AFIT
COMMAND- TOTAL
WELCOME TO TOTAL -- VERSION 3.0
(C) 1980  -- STANLEY J. LARIMER


OPTION >11
INPUT OF [ AMAT ] MATRIX:
ENTER MATRIX SIZE: ROWS,COLUMNS >5 5
ENTER 5 ELEMENTS PER ROW:
ROW 1 >0 -.1123E-2 -.1596E-3 -1.896 .9886
ROW 2 >0 0 0 0 1
ROW 3 >0 -.5617 -.01258 .8522 -.5232
ROW 4 >0 -.1211E-2 -.9782E-4 -1.502 .7764
ROW 5 >0 .3213E-3 -.01068 5.455 -.7595
```

COL >	1	2	3	4	5
ROW					
1	0.	-.1123E-02	-.1596E-03	-1.896	.9886
2	0.	0.	0.	0.	1.000
3	0.	-.5617	-.1258E-01	.8522	-.5232
4	0.	-.1211E-02	-.9782E-04	-1.502	.7764
5	0.	.3213E-03	-.1068E-01	5.455	-.7595

```
OPTION >COPY,AMAT,IMAT
COPY COMPLETE

OPTION >11
INPUT OF [ AMAT ] MATRIX:
ENTER MATRIX SIZE: ROWS,COLUMNS >5 2
ENTER 5 ELEMENTS PER COLUMN:
COLUMN 1 >-.1492 0 .03492 -.03891 -24.06
COLUMN 2 >-.2449 0 .0403 -.1706 -6.473
```

```
       COL >   1          2
ROW
  1      -.1492     -.2449
  2       0.         0.
  3       .3492E-01   .4030E-01
  4      -.3891E-01  -.1706
  5      -24.06      -6.473




OPTION >COPY,AMAT,IMAT
COPY COMPLETE

OPTION >11
INPUT OF [ AMAT ] MATRIX:
ENTER MATRIX SIZE: ROWS,COLUMNS >2 5
ENTER 5 ELEMENTS PER ROW:
ROW 1 >0 0 0 1 0
ROW 2 >0 0 0 0 1

    COL >   1          2          3          4          5
ROW
  1    0.         0.         0.         1.000      0.
  2    0.         0.         0.         0.         1.000




OPTION >COPY,AMAT,JMAT
COPY COMPLETE

OPTION >11
INPUT OF [ AMAT ] MATRIX:
ENTER MATRIX SIZE: ROWS,COLUMNS >2 2
ENTER 2 ELEMENTS PER ROW:
ROW 1 >-.1064 .07496
ROW 2 >0 0

    COL >   1          2
ROW
  1     -.1064      .7496E-01
  2     0.         0.




OPTION >COPY,AMAT,IMAT
COPY COMPLETE
```

(All the required matrices have been entered. The $\underline{M}$ matrix is now placed in AMAT with Option 11 and AKEY is typed.)

```
OPTION >11
INPUT OF [ AMAT ] MATRIX:
ENTER MATRIX SIZE: ROWS,COLUMNS >2 5
ENTER 5 ELEMENTS PER ROW:
ROW 1 >0 0 0 0 0
ROW 2 >0 0 0 0 .25


   COL >   1            2            3            4            5
ROW
  1   0.          0.          0.          0.          0.
  2   0.          0.          0.          0.           .2500




OPTION >AKEY
COPY COMPLETE
COPY COMPLETE
(CMAT) = (AMAT) * (BMAT)

[ CMAT ] MATRIX:



   COL >   1            2            3            4            5
ROW
  1   0.          0.          0.          0.          0.
  2   0.           .8033E-04  -.2670E-02   1.364       -.1899




COPY COMPLETE
COPY COMPLETE
(CMAT) = (AMAT) + (BMAT)

[ CMAT ] MATRIX:



   COL >   1            2            3            4            5
ROW
  1   0.          0.          0.          1.000       0.
  2   0.           .8033E-04  -.2670E-02   1.364        .8101




COPY COMPLETE
COPY COMPLETE
COPY COMPLETE
(CMAT) = (AMAT) * (BMAT)
```

[CMAT] MATRIX:

```
    COL >    1            2
ROW
  1     0.           0.
  2    -6.015       -1.618
```

COPY COMPLETE
COPY COMPLETE
(CMAT) = (AMAT) + (BMAT)

[CMAT] MATRIX:

```
    COL >    1            2
ROW
  1    -.1064        .7496E-01
  2    -6.015       -1.618
```

COPY COMPLETE
COPY COMPLETE
STORING INVERSE OF (AMAT) TO (CMAT):

[CMAT] MATRIX:

```
    COL >    1            2
ROW
  1    -2.597       -.1203
  2     9.654       -.1708
```

COPY COMPLETE
COPY COMPLETE
(CMAT) = (AMAT) * (BMAT)

[CMAT] MATRIX:

301

COL >	1	2	3	4	5
ROW					
1	0.	-.9664E-05	.3212E-03	-2.761	-.9746E-01
2	0.	-.1372E-04	.4560E-03	9.421	-.1383

COPY COMPLETE
COPY COMPLETE
(CMAT) = (AMAT) * (BMAT)

[CMAT] MATRIX:

COL >	1	2	3	4	5
ROW					
1	0.	.4801E-05	-.1596E-03	-1.895	.4842E-01
2	0.	0.	0.	0.	0.
3	0.	-.8903E-06	.2959E-04	.2832	-.8979E-02
4	0.	.2716E-05	-.9028E-04	-1.500	.2739E-01
5	0.	.3213E-03	-.1068E-01	5.455	3.241

COPY COMPLETE
COPY COMPLETE
(CMAT) = (AMAT) - (BMAT)

[CMAT] MATRIX:

COL >	1	2	3	4	5
ROW					
1	0.	-.1128E-02	-.1099E-07	-.7878E-03	.9402
2	0.	0.	0.	0.	1.000
3	0.	-.5617	-.1261E-01	.5690	-.5142
4	0.	-.1214E-02	-.7536E-05	-.2222E-02	.7490
5	0.	.3469E-17	.1665E-15	.5400E-12	-4.000

COPY COMPLETE
STORING CHARACTERISTIC EQN & EIGENVALUES OF (AMAT)
TO POLYA AND ROOTA RESPECTIVELY:

```
        CHARACTERISTIC EQN              EIGENVALUES OF A'1AT
        POLYA COEFFICIENTS              POLYA ROOTS    (ROOTA)

      (    1.000    )S** 5       (      .2100E-06) + J(    .3023E-04)
      (    4.015    )S** 4       (      .2100E-06) + J(   -.3023E-04)
      (    .5936E-01)S** 3       (     -.2654E-02) + J(   0.        )
      (    .1292E-03)S** 2       (     -.1218E-01) + J(   0.        )
      (   -.4914E-13)S** 1       (     -4.000     ) + J(   0.        )
      (    .1181E-12)            POLYNOMIAL CONSTANT=    1.000

        COPY COMPLETE
        COPY COMPLETE
```

(The roots are the transmission zeros. The first two are assumed to be zero, thus Z_t = 0, 0, -0.0026, -0.0122, -4.0. A new $\underline{M}$ matrix is now entered, and AKEY is used to evaluate transmission zeros with a different measurement matrix.)

```
OPTION >11
INPUT OF [ AMAT ] MATRIX:
ENTER MATRIX SIZE: ROWS,COLUMNS >2 5
ENTER 5 ELEMENTS PER ROW:
ROW 1 >0 0 0 0 0
ROW 2 >0 0 0 0 .1

   COL >    1              2             3            4            5
ROW
  1    0.            0.            0.           0.           0.
  2    0.            0.            0.           0.            .1000




OPTION >AKEY
COPY COMPLETE
COPY COMPLETE
(CMAT) = (AMAT) * (BMAT)

[ CMAT ]  MATRIX:



   COL >    1            2            3            4            5
ROW
  1    0.            0.           0.           0.           0.
  2    0.             .3213E-04  -.1068E-02    .5455        -.7595E-01


COPY COMPLETE
COPY COMPLETE
(CMAT) = (AMAT) + (BMAT)

[ CMAT ]  MATRIX:



   COL >    1            2            3            4            5
ROW
  1    0.            0.           0.           1.000        0.
  2    0.             .3213E-04  -.1068E-02    .5455         .9241


COPY COMPLETE
COPY COMPLETE
COPY COMPLETE
(CMAT) = (AMAT) * (BMAT)
```

[CMAT] MATRIX:


```
    COL >    1            2
ROW
  1     0.          0.
  2    -2.406      -.6473
```

COPY COMPLETE
COPY COMPLETE
(CMAT) = (AMAT) + (BMAT)

[CMAT] MATRIX:


```
    COL >    1            2
ROW
  1    -.1064       .7496E-01
  2    -2.406      -.6473
```

COPY COMPLETE
COPY COMPLETE
STORING INVERSE OF (AMAT) TO (CMAT):

[CMAT] MATRIX:


```
    COL >    1            2
ROW
  1    -2.597      -.3008
  2     9.654      -.4269
```

COPY COMPLETE
COPY COMPLETE
(CMAT) = (AMAT) * (BMAT)

[CMAT] MATRIX:

COL >	1	2	3	4	5
ROW					
1	0.	-.9664E-05	.3212E-03	-2.761	-.2779
2	0.	-.1372E-04	.4560E-03	9.421	-.3945

COPY COMPLETE
COPY COMPLETE
(CMAT) = (AMAT) * (BMAT)

[CMAT] MATRIX:

COL >	1	2	3	4	5
ROW					
1	0.	.4801E-05	-.1596E-03	-1.895	.1381
2	0.	0.	0.	0.	0.
3	0.	-.8903E-06	.2959E-04	.2832	-.2560E-01
4	0.	.2716E-05	-.9028E-04	-1.500	.7812E-01
5	0.	.3213E-03	-.1068E-01	5.455	9.240

COPY COMPLETE
COPY COMPLETE
(CMAT) = (AMAT) - (BMAT)

[CMAT] MATRIX:

COL >	1	2	3	4	5
ROW					
1	0.	-.1128E-02	-.1099E-07	-.7878E-03	.8505
2	0.	0.	0.	0.	1.000
3	0.	-.5617	-.1261E-01	.5690	-.4976
4	0.	-.1214E-02	-.7536E-05	-.2222E-02	.6983
5	0.	.3469E-17	-.1665E-15	.5400E-12	-10.00

COPY COMPLETE
STORING CHARACTERISTIC EQN & EIGENVALUES OF (AMAT)
TO POLYA AND ROOTA RESPECTIVELY:

```
CHARACTERISTIC EQN                    EIGENVALUES OF AMAT
POLYA COEFFICIENTS                      POLYA ROOTS    (ROOTA)

(    1.000    )S** 5      (      .3238E-05) + J(    -.1188E-03)
(    10.01    )S** 4      (      .3238E-05) + J(     .1188E-03)
(    .1484    )S** 3      (    -.2660E-02) + J(    0.        )
(    .3231E-03)S** 2      (    -.1218E-01) + J(    0.        )
(  -.7624E-12)S** 1      (    -10.00    ) + J(    0.        )
(    .4577E-11)          POLYNOMIAL CONSTANT=      1.000
```

COPY COMPLETE
COPY COMPLETE

OPTION >

Appendix F

A TOTAL Macro Program For Determining the Closed-Loop System Matrices

Macro programming of TOTAL is used to formulate the closed-loop system matrices designated $\underline{A}_{c\ell}$, $\underline{B}_{c\ell}$, and $\underline{C}_{c\ell}$. To perform the necessary operations, a Macro program called CKEY is developed using the CREATE command in TOTAL. The instructions in CKEY are automatically executed anytime the key name is typed while in TOTAL. A complete listing for CKEY is given in this appendix.

For a system that is in zero-B_2 form, the partitioned matrix $\underline{A}_{21}$ is input into PMAT, and $\underline{A}_{22}$ is input into QMAT. If AKEY and BKEY (see Appendix E) have been run, $\underline{F}_1$ and $\underline{F}_2$ are stored in NMAT and OMAT respectively; otherwise, they must be obtained from Option 14 in the MULTI program and input into NMAT and OMAT. The $\underline{K}_0$ gain matrix is loaded into RMAT. $\underline{K}_1$ is input into BMAT, $g\underline{B}_2$ is placed in AMAT, and CKEY is typed. TOTAL prints intermediate calculations as they are performed. These aid in checking the proper operation of the Macro program. The final results are printed after a message of "ECHO, OFF" is output. Following this message $\underline{F}_1$, $\underline{F}_2$, $\underline{A}_{11}$, $\underline{A}_{12}$, $g\underline{B}_2\underline{K}_1$, $\underline{A}_{21} - g\underline{B}_2\underline{K}_0\underline{F}_1$, $\underline{A}_{22} - g\underline{B}_2\underline{K}_0\underline{F}_2$, and $g\underline{B}_2\underline{K}_0$ are output in the order just listed. The message "ECHO, ON" signals the end of the output. These matrices are then assembled to yield the closed-loop $\underline{A}_{c\ell}$, $\underline{B}_{c\ell}$, and

$\underline{C}_{c\ell}$ matrices as follows from Reference 6.

$$
\begin{bmatrix} \dot{\underline{z}}(t) \\ \dot{\underline{x}}_1(t) \\ \dot{\underline{x}}_2(t) \end{bmatrix} = \begin{bmatrix} 0 & -\underline{F}_1 & -\underline{F}_2 \\ 0 & \underline{A}_{11} & \underline{A}_{12} \\ g\underline{B}_1\underline{K}_1 & \underline{A}_{21}-g\underline{B}_2\underline{K}_0\underline{F}_1 & \underline{A}_{22}-g\underline{B}_2\underline{K}_0\underline{F}_2 \end{bmatrix} \begin{bmatrix} \underline{z}(t) \\ \underline{x}_1(t) \\ \underline{x}_2(t) \end{bmatrix} + \begin{bmatrix} \underline{I}_\ell \\ 0 \\ g\underline{B}_2\underline{K}_0 \end{bmatrix} \underline{v}(t)
$$

$$\text{(F-1)}$$

$$
\underline{y}(t) = [\; 0 \quad \underline{C}_1 \quad \underline{C}_2 \;] \begin{bmatrix} \underline{z}(t) \\ \underline{x}_1(t) \\ \underline{x}_2(t) \end{bmatrix}
$$

$$\text{(F-2)}$$

These composite $\underline{A}_{c\ell}$, $\underline{B}_{c\ell}$, $\underline{C}_{c\ell}$ matrices can be used in any appropriate routine to obtain the closed-loop transfer functions by $\underline{G}(s) = \underline{C}_{c\ell}(s\underline{I} - \underline{A}_{c\ell})^{-1} \underline{B}_{c\ell}$

This can be accomplished with Option 25 in TOTAL. $\underline{A}_{c\ell}$, $\underline{B}_{c\ell}$, and $\underline{C}_{c\ell}$ are input, and the $\underline{K}$ and $\underline{D}$ matrices are set to zero. Performing Option 25 will yield the system transfer function as GTF for any input/output combination specified. A note of caution must be provided at this point if Options 18 and 25 of TOTAL are used to obtain the closed-loop system transfer functions. Because of the numerical method used by TOTAL, if the closed-loop matrices are ill defined, errors may result in the characteristic roots that are calculated.

```
CREATE, CKEY, COPY, AMAT, TMAT,
              COPY, BMAT, SMAT, 74,
              COPY, CMAT, UMAT,
              COPY, RMAT, BMAT, 74,
              COPY, CMAT, VMAT,
              COPY, CMAT, AMAT
              COPY, NMAT, BMAT, 74,
              COPY, CMAT, BMAT,
              COPY, PMAT, AMAT, 73,
              COPY, CMAT, WMAT,
              COPY, VMAT, AMAT,
              COPY, OMAT, BMAT, 74,
              COPY, CMAT, BMAT,
              COPY, QMAT, AMAT, 73,
              COPY, CMAT, XMAT, ECHO, OFF,
              NMAT, OMAT, HMAT, IMAT,
              UMAT, WMAT, XMAT, VMAT, ECHO, ON
```

VITA

Finley Barfield is a native of Norfolk, Virginia.
He graduated from the Virginia Military Institute in
Lexington, Virginia, in 1968 with a Bachelor of Science in
Electrical Engineering. He was commissioned through the
Air Force ROTC program and served on active duty for four
years. During that time he was assigned to the Control
System Development Branch, Flight Control Division of the
Air Force Flight Dynamics Laboratory. His work involved the
flight testing of an advanced terrain following system,
development of multiplexing techniques for flight control
application and research into self-adaptive control methods
for tactical missiles.

In 1972 he became a civilian employee of the Advanced
Development Branch of the Air Force Flight Dynamics Labora-
tory's Flight Control Division. He has been assigned to
both the Controlled Configured Vehicle (CCV) Bomber and
Fighter Advanced Development Programs. Recently he served
as the responsible Air Force engineer for flight control law
development on the AFTI/F-16 Program. He is currently
working towards an advanced degree at the Air Force Institute
of Technology, Wright-Patterson AFB, Ohio.

REPORT DOCUMENTATION PAGE	READ INSTRUCTIONS BEFORE COMPLETING FORM

1. REPORT NUMBER	2. GOVT ACCESSION NO.	3. RECIPIENT'S CATALOG NUMBER
AFIT/GE/EE/83S-4	AD-A135 870	

4. TITLE *(and Subtitle)*	5. TYPE OF REPORT & PERIOD COVERED
MULTIVARIABLE CONTROL LAWS FOR THE AFTI/F-16	MS Thesis
	6. PERFORMING ORG. REPORT NUMBER

7. AUTHOR(s)	8. CONTRACT OR GRANT NUMBER(s)
A. Finley Barfield	

9. PERFORMING ORGANIZATION NAME AND ADDRESS	10. PROGRAM ELEMENT, PROJECT, TASK AREA & WORK UNIT NUMBERS
Air Force Institute of Technology (AFIT/EN) Wright-Patterson AFB, Ohio 45433	

11. CONTROLLING OFFICE NAME AND ADDRESS	12. REPORT DATE
AFTI/F-16 Advanced Development Program Ofc AFWAL/FII Wright-Patterson AFB, Ohio 45433	July 1983
	13. NUMBER OF PAGES
	311

14. MONITORING AGENCY NAME & ADDRESS *(if different from Controlling Office)*	15. SECURITY CLASS. *(of this report)*
	UNCLASSIFIED
	15a. DECLASSIFICATION/DOWNGRADING SCHEDULE

16. DISTRIBUTION STATEMENT *(of this Report)*

Approved for public release; distribution unlimited

17. DISTRIBUTION STATEMENT *(of the abstract entered in Block 20, if different from Report)*

18. SUPPLEMENTARY NOTES

19. KEY WORDS *(Continue on reverse side if necessary and identify by block number)*

Multivariable Control Laws	Measurement Matrix
Digital Control	CCV Modes
Regular Plant	
Irregular Plants	
Transmission Zeros	

20. ABSTRACT *(Continue on reverse side if necessary and identify by block number)*

Recently evolved multivariable design techniques are used to develop control laws for the AFTI/F-16. The techniques were developed by Professor Brian Porter of the University of Salford, England. In the study, designs are investigated to provide pilot control of vehicle rotational rates and accelerations. This line of inquiry is in contrast to the angle control concepts required in previous applications of these new techniques. A computer-aided design package called "MULTI" is used in refining the control laws

DD _{1 JAN 73} **1473**   EDITION OF 1 NOV 65 IS OBSOLETE

to the preliminary design stage. It proves to be invaluable. An aircraft model is developed in state space form for the AFTI vehicle from linearized aerodynamic data. This is accomplished at several points in the flight envelope. After validation, these models are used for the design and evaluation of the control laws. AFTI is equipped with additional control surfaces to provide Direct Force (CCV) control. A requirement of the design is to demonstrate specific CCV capabilities. Major emphasis is placed on the ability to properly blend CCV and conventional control capabilities for combat maneuvering. The methods employed to obtain a design are presented along with the evaluations of the final control laws. Several instabilities encountered during the investigation are discussed. The multivariable techniques are shown to provide good designs with a very moderate expenditure of manpower. Additional areas of research are discussed along with proposed modifications to the "MULTI" package.